INFORMATION TO USERS

This manuscript has been reproduced from the microfilm master. UMI films the text directly from the original or copy submitted. Thus, some thesis and dissertation copies are in typewriter face, while others may be from any type of computer printer.

The quality of this reproduction is dependent upon the quality of the copy submitted. Broken or indistinct print, colored or poor quality illustrations and photographs, print bleedthrough, substandard margins, and improper alignment can adversely affect reproduction.

In the unlikely event that the author did not send UMI a complete manuscript and there are missing pages, these will be noted. Also, if unauthorized copyright material had to be removed, a note will indicate the deletion.

Oversize materials (e.g., maps, drawings, charts) are reproduced by sectioning the original, beginning at the upper left-hand corner and continuing from left to right in equal sections with small overlaps.

Photographs included in the original manuscript have been reproduced xerographically in this copy. Higher quality 6" x 9" black and white photographic prints are available for any photographs or illustrations appearing in this copy for an additional charge. Contact UMI directly to order.

ProQuest Information and Learning
300 North Zeeb Road, Ann Arbor, MI 48106-1346 USA
800-521-0600

Synthesis and Characterization of Complexes Involving Phosphino-centres as Lewis Acids

by

Andrew Douglas Phillips

Submitted in partial fulfillment of the requirements
for the degree of Doctor of Philosophy

at

Dalhousie University
Halifax, Nova Scotia
February, 2001

© Copyright by Andrew Douglas Phillips, 2001

National Library of Canada
Acquisitions and Bibliographic Services
395 Wellington Street
Ottawa ON K1A 0N4
Canada

Bibliothèque nationale du Canada
Acquisitions et services bibliographiques
395, rue Wellington
Ottawa ON K1A 0N4
Canada

Your file Votre référence

Our file Notre référence

The author has granted a non-exclusive licence allowing the National Library of Canada to reproduce, loan, distribute or sell copies of this thesis in microform, paper or electronic formats.

L'auteur a accordé une licence non exclusive permettant à la Bibliothèque nationale du Canada de reproduire, prêter, distribuer ou vendre des copies de cette thèse sous la forme de microfiche/film, de reproduction sur papier ou sur format électronique.

The author retains ownership of the copyright in this thesis. Neither the thesis nor substantial extracts from it may be printed or otherwise reproduced without the author's permission.

L'auteur conserve la propriété du droit d'auteur qui protège cette thèse. Ni la thèse ni des extraits substantiels de celle-ci ne doivent être imprimés ou autrement reproduits sans son autorisation.

0-612-66642-5

Canada

DALHOUSIE UNIVERSITY

FACULTY OF GRADUATE STUDIES

The undersigned hereby certify that they have read and recommend to the Faculty of Graduate Studies for acceptance a thesis entitled "Synthesis and Characterization of Complexes Involving Phosphino-centres as Lewis Acids"

by Andrew D. Phillips

in partial fulfillment of the requirements for the degree of Doctor of Philosophy.

Dated: January 12, 2001

External Examiner

Research Supervisor

Examining Committee

DALHOUSIE UNIVERSITY

DATE: February 14th, 2001

AUTHOR: Andrew Douglas Phillips

Title: Synthesis and Characterization of Complexes Involving Phosphino-centres as Lewis Acids

DEPARTMENT OR SCHOOL: Chemistry

DEGREE: Ph. D. CONVOCATION: May YEAR: 2001

Permission is herewith granted to Dalhousie University to circulate and to have copied for non-commercial purposes, at its discretion, the above title upon the request of individuals or institutions.

Signature of Author

The author reserves other publication rights, and neither the thesis nor extensive extracts from it may be printed or otherwise reproduced without the author's written permission.

The author attests that permission has been obtained for the use of any copyrighted material appearing in this thesis (other than brief excerpts requiring only proper acknowledgement in scholarly writing), and that all such use is clearly acknowledged.

For Mum, Dad and Stuart

To be conscious that you are ignorant is a great step to knowledge.

Benjamin Disraeli

Table of Contents

List of Figures

List of Tables

Abstract

Phosphines, where there is a lone pair of electrons on phosphorus, are typically regarded as Lewis bases, whereas hypervalent bonding environments with electronegative substituents are effective Lewis acids. The discovery of compounds with mono- and di-substituted phosphine centres, such as the phosphadiazonium cation Mes^*NP^+ (Mes* = 2,4,6-tri-*tert*-butylphenyl) and iminophosphines, RNPR', provide access to new phosphorus bonding environments. The complexes reported in this thesis represent the development of phosphines as Lewis acids.

A series of phosphadiazonium-ligand-triflate complexes $[Mes^*NP{\bullet}Lg]OSO_2CF_3$, (Lg = Ligand), (**A**) have been isolated and comprehensively characterized. This involved a series of ligands having a range of basicities and polarizabilities (pyridine, 1-azabicyclo[2.2.2]-octane, imidazol-2-ylidene, tertiary phosphine chalcogenides and chalcogenoimidazolines). Spectroscopic and structural properties of these complexes are discussed in the context of data available for other established bonding environments of phosphorus. A complex (**B**) containing a chelated phosphine centre has been prepared and characterized using the bidentate 2,2'-dipyridyl ligand.

The synthesis of previously unknown *P*-functionalized iminophosphines (i.e., *P*-silyl-iminophosphines) was accomplished using $Mes^*NPOSO_2CF_3$ as a Lewis acid. The Lewis acidic properties of *P*-chloro-iminophosphine (Mes*NPCl) have been demonstrated using imidazol-2-ylidene as a ligand affording a complex (**C**) which represents a definitive example of an iminophosphide bonding environment. The adduct features a trisubstituted phosphorus centre with pyramidal geometry and P–N π-bonding.

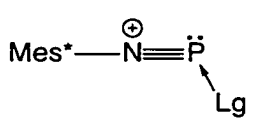

A

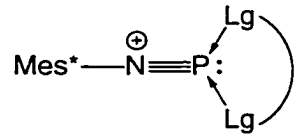

B

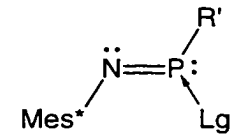

C

List of Abbreviations and Symbols

Unless otherwise listed in the table below, standard letter symbols, SI prefixes, units and chemical abbreviations used in this thesis are as defined in Dean, J. A. *Lange's Handbook of Chemistry*; 15th ed.; McGraw-Hill: New York, 1999, Table 2.6. Crystallographic abbreviations follow those approved by the International Union of Crystallographers (IUCr).

$\{A\}$	Decoupled nucleus A	Cp	Cyclopentadienyl
acac	Acetylacetonate anion (2,4-Pentanedionato)	Cp*	Pentamethylcyclopenta-dienyl
Ad	Adamantyl	CSD	Cambridge Structural Database
An	Generalized anion	Cy	Cyclohexyl
APCI	Atmospheric pressure chemical ionization	d	Doublet
Ar	Generalized aryl substituent	$d(A–B)$	Distance between atoms A and B
br.	Broad	$\delta(A)$	Chemical shift of nucleus A (solution NMR)
χ	Electronegativity		
χ_{spec}	Electronegativity (from spectroscopic data)	δ_{ii}	Principal component ii of the chemical shift tensor
Cat	Generalized cation	$\delta_{iso}(A)$	Isotropic chemical shift of nucleus A (solid-state NMR)
CCD	Charge coupled device		
CEPA-1	Coupled Electron Pair Approximation (Level 1)	DAB	1,4-Di-*tert*-butyl-diazabutadiene
Ch	Chalcogen	dsp	Doublet of septets
COD	1,5-Cyclooctadiene	D_x	Crystallographically determined density
CP	Cross polarization		

E	Group 13,14, or 15 element
$\Delta E(A–B)$	Transition energy from MO *A* to MO *B*
ECP	Effective core potential
ESD	Estimated standard deviation
fc	Frozen core
Fln	Fluorenyl
FMes	2,4,6-Tris-trifluoromethyl-phenyl
FT	Fourier Transform
η	Absolute hardness
ΔH_B	Bond enthalpy
HF	Hartree-Fock
H_o	Acidity function
HOMO	Highest occupied molecular orbital
HSAB	Hard-soft acid-base
hν	Radiation
i	*Ipso*
$I(A)$	Intensity of signal *A*
ISEE	Inner shell electron excitation
iso	Isotropic
Lg	Generalized ligand
LUMO	Lowest unoccupied molecular orbital
m-	*Meta*
M	Generalized metal
m	Multiplet
μ	Dipole moment
MAS	Magic-angle spinning
Ment	Menthyl
Mes	2,4,6-Tri-methylphenyl
Mes*	2,4,6-Tri-*tert*-butylphenyl
MO	Molecular orbital
MP*n*	*n*th-order Møller-Plesset
M_r	Crystallographically determined molecular mass
$^nJ(A,B)$	Coupling constant between nuclei *A* and *B*, connected through *n* number of bonds
Np	Neopentyl
NQR	Nuclear quadrupolar resonance
o-	*Ortho*
OTf	Trifluoromethylsulphonate (triflate)
p-	*Para*
PE	Photoelectron
Pip	Piperidino

pK_a	Acidity constant, in logarithmic units
q	Quartet
R	Substituent
R	Residual factor
R_w	Weighted residual factor
$r_W(A)$	van der Waals radius of element A
$r_I(A)$	Ionic radius of element A
s	Singlet
S	Goodness-of-fit
$\Sigma \angle(A)$	Sum of bond angles about element centre A
sept	Septet
t	Triplet
TMP	Tetramethylpiperidino
Tipp	Triisopropylphenyl
vis	Visible
X	Halogen
$\nu(A)$	Frequency of signal A
$\nu_{1/2}$	Line width at half height
V	Volume
Z	Unit cell mass divided by the defined formula mass (integer value)
ZPVE	Zero-point vibrational energy

Qncd	1-Azabicyclo[2.2.2]octane (quinuclidine)
DBN	1,5-Diazabicyclo[4.3.0]-non-5-ene
DABCO	1,4-Diazabicyclo[2.2.2]-octane
DBU	1,8-Diazabicyclo[5.4.0]-undec-7-ene
SeIm	1,3-Diisopropyl-4,5-dimethylimidazole-2(3*H*)-selenone
TeIm	1,3-Diisopropyl-4,5-dimethylimidazole-2(3*H*)-tellurone
SIm	1,3-Diisopropyl-4,5-dimethylimidazole-2(3*H*)-thione
Im	Diisopropyl-4,5-dimethylimidazol-2-ylidene
4-DMAP	4-Dimethylaminopyridine
DMSO	Dimethyl sulphoxide

Dipy	2,2'-Dipyridyl
SiDAB	1,3-Di-*tert*-butyl-2,3-dihydro-1*H*-1,3,2-diazolsilol-2-ylidene
Pyz	Pyrazine
THF	Tetrahydrofuran
Tmeda	*N*,*N*,*N*',*N*'-Tetramethylethylenediamine

Conventions and Nomenclature

For the Lewis drawings in this thesis, lone pairs are placed on the principal atom or atoms of interest, and for clarity, omitted from peripheral substituents. In addition, bonds drawn as arrows represent a coordinate or dative interaction. In Lewis drawings and in molecular formulae, cationic and anionic entities are separated by square brackets.

Nomenclature follows that found in the published literature, which does not often follow the guidelines recommended by IUPAC (international union of pure and applied chemists). However, at the introduction of each class of compounds, alternative names (including IUPAC nomenclature) are given.

Bond lengths, bond angles, and torsion angles without reported standard errors values are indicated by the symbol †. Standard deviations for means of bond lengths obtained from statistical analyses are given inside square brackets, whereas crystallographic obtained standard errors are quoted in parentheses.

Unless otherwise specified, pK_a values refer to those obtained from measurements using aqueous solutions.

Acknowledgements

I am much indebted to numerous individuals for their guidance and support during my stay here at Dalhousie. First, and foremost, I would specially like to thank my supervisor and friend, Dr. Neil Burford. This thesis would have not been possible without his devotion towards new "structure and bonding". Special mention goes to Dr. Roderick E. Wasylishen and his family for their encouragement.

I would also like to thank previous and current postdoctoral fellows, graduate, and undergraduate students of the Burford research group. I would like to highlight several colleagues that I have enjoyed working with: Denise Walsh, Dr. Glen Briand, Dr. Daren J. LeBlanc, Doug Jackson, Paul Ragogna, Heather Spinney, Laura Stark, Natasha Zwarun, Luke Chen, Dr. Jason A. C. Clyburne and Donna Silvert. A special thanks goes to Dr. Charles L. B. Macdonald for his friendship and excellent insights. My appreciation goes to Dr. Edgar Ocando-Mavarez for his assistance.

Today's synthetic chemist must work in cooperation with many other people in various fields of chemistry. I am certainly no exception. I wish to thank Dr. T. Stanley Cameron of DALX, Dr. Hilary A. Jenkins (St. Mary's University), Dr. Robert McDonald (University of Alberta) and members of Dr. A. L. Rheingold's (University of Delaware) research group for their assistance with crystallography. I would especially like to thank Katherine N. Robertson (DALX) for the exceptional amount of time and effort devoted to solving my crystal structures. Thanks to past and present friends in the Wasylishen research group for solid state NMR advice, especially Dr. Guy M. Bernard, David Bryce, Dr. Robert W. Schurko, Myrlene Gee and Dr. Klaus Eichele. I thank the members of ARMRC, Dr. Don L. Hooper and Dr. Michael D. Lumsden for spectral collection. I am

indebted to Dr. Russell J. Boyd for allowing me to indulge my interests in theoretical chemistry. I wish to thank Dalhousie University and the Walter C. Sumner Foundation for a scholarship and financial assistance. Thanks to Anna Gubskaya for assistance with translation of papers. I am also indebted to Dr. T. Stanley Cameron and Bruce T. Grindley for their insightful comments and suggestions regarding the drafts of this thesis.

The administrative and technical staff at Dalhousie has been most helpful. Thanks to Gail E. Power, Giselle M. Andrews and Deanna J. Wentzell. Ross Shortt and Rick Conrad were essential in keeping my vacuum pump healthy. My deepest gratitude to Jurgen Müller, master glassblower and friend. I will miss you.

Outside of Dalhousie University, I would like to thank Dr. Martin Nieger, University of Bonn and Mrs. Gill Heale, Senior Scientific Editor for Cambridge Crystallographic Data Centre for meeting my requests for crystallographic information with dispatch. Furthermore, I thank Dr. Anthony. J. Arduengo III, University of Alabama, Dr. Rainer Glaser, University of Missouri, and Dr. Norbert Kuhn, University of Tübingen for their correspondence.

To friends at home in Toronto, Billy Quan, Hoang Letien, Mark Lee, Mike Young, and here in Halifax; Dino Mangion, Todd Melville, Cameron Dickinson and Cassie (*mon minou francophone*). Special thanks to my room-mate Geneviève Mercier for her friendship, translation of papers, and cooking! My most sincere gratitude to Karen Won Yan Anne Cheng for her encouragement and support. In the end, I will always be greatly indebted to two individuals. Their advice and insights were essential to this production of this thesis. My sincere thanks to Dr. *Roland Rösler* and Dr. *James W. Gauld*!

Chapter 1: Introduction

1.1: Why Discover New Bonding Environments for Main-group Elements?

During the past twenty years significant developments have occurred in regards to our fundamental understanding of main-group chemistry. Molecules with elements in bonding environments previously thought to be highly unstable and not to exist, are now being successfully isolated under normal laboratory conditions.[1] Furthermore, the structural and spectroscopic characterization of these compounds is revealing surprising new patterns of molecular bonding. Therefore by discovering new bonding environments for elements such as phosphorus, present and future chemists can modify or develop molecular bonding theories that are consistent with experimental findings.

The question as to why certain bonding environments are unstable and difficult to isolate is an important one to understand. Knowledge of the factors responsible for compound instability assist chemists in developing new synthetic strategies (vide infra) for overcoming these challenges.

An often-cited explanation for the instability associated with heavy-element multiple bonding is the comparatively low enthalpy of π-bonding versus σ-bonding for atoms having valence electrons with a principal quantum number $n > 2$.[1-4] In general, for elements from the second row (i.e., $n = 2$), the total bond enthalpy (ΔH_B) of double and triple bonds (i.e., $\Delta H_B = \sigma + \pi$ or $\Delta H_B = \sigma + 2 \times \pi$) exceeds the combined energies of two or three single σ-bonds (Table 1.1). Consequently, the second row elements form π-bonded compounds, which are highly stable towards oligomerization and catenation. In contrast, for the heavier elements with $n > 2$, including phosphorus ($n = 3$), the ΔH_B of

[1] "Normal laboratory conditions" means that the compounds can be manipulated and stored for months at ambient temperature. However, for the purposes of this thesis, synthesis and characterization of compounds where air and moisture are excluded is considered a "normal condition".

two σ-bonds is greater than that of a double or a triple bond (Table 1.1). Thus, these elements often are found in σ-bonded ring or polymeric systems.

Some main-group compounds are inherently unstable due to low bond polarity. Heteronuclear covalent bonds are partially stabilized through ionic-covalent resonance, that is, electrostatic interactions contribute to ΔH_B. The ionic-covalent resonance energy of a bond is proportional to the electronegativity difference ($\Delta\chi$) of the two atoms involved.[5] Generally, within a given period, element electronegativity decreases with increasing *n*. Hence, heavy element heteronuclear bonds (A–B) with a small $\Delta\chi$ have ΔH_B values that are comparable with those ΔH_B for homonuclear bonds (A–A and B–B), where $\Delta\chi = 0$. For example, the $\Delta\chi_{spec}$ for the selenium-iodine bond is small (0.065)[6] and consequently, alkyl- and aryl-selenyl iodides RSeI, are difficult to isolate due to their tendency to decompose into diselenides RSeSeR, and molecular iodine.[7]

Table 1.1: Approximate enthalpies for the σ- and π-components of homonuclear bonds for selected main-group elements. All values in kJ mol^{-1}, reproduced from reference 4.

	Element								
	C	N	O	Si	P	S	Ge	As	Se
Component Enthalpy									
σ	335	160	145	195	200	270	165	175	210
π	295	395	350	120	145	155	110	120	125
Total Bond Enthalpy									
σ + π	630	555	495	315	345	425	275	295	335
2 × σ	670	320	290	390	400	540	330	350	420

1.2: New Synthetic Methodology for the Isolation of Unusual Bonding Environments

Three important synthetic strategies are increasingly being utilized for the isolation of new bonding environments for transition metals, main-group, lanthanide, and other heavier elements of the periodic table.[8] These are steric protection, coordination, and for ionic systems, use of weakly interacting counter-ions. All three synthetic strategies are commonly used in the isolation of unusual bonding environments for phosphorus.

Steric protection is achieved through the attachment of voluminous organic substituents, alkyl, or aryl groups (e.g., $(Me_3Si)_3C$ and Mes*), where the majority of bulk is positioned relatively close to a central reactive element. The sterically demanding "bulky" substituent behaves as a "molecular shield", preventing interactions between the central element and other potentially reactive molecules.[9,10] Hence, the resulting compound is kinetically stabilized with respect to other structural alternatives. However, bulky substituents also impart stabilization, through steric strain, by causing alternative bonding combinations to be higher in overall energy.[2,11] Therefore, it is thermodynamically favorable to form π-bonded compounds so as to minimize the number of bulky substituents surrounding the reactive centre within the molecule and reduce internal steric strain.[2,8]

Thermodynamic contributions to steric stabilization are demonstrated by the formation of a *P*-amino-iminophosphine **1.1**, through the spontaneous elimination of a secondary amine from a trisaminophosphine **1.2** (Figure 1.1). Under ambient conditions, this reaction occurs when the *P*- and *N*-substituents on **1.1** are extremely bulky (i.e., **1.1**, R = ^{i}Pr). However, when the *N*-substituent R, is smaller than ^{i}Pr, (e.g., **1.1**, R = Me, Et), the reaction rate is considerably slower.[12]

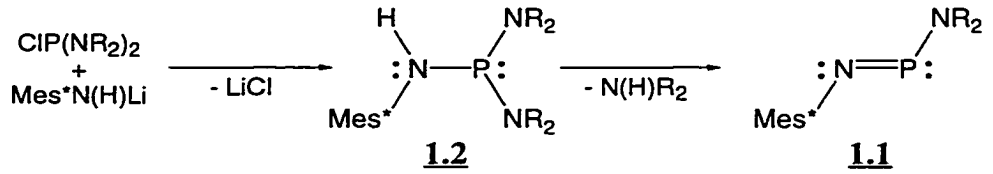

Figure 1.1: The formation of a *P*-amino-iminophosphine **1.1** by the elimination of a secondary amine from a *N*-Mes* substituted trisaminophosphine **1.2**. Minimization of internal steric hindrance is the primary driving force behind this reaction. The rates of reaction increase in the order R = Me < Et < ^{i}Pr, which is correlated with the size of the substituent R.[12]

In contrast, secondary amines are known to add to *P*-alkyl-iminophosphines which have less steric bulky *P*- and *N*-substituents, for example, ^{t}BuNP^{t}Bu and ^{t}BuNPSiMe$_3$.[13-15]

Some unusual bonding environments can be stabilized as complexes by deactivation of the site of reactivity for the central element, the HOMO for a Lewis base and the LUMO for a Lewis acid. The resulting complex must be resistant to further reactivity, such as structural rearrangement (e.g., hydrogen migration or orthometallation), but allow for exchange or substitution. The Lewis acid-base complex features a prototypical example of the unusual bonding environment that is stable enough for further study. For example, at present, there are no isolated examples of donor-free phosphorus-nitrogen or sulphur-phosphorus analogues of allene R_2CCCR_2 (i.e., bisiminophosphonium cations **1.3** (E = NR), or bisthiophosphonium cations **1.3** (E = S)). However, donor-stabilized examples have been isolated, including bis-(4-DMAP)-bisiminophosphonium bromide[16] **1.4** and bispyridino-bisthiophosphonium bromide[17] **1.5**. Structural characterization of the former has helped in the development of a theoretical bonding model for the bisiminophosphonium cation **1.3** E = (NH).[16]

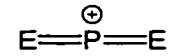

1.3

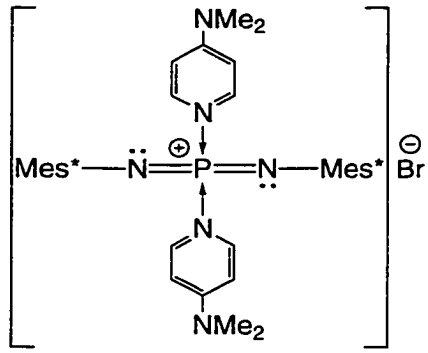

1.4

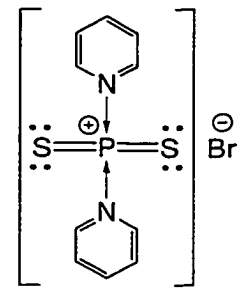

1.5

Use of substituents such as amino NR_2 and thio SR groups, where the attaching atom contains a non-bonding pair of valence electrons, can stabilize a reactive central element through π-bonding, hereafter referred to as lone-pair π-conjugation.[18,19] The majority of compounds featuring a disubstituted cationic phosphorus centre, phosphenium or phospharylium cations PR_2^+ (e.g., **1.6**-**1.11**), are isolated with at least one *P*-substituent which is capable of lone-pair π-conjugation.[20-45] Alternatively, complexes containing a donor-stabilized phosphenium cation can be prepared using a donor group integrated into part of a pendant substituent (e.g., **1.12**),[46,47] or in the form of a ligand (e.g., **1.13**[48]). The Lewis acidity of reactive element centres can, in some cases, be exploited for the synthesis of new bonding environments (vide infra).

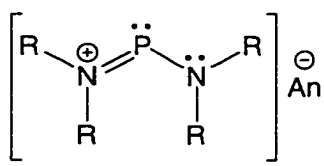

1.6

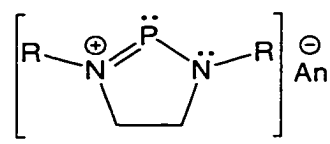

1.7

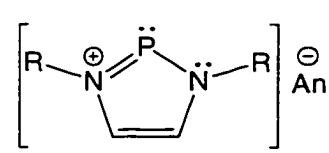

1.8

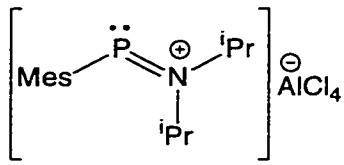

1.9

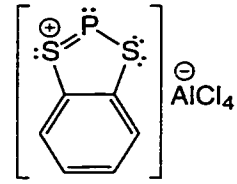

1.10

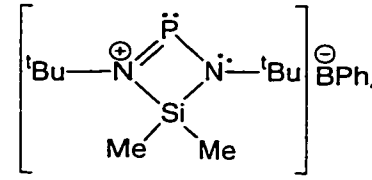

1.11

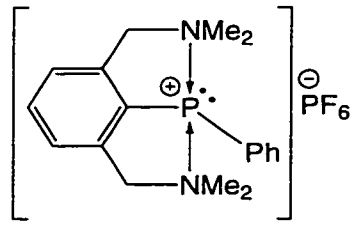

1.12

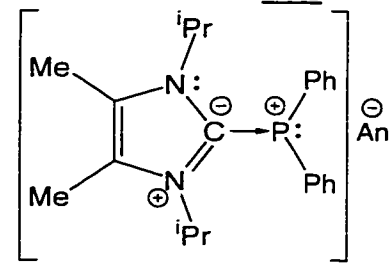

1.13

The nature of cation-anion interactions is an important issue in main-group and transition metal chemistry.[49-51] Of specific interest is how this interaction affects both spectroscopic and structural parameters in the cation and anion. When the distance between two separate assemblies is greater than the sum of van der Waals radii for the closest atomic centres involved, the two assemblies are considered non-bonded. However, their electron density can be polarized directionality towards each other.[52] An intermolecular interaction of this type is regarded as predominantly ionic. In many compounds featuring a cation-anion pairing with a predominantly ionic interaction, the exchange of different anions or cations has a minor or no effect on the bonding character on the corresponding partner ion. For example, the solution phosphorus chemical shifts of the diazaphospholenium cation **1.8** (R = ^{t}Bu) are similar regardless of the type of anion in the complex (e.g., An = $GaCl_4^-$ or PF_6^-).[32]

As the distance between the two entities decreases (i.e., becomes increasingly less than the sum of van der Waals radii[2] for the closest atomic centres involved), the covalent character of the interaction increases. There are no established threshold

[2] A discussion of the variations in van der Waals radii is provided on page 8.

distances for determining when the two entities are considered formally bonded. This problem is illustrated in Figure 1.2, which shows chlorine-phosphorus distances for various diaminochlorophosphines and complexes containing a diaminophosphenium cation. Hence, there is a region where compound classification is ambiguous. Therefore, it is more appropriate to consider the Cl–P interactions in these compounds as a part of a continuum, ranging from predominantly covalent to ionic. Thus, for these types of compounds with a chlorine-phosphorus distance less than the combined van der Waals

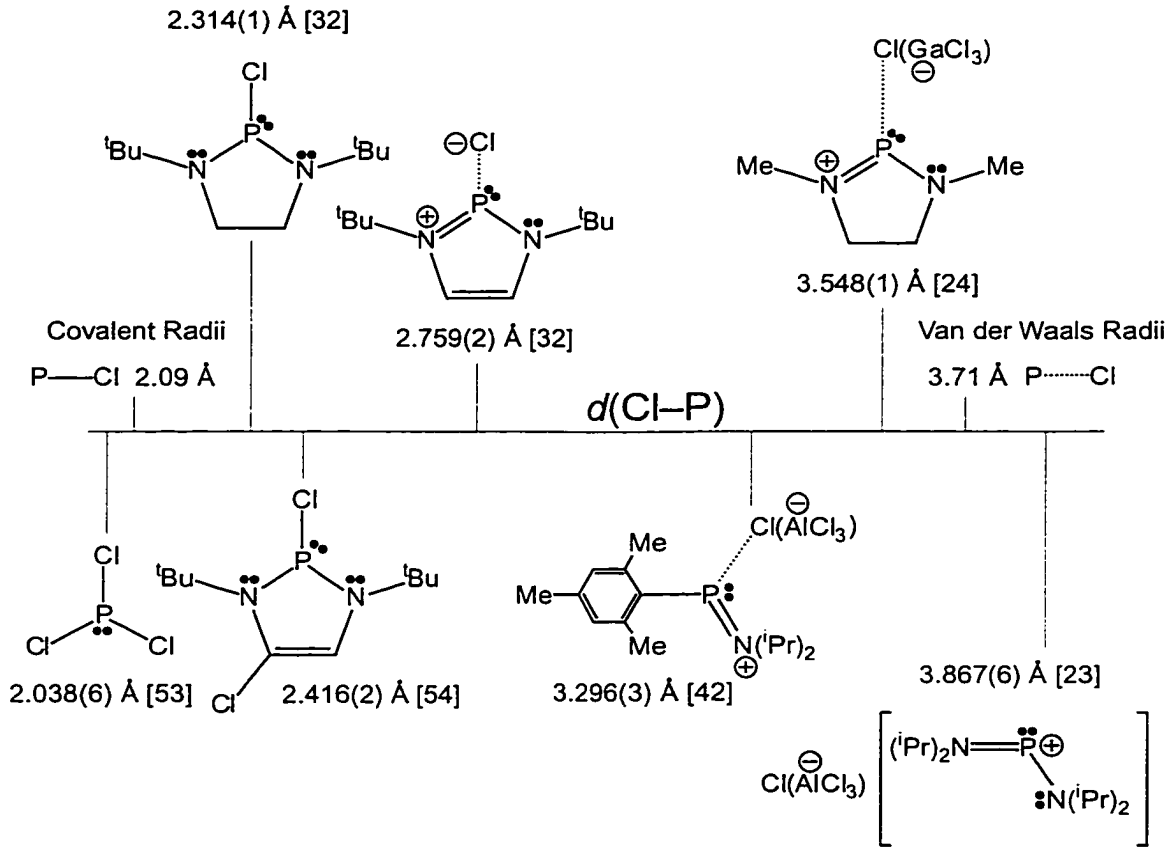

Figure 1.2: Comparison of distances between the phosphorus and chlorine centres in phosphines and phosphenium complexes. A dotted line drawn between a cation and anion represents an interaction, which is not considered a formal covalent bond (i.e. auto-ionization of the chlorine-phosphorus bond occurs in solution). References for the complexes are quoted inside square brackets.

radius of chlorine and phosphorus, 3.71 Å[82] (from $\Sigma\, r_w(Cl) + r_w(P)$), they can be considered as having some degree of both diaminochlorophosphine and diaminophosphenium bonding character.

The valence orbital radius for a particular atomic centre is dependent on its bonding environment, in particular, on the oxidation state of the element involved. The valence orbital radius of an atom increases with decreasing oxidation number. In an anionic bonding environment where the atomic centre has an excess of electrons, electron-electron repulsion is greater than total nuclear attraction, and hence the size of the atomic centre increases. Conversely, in a cationic bonding environment, nuclear charge is greater than total electron charge, the attractive nuclear-electron force is slightly greater than the electron-electron repulsion force, and the size of the atomic centre is contracted. For example, the valence orbital radius of phosphorus in an uncharged bonding environment is 1.90 Å,[55] whereas the ionic radius for phosphorus in an anionic phosphide bonding environment with an oxidation state of -3 is 2.12 Å.[56] In contrast, phosphorus in a cationic bonding environment with a formal charge of +3 and +5, has a radius of 0.44 Å and 0.38 Å, respectively.[56] The van der Waals radius of atoms which can exist as independent anions is roughly equivalent to their ionic radius,[57] for example, $r_w(Br) = 1.95$ Å, whereas $r_i(Br^-) = 1.96$ Å.[55] However, for an atomic centre in a cationic bonding environment, the van der Waals radius will be smaller than that in a neutral molecule. The following r_w values, based on an oxidation state of zero, are used in this thesis and were obtained from reference 55; C (1.85 Å), Cl (1.81 Å), N (1.54 Å), O (1.40 Å), P (1.90 Å), S (1.85 Å), and Se (2.00 Å). Hence, the use of these van der Waal radii provides only a crude estimate for considering when a cation and anion have a covalent interaction, as they are not corrected for different oxidation states.

Cations can be made more Lewis acidic by pairing them with weakly Lewis basic anions. For example, a phosphenium complex **1.11** was synthesized with tetraphenylborate BPh_4^-.[45] The crystal structure shows predominantly ionic interactions between the cation and anion.[45] The stabilization of highly Lewis acidic main-group and transition metal cations requires the use of a counter-ion with certain characteristics,[51] including minimal covalent interactions with the cation and stability with respect to oxidation or substituent abstraction. Ideal weakly coordinating anions have charge that is evenly distributed across their molecular framework. Moreover, they should contain substituents with no or little donor ability (i.e., fluorocarbon or hydrocarbon groups).[51]

For compounds containing a strongly Lewis acidic centre, the choice of reaction or crystallization solvent is crucial,[51] as was demonstrated by the σ-coordination of the triethylsilylium cation by toluene in complex **1.14**.[58-60]

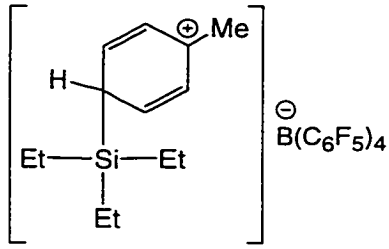

1.14

1.3: Brief Introduction to the Unusual Bonding Environments involving Phosphorus as the Central Element

Phosphorus and its heavier group 15 homologues can undergo valence expansion forming penta- and hexa-substituted compounds including pentafluorophosphorane PF_5, and hexafluorophosphate PF_6^-. In contrast, tetrasubstitution represents the maximum valency for nitrogen with the exception of interstitial compounds. Nevertheless, nitrogen in most oxidation states is capable of forming strong π-bonds with boron, oxygen, and

carbon, whereas the isolation of compounds with π-bonding for phosphorus in low oxidation states usually requires the use of the synthetic methodologies discussed in Section 1.2.

The representative structures of some common and unusual phosphorus bonding environments are shown in Figure 1.3. The phosphorus compounds described in this thesis are occasionally designated using a sigma-lambda notation[61,62] σ^x,λ^y, where x represents the number of substituents and y is the total bond order or classical valency[63] of the phosphorus centre.

Two distinct classifications of phosphorus compounds can be considered based on the bonding nature of the valence electrons. When all the valence electrons on phosphorus are involved in bonding, the compound is described as having a "phosphorano" bonding environment. This bonding environment is typically represented by phosphoranes PR_5, phosphoranides PR_6^-, or phosphorylic $P(=R)R_4$ compounds. A compound labeled as "phosphino" features one or more pairs of non-bonding valence electrons that reside on the phosphorus centre. Further distinctions are made based on the presence of a σ- or π-bonded phosphorus centre (vide infra).

Undoubtedly, the most commonly encountered phosphino-bonding environments are the trisubstituted σ-phosphines R_3P, and σ-phosphites $(RO)_3P$.[64] The combined stereochemical, σ-donor and π-acceptor properties of trisubstituted σ-phosphines are ideal characteristics for ligands and accordingly, tertiary phosphines play a fundamental role in the coordination chemistry of transition metals.[64-66]

Phosphino-bonding environments which feature a π-bonded phosphorus centre, hereafter referred to as "π-phosphino", are much less common than σ-phosphines, with the majority of species discovered only within the past twenty years.

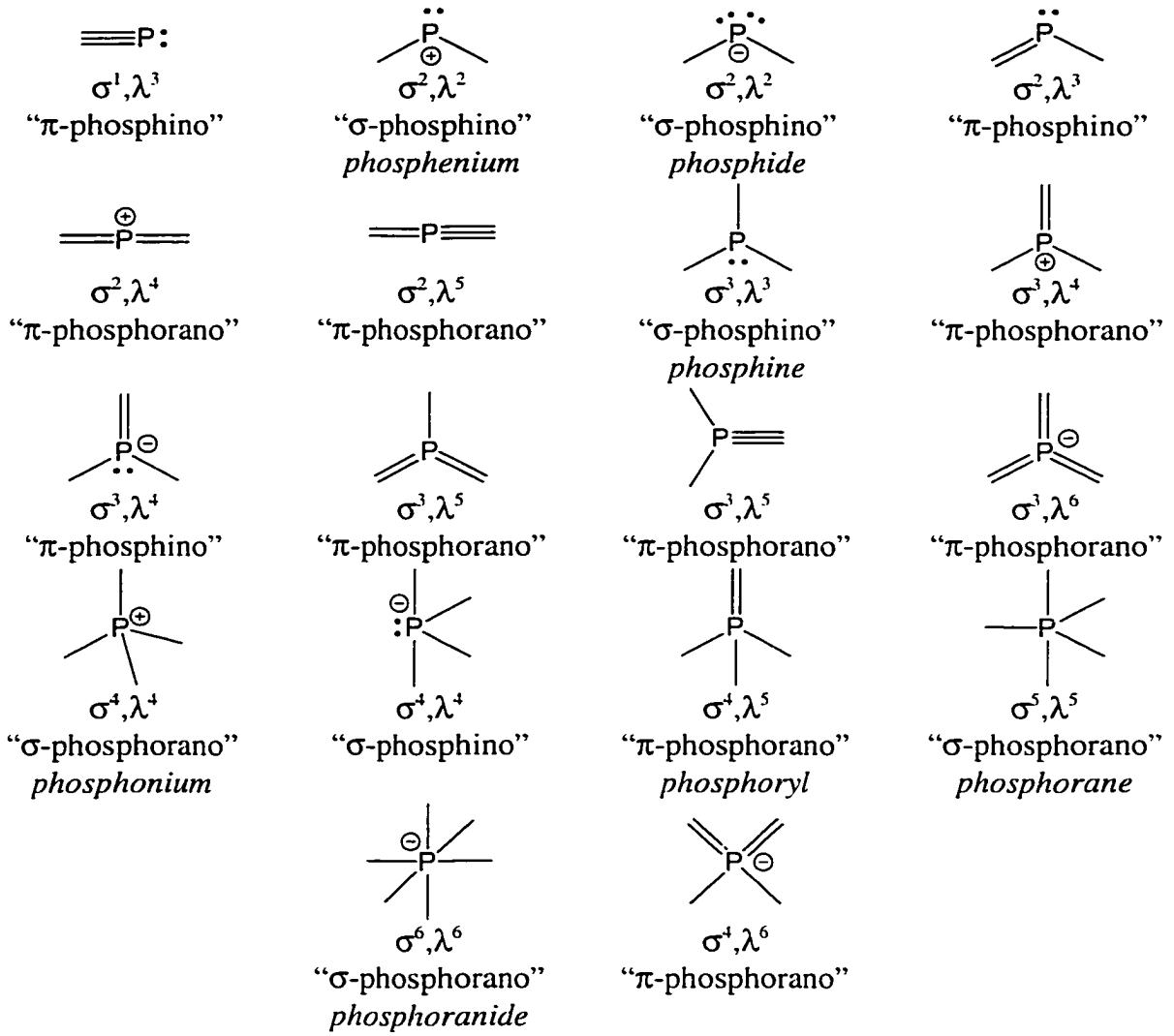

Figure 1.3: Structural representations of various bonding environments with phosphorus as the central element. Each representation is designated by sigma-lambda notation. The type of bonding environment is given inside quotes. Type in italics represents the common class name for that particular phosphorus bonding environment.

Isolation of π-phosphino-bonding environments usually requires special synthetic strategies as described in Section 1.2. Several classes of π-phosphino-bonding environments are known, and some examples are given in Figure 1.4. Of the

monosubstituted π-phosphino-compounds, the phosphaalkynes (alkylidynephosphines) have been the most studied in terms of synthesis, characterization, and chemical reactivity.[67-69]

Monosubstituted π-Phosphino-bonding Environments

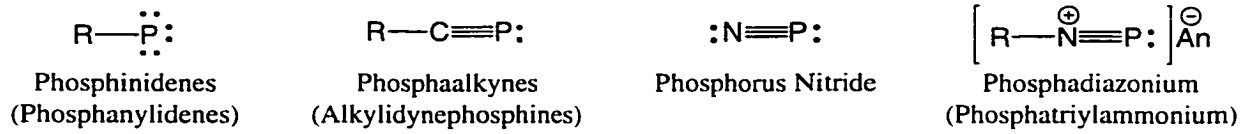

Disubstituted π-Phosphino-bonding Environments

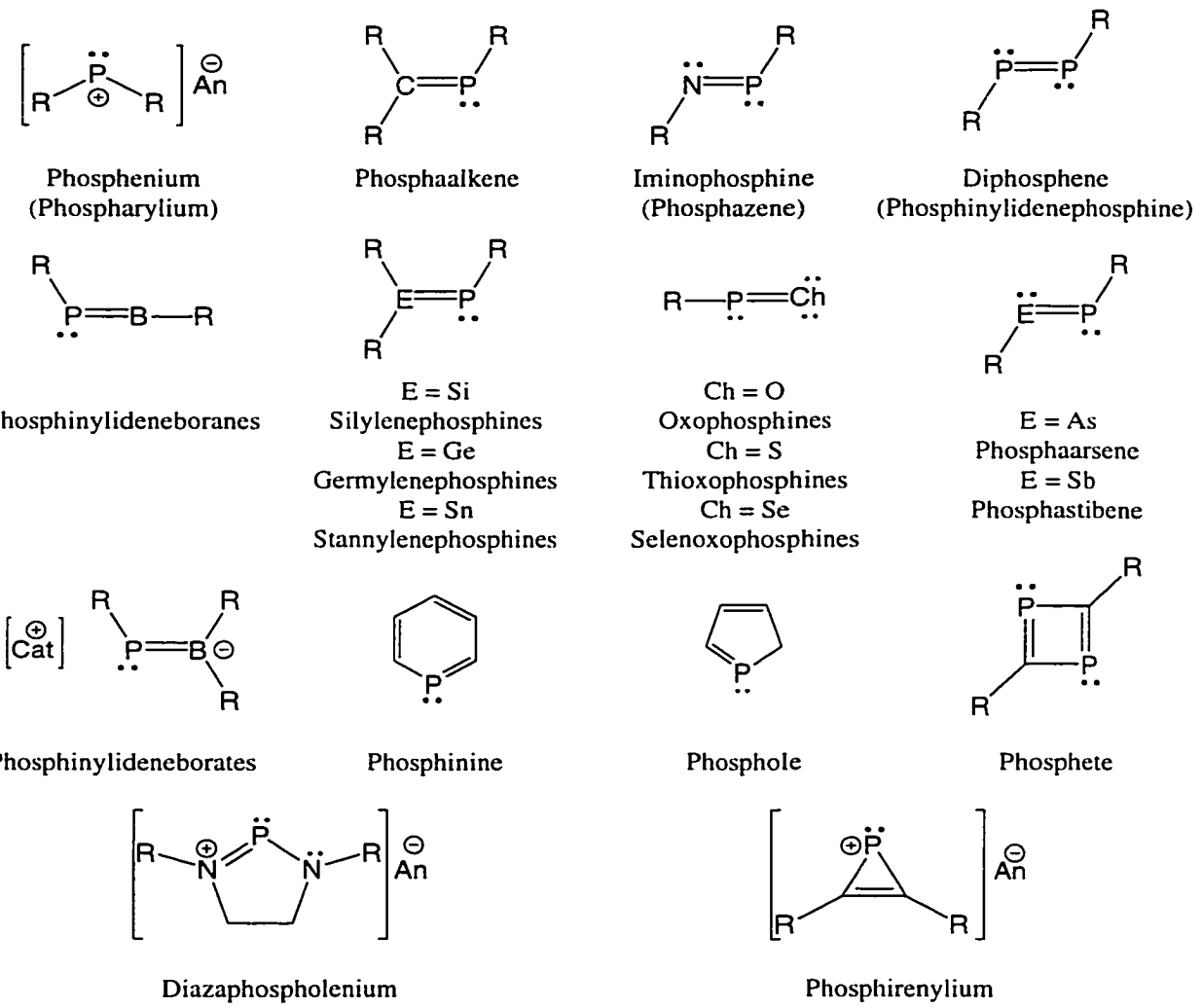

Figure 1.4: Some examples of common π-phosphino-bonding environments.

Iminophosphines (phosphazene or phosphinimines), phosphenium cations, diazaphospholenium cations,[30,41] phosphaalkenes (alkylidenephosphines),[70] and several forms of λ^3-phosphorus heterocycles, including phosphinines and phospholes,[71,72] are the most studied disubstituted π-phosphino-bonding environments. Examples of compounds with a trisubstituted π-phosphino- or phosphorano-centre are discussed in Section 3.3.

Interest in mono- and di-substituted π-phosphino-bonding environments has grown primarily because many of these types of compounds have demonstrated chemical reactivity, which mimics that of organic carbon and nitrogen compounds.[73-76] For example, phosphenium cations PR_2^+, have both σ-donor and π-acceptor capabilities.[20,41,77] Accordingly, these compounds, as ligands form, coordination complexes with transition metal centres.[20,41,77] In this respect, phosphenium cations have a reactivity that is analogous with isoelectronic carbon monoxide.[20,77] A partial listing of different π-phosphino-bonding environments with isoelectronic nitrogen and carbon compounds is provided in Figure 1.5.

The reactivity of π-phosphino-compounds, in general, can be classified as either that of a carbene or olefin (Figure 1.6). For example, phosphaalkenes **1.20**, and diphosphenes **1.22**, like alkenes undergo "Diels-Alder-like" [2+4] cycloaddition with 2,3-dimethyl-1,3-butadiene, forming phosphanocyclohexenes[70] **1.24** and 1,2-diphosphano-cyclohexenes[78,79] **1.25**, respectively. In contrast, phosphenium cations **1.6** and *P*-alkyl-iminophosphines **1.21**, generally, have carbenic-like reactivity and undergo [2+1] chelotropic cycloadditions with 2,3-dimethyl-1,3-butadiene, forming phospholenium cations[80-82] **1.26** and λ^5-iminophospholenes[83,84] **1.27**, respectively.

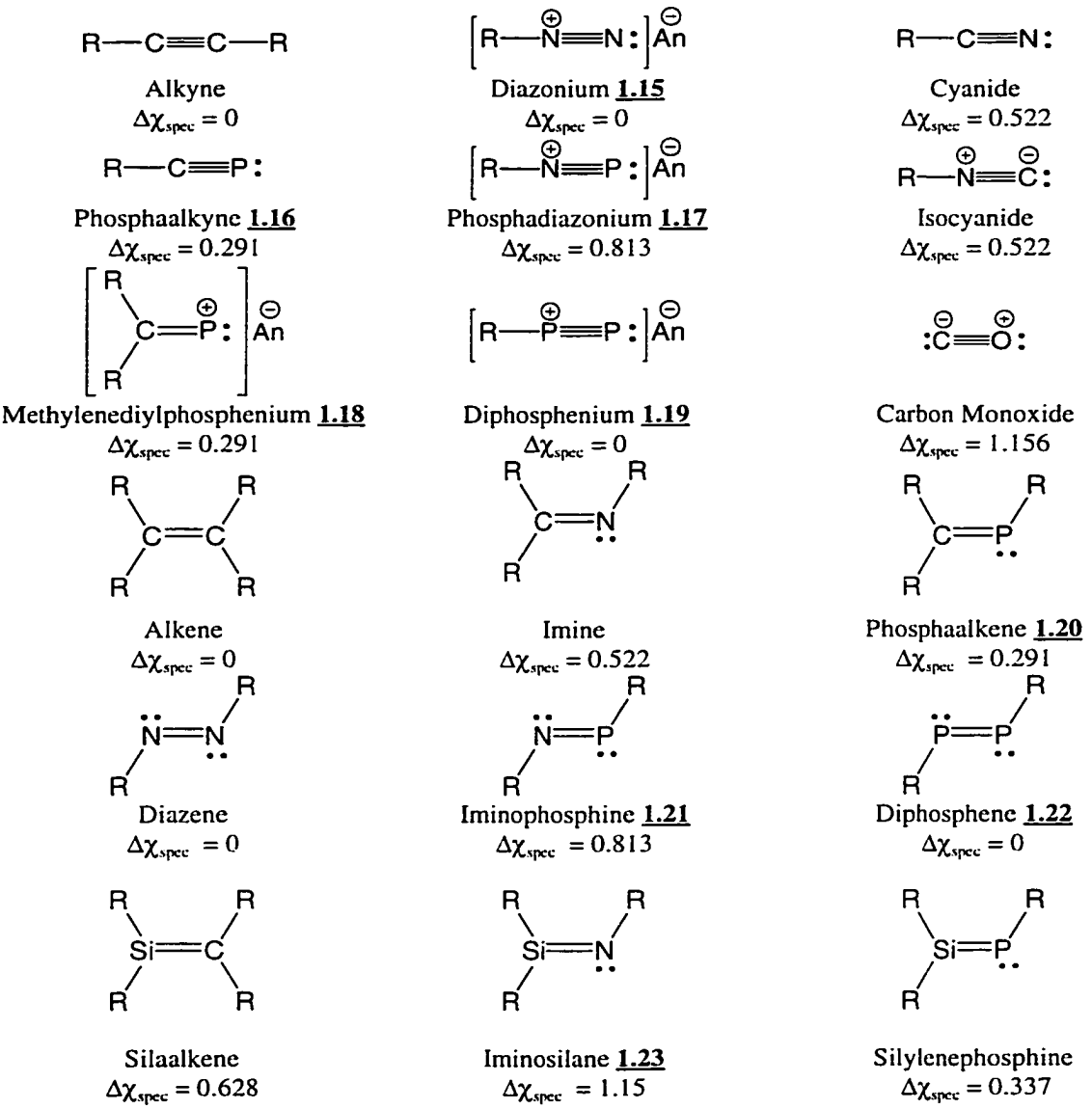

Figure 1.5: Comparison of mono- and di-substituted π-phosphino compounds **1.15**-**1.23** with isoelectronic carbon, silicon, and nitrogen species. The differences in electronegativity ($\Delta\chi_{spec}$) of atomic centres composing the π-bond are also provided. Values for χ_{spec} were obtained from reference 6.

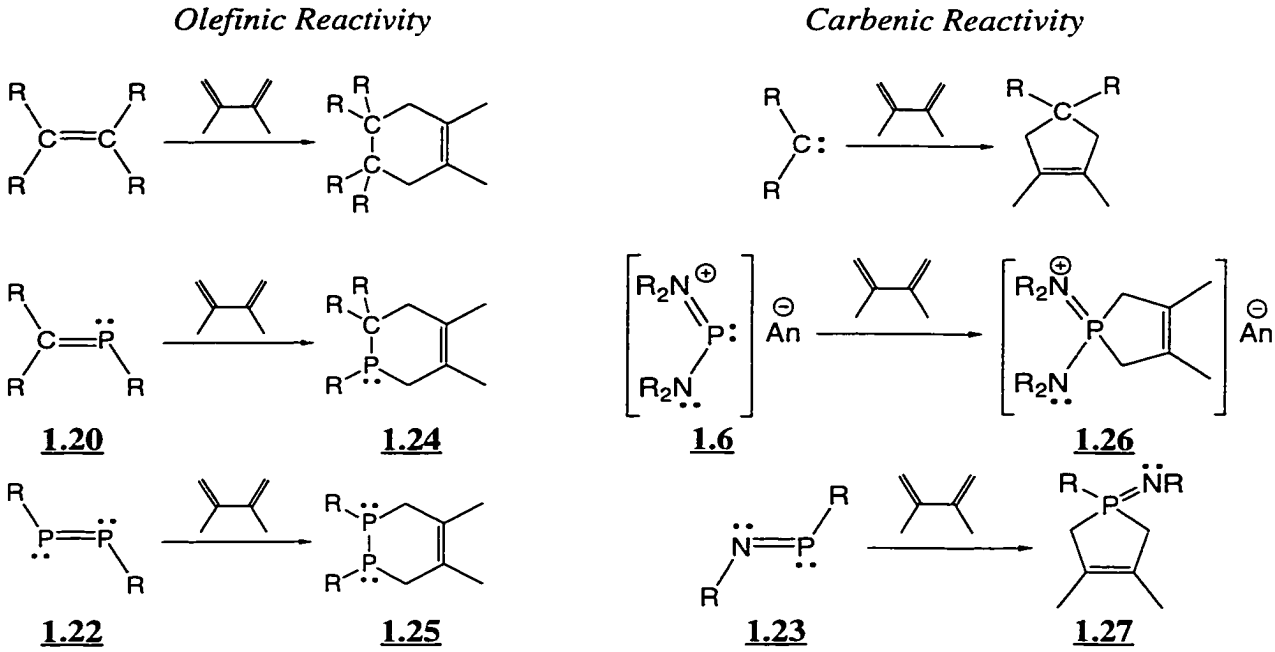

Figure 1.6: Comparative reactivity of alkenes, carbenes, and π-phosphino-compounds with 2,3-dimethyl-1,3-butadiene.

The type of reactivity for π-phosphino-compounds is determined by the bonding nature of the HOMO in these molecules.[85-87] Compounds with carbenic-like reactivity have a frontier orbital sequence with the HOMO as non-bonding.[86] Alternatively, compounds with a HOMO of π-bonding character have reactivity analogous to alkenes.[3,86] From uv-vis and uv-PE spectroscopy, it is suggested that iminophosphines **1.21**, with an alkyl *P*-substituent, possess a HOMO of non-bonding character. In contrast, phosphaalkenes **1.20**, have a HOMO which is π-bonding, the frontier orbital sequence for both types of compounds are shown in Figure 1.7.[88]

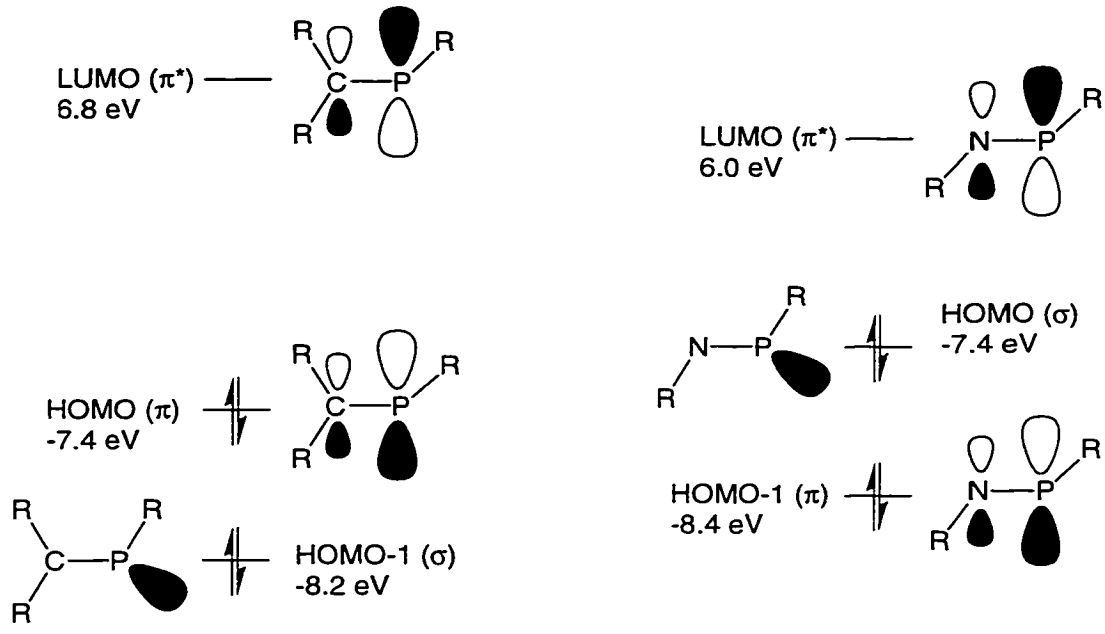

Figure 1.7: A comparison of the relative energy levels (not to scale) for the frontier orbital sequence in a phosphaalkene **1.20** (left) and an iminophosphine **1.21** (right). The values shown are from calculations using ab initio methods (HF/STO-3G level of theory).[86] The relative differences between MOs are consistent with experimental observations.[88]

Many disubstituted π-phosphino-compounds, analogous with trisubstituted σ-phosphines, have Lewis basic properties and are capable of coordinating to a transition metal or Lewis acidic main-group centre.[69,89] The mode of coordination (η^1 (σ) or η^2 (π)) is dependent on the electronic properties of the metal centre and, in particular, the nature of the HOMO in the π-phosphino-compound. The η^1 coordination mode is generally observed when the HOMO of the π-phosphino-compound is non-bonding, such as an iminophosphine (e.g., **1.28**),[90] whereas the η^2 mode is typical for coordinating π-phosphino-compounds with a π-type HOMO, such as a phosphaalkyne (e.g., **1.29**[69]).

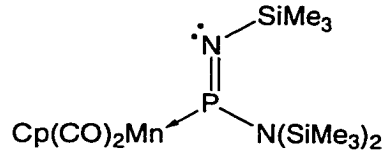

1.28

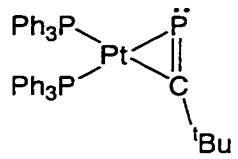

1.29

All π-phosphino-bonding environments contain an unoccupied LUMO of π*-character and in principle these compounds can behave as Lewis acids. The Lewis acidic behaviour of iminophosphines **1.21**, is a primary focus of the research presented in this thesis. π-Phosphino-compounds with strong Lewis acidity are either cationic or possess a phosphorus-element π-bond that is highly polarized (i.e., a large $\Delta\chi$), or both. Thus, only a few π-phosphino-compounds are known to behave as Lewis acids. These compounds include iminophosphines **1.21**,[91] methylenediylphosphenium **1.18**,[92] phosphadiazonium **1.17**,[93,94] diphosphenium **1.19**,[95] phosphenium cations **1.6**,[43,48,96-98] and their related cyclic anagloues, diazaphospholenium cations **1.8**.[20,34,40] Iminosilanes **1.23** are strong Lewis acids,[99] which is due to the large electronegativity difference between silicon and nitrogen ($\Delta\chi_{spec}$ = 1.15[6]). The π-P–N bond in iminophosphines **1.21** is also polarized ($\Delta\chi_{spec}$ = 0.81)[6] as indicated by large dipole moments measured in solution (e.g., μ(P–N) = 2.70 D[100] in Mes*NPN(SiMe$_3$)$_2$). The comparable electronegativity of phosphorus and carbon ($\Delta\chi_{spec}$ = 0.29) results in weakly polarized P–C π-bonds (e.g., μ(P–C) in phosphaalkynes **1.16** R = ^{t}Bu is 1.24 D,[101] and 1.58 D[101] with R = Ad). Consequently, no complexes are currently known with a phosphaalkyne **1.16** or phosphaalkene **1.20** as the Lewis acidic component.

1.4: The π-Imino-phosphino-bonding Environment: Iminophosphines and Phosphadiazonium Cations

A plethora of iminophosphines **1.23** has been isolated and spectroscopically characterized.[74,90,102-105] The majority of known iminophosphines are synthesized using the sterically demanding Mes* substituent attached to the nitrogen (imino) centre for protection against cyclodimerization. Other types of imino-substituents include Mes,[106] FMes,[107] ^{t}Bu,[108] $SiMe_3$,[13,106] and $OSi(Me)_2{}^t$Bu.[109] However, the Mes* *N*-substituted iminophosphines are solids at room temperature and many have been characterized through crystallography (Figure 1.8). Most synthetic studies on iminophosphines have focused on the attachment of various kinds of substituents to the phosphorus centre. Iminophosphines are also found as functional groups, for example, a 1,3,2,4-diazadiphosphetidine **1.30** was prepared featuring two Mes*NP units attached to the nitrogen centres of the four-membered ring.[110] 1,3,5-Triaza-2,4-diphospha-1,4-pentadienes **1.31** (R' = Mes*; R = ^{t}Bu, Ad, Mes, Tipp, Mes*; R' = CPh_3, R = Mes*) are composed of two Mes*NP units bridged through a common amino-substituent.[111,112]

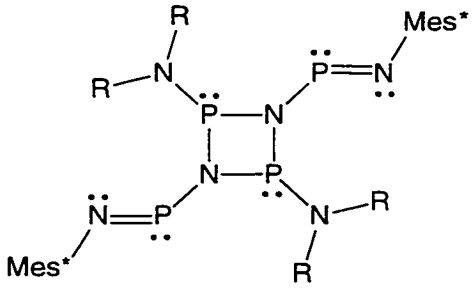

1.30

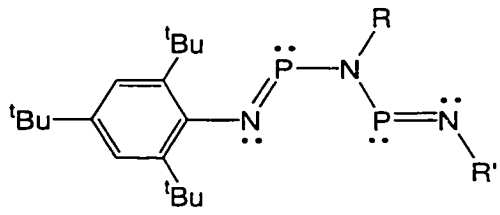

1.31

Iminophosphines

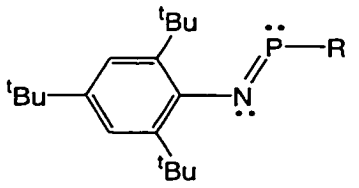

R = Me, Et, **C(Ph)$_3$**, **C(Et)$_3$** ^{t}Bu, ^{i}Pr, CH(SiMe$_3$)$_2$, **C(SiMe$_3$)$_3$**, Ph, Mes, Tipp, Mes*, **S^{t}Bu**, Se^{t}Bu, **P(^{t}Bu)$_2$**, As(^{t}Bu)$_2$, Styryl, **Fe(CO)$_2$Cp**, (-)**MentO**, **OSiMe$_3$**, **O^{t}Bu**, O^{i}Pr, AdO, OCH$_2$(^{t}Bu), **OCH(^{t}Bu)$_2$**, **OC(^{t}Bu)$_3$**, **OC$_6$H$_4$-Me-2**, OMes, OPh, **OC$_6$H$_2$(^{t}Bu)$_2$-2,6-Me-4**, **OSO$_2$C$_6$H$_4$Me-4**, **OSO$_2$CF$_3$**, **OC(O)CF$_3$**, **CH(CF$_3$)$_2$**, **Cp***, F, Cl, Br, I, **S$_2$P(^{t}Bu)$_2$**, **Se$_2$P(^{t}Bu)$_2$**

R = 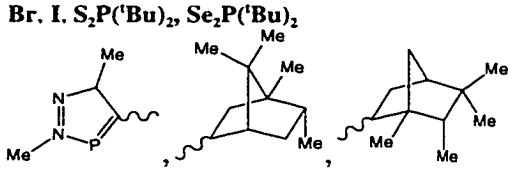

Amino-iminophosphines

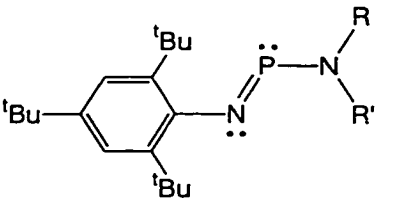

R = R' (**Me**, Et, **SiMe$_3$**, **^{i}Pr**, ^{t}Bu, **TMP**, Pip)
R = H (R' = **^{t}Bu**, Ad, **CPh$_3$**, Mes, Tipp, **Mes***)
R = Mes* (R' = **P(Me)Si(SiMe$_3$)$_3$**, **P(NCPh$_2$)$_2$**)
R = SiMe$_3$ (R' = **N(SiMe$_3$)$_2$**)
R = Mes* (R' = P(Styryl)Et, R' = P(Cl)Et)

π–Conjugated Iminophosphines

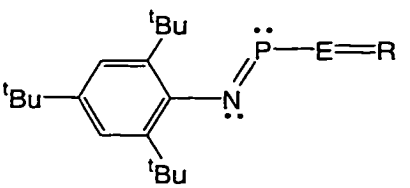

E = N (R = C(NMe$_2$)$_2$, **C(^{t}Bu)$_2$**, **Fln**, **PPh$_3$**, P(^{t}Bu)$_2$Ph, P(NMe$_2$)$_3$, **PH(N^{i}Pr$_2$)$_2$**)
E = P (R = C(NMe$_2$)$_2$, C(NMe$_2$)NEt$_2$)

Figure 1.8: A listing of known *N*-Mes*, *P*-substituted iminophosphines. Words in bold type represent compounds whose structure has been determined by crystallography.

Comparisons of iminophosphine RNPR', crystal structures have shown that the electronic and steric properties of the *N*- and *P*-substituents considerably influence the structural parameters of the central PN unit. This includes the P–N, P–R' bond lengths, the R-N-P bond angle, and to a lesser extent, the R–N bond length and the N-P-R bond angle. The electronic effect imparted by different types of substituents was modeled

from ab initio calculations using the CEPA-1 level of theory with a Huzinaga basis set. The calculations revealed that the greatest changes occurred when the *P*- and *N*-substituents operate in tandem.[3,113,114] For example, an iminophosphine with both a σ-donating *P*-substituent and an σ-accepting *N*-substituent has a long π-P–N bond, (*d*(P–N) = 1.578 Å $FNPSiH_3$; 1.572 Å FNPH).[113] In contrast, an σ-accepting *P*-substituent combined with a σ-donating *N*-substituent results in an iminophosphine with a shortened P–N bond (*d*(P–N) = 1.490 Å H_3SiNPF; 1.515 Å HNPF).[113]

If the *P*-substituent is removed entirely from the iminophosphine, the resulting species is referred to as a phosphadiazonium cation **1.17**, also referred to as a phosphoazonium or phosphanetriylammonium cation. Calculations suggest that these molecules have a very short P–N bond (*d*(P–N) = 1.43 Å in HNP^+ c.f., 1.548 Å in HNPH)[113] with a R-N-P unit that is collinear (i.e., a R-N-P bond angle of 180°).[113] Ab initio calculations show that if the *N*-substituent were to be removed, the resulting compound NPR^+ would be highly unstable and revert through substituent bridging to a phosphadiazonium cation.[115,116]

The structural modifications within an iminophosphine that are due to electronic properties of the *P*- and *N*-substituents, are termed "σ-push-pull substitution". This effect has been experimentally observed in iminophosphines, but also for asymmetric diphosphenes RPPR'.[3,113,114]

In general, the phosphorus and nitrogen centres as well as the connecting atoms of the *P*-, and *N*-substituents in iminophosphines are co-planar. Hence, the configuration of the *P*-, *N*-substituents is either *cis* (i.e., the R-N-P-R torsion angle is close or equal to 0°) or *trans* (i.e., the R-N-P-R torsion angle is close or equal to 180°). However, there are a few exceptions, which are discussed in Chapter 6. *Cis*- and *trans*-isomers of

iminophosphines have different spectroscopic properties and from NMR spectroscopy, it is possible to assign stereochemistry without the aid of crystallography.[117-119]

It has been postulated that the conversion between *cis*- and *trans*-isomers of iminophosphines involves an in-plane rotation of the *N*-substituent. A low activation barrier for stereochemical interconversion has been put forth as a reason why *cis*- and *trans*-isomers pairs are not observed together in solution or isolated separately in the solid state.[102,119] In contrast, *cis*- and *trans*-isomers pairs of diazaphosphetidene $(RNPR)_2$[120,121] and optically active (+) and (-) tertiary phosphines[122] are observed in solution NMR spectra. Nevertheless, it has been recently reported that a rapid equilibrium between *cis*- and *trans*-isomers occurs for amino-iminophosphines Mes^*NPNR_2 (R = Me and Et), in solution.[119] Ab initio calculations, at CEPA-1 level of theory with a Huzinaga basis set, suggest that an iminophosphine with an electron-withdrawing *P*-substituent (e.g., HNPF) has a lower activation energy barrier for stereochemical conversion (30.5 kJ mol^{-1} c.f., 58.5 kJ mol^{-1} for HNPH),[113] a larger H-N-P bond angle (128.4° c.f., 112.3° in HNPH),[113] and a shorter P–N bond (d(P–N) = 1.503 Å, HNPF; 1.548 Å, HNPH).[113] Furthermore, for these types of iminophosphines, the *cis*-isomer is thermodynamically favoured over the *trans*-isomer.[113] This is in accordance with crystal structure observations of only *cis*-isomers for *P*-halogeno-iminophosphines Mes^*NPX (X = Cl and Br).[123,124]

Structurally, the *P*-halogeno-iminophosphines Mes^*NPX (X = Cl, Br and I), have phosphorus-halogen bonds (d(P–X) = 2.127(1) Å,[124] Cl; 2.337(2) Å, Br[124]; 2.895(1) Å, I[102]) which are significantly longer than those in trisubstituted halogeno-phosphines PX_3, (d(P–X) = 2.038(6) Å, Cl;[53] 2.216(4) Å, Br;[125] 2.463(5) Å, I[126]), and *P*-halogeno-phosphaalkenes $(Me_3Si)_2CPX$, (d(P–X) = 2.094(1) Å, Cl;[127] 2.262(1) Å, Br;[127] 2.502(1) Å, I[128]). It is postulated that the longer P–X bonds in *P*-halogeno-iminophosphines

Mes*NPX, are due to interactions between the non-bonding valence electrons on the imino nitrogen centre and the σ* MO of the P–X bond. This type of interaction is referred to as negative hyperconjugation.[124] A similar effect is also proposed to account for the longer than typical P–O bonds in *P*-aryloxy-iminophosphines (*d*(P–O) = 1.658(1) Å Mes*NPOC$_6$H$_2$(^{t}Bu)$_2$-2,6,Me-4 c.f., *d*(P–O) = 1.573[11] Å[131] in (R$_2$N)$_2$P–O).[129]

The crystal structure of the triflate *P*-substituted iminophosphine Mes*NPOTf, shows that the P–O(Tf) interaction is significantly longer (*d*(P–O) = 1.923(3) Å)[130] than that of a typical phosphorus-oxygen single bond (e.g., *d*(P–O) = 1.573[11] Å,[131] (R$_2$N)$_2$P–O). Furthermore, Mes*NPOTf has, at present, the smallest P-N bond length (*d*(P–N) = 1.467(4) Å)[130] observed for any iminophosphine or complex containing a cationic phosphadiazonium unit.[130] The triflate group O_3SCF_3, is highly electron withdrawing, and consequently, a very weak base (H_o of HOTf = -14.1[132] c.f., H_o of 100 % H_2SO_4 = -12). In a covalent bonding situation, the triflate group is readily displaced by a stronger nucleophile, including many anionic and neutral Lewis bases.[133,134] The triflate anion, in the presence of a strong Lewis base, is more stable with regards to abstraction than many other types of common anions (viz., $AlCl_4^-$, $GaCl_4^-$, BPh_4^- and PF_6^-).[132,133] Hence, Mes*NPOTf is a suitable candidate for studies on the coordination chemistry of a π-phosphino-bonding environment as a Lewis acid.

Other types of iminophosphines with an electron-withdrawing *P*-substituent include the Cp*-iminophosphines, where the *P*-substituent has structural and spectroscopic features that suggest pentamethylcyclopentadienyl-like bonding character, Cp^{*-}. The crystal structures of Mes*NPCp* and $Et_3SiNPCp^*$, show either η^1 or η^2 coordination by the Cp* substituent to the phosphorus centre.[135] The phosphorus-carbon bond lengths (*d*(P–C) = 1.94(1) Å and 2.168(4), 2.122(4) Å, respectively),[135] are

significantly longer than those observed in *P*-alkyl-iminophosphines, (e.g., *d*(P–C) = 1.566(2) Å,[136] Mes*NPCEt$_3$). Solid-state $^{13}C\{^1H\}$MAS, and solution ^{13}C spectra of Mes*NPCp* and $Et_3SiNPCp^*$ contain a single averaged $\delta(^{13}C)$ resonance associated with the Cp* group and it is postulated that the substituent is undergoing continuous [1,5]-sigmatropic rearrangements.[135,137] Furthermore, the Cp*-iminophosphines can undergo nucleophilic substitution or migration reactions where the Cp* substituent is replaced by a stronger nucleophile or is transferred to a transition metal centre.[35]

The phosphadiazonium-dichalcogenophosphinate complexes [Mes*NP]$Ch_2P(^tBu)_2$, (Ch = S or Se) exhibit close pairing cation-anion in the solid state, but not in solution.[137,138] Specific structural and spectroscopic features of the these complexes are described in Chapters 5 and 6.

In some cases, the structural parameters of the Mes*NP unit in iminophosphines with an electron-withdrawing *P*-substituent are similar to those in complexes containing a cationic phosphadiazonium unit RNP^+, see Chapter 6. Consequently, these types of iminophosphines have a bonding character which is in between the ionic bonding extreme represented by a phosphadiazonium cation **1.17**, and the covalent bonding extreme as represented by an iminophosphine **1.21**, with an alkyl or aryl group as the *P*-substituent (Figure 1.9).[77,130]

For *P*-halogeno-iminophosphines, the large $\Delta\chi_{spec}$ of the phosphorus-halogen bond results in an iminophosphine with substantial positive charge at phosphorus, as suggested from ab initio calculations.[124] Hence, the *P*-halogeno-iminophosphines, such as Mes*NPCl, are stronger Lewis acids than iminophosphines with an aryl, alkyl or amino group as the *P*-substituent.

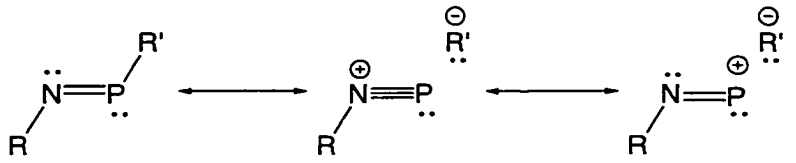

Figure 1.9: The overall bonding character of iminophosphines with an electron-withdrawing *P*-substituent R' as represented by resonance contributions from an iminophosphine (left) and a phosphadiazonium-anion complex (middle and right).

A number of methods have been devised for synthesizing iminophosphines.[90,102,103] The most common procedures involve organic base or thermal assisted elimination of hydrochloride or chlorotrimethylsilane from a *P*-halogeno-aminophosphine R(R')NPCl(R''), (R' = H or $SiMe_3$), (Figure 1.10). The *P*-chloro-iminophosphine Mes*NPCl, is a particularly useful synthon and, through metathesis reactions, provides access to a variety of *P*-substituted iminophosphines[25,130,139-144] and other types of π-phosphino-bonding environments.[111,112,136,145-151] The synthesis of Mes*NPCl is performed as a single pot reaction by combining $Mes*NH_2$ with excess quantities of Et_3N and PCl_3.[123,152] Alternatively, Mes*NPCl can be isolated through thermal assisted elimination of Me_3SiCl from $Mes*(SiMe_3)NPCl_2$[153] or the addition of base to dichloroaminophosphine $Mes*N(H)PCl_2$, which is obtained by the reaction of [Li]N(H)Mes* with PCl_3. The triflate *P*-substituted iminophosphine Mes*NPOTf, the precursor for the majority of new compounds reported in thesis, is synthesized by a metathesis reaction between Mes*NPCl and silver triflate [Ag]OTf (Figure 1.11).[130]

The reactivity of iminophosphines has been a subject of some interest and a number of new phosphorus bonding environments have been synthesized using iminophosphines as precursors.[102,105] Iminophosphines are important building blocks for phosphorus-nitrogen heterocycles.[74,75,90,102,154] However, for the purposes of this thesis, only the reactivity of iminophosphines with Lewis acids and Lewis bases is summarized.

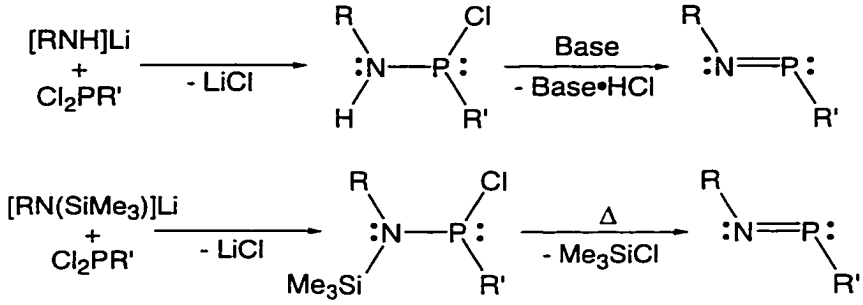

Figure 1.10: Common synthetic routes for the preparation of iminophosphines, including Mes*NPCl.

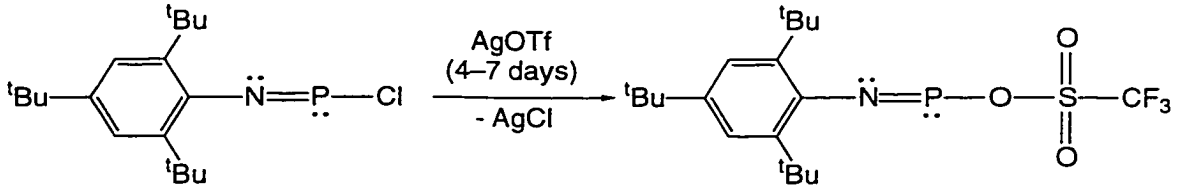

Figure 1.11: The synthetic route for the preparation of the triflate *P*-substituted iminophosphine Mes*NPOTf.

Lewis acids will react with iminophosphines, specifically at the imino-centre if the *P*-substituent is an electron-donor (e.g., an alkyl, amino or aryl group). Strong acids such as triflic acid ($HOSO_2CF_3$, $H_o = -14.1$)[132] readily protonate *P*-alkyl-iminophosphines or amino-iminophosphines, resulting in the formation of aminophosphenium cations **1.6** (R = Mes*/H, An = OTf^-).[33,35,93]

The addition of a group 13 chloride ($AlCl_3$ or $GaCl_3$) to the tris-trimethylsilylamino-iminophosphine $Me_3SiNPN(SiMe_3)_2$, results in a Lewis acid-base complex **1.32** (E = Al or Ga) featuring an Al–N or Ga–N coordinate bond (Figure 1.12).[155,156] When complex **1.32** (E = Al or Ga) is heated, chlorotrimethylsilane is eliminated resulting in the formation of a cyclic dichloroaluminum or a dichlorogallium bridged amino-iminophosphine **1.33** (E = Al or Ga), (Figure 1.12).[155,156] This zwitterionic

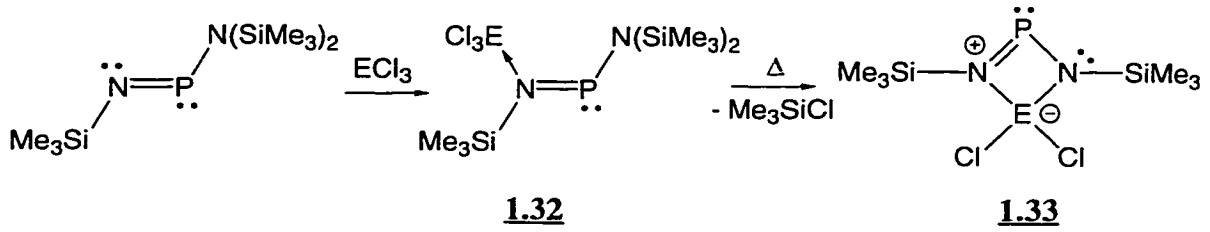

1.32 **1.33**

Figure 1.12: Synthesis of a bridged zwitterionic amino-iminophosphine **1.33** (E = Al or Ga) by the addition of a Lewis acid ($AlCl_3$ or $GaCl_3$) to the amino-iminophosphine $Me_3SiNPN(SiMe_3)_2$.

iminophosphine **1.33** (E = Ga) has been shown to exhibit Lewis acidic properties, forming complexes with amines and cyclic ethers.

The addition of $AlCl_3$ to an iminophosphine with an electron-withdrawing *P*-substituent, Mes*NPCl or Mes*NPOAr (Ar = $C_6H_2(^tBu)_2$-2,6,Me-4), results in the abstraction of a chloride Cl^- or arylolate group ArO^-, and yielding complex **1.34**, which features a phosphadiazonium cation (Figure 1.13).[33,123] Abstraction of Mes*NPCl can also be accomplished using $GaCl_3$.[93,94] The synthesis of complexes containing a phosphadiazonium cation $Mes*NP^+$, has only been successful using group 13 halides. Attempts at abstraction using $[Na]BPh_4$ or $[Ph_3C]BF_4$ has led to the formation of either a *P*-phenyl-iminophosphine Mes*NPPh, or an alkyl-difluoro-iminophosphorane $Mes*NPF_2CPh_3$.[93,150]

Few reactivity studies between iminophosphines and Lewis bases have been reported. Calculations suggest that Lewis bases will preferentially react with iminophosphines at the phosphorus centre.[85] Hydride transfer reagents such as lithium aluminum hydride are hypothesized to add first to the phosphorus centre of an amino-iminophosphine, forming the *P*-hydro-phosphinoamide salt **1.35**, (Figure 1.14) which is then hydrolyzed to form the bisaminophosphine **1.36**, (Figure 1.14) as demonstrated through deuterium labeling experiments.[157,158]

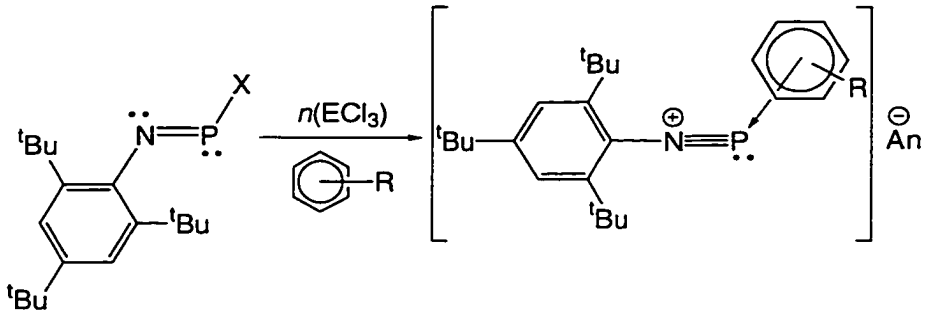

1.34

X = Cl (*n* = 1, E = Al, An = $AlCl_4^-$, arene = C_6H_5Me) [123]
X = $OC_6H_2(^tBu)_2$-2,6-Me-4 (*n* = 1, E = Al, An = $AlCl_4^-$, arene = C_6H_5Me) [33]
X = Cl (*n* = 1, E = Ga, An = $GaCl_4^-$, arene = C_6H_6, C_6H_5Me) [93,94]
X = Cl (*n* = 2, E = Ga, An = $Ga_2Cl_7^-$, arene = C_6H_6, C_6H_5Me, $C_6H_3(Me)_3$-1,3,5) [93,94]

Figure 1.13: Generalized synthesis of a η^6 arene-phosphadiazonium complex through chloride or arylolate abstraction from a *P*-halogeno- or *P*-aryloxy-iminophosphine using a group 13 Lewis acid. References are quoted inside square brackets.

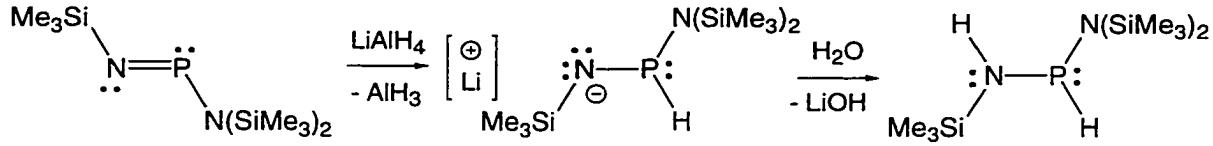

1.35 **1.36**

Figure 1.14: The reactivity of the amino-iminophosphine $Me_3SiNP(SiMe_3)_2$, with lithium aluminum hydride. The intermediate, a *P*-hydro-phosphinoamide salt **1.35**, is hydrolyzed forming a trisubstituted σ-bisaminophosphine **1.36**.

Phosphadiazonium cations RNP^+, are isoelectronic analogues of diazonium cations **1.15**, diphosphadiazonium cations **1.19**, and phosphaalkynes **1.16**. They are structurally characterized by a collinear (Mes*)C-N-P fragment and a short P–N bond (d(P–N) < 1.5 Å).[123] Phosphadiazonium cations with a less bulkier substituent (e.g., $MeNP^+$, $EtNP^+$) are observed as fragmentation products in the APCI mass spectra of diazaphospholenium salts **1.7** (R = Me, An = $GaCl_4^-$).[159] Ab initio calculations suggest that the electronic structure of a phosphadiazonium cation is similar to that of a

diazonium cation **1.15**, in that the highest accumulation of positive charge is situated at the terminal atom (Figure 1.15), but that the P–N bond is significantly more polarized than the N–N bond in RNN^+.[115,116] In addition, the calculations propose that the cleavage of a PN fragment from the substituent is not energetically favourable,[115] whereas the loss of N_2 from the substituent is a predominant reaction pathway in diazonium chemistry.[160] A theoretical study of the model *N*-phenyl-phosphadiazonium cation $PhNP^+$, shows that the HOMO is comprised of two degenerate π-bonding orbitals and the LUMO is a set of two degenerate π*-bonding orbitals.[76,161] The HOMO-1 is a σ-type molecular orbital, which contains the non-bonding valence electrons for phosphorus. This bonding model suggests that the chemical reactivity of the phosphadiazonium cation should be analogous to that of alkenes and phosphaalkynes.

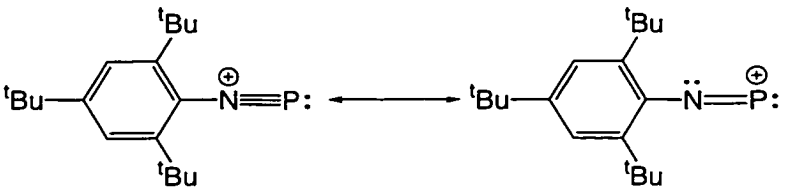

Figure 1.15: The overall bonding character of a phosphadiazonium cation as represented by resonance structures.

A summary of the reactions involving the phosphadiazonium complex **1.34** (An = $AlCl_4^-$) is shown in Figure 1.16. Analogous with iminophosphines, phosphadiazonium cations are useful in the synthesis of phosphorus-nitrogen heterocycles. Examples include the heterocyclic phosphenium salt[145] **1.37** (R = ^{i}Pr or $SiMe_3$), tetraazaphospholylium salts[145] **1.38** (R = ^{t}Bu or Et_3C) and the phosphaquinolinum salt[162] **1.39**.

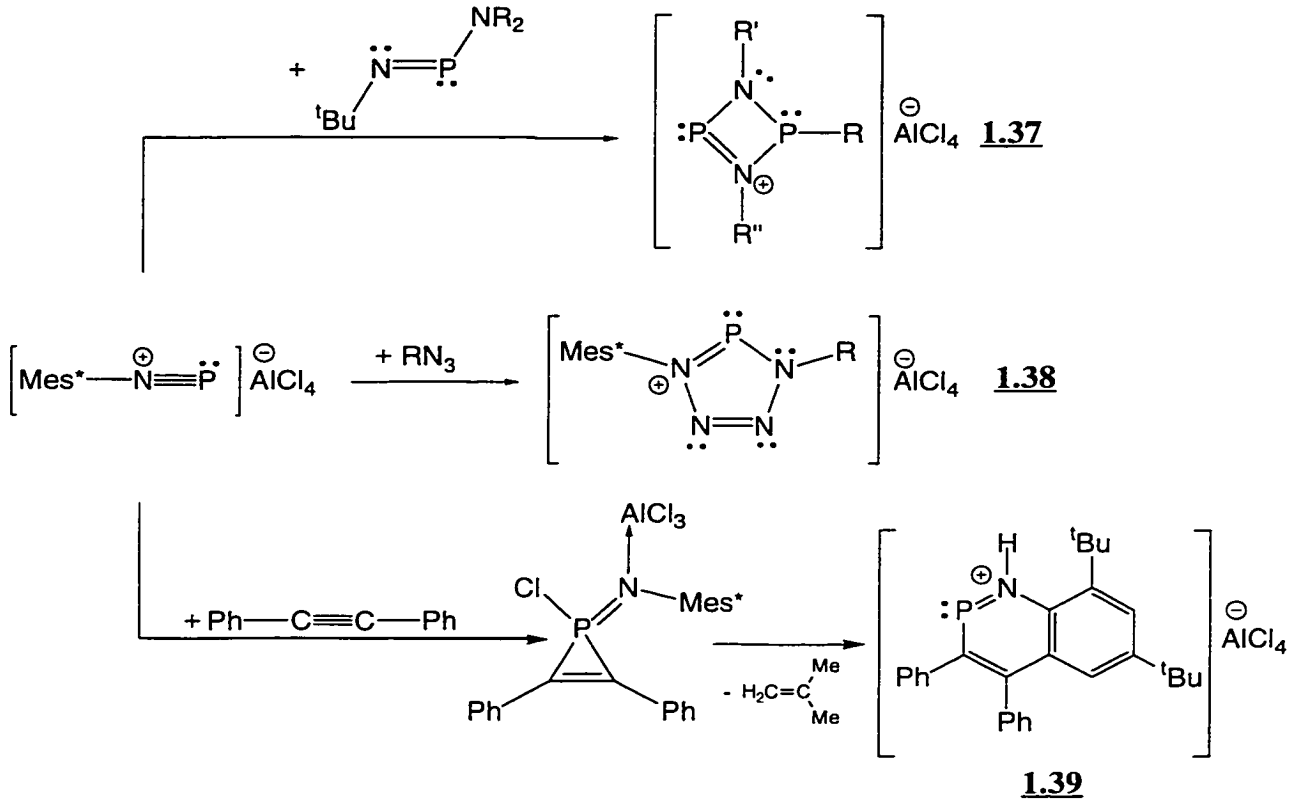

Figure 1.16: Examples of phosphorus-nitrogen heterocycles synthesized from a phosphadiazonium cation precursor.

Two complexes **1.40** and **1.41** have been isolated and characterized and feature a phosphadiazonium cation RNP^+, that is behaving as a Lewis base with respect to a transition metal centre.[163,164]

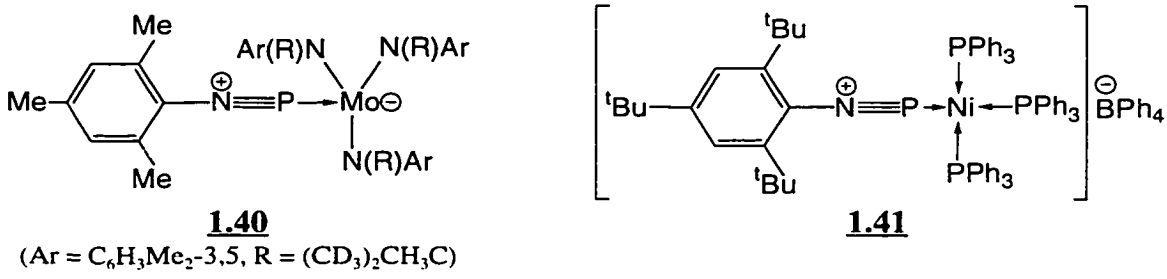

1.40
(Ar = $C_6H_3Me_2$-3,5, R = $(CD_3)_2CH_3C$)

1.41

Complexes containing phosphadiazonium cations are known to react with Lewis bases. The primary amine Mes*NH_2, or the primary alcohol Mes*OH, when combined with the phosphadiazonium tetrachlorogallate complex **1.34** (An = $GaCl_4^-$) results in the formation of a diaminophosphenium **1.42** (E = NH) or a *P*-amino-*P*-aryloxy-iminophosphenium **1.42** (E = O) cation, respectively (Figure 1.17).[25] These reactions presumably involve a 1,3-hydride shift from the coordinating Lewis base to imino-nitrogen centre.[25]

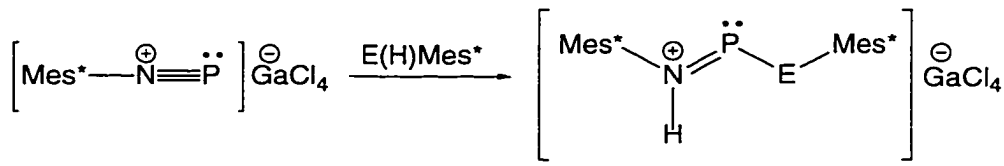

1.42

Figure 1.17: The formation of an acyclic diaminophosphenium **1.42** (E = NH) or *P*-amino-*P*-aryloxy-phosphenium **1.42** (E = O) cation by the reaction of a phosphadiazonium cation with a primary amine or alcohol.

1.5: Coordination Chemistry of Phosphadiazonium Cations as Lewis Acids

Traditionally, the main-group elements have been divided into metals, metalloids, and non-metals. Metals are regarded as Lewis acids and the non-metals as Lewis bases. The Lewis acidic behaviour of many main-group elements including members of group 13 and the heavier members of group 14, 15, 16 and 17 are well known and have been ranked using different scales (e.g., Table 1.2).[165,166] However, some main-group elements have amphoteric properties. That is, under specific conditions, the element in a particular bonding environment can be a Lewis acid and in others, it is has properties of a Lewis base.

Table 1.2: Comparison of Lewis acid strength for main-group elements using the Brown scale. The scale is based on the oxidation state of a cation and the average number of oxygen substituents bound to the cationic centre. Smaller values indicate greater Lewis acidity. Values are based on the highest oxidation state for each element. Reproduced from reference 165.

B	0.87	C	1.35	N	1.67	O	–	F	–
Al	0.57	Si	1.00	P	1.25	S	1.5	Cl	1.75
Ga	0.65	Ge	0.89	As	1.13	Se	1.5	Br	–
In	0.50	Sn	0.68	Sb	0.83	Te	1.0	I	1.2

Phosphorus, as σ-phosphines, has been classically viewed as a Lewis base. However, in a bonding environment where all the valence electrons on phosphorus are involved in bonding, (e.g., phosphoranes, and phosphoryl species) the compound has Lewis acidic properties. Lewis acidity is substantially increased when electron-withdrawing substituents are attached to the phosphorus centre. Pentafluorophosphorane PF_5, is considered a strong Lewis acid,[167] although weaker than its heavier homologues (i.e., EF_5, E = As, Sb, and Bi).[132,168] The σ-phosphino-bonding environment is a very weak Lewis acid, due to presence of a pair of non-bonding valence electrons on phosphorus. However, the amphoteric nature of phosphorus in the lower oxidation states is beginning to be realized as more complexes are discovered with a σ-phosphino-centre as the Lewis acidic component. For example, the anion in compound $[NEt_4]$**1.43** can be envisioned as a Lewis acid-base complex between a bromide ion and phosphorus tribromide.[169,170]

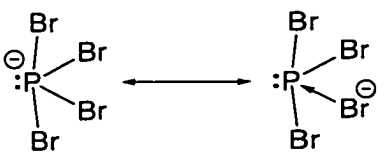

1.43

From their initial discovery, phosphadiazonium cations were shown to behave as Lewis acids. The crystal structure of the first reported complex containing a phosphadiazonium cation [Mes*NP]$AlCl_4$ **1.34** (An = $AlCl_4^-$), revealed the presence of a toluene molecule in close proximity to the phosphorus centre of the phosphadiazonium unit.[123] Furthermore, the tetrachloroaluminate anion has a stronger than usual interaction with the cation, that is, the shortest phosphorus-anion distance ($d((Cl_3Al)Cl–P)$ = 3.084(4) to 3.513(4) Å)[123] is less than 3.71 Å (from $\Sigma\, r_w(Cl) + r_w(P)$). A more detailed structural and spectroscopic investigation of complexes with a phosphadiazonium cation and tetrachlorogallate $GaCl_4^-$, or heptachlorodigallate $Ga_2Cl_7^-$, counter-ions showed that an arene is η^6 π-coordinated to the phosphorus centre of the $Mes*NP^+$ unit.[93,94] The P–C(arene) interaction in the [Mes*NP•arene]Ga_2Cl_7 complexes are directly related to the π-donor strength of the arene, decreasing in the order, benzene (2.820(4) Å) > toluene (2.767(7) Å) > mesitylene (2.687(7) Å), (Table 1.3). Similarly, the (anion)Cl–P distances in the [Mes*NP•arene]Ga_2Cl_7 complex, also related with the Lewis basicity of the arene, increasing in the order benzene (3.295(3) Å) < toluene (3.487(4) Å) < mesitylene (3.513(4) Å), (Table 1.3). Solution ^{31}P NMR spectra of the [Mes*NP•arene]An (An = $GaCl_4^-$, or $Ga_2Cl_7^-$) complexes, redissolved in CD_2Cl_2, showed that the arene maintains coordination to the phosphadiazonium unit. However, for complexes featuring a tetrachloroaluminate or tetrachlorogallate anion, the arene can be removed when exposed to a dynamic vacuum.

The [Mes*NP•arene]An complexes **1.34** (An = $AlCl_4^-$, $GaCl_4^-$, or $Ga_2Cl_7^-$) represent the first compounds to feature a π-coordinated phosphorus centre and are experimental models of the π-coordination complex intermediates that are postulated to form during aromatic electrophilic substitution reactions.[93]

Table 1.3: Comparison of selected structural features; *d*(P–N), *d*(P–C(arene)), *d*(Cl–P), and the ∠((Mes*)C-N-P) values for η^6 arene-phosphadiazonium complexes **1.34**.

Compound	*d*(P–N) (Å)	∠((Mes*)C-N-P) (°)	*d*(P–C(arene))[a] (Å)	*d*(Cl–P) (Å)	Reference
[Mes*NP•C_6H_5Me]$AlCl_4$	1.475(8)	177.0(7)	–	3.16†	123
[Mes*NP•C_6H_6]$GaCl_4$	1.484(7)	175.5(7)	3.001(1)	3.084(4)	93
[Mes*NP•C_6H_5Me]$GaCl_4$	1.53(2)	177.0(1)	3.08(1)	3.139(9)	93
[Mes*NP•C_6H_6]Ga_2Cl_7	1.463(5)	178.5(4)	2.820(4)	3.395(3)	93
[Mes*NP•C_6H_5Me]Ga_2Cl_7	1.464(9)	178.7(8)	2.767(7)	3.487(4)	93
[Mes*NP•$C_6H_3Me_3$-1,3,5]Ga_2Cl_7	1.471(6)	175.7(5)	2.687(7)	3.513(4)	93

([a]) Distance between the phosphorus centre and the centroid of the arene ring.

The first reported σ-coordination complex [Mes*NP•Lg]An featuring a phosphadiazonium cation was synthesized using triphenylphosphine as the ligand (Lg = PPh_3), but was characterized only by solution ^{31}P NMR spectroscopy.[38] The reaction between [Mes*NP•C_6H_5Me]$AlCl_4$ **1.34** (An = $AlCl_4^-$), and PPh_3, using a 1:1 stoichiometry, afforded [Mes*NP•PPh_3]$AlCl_4$ as postulated by a $^1J(^{31}P,^{31}P)$ value of 340 Hz.[38] An analogous reaction was performed using [Mes*NP•C_6H_5Me]Al(OAr)Cl_3 (Ar = 2,6-di-*tert*-butyl-4-methylphenyl) and PPh_3 in toluene at -30°C.[33] The ^{31}P NMR spectrum of the complex [Mes*NP•PPh_3]Al(OAr)Cl_3, prepared *in situ*, showed a doublet of doublets with $^1J(^{31}P,^{31}P)$ value of 338 Hz.[33] The complex was found to be unstable at ambient temperature, decomposing into the *P*-aryloxy-iminophosphine Mes*NPOAr and the phosphine-trichloroaluminum complex Cl_3Al•PPh_3.[33]

A stable phosphadiazonium-triphenylphosphine complex **1.44** was synthesized from the addition of Mes*NPOTf to PPh_3, using a 1:1 stoichiometry, at room temperature with hexane as the reaction solvent.[25] The complex was characterized as [Mes*NP•PPh_3]OTf **1.44** by solid-state ^{31}P NMR, IR, elemental analysis and crystallography.[25] However, there is no conclusive evidence of the complex in reaction

mixtures or when redissolved in solvent.[25] Solution ^{31}P NMR spectra fail to resolve a $^{1}J(^{31}P,^{31}P)$ value even at low temperature (-80 °C) or in different solvents.[25]

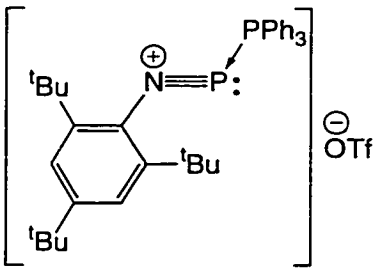

1.44

The crystal structure of [Mes*NP•PPh_3]OTf **1.44** shows a P–P(Lg) bond length (d(P–P) = 2.625(2) Å),[25] which is significantly greater than a typical single P–P bond distance as observed in diphosphines R_2P–PR_2, (d(P–P) = 2.214[22] Å),[131] and in the *P*-phosphino-iminophosphine Mes*NPP(^{t}Bu)$_2$, (d(P–P) = 2.192(1) Å[171]). The long P–P(Lg) bond in [Mes*NP•PPh_3]OTf **1.44** is attributed to a close interaction between the phosphorus centre of the Mes*NP unit and an oxygen centre of the triflate group. The P–O(Tf) distance (d(P–O) = 2.298(4) Å)[25] is longer than that reported for Mes*NPOTf, (d(P–O(Tf)) = 1.923(3) Å[130]). Structural parameters for the phosphadiazonium Mes*NP, and triflate units in [Mes*NP•PPh_3]OTf **1.44** are presented in Chapter 6.

Solid-state ^{31}P CP/MAS NMR spectra of [Mes*NP•PPh_3]OTf **1.44** show a large $^{1}J(^{31}P,^{31}P)$ value of 405 Hz,[25] which is unusual considering that the complex has a long P–P(Lg) bond. Thus, the magnitude of $^{1}J(^{31}P,^{31}P)$ cannot be correlated with d(P–P) values.[172] In addition, the spectra show that from the isotropic $\delta(^{31}P)$ value, the phosphorus nucleus of the Mes*NP unit is shielded ($\delta(^{31}P)$ = 71 ppm)[25] with respect to that reported for Mes*NPOTf ($\delta(^{31}P)$ = 52 ppm[130]). Solution ^{31}P NMR spectra reveal that the phosphorus nucleus associated with the phosphadiazonium unit in the [Mes*NP•PPh_3]$AlXCl_3$ (X = Cl or OAr') complexes are also slightly deshielded

($\delta(^{31}P)$ = 87 and 84 ppm, respectively)[33,38] as compared with that in the η^6 arene-phosphadiazonium complexes [Mes*NP•C_6H_5Me]$AlXCl_3$ ($\delta(^{31}P)$ = 79 ppm Cl;[123] 77 ppm $OC_6H_2(^tBu)_2$-2,6-Me-4 [33]). The phosphorus nucleus of the PPh_3 fragment in [Mes*NP•PPh_3]$AlXCl_3$ (X = Cl or OAr) is deshielded ($\delta(^{31}P)$ = 22 ppm)[33,38] as compared with that of the free PPh_3 ($\delta(^{31}P)$ = -8 ppm), whereas the solution $\delta(^{31}P)$ value of the PPh_3 unit in [Mes*NP•PPh_3]OTf **1.44** is identical to the free ligand.[25] Furthermore, solid-state NMR spectra reveal that the isotropic ^{31}P chemical shift for the PPh_3 unit in [Mes*NP•PPh_3]OTf **1.44** ($\delta_{iso}(^{31}P)$ = -1 ppm)[25] is not much different from that reported for the free ligand ($\delta_{iso}(^{31}P)$ = -10 ppm[173]). Therefore, the bonding character of PPh_3 in **1.44** appears relativity unchanged from that of the free ligand.

The seminal isolation and structural characterization of [Mes*NP•PPh_3]OTf **1.44** demonstrates that phosphorus-element bonds can be formed through Lewis acid-base interactions.[25] The Lewis acidic properties of iminophosphines, such as Mes*NPOTf, has led to the development of a new synthetic methodology for the creation of phosphorus bonding environments, for example, [Mes*NP•PPh_3]OTf **1.44**. The work presented in thesis utilizes this synthetic methodology; creating and characterizing new examples of [Mes*NP•Lg]OTf complexes using other Lewis basic main-group compounds as ligands.

1.6: Characterization of Phosphorus Compounds by 31-P NMR Spectroscopy

The 100% abundance of the ^{31}P nucleus with a nuclear spin (I) of $^1/_2$, provides an ideal condition for NMR spectroscopy and accordingly its use in the characterization of phosphorus compound is standard. However, phosphorus chemical shifts $\delta(^{31}P)$, cannot be used as a measure of electron density about the phosphorus nucleus,[174] as is generally the case with $\delta(^1H)$ values for protons. The shielding of the phosphorus nucleus is dominated by paramagnetic factors, which have a dependence on the energetic

accessibility of molecular excited states.[174] Hence, for some phosphorus compounds, including iminophosphines, the $\delta(^{31}P)$ values appear related with the energy difference between the HOMO and LUMO.[137,175] Therefore, the magnitude of $\delta(^{31}P)$ can only be used as a qualitative, but not a definitive guide, about the structure and bonding within a phosphorus compound. More importantly for the purposes of this thesis, the observation of a change in $\delta(^{31}P)$ indicates that a Lewis acid-base complex is formed. The number of peaks in a ^{31}P NMR spectrum provides information on the number of different phosphorus containing species present in a reaction mixture. Spin-spin coupling values J, if present, also can provide evidence for complex formation, but only if the coordinating centre of the ligand has an $I = {}^1/_2$. Moreover, there are no well-defined relationships between the magnitude of J values and molecular structure (e.g., bond length).[172]

1.7: Overview of Chapters in the Thesis

The contents of Chapters 2 through 5 describe the syntheses and characterization of phosphadiazonium-ligand-triflate complexes [Mes*NP•Lg]OTf and iminophosphine-ligand complexes of the type Mes*NP(R)•Lg. They are organized according to the donating element of the ligand involved (nitrogen, carbon, silicon, and chalcogen). At the beginning of Chapters 2 through 5, a brief overview of the different aspects regarding the coordination chemistry of phosphorus as a Lewis acid is provided. Tables for Chapters 2 through 8 are located at the end of each chapter.

The complexes described in Chapters 2 through 8 represent original research and interpretation performed by the author with crystallographic and solid-state NMR results provided by the collaborators mentioned in Sections 8.1 and 8.2.

In Chapter 6, the structural and spectroscopic features of the Mes*NP and triflate units for the phosphadiazonium-ligand-triflate complexes [Mes*NP•Lg]OTf are

compared with each other, with iminophosphines, and with other related phosphorus compounds. Chapter 7 contains conclusions and proposals for the further development of the coordination chemistry for π-phosphino-compounds. Specific experimental descriptions for syntheses and spectroscopic characterizations for all new compounds described in this thesis are presented in Chapter 8.

Chapter 2: Synthesis and Characterization of Phosphadiazonium-ligand-triflate Complexes featuring Phosphorus-nitrogen Coordination

2.1: Introduction: Overview of Phosphorus-nitrogen Coordination Chemistry

The role of phosphorus as a Lewis acid was first recognized with the discovery of complexes synthesized with nitrogen Lewis bases.[176] Subsequently, compounds containing a variety of Lewis acidic phosphorus bonding environments have been synthesized which involve a nitrogen centre as the Lewis basic component. Most of the isolated complexes contain a phosphorano-bonding environment and they include strongly Lewis acidic pentasubstituted phosphoranes PR_5, with electronegative substituents (e.g., R = fluoro, chloro, bromo, or *ortho*-phenylenedioxy groups).[167,176,177] There are a number of phosphorano-complexes intermolecularly coordinated with ligands such as amines,[178-180] pyridine,[17,179,181-187] pyrazine,[188,189] pyrazole,[190,191] and complexes featuring intramolecular coordination with oxyquinolines,[192-194] *N*,*N*',*N*'-trimethylethylenediamine,[195-197] pendant amino,[47,194,198,199] imino,[200] or diazo[200] groups attached as substituents. Phosphorano-complexes with chelating nitrogen ligands such as such as 2,2'-dipyridyl[181,201,202] and *N*,*N*'-dialkylamidinium,[203] have been isolated and characterized. The structures of the majority of phosphorano-nitrogen coordination complexes are formulated from data obtained from spectroscopic[176] (e.g., ^{31}P, ^{1}H, ^{13}C, ^{19}F NMR, ^{35}Cl NQR, IR, Raman, uv-vis) and physical measurements (e.g., molar conductivity, vapour pressure, elemental analysis, or calorimetry).[176] Conclusive evidence of phosphorus-nitrogen coordination is provided through crystallography. However, relatively few phosphorano-nitrogen complexes have been characterized by this method.

In contrast to complexes featuring a phosphorano-bonding environment, there are fewer known examples of phosphino-complexes containing a nitrogen centre as the Lewis basic component. The presence of non-bonding valence electrons on phosphorus results in bonding environments with weak Lewis acidity as compared with those compounds containing a phosphorano-centre.[204] There are currently no crystallographically characterized examples of complexes featuring intermolecular coordination between a nitrogen centre and a σ-phosphino-bonding environment PR_3. Nevertheless, spectroscopic and physical chemical data are available for such compounds. The existence of $Cl_3P{\bullet}NMe_3$[205] and related derivatives have been postulated based on data from vapour-pressure and solution ^{31}P NMR measurements. No reaction is observed between phosphorus trifluoride and organic nitrogen bases.[179] However, complexes featuring a σ-phosphino-centre with intramolecular mono-, di-, or tri-coordination by the 8-dimethylamino-1-naphthyl substituent have been reported.[206-209] At present, there are no examples of complexes containing a chelated σ-phosphino-centre. Experiments have revealed that complexes are not formed on the addition of phosphorus trihalides (PCl_3 or PBr_3) to 2,2'-dipyridyl.[210]

Cationic π-phosphino-compounds are stronger Lewis acids than σ-phosphines. Hence, there are more characterized examples of complexes containing a phosphenium PR_2^+, or phosphinidene PR^{2+} bonding environment with a nitrogen centre as the Lewis basic component. Complexes featuring the latter type of bonding environment are isolated with two ligands attached to the phosphorus centre.[96,97,211] A complex with a tricoordinated P^{3+} ion is postulated based on data from ^{31}P NMR spectroscopy.[96] Acyclic diaminophosphenium and diazaphospholenium cations have been shown, on the basis of data from crystallography and or ^{31}P, ^{19}F, ^{1}H, ^{13}C NMR spectroscopy,[34,36,37,40,44] to form complexes with Lewis bases such as 1,8-diazabicyclo[5.4.0]-undec-7-ene,

1,5-diazabicyclo[4.3.0]-non-5-ene, or pyridine. Complexes containing a phosphenium-bonding environment without the benefit of lone pair π-conjugation have been isolated from two-fold σ-coordination by pendant dialkylamino groups.[212]

There are very few examples of complexes which feature an iminophosphine behaving as the Lewis acidic component. Evidence from ^{31}P and ^{1}H NMR spectra of the *P*-8-dimethylamino-1-naphthyl substituted iminophosphine **2.1** suggest, based on differences in phosphorus chemical shift, the presence of a weak interaction between the phosphorus and amino-centres.[98] However, protonation of the iminophosphine **2.1** with triflic acid resulted in the formation of a complex **2.2** (Figure 2.1). This complex features an intramolecularly coordinated phosphenium cation, as shown by the presence of anisochronous methyl groups in the ^{1}H NMR spectra and a phosphorus nucleus that is shielded as compared with complexes containing a non-coordinated aminophosphenium cation.[98] This suggests that the resulting phosphenium cation is more Lewis acidic than the parent iminophosphine **2.1**. Nevertheless, other types of iminophosphines have demonstrated Lewis acidic behaviour. Lewis acid-base complexes containing aluminatodiiminophosphane **2.3**, were synthesized by the addition of tertiary amines (quinuclidine **2.4**, *N*,*N*,*N'*,*N'*-tetramethylethylenediamine **2.5**, and 1,4-diazabicyclo[2.2.2]-octane **2.6**) in a 1:1 stoichiometry.[91,213] The complexes **2.4**-**2.6** were shown, based on data from crystallography, solid-state and solution ^{31}P NMR spectroscopy, to possess intermolecular phosphorus-nitrogen coordination.[91,213] The mono- and bis-coordination of the *P*-chloro-iminophosphine Mes*NPCl, with 4-dimethylaminopyridine has been mentioned.[214]

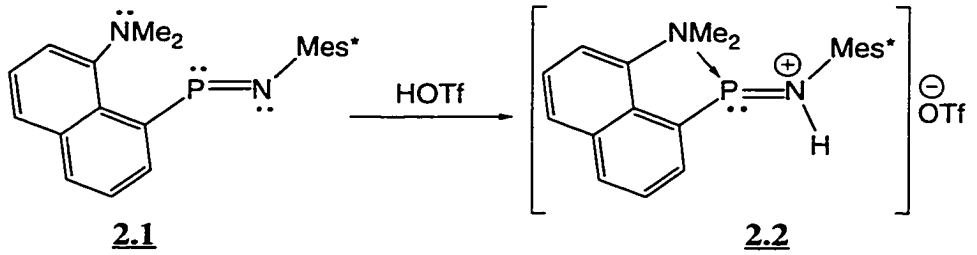

2.1 2.2

Figure 2.1: Protonation of the *P*-aryl-iminophosphine 2.1, results in the formation of an amino-phosphenium salt 2.2, featuring intramolecular coordination between the phosphorus centre and a dimethylamino-group.

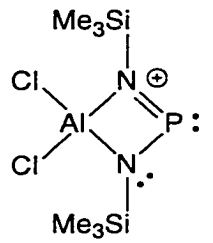

2.3

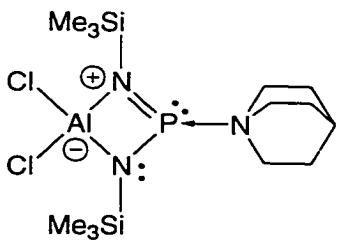

2.4

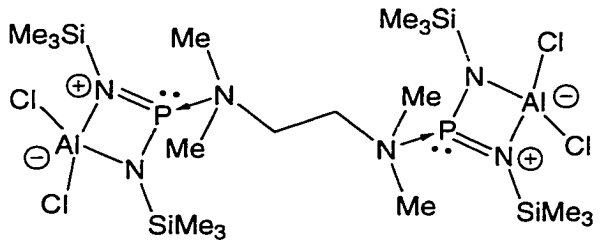

2.5

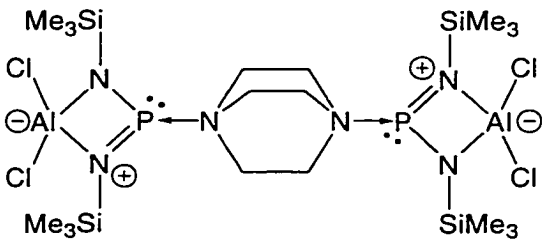

2.6

The coordination of many of the above mentioned phosphorus bonding environments with nitrogen bases has led to the formation of new bonding environments for phosphorus. In some cases, the resulting complexes represent a previously known phosphorus-bonding environment. However, their isolation demonstrates accessibility using coordination chemistry. Hence, a study by the author of this thesis was undertaken to show that coordination of nitrogen bases with the Lewis acidic triflate-substituted iminophosphine Mes*NPOTf, results in complexes 2.7-2.9, which represent examples of

new bonding environments for phosphorus.[215,216] Descriptions and comparisons of these complexes are presented in the following sections.

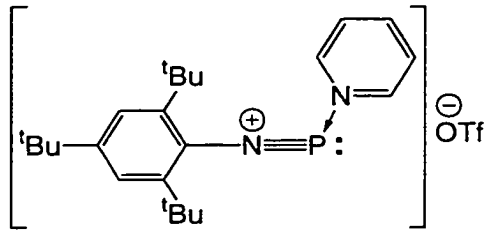

2.7

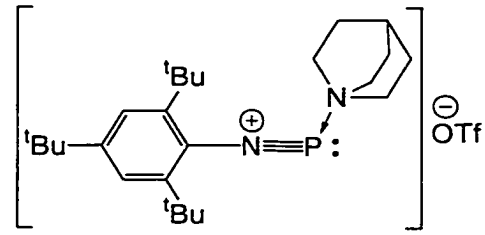

2.8

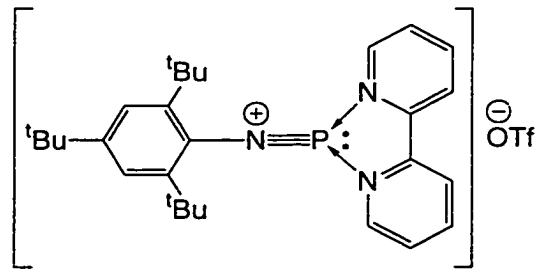

2.9

2.2: Results and Discussion

2.2.1: Synthesis of Phosphadiazonium-ligand-triflate Complexes, [Mes*NP•Lg]OTf, where Lg is Py (2.7), Qncd (2.8), or Dipy (2.9)

Complexes 2.7-2.9 were prepared by the addition of base (1:1 stoichiometry for quinuclidine and 2,2'-dipyridyl, 2.4:1 stoichiometry for pyridine) to Mes*NPOTf in benzene.[215,216] The complexes precipitated out of solution on mixing of the reagents and were characterized using solution NMR spectroscopy and single crystal X-ray diffraction studies. Elemental analyses confirmed the formulation for [Mes*NP•Lg]OTf (Lg = Py 2.7 or Qncd 2.8).[215,216] Furthermore, solid-state ^{31}P NMR spectra (static and CP/MAS) were obtained for complexes [Mes*NP•Lg]OTf, Lg = Py 2.7 or Dipy 2.9. Solution ^{31}P NMR spectra of reaction mixtures prepared in dichloromethane exhibited a dominant signal corresponding to the complexes, but were accompanied by smaller intensity peaks

which are tentatively assigned as Mes*NPCl ($\delta(^{31}P)$ = 136 ppm)[152] and [(Mes*NH)$_2$P]OTf ($\delta(^{31}P)$ = 279 ppm),[33] based on comparisons of reported $\delta(^{31}P)$ values for isolated compounds. The isolation of analytically pure samples of **2.7**-**2.9** was dependent primarily on the choice of reaction solvent. Reaction mixtures containing [Mes*NP•Py]OTf **2.7**, prepared in dichloromethane, showed that the Mes*NPCl signal grew in intensity over a period of several weeks, consistent with previous reports of other cationic π-phosphino-compounds in dichloromethane.[23,24,92,93] The complexes **2.7**-**2.9** are insoluble in hydrocarbon solvents such as n-hexane, pentane, and only slightly soluble in benzene. Crystals of the complexes **2.8** and **2.9** were obtained through slow diffusion of n-hexane into a solution of the compound in dichloromethane. Crystals of **2.7** were obtained by slow evaporation of the compound in a solution composed of dichloromethane and n-hexane. Specific details on the crystallization process are provided in Section 8.2.

2.2.2: Structural Features of the Phosphadiazonium-ligand-triflate Complexes, [Mes*NP•Lg]OTf, where Lg is Py (2.7), Qncd (2.8), or Dipy (2.9)

The crystal structures of [Mes*NP•Lg]OTf (Lg = Py **2.7** and Qncd **2.8**) reveal a single interaction between the nitrogen centre of the ligand and the phosphorus centre of the phosphadiazonium unit (Figures 2.2 and 2.3).[215,216] The crystal structure of [Mes*NP•Dipy]OTf **2.9**, shows chelation of the phosphadiazonium unit by the 2,2'-dipyridyl ligand with two equivalent phosphorus-nitrogen interactions (Figure 2.4).[216] The [Mes*NP•Py]OTf complex **2.7** is a dimer in the solid state, composed of two Mes*NP•Py units bridged by two triflate groups (vide infra). The crystal structures of [Mes*NP•Lg]OTf (Lg = Dipy or Qncd) show individual molecular units consisting of a single cation paired with one anion and no bridging triflate interactions. However, in the case of [Mes*NP•Dipy]OTf **2.9**, each molecular unit is paired with one disordered

dichloromethane molecule. Furthermore, the trifluoromethyl group of the triflate anion in **2.9** is rotationally disordered.

The P–N(Lg) bond in [Mes*NP•Qncd]OTf, (d(P–N(Qncd)) = 1.933(2) Å)[216] is slightly shorter than that in [Mes*NP•Py]OTf, (d(P–N(Py)) = 1.958(8) Å) and both are significantly shorter than those in [Mes*NP•Dipy]OTf, (d(P–N(Dipy)) = 2.065(4), 2.066(4) Å[216]). The increased length of the P–N(Lg) bonds in [Mes*NP•Dipy]OTf is possibly due to a competing interaction between the nitrogen centres of the 2,2'-dipyridyl ligand.

The P–N(Lg) bond lengths in **2.7**-**2.9** are considerably longer than the P–N bond lengths in other disubstituted π-phosphino-species, including amino-iminophosphines Mes*NPNR$_2$, (d(P–N(R$_2$)) = 1.624(2) to 1.674(1) Å), and diaminophosphenium salts [P(NR$_2$)$_2$]An, (d(P–N(R$_2$)) = 1.59(1) to 1.617(3) Å). A survey of individual values for amino-iminophosphines and diaminophosphenium salts is given in Table 2.1. Theoretical calculations show that for phosphorus-nitrogen interactions, in which the nitrogen centre has an available pair of non-bonding valence electrons, the P–N bonds are contracted due to lone pair π-conjugation.[105,217] It is postulated that this interaction accounts for the shortened P–N(R$_2$) bonds in both amino-iminophosphines and diaminophosphenium salts and is consistent with the observation of planar geometry for the amino-substituent in these compounds.[18,103] The potassium phosphoramidate salt [K]OP(O)$_2$•NH$_3$, has a d(P–N(Lg)) value of 1.800(4) Å,[180] which is longer than those reported for amino-iminophosphines and diaminophosphenium salts. Importantly, the potassium phosphoramidate salt [K]OP(O)$_2$•NH$_3$, is recognized has having a quaternized nitrogen centre.[180]

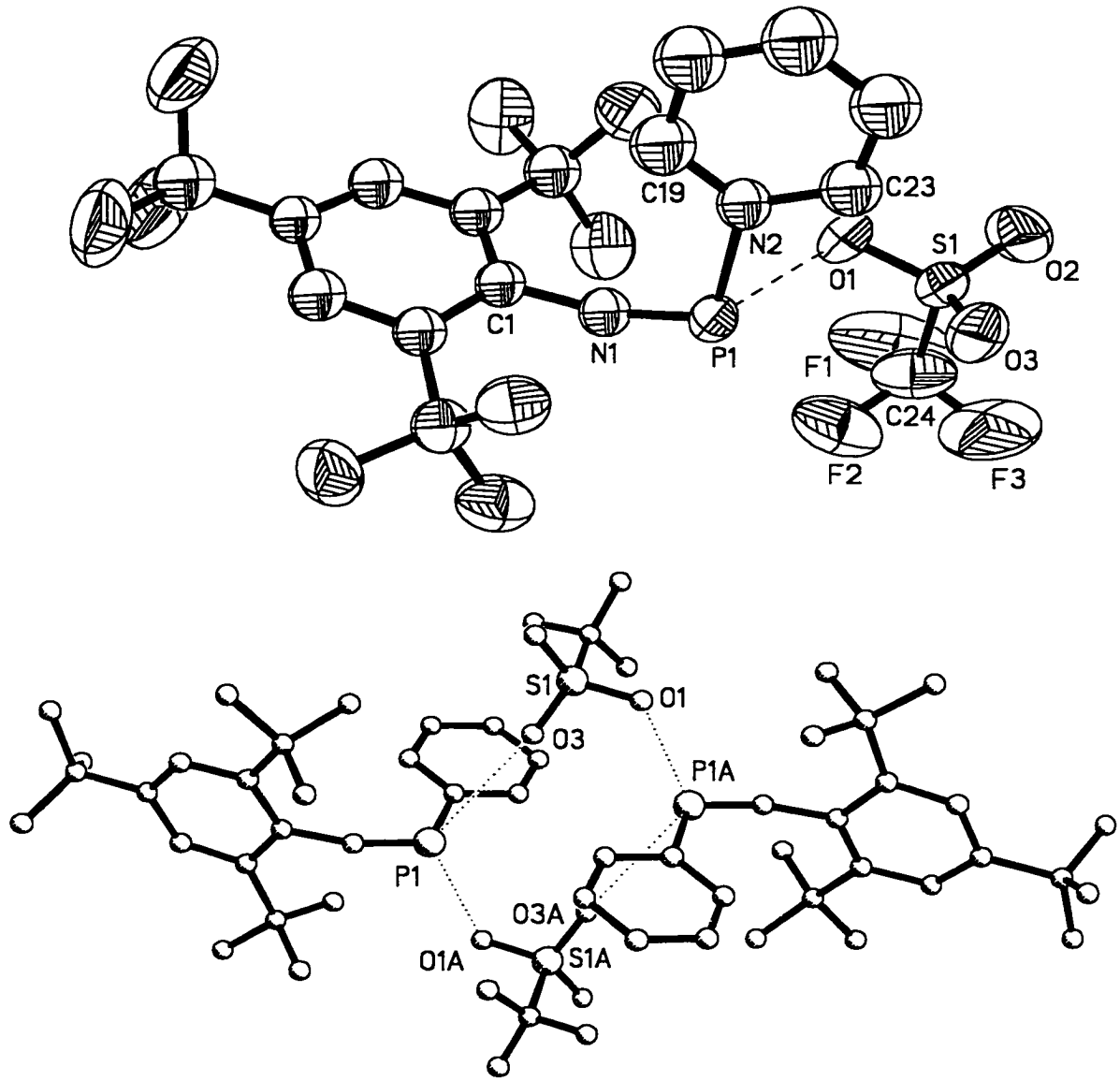

Figure 2.2: (Top) ORTEP-like view of a single unit of [Mes*NP•Py]OTf **2.7**, drawn with 50% probability ellipsoids. The hydrogen atoms have been omitted for clarity. Important bond lengths (Å) and angles (°): P(1)–N(1) 1.472(8), P(1)–N(2) 1.958(8), N(1)–C(1) 1.42(1), C(1)-N(1)-P(1) 161.7(7), N(1)-P(1)-N(2) 107.8(4), P(1)-N(2)-C(19) 121.6(7), P(1)-N(2)-C(23) 116.4(7), C(19)-N(2)-C(23) 121.7(9). (Bottom) PLUTO-like view of [Mes*NP•Py]OTf **2.7**, showing the bridging triflate interactions. The hydrogen atoms have been omitted for clarity. Important bond lengths (Å): P(1)–O(1A), P(1A)–O(1) 2.712(7), P(1)–O(3), P(1A)–O(3A) 3.064(7). Values reproduced from reference 215.

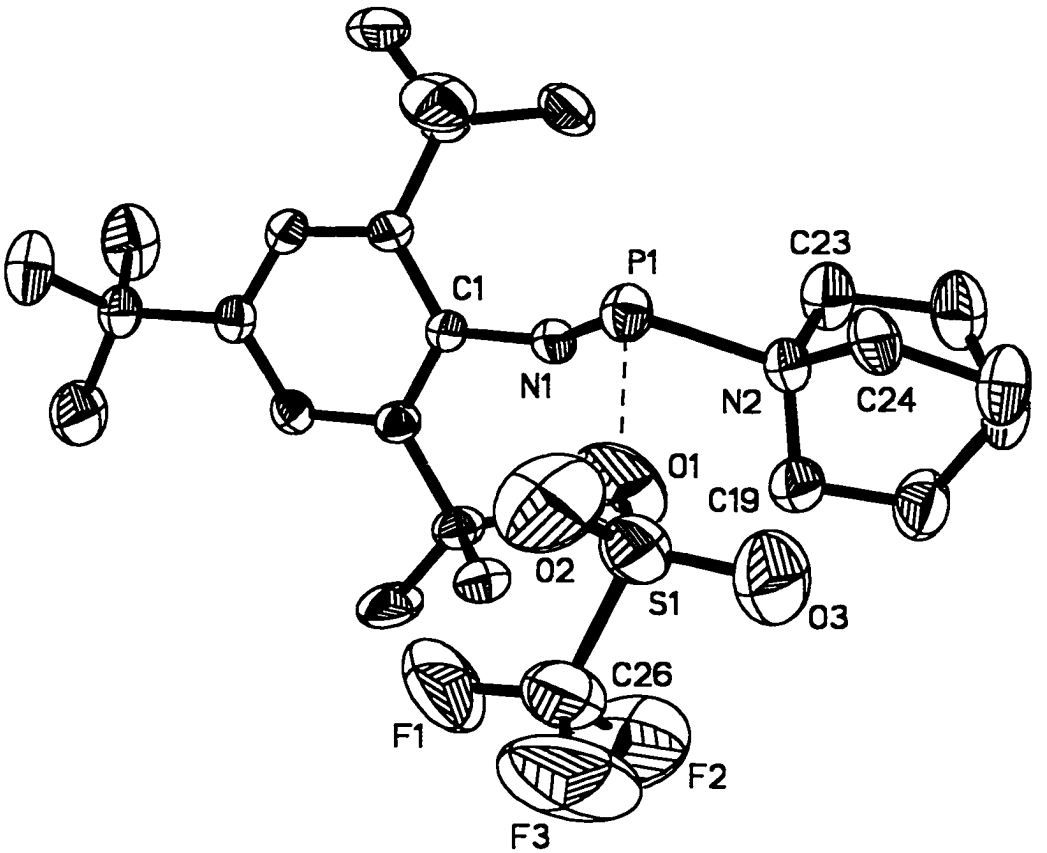

Figure 2.3: ORTEP-like view of [Mes*NP•Qncd]OTf **2.8**, drawn with 50% probability ellipsoids. The hydrogen atoms have been omitted for clarity. Important bond lengths (Å) and angles (°): P(1)–N(1) 1.519(2), P(1)–N(2) 1.933(2), N(1)–C(1) 1.415(3), N(2)–C(19) 1.501(3), N(2)–C(23) 1.499(3), N(2)–C(24) 1.513(3), P(1)–O(1) 2.697(3), C(1)-N(1)-P(1) 143.9(2), N(1)-P(1)-N(2) 103.7(1), P(1)-N(2)-C(19) 116.6(2), P(1)-N(2)-C(23) 106.8(2), P(1)-N(2)-C(24) 106.0(2), C(19)-N(2)-C(23) 110.0(2), C(19)-N(2)-C(24) 109.0(2), C(23)-N(2)-C(24) 108.1(2). Values reproduced from reference 216.

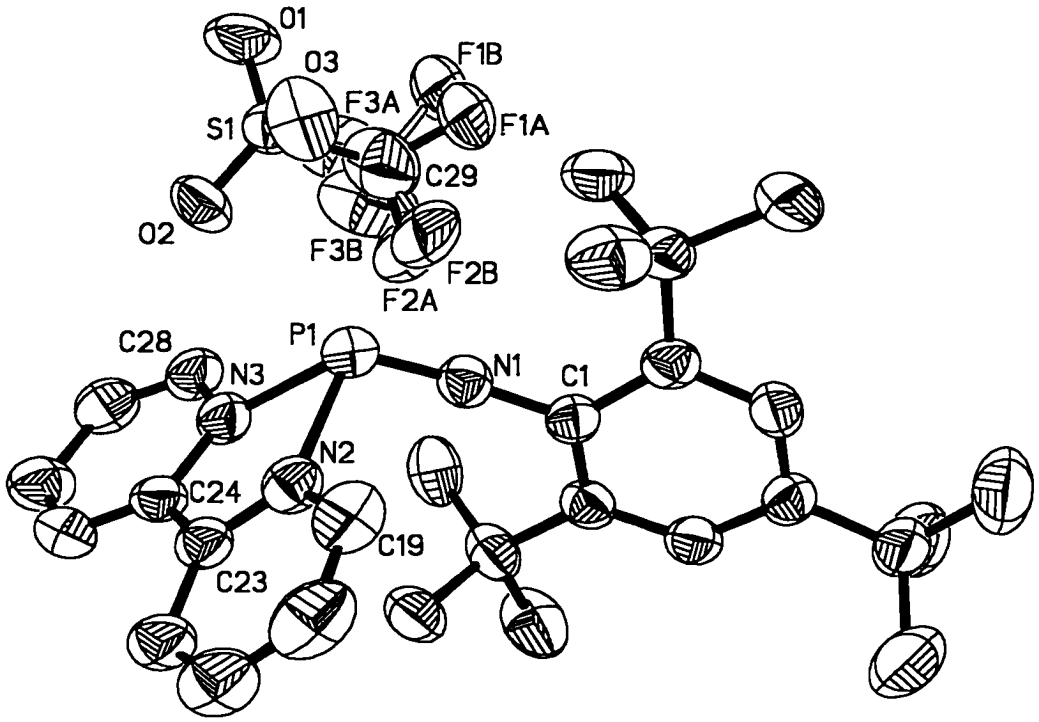

Figure 2.4: ORTEP-like view of [Mes*NP•Dipy]OTf **2.9**, drawn with 50% probability ellipsoids. The hydrogen atoms and the dichloromethane solvate have been omitted for clarity. The CF_3 group of the anion is disordered. Important bond lengths (Å) and angles (°): P(1)–N(1)1.497(4), P(1)–N(2) 2.065(4), P(1)–N(3) 2.066(4), N(1)–C(1) 1.401(6), N(2)–C(19) 1.347(6), N(2)–C(23) 1.331(6), N(3)–C(24) 1.363(6), N(3)–C(28) 1.347(6), P(1)-N(1)-C(1) 169.4(4), N(1)-P(1)-N(2) 106.3(2), N(1)-P(1)-N(3) 113.0(2), N(2)-P(1)-N(3) 75.1(2), P(1)-N(2)-N(19) 120.0(5), P(1)-N(2)-C(23) 119.6(3), P(1)-N(3)-C(24) 119.0(3), P(1)-N(3)-C(28) 121.2(4), N(2)-C(23)-C(24) 113.6(4), N(3)-C(24)-C(23) 111.9(4). Values reproduced from reference 216.

The phosphorus and quaternized (sp^3 hybridized) nitrogen centres are strictly σ-bonded, and hence [K]$OP(O)_2$•NH_3 is presented as an example of a system with an 'idealized' P–N single bond with no lone pair π-conjugation.[180] Similarly, the long length of the P–N(Lg) interaction in complexes **2.7**-**2.9** suggest that there is no lone pair π-conjugation between the nitrogen centre(s) of the ligand and the phosphorus centre of the phosphadiazonium unit (vide infra).

Ligand basicity may be a contributing factor in P–N(Lg) bond length for complexes **2.7** to **2.9**. Hence, a shorter phosphorus and ligand interaction is correlated with greater ligand basicity, (i.e., *d*(P–N(Lg)) {pK_a}: Qncd 1.933(2) Å {Qncd•H^+ 10.95}[218] < Py 1.958(8) Å {Py•H^+ 5.25}[219] < Dipy 2.065(4), 2.066(4) Å {Dipy•H^+ 4.23}[220]). Similarly, high level ab initio calculations, at the MP2/6-31G(d) level of theory, on a simplified version of the bisiminiophosphonium-base complex $(MeN)_2P$•Lg^+ (Lg = NH_3, Py, or 4-DMAP), show that the P–N(Lg) bond length is related with ligand basicity (i.e., *d*(P–N(Lg)) {pK_a}, 4-DMAP 1.879 Å {4-DMAP•H^+ 10.14}[221] < NH_3 1.913 Å {NH_4^+ 9.24}[222] < Py 1.959 Å {Py•H^+ 5.25}[219]).[16]

In general, complexes featuring a phosphorano-centre (i.e., phosphorane (σ^5,λ^5) *d*(P–N) = 1.842(2) to 2.143(3) Å; (σ^4,λ^4) *d*(P–N) = 1.896(4) to 1.987(1) Å), phosphoryl ((σ^5,λ^4) *d*(P–N) = 1.838(3) Å; (σ^3,λ^5) *d*(P–N) = 1.185(5) to 2.023(8) Å), have shorter P–N(Lg) interactions than those containing a π- or σ-phosphino-centre (i.e., phosphine (σ^3,λ^3) *d*(P–N) = 2.076(6) to 2.999† Å; iminophosphine (σ^2,λ^3) *d*(P–N) = 2.038(9) to 2.1 10(6) Å; or phosphenium (σ^2,λ^2) *d*(P–N) = 2.068(4) Å), individual values are provided in Table 2.2. The exceptions are complexes, which feature a phosphinidene-centre ((σ^1,λ^1) *d*(P–N) = 1.752(4) to 1.766(5) Å). This reflects the greater Lewis acidity of phosphorano-compounds versus that of σ- and π-phosphino-bonding environments. This argument is consistent with the observation that pyridine complexes featuring a

phosphorane **2.10** (d(P–N(Py)) = 1.885(4) Å),[185] dithiophosphonium **2.11** (d(P–N(Py)) = 1.77(1), 1.87(1) Å, An = Br; d(P–N(Py) = 1.831(1) Å, An = I),[17] or dithiophosphoryl **2.12** (d(P–N(Py)) = 1.849(2) Å)[186] centre have a shorter P–N(Py) interaction than that in [Mes*NP•Py]OTf **2.7**, (d(P–N(Py)) = 1.958(8) Å[215]). Similarly, the P–N(Dipy) bonds in [Mes*NP•Dipy]OTf **2.9**, (d(P–N(Dipy)) = 2.065(4), 2.066(4) Å)[216] are considerably longer than those reported for the 2,2'-dipyridyl-spirophenylenedioxyphosphorane complex **2.13** (d(P–N(Dipy)) = 1.896(4), 1.898(4) Å[202]).

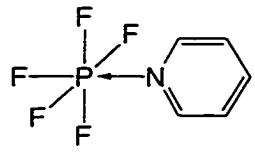

2.10

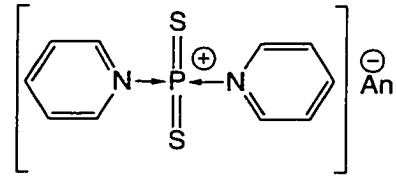

2.11

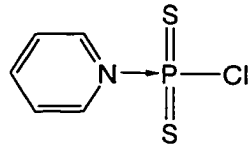

2.12

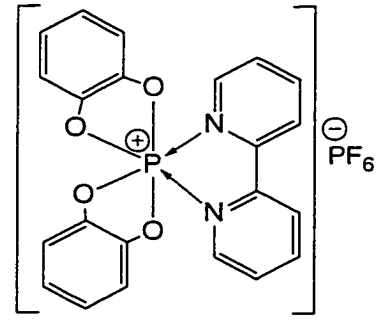

2.13

The P–N(Qncd) bond in [Mes*NP•Qncd]OTf **2.8** (d(P–N(Qncd)) = 1.933(2) Å)[216] is significantly shorter than that in the aluminatodiiminophosphane-quinuclidine complex **2.4** (d(P–N(Qncd)) = 2.038(9) Å[91]). This suggests that the Lewis acidity of the phosphorus centre in phosphadiazonium cation Mes*NP$^+$, is greater than that of the aluminatodiiminophosphane **2.3**. This is expected, as the latter bonding environment contains a disubstituted phosphorus centre with lone pair π-conjugation from both amino-substituents.

The [Mes*NP•Lg]OTf (Lg = Py **2.7** or Qncd **2.8**) complexes have N-P-N bond angles (Lg = Py, 103.7(1)°; Lg = Qncd, 107.8(4)°)[215,216] that fit inside the range observed for amino-iminophosphines (104.0(1) to 115.9(3) °) and diaminophosphenium salts (103.9(2) to 117.0(7) °), individual values for the amino-iminophosphines and diaminophosphenium salts are given in Table 2.1. The smallest (Mes*)N-P-N(Lg) bond angle in [Mes*NP•Dipy]OTf **2.9** (106.3(2)°)[216] is close to those in complexes with Lg = Py **2.7** (103.7(1)°)[215] or Qncd **2.8** (107.8(4)°[216]). Furthermore, the largest (Mes*)N-P-N(Dipy) bond angle (113.0(2)°) is comparable to the (Mes*)N-P-O(Tf) bond angle in [Mes*NP•Qncd]OTf **2.8** (112.5(1)°[216]).

The pyramidal geometry of the phosphorus centre in [Mes*NP•Dipy]OTf **2.9** is indicated by the sum of the bond angles around phosphorus ($\Sigma \angle(P) = 294.4(3)°$).[216] Thus indicating that the phosphorus centre in [Mes*NP•Dipy]OTf **2.9** has a pair of non-bonding valence electrons which are stereochemically active.

The C(Mes*)-N-P-N(Lg) torsion angles in [Mes*NP•Py]OTf **2.7** and [Mes*NP•Qncd]OTf **2.8** are 12(2)° and 175.7(3)°, respectively.[215,216] Therefore, [Mes*NP•Py]OTf **2.7** has a *cis*-configuration about the P–N bond, whereas [Mes*NP•Qncd]OTf **2.8** has a *trans*-configuration. For [Mes*NP•Dipy]OTf **2.9**, the two C(Mes*)-N-P-N(Dipy) torsion angles (28(2)°, 109(2)°)[216] differ from those in [Mes*NP•Lg]OTf (Lg = Pyr **2.7** or Qncd **2.8**), and may be a consequence of the rigid structure of the 2,2'-dipyridyl ligand maintaining a bidentate interaction with the phosphorus centre. The difference between both C(Mes*)-N-P-N(Lg) torsion angles, ϕ = 80(3)° (Lg = Dipy **2.9**),[216] is less than the $\phi = 90°$ (Lg = NH_3) determined from ab initio calculations, at the MP2/ECP 6-31g(d,p)+ZPVE level of theory, on the model bis-ammine-phosphadiazonium complex $HNP(•NH_3)_2^+$.[223] The smaller ϕ value in

[Mes*NP•Dipy]OTf **2.9** is probably due to structural constraints of the 2,2'-dipyridyl ligand.

In [Mes*NP•Py]OTf **2.7**, the ligand is planar (i.e., mean deviation of the non-hydrogen atoms from the plane is 0.007(5) Å). The plane containing the non-hydrogen atoms of the pyridine ligand is tilted 9.81†° with respect to the plane defined by C(1), N(1) and P (Figure 2.2).[215] The pyridine ring plane is twisted by 84.1†° with respect to the aryl ring plane of the Mes* substituent, presumably minimizing steric repulsion within the complex.[215] The bond lengths and angles within the pyridine ligand of [Mes*NP•Py]OTf **2.7** are identical to those found in the free ligand,[224] pyridine-*N*-oxide,[225] and pyridine complexes featuring phosphorus or other main-group elements as the Lewis acidic component (e.g., **2.10**-**2.12**, F_3B•Py).[17,185,186,226]

The bond lengths and angles of the quinuclidine unit in [Mes*NP•Qncd]OTf **2.8** are the same as those found in F_3B•Qncd,[227] the aluminatodiiminophosphane-quinuclidine complex **2.4**,[91] and Qncd•CBr_4 where the nitrogen centre has a weak interaction with one of the bromine atoms (d(Br–N) = 2.531(6) Å[228]). A comparison with the bond parameters for the free quinuclidine is not feasible due to disorder in the crystal structure.[229] The ligand in [Mes*NP•Qncd]OTf **2.8** has a staggered arrangement with respect to the N–C(Mes*) bond (i.e., the (Mes*)N-P-N-C(Qncd) torsion angles are -179.3(2)°, 65.6(2)°, and -57.9(2)°),[216] thus minimizing steric interactions between the Mes* substituent and the ligand.

The 2,2'-dipyridyl group in [Mes*NP•Dipy]OTf **2.9** has a *cisoid* configuration, in that the N(Lg)-C-C-N(Lg) torsion angle is small (7.7(6)°)[216] and hence the nitrogen centres are adjacent to each other. This *cisoid* configuration in [Mes*NP•Dipy]OTf is consistent with other complexes featuring a chelating 2,2'-dipyridyl ligand. Both pyridyl rings are planar in **2.9** (i.e., mean deviation of the non-hydrogen atoms from the plane is

0.011(4) Å and 0.005(4) Å), with the rings slightly twisted (8.4(2)°)[216] with respect to each other.[216] In contrast, the pyridyl rings in the 2,2'-dipyridyl-spirophenylenedioxyphosphorane complex **2.13** are less twisted (i.e., the N(Lg)-C-C-N(Lg) torsion angle is 4.7†°).[202] The N(Lg)-P-N(Lg) bond angle in [Mes*NP•Dipy]OTf **2.9** (75.1(2)°)[216] is smaller than that in **2.13** (81.7(2)°[202]). This is the result of longer P–N(Lg) bonds in **2.9**. The bond lengths and angles within the pyridyl rings for [Mes*NP•Dipy]OTf **2.9** are equivalent to those in free 2,2'-dipyridyl,[230] with exception of the N-C-C(N) bond angles which are smaller in **2.9** (113.6(4)°, 111.9(4)°)[216] than that reported for the free ligand (116.1(2)°[230]). Bending of the pyridyl rings towards the Lewis acidic centre is commonly observed for the 2,2'-dipyridyl ligand in a chelating coordination mode and can be rationalized in terms of maximizing interaction between the Lewis basic and Lewis acidic centres. The aryl ring plane of the Mes* substituent in [Mes*NP•Dipy]OTf **2.9** is positioned 81.8(2)° and 76.4(2)° with respect to the pyridyl ring planes,[216] thereby minimizing steric interactions.

The structural parameters of the phosphadiazonium Mes*NP$^+$, and triflate units in **2.7**, **2.8**, and **2.9** are discussed and compared to other phosphadiazonium-ligand complexes in Chapter 6. The crystal structures show that the phosphorus-oxygen(Tf) distances in **2.7** (d(P–O(Tf)) = 2.712(7), 3.064(7) Å) and **2.8** (d(P–O(Tf)) = 2.697(3) Å)[216] are significantly longer than a typical P–O bond (d(P–O) = 1.573[11] Å[131] $(R_2N)_2$P–O), but are less than 3.30 Å (from $\Sigma\, r_w$(P) + r_w(O)). In contrast, the P–O(Tf) distance in [Mes*NP•Dipy]OTf is 3.490(5) Å.[216] The shortest cation-anion distance is between N(2) and O(3), (d(O–N) = 3.208(6) Å[216]). This distance is significantly greater than 2.94 Å (from $\Sigma\, r_w$(O) + r_w(N)). Therefore, the cation-anion interaction in [Mes*NP•Dipy]OTf **2.9** is considered predominantly ionic. The [Mes*NP•Py]OTf **2.7** complex has a second considerably longer P–O(Tf) interaction (d(P–O(Tf)) = 3.064(7) Å)

which is less than 3.30 Å (from $\Sigma\, r_w(P) + r_w(O)$). Consequently, [Mes*NP•Py]OTf is a dimer when crystallized in the solid state (Figure 2.2). The phosphorus centres of the two Mes*NP•Py units are bridged through two separate oxygen atoms on independent triflate groups. The two [Mes*NP•Py]OTf units of the dimer are related through a centre of inversion. This particular coordinating mode for triflate has been observed in other complexes including those with a transition metal centre, for example, $Cu_4(OH)_4(OTf)_2(C(Py\text{-}2)_3)_4^{2+}$ **2.14**.[231]

The phosphorus centre in [Mes*NP•Py]OTf **2.7** has a distorted tetrahedral geometry, as defined from two P–N bonds and two P–O(Tf) interactions. This is similar to that observed for the phosphorus centre in the η^6 arene-phosphadiazonium complexes with a heptachlorodigallate anion [Mes*NP•arene]Ga_2Cl_7 **1.34** (An = $Ga_2Cl_7^-$).[93,94]

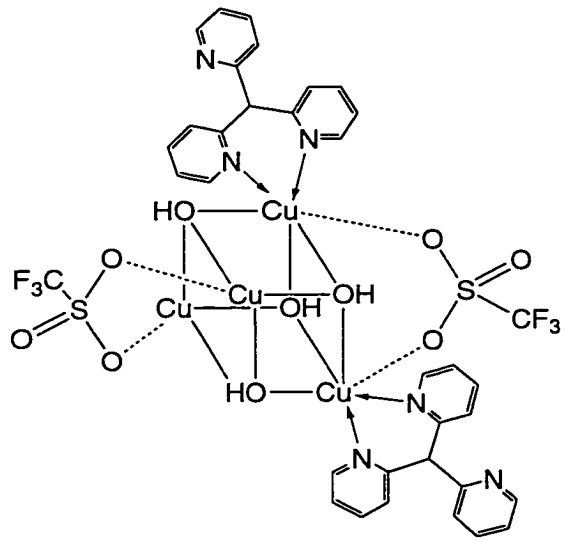

2.14

(Two ligands have been omitted for clarity)

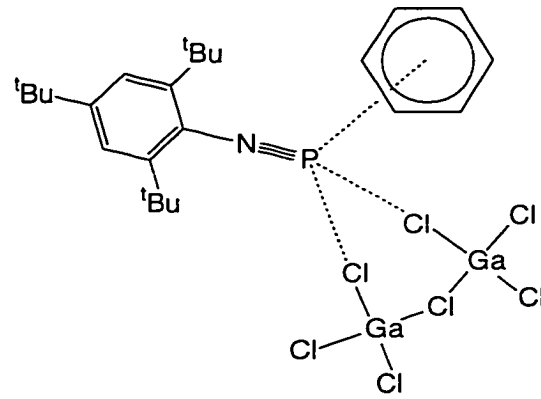

1.34

(Arene = C_6H_6, An = $Ga_2Cl_7^-$)

2.2.3: Spectroscopic Features of Phosphadiazonium-ligand-triflate Complexes, [Mes*NP•Lg]OTf, where Lg is Py (2.7), Qncd (2.8), or Dipy (2.9)

Solution ^{31}P NMR spectra of [Mes*NP•Lg]OTf (Lg = Py **2.7** or Qncd **2.8**) have revealed that both complexes ($\delta(^{31}P)$ = 71 ppm,[215] Lg = Py; 144 ppm,[216] Lg = Qncd) feature a deshielded phosphorus nucleus as compared with that observed in Mes*NPOTf ($\delta(^{31}P)$ = 55 ppm[130]). The phosphorus nucleus in [Mes*NP•Qncd]OTf **2.8** exhibited the greatest shielding difference ($\Delta\delta(^{31}P)$ = 89 ppm) in complexes **2.7**-**2.9**, although not as large as the 176 ppm difference in $\delta(^{31}P)$ for the aluminatodiiminophosphane **2.3** ($\delta(^{31}P)$ = 129 ppm)[155] when it is coordinated by quinuclidine **2.4**, ($\delta(^{31}P)$ = 205 ppm[91]). Similarly, $\delta(^{31}P)$ for the diazaphospholenium salt **2.15**, ($\delta(^{31}P)$ = 271 ppm)[36] changes by 103 ppm when it is coordinated by pyridine ($\delta(^{31}P)$ = 168 ppm),[36] whereas only a 16 ppm difference is observed between [Mes*NP•Py]OTf **2.7** and Mes*NPOTf.

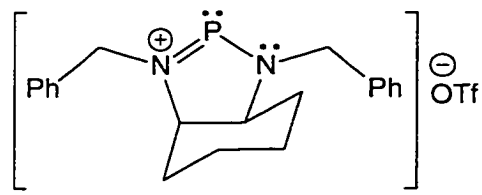

2.15

The $\delta(^{31}P)$ value for the [Mes*NP•Dipy]OTf **2.9** complex ($\delta(^{31}P)$ = 54 ppm)[216] is identical to that of Mes*NPOTf ($\delta(^{31}P)$ = 55 ppm[130]). However, the phosphorus nucleus in [Mes*NP•Dipy]OTf **2.9** ($\delta_{iso}(^{31}P)$ = 67 ppm), as determined from solid state ^{31}P CP/MAS NMR spectra, is deshielded with respect to that in Mes*NPOTf ($\delta_{iso}(^{31}P)$ = 52 ppm[232]). This suggests the molecular structure of [Mes*NP•Dipy]OTf **2.9** varies slightly between solution and in the solid state. The isotropic ^{31}P chemical shift of [Mes*NP•Py]OTf **2.7** ($\delta_{iso}(^{31}P)$ = 64 ppm) is marginally different from the solution value ($\delta(^{31}P)$ = 71 ppm[215]). The phosphorus nucleus in the phosphadiazonium-ligand-triflate

complexes **2.7**-**2.9** is considerably shielded with respect to the range of values reported for acyclic diaminophosphenium cations ($\delta(^{31}P)$ = 263 to 280 ppm; $\delta(^{31}P)$ of $[(Mes^*N(H))_2P]GaCl_4$ = 281 ppm[25]), but are nearer to those reported for amino-iminophosphines ($\delta(^{31}P)$ = 198 to 305 ppm; $\delta_{iso}(^{31}P)$ = 144 to 182 ppm), individual values for diaminophosphenium cations and are given amino-iminophosphines in Table 2.3.

Solution ^1H NMR spectra of [Mes*NP•Lg]OTf (Lg = Py **2.7** or Qncd **2.8**) show that the protons associated with the ligand are deshielded (Lg = Py **2.7**, $\delta(^1H)$ = 7.88, 8.35, 8.82 ppm; Lg = Qncd **2.8**, $\delta(^1H)$ = 1.98, 2.16, 3.43 ppm)[215,216] with respect to those in the free ligand (Py $\delta(^1H)$ = 7.16, 7.55, 8.52 ppm; Qncd $\delta(^1H)$ = 1.48, 1.65, 2.76 ppm), but for Lg = Qncd **2.8**, the values are comparable to those found in the aluminatodiiminophosphane-quinuclidine complex **2.4** ($\delta(^1H)$ = 1.81, 2.03, 2.90 ppm[91]). This suggests that the complexes [Mes*NP•Lg]OTf (Lg = Py **2.7** or Qncd **2.8**), are present in solution. The $\delta(^1H)$ and $\delta(^{13}C)$ resonances corresponding to the ligand in [Mes*NP•Lg]OTf (Lg = Py **2.7**, Qncd **2.8**, or Dipy **2.9**) show no indication of coupling with the phosphorus nucleus. The carbon nuclei of the quinuclidine unit in [Mes*NP•Qncd]OTf **2.8** are more shielded ($\delta(^{13}C)$ = 20.8, 24.6, 31.4 ppm)[216] than those in the free ligand ($\delta(^{13}C)$ = 24.0, 27.2, 48.2 ppm) and in the aluminatodiiminophosphane-quinuclidine complex **2.4** ($\delta(^{13}C)$ = 21.5, 25.1, 45.7 ppm[91]). The greater shielding is perhaps a consequence of the stronger interaction between the ligand and phosphorus centres in [Mes*NP•Qncd]OTf **2.8** than that in the aluminatodiiminophosphane-quinuclidine complex **2.4**. For [Mes*NP•Lg]OTf (Lg = Py **2.7** or Qncd **2.8**), the chemical shifts of the hydrogen and carbon nuclei nearest the nitrogen centre of the ligand exhibited the largest differences. The solution ^1H and ^{13}C NMR spectra of [Mes*NP•Py]OTf **2.7** reveal one set of signals for the *ortho*- and *meta*-protons and carbon nuclei associated with the pyridine ligand. Similarly, a single resonance for each

type of methylene group on the quinuclidine ligand was observed for [Mes*NP•Qncd]OTf **2.8**. Consequently, this suggests that the ligands have free rotation about the P–N(Lg) bond in solution.

The proton and carbon chemical shifts associated with the Mes* substituent in the [Mes*NP•Lg]OTf complexes (Lg = Py **2.7**, Qncd **2.8**, or Dipy **2.9**) showed small differences from that observed for Mes*NPOTf. The Mes* ring carbons and the *meta*-protons in complex [Mes*NP•Dipy]OTf **2.9** have larger phosphorus coupling J values.

The solution ^{1}H NMR spectra of [Mes*NP•Dipy]OTf **2.9** shows a single set of pyridyl resonances in which the protons are slightly deshielded ($\delta(^{1}H)$ = 7.98, 8.54, 8.88, 8.99 ppm)[216] with respect to those in the free ligand ($\delta(^{1}H)$ = 7.22, 7.73, 8.36, 8.56 ppm). Furthermore, the $\delta(^{13}C)$ values associated with the 2,2'-dipyridyl unit in [Mes*NP•Dipy]OTf **2.9** ($\delta(^{13}C)$ = 122.3, 124.6, 128.7, 144.8, 148.1 ppm)[216] also differ from those observed in free ligand ($\delta(^{13}C)$ = 121.3, 124.3, 137.4, 149.7, 156.7 ppm). Both observations from the ^{1}H and ^{13}C NMR spectra indicate a retention of the phosphadiazonium-2,2'-dipyridyl interaction in solution, whereas the $\delta(^{31}P)$ value does not provide conclusive evidence for complex formation. Of note is the deshielding of the protons in the 3,3' position of the ligand in **2.9** ($\delta(^{1}H)$ = 8.88 ppm, $\Delta\delta(^{1}H)$ = 0.52 ppm),[216] resulting from the steric repulsion generated by the *cisoid* conformation of the 2,2'-dipyridyl ligand in [Mes*NP•Dipy]OTf **2.9** as depicted in Figure 2.5. This observation is consistent with other transition metal complexes containing a chelating 2,2'-dipyridyl ligand.[233-235]

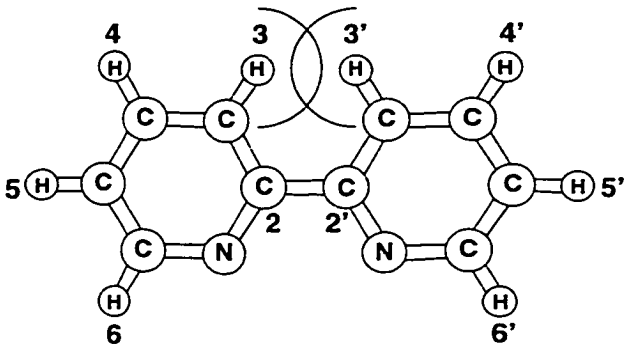

Figure 2.5: Hydrogen and carbon labeling scheme for the 2,2'-dipyridyl ligand in [Mes*NP•Dipy]OTf **2.9**. The steric interaction between the 3,3' protons is illustrated by the overlapping arcs.

IR spectra of the [Mes*NP•Lg]OTf (Lg = Py **2.7**, Qncd **2.8**, or Dipy **2.9**) complexes, prepared as paraffin oil mulls, show strong intensity peaks corresponding to stretching frequencies for the SO_3 and CF_3 fragments of the triflate group. Spectroscopic features including $\delta(^{19}F)$ values and IR stretching frequencies related to the triflate group in complexes **2.7**-**2.9** are discussed in Chapter 6. In general, the IR spectra are too complicated to assign stretching frequencies to specific bond types within the complexes. Nevertheless, the IR spectrum of [Mes*NP•Dipy]OTf **2.9** exhibits a resonance at 1446 cm^{-1}.[216] This corresponds to a N–C bond stretching frequency in the 2,2'-dipyridyl ligand and its value is consistent with that observed in 2,2'-dipyridyl-aluminum trihalide complexes where the ligand has a bidentate interaction with the aluminum centre.[236]

2.3: Conclusions: General Bonding and Structural Implications for [Mes*NP•Lg]OTf, where Lg = Py (2.7), Qncd (2.8), or Dipy (2.9)

Data from the crystallographic and NMR spectroscopic measurements show that new compounds, [Mes*NP•Lg]OTf (Lg = Py **2.7**, Qncd **2.8**, or Dipy **2.9**) are formed by the reaction of Mes*NPOTf with nitrogen bases. Furthermore, the data suggest that these complexes are structurally similar in solution and in the solid state.

The monodentate [Mes*NP•Lg]OTf complexes (Lg = Py **2.7** or Qncd **2.8**) represent a new class of disubstituted π-phosphino-bonding environment and are distinct from other disubstituted phosphino-environments such as amino-iminophosphines and compounds with a diaminophosphenium cation. These new phosphorus bonding environments including [Mes*NP•Dipy]OTf **2.9**, are only accessible via coordination, as a consequence of the Lewis acidic properties of the triflate-substituted iminophosphine Mes*NPOTf.[216]

The cationic unit of the [Mes*NP•Qncd]OTf complex **2.8**, can be envisaged as a structural isomer of the diaminophosphenium cation $P(NR_2)_2^+$, where both fragments are related by a hypothetical 1,3-migration of a substituent on nitrogen, as illustrated in Figure 2.6. Hence, the [Mes*NP•Qncd]OTf complex **2.8**, represents a model of the σ-coordination intermediate **2.16**, which is postulated to form during the synthesis the diaminophosphenium salt $[(Mes*N(H))_2P]GaCl_4$ **2.17**, (Figure 2.7) from the addition of $Mes*NH_2$ to $[Mes*NP•C_6H_6]GaCl_4$.[25]

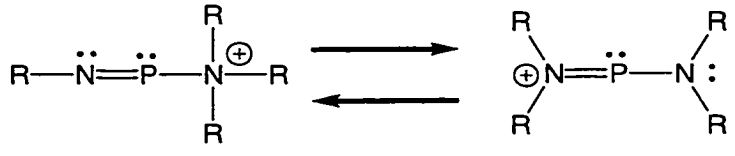

Figure 2.6: The relationship between an ammonium-iminophosphine cation (left), the cationic unit found in [Mes*NP•Qncd]OTf **2.8**, and a diaminophosphenium cation (right), through a hypothetical 1,3-migration of a substituent on nitrogen.

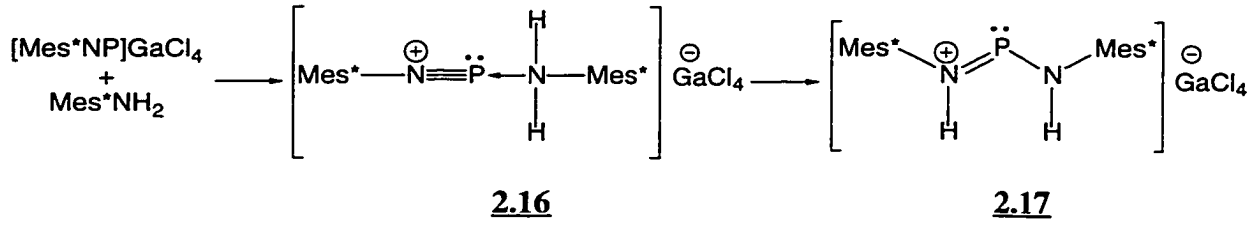

2.16 **2.17**

Figure 2.7: The postulated formation of an intermediate, σ-amino-phosphadiazonium complex **2.16**, from the reaction of a phosphadiazonium cation and a primary amine.

The bonding relationship between the [Mes*NP•Lg]OTf complexes (Lg = Py **2.7** or Qncd **2.8**), amino-iminophosphines, $RNPNR_2$ and diaminophosphenium cations, $(R_2N)_2P^+$ is shown by the relationship of resonance structures in Figure 2.8. It is apparent from comparisons of the P–N(Lg) bond lengths in [Mes*NP•Lg]OTf (Lg = Py **2.7** or Qncd **2.8**) that the interaction between the ligand and phosphorus centre involves only σ-bonding, whereas the phosphorus-substituent bonding in amino-iminophosphines and diaminophosphenium salts has a π-component resulting from lone pair π-conjugation. The P–N(Lg) bonding in [Mes*NP•Qncd]OTf has no π-component due to the quaternized nitrogen centre of the ligand, but both pyridine and 2,2'-dipyridyl contain a low-energy LUMO of π* character. Hence these compounds can act as π-Lewis acids and accordingly both types of ligands are used frequently to coordinate metals in low-oxidation states.[237] However, the long P–N(Lg) bond lengths in the [Mes*NP•Lg]OTf complexes (Lg = Py or Dipy) suggest that any π-component of the P–Lg bond is weak or negligible. Therefore, the phosphadiazonium-ligand-triflate complexes **2.7**-**2.9** have only one set of π-interactions involving phosphorus and that is with the imino-centre.

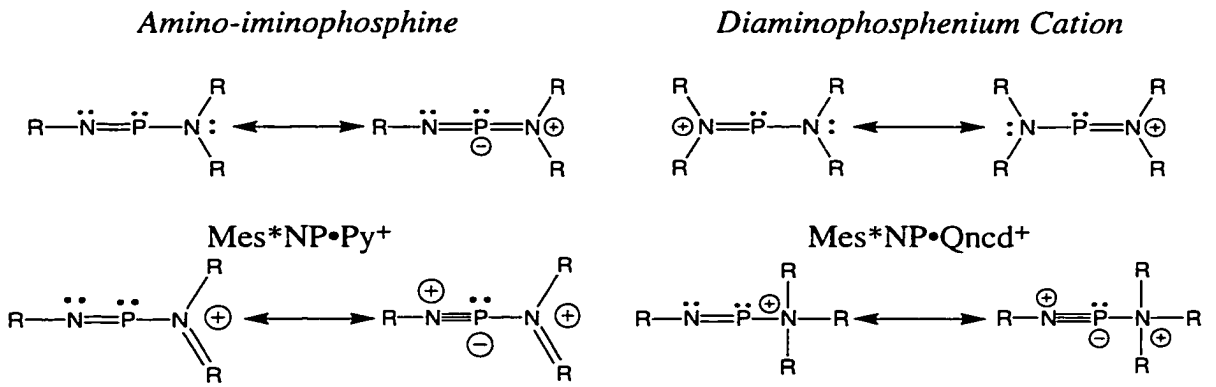

Figure 2.8: Comparison of bonding models for amino-iminophosphines and diaminophosphenium cations with those of the phosphadiazonium-ligand-triflate complexes [Mes*NP•Lg]OTf (Lg = Py **2.7** or Qncd **2.8**).

The [Mes*NP•Dipy]OTf complex **2.9**, represents an isolated and characterized example of a chelated π-phosphino-bonding environment that exists in both solution and the solid state. In contrast, the phosphadiazonium-diselenophosphinate complex [Mes*NP]$Se_2P(^tBu)_2$, is reported to dissociate in solution.[137] The [Mes*NP•Dipy]OTf complex **2.9** features a trisubstituted, pyramidal phosphorus centre and is an example of an iminophosphide bonding environment which is discussed further in Section 3.3. The bis-coordinated phosphinidene complex **2.18**,[97] differs from [Mes*NP•Dipy]OTf **2.9**, by having an amino NR_2, rather than imino NR, substituent. However, **2.18** can be considered as having some iminophosphide bonding character (Figure 2.9). There is evidence to support lone pair π-conjugation between the phosphorus centre and the amino-substituent (i.e., planar PNR_2 geometry) in **2.18**. However, the shorter P–N bond in [Mes*NP•Dipy]OTf (d(P–N(Mes*) = 1.497(4) Å)[216] as compared with $[Cy_2NP•DBN_2](PF_6)_2$ **2.18**, (d(P–N) = 1.628(5) Å),[97] suggests a stronger π-bonding in the former.[97]

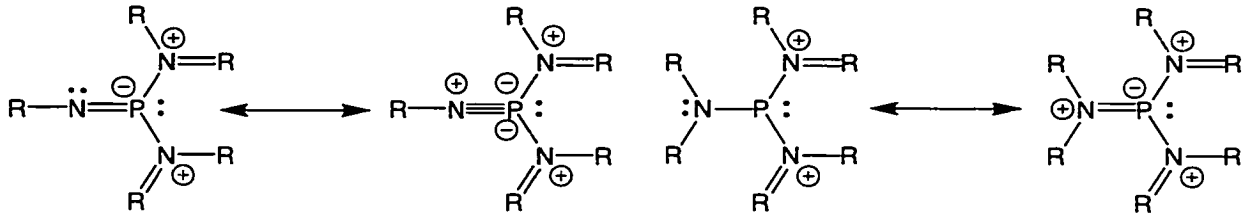

Mes*NP•Dipy$^+$ **2.9** $\qquad$ $(Cy_2N)P•DBN_2^{2+}$ **2.18**

Figure 2.9: Comparison of bonding models for the phosphadiazonium-ligand unit in [Mes*NP•Dipy]OTf **2.9** and the bis-amine-phosphinidene fragment in the $[Cy_2NP•DBN_2](PF_6)_2$ complex **2.18**.

The bidentate chelation of the phosphorus centre in [Mes*NP•Dipy]OTf **2.9** is expected on the premise that the Lewis basicity of each nitrogen centre in 2,2'-dipyridyl is greater than that of the triflate group. Although transition metal complexes with a mono-coordinating 2,2'-dipyridyl ligand are known,[238] there is no evidence to support this mode of ligand coordination in [Mes*NP•Dipy]OTf. Furthermore, from calculations, using ab initio methods, the coordination of two ammonia ligands to a model phosphadiazonium cation HNP^+, is energetically favourable.[223] The [Mes*NP•Lg]OTf complexes (Lg = Py **2.7** or Qncd **2.8**) may have a bonding interaction with the triflate anion, albeit, extremely weak, whereas the bidentate coordination of the ligand in [Mes*NP•Dipy]OTf **2.9**, causes a predominantly ionic cation-anion interaction. Importantly, this suggests that the Lewis acidity of the Mes*NP•Dipy$^+$ unit is weaker than that for complexes Mes*NP•Lg$^+$ with a monodentate ligand interaction (Lg = Py or Qncd). It is known that complexes with polydentate ligands are kinetically and thermodynamically more stable than complexes containing multiple ligand of a similar type, but with a single donor site,[239] and it is possible that the phosphorus-ligand interactions in [Mes*NP•Dipy]OTf **2.9** are stabilized by the chelate effect.

Table 2.1: Comparison of P–N(Lg) bond lengths and N-P-N bond angles for [Mes*NP•Lg]OTf (Lg = Py **2.7**, Qncd **2.8**, or Dipy **2.9**) with the P–N(R_2) bond lengths and N-P-N bond angles in amino-iminophosphines and acyclic diaminophosphenium salts.

Compound	*d*(P–N(Lg/R)) (Å)	∠(N-P-N) (°)	∠((Mes*)N-P-O(Tf)) (°)	Reference
Phosphadiazonium-ligand-triflate Complexes				
[Mes*NP•Qncd]OTf (**2.8**)	1.933(2)	103.7(1)	112.5(1)	216
[Mes*NP•Py]OTf (**2.7**)	1.958(8)	107.8(4)	128.8(2)	215
[Mes*NP•Dipy]OTf (**2.9**)	2.065(4)	106.3(2)		216
	2.066(4)	113.0(2)		
Amino-iminophosphines				
Mes*NPN(H)Mes*	1.624(2)	104.0(1)		171
Mes*NPN(H)^{t}Bu	1.632(6)	110.4(3)		112
Mes*NPN(H)Mes*	1.633(8)	103.8(5)		240
Mes*NPNTmp	1.646(5)	105.0(2)		241
Mes*NPNMe_2	1.651(3)	115.9(3)		242
Mes*NPN(H)CPh_3	1.651(4)	107.4(2)		112
Mes*NPN(^{i}Pr)$_2$	1.656(2)	105.6(1)		242
^{t}BuNPN($SiMe_3$)^{t}Bu	1.658(4)	104.9(2)		243
Mes*NPN($SiMe_3$)$_2$	1.668(2)	109.3(1)		244
Mes*NPN($SiMe_3$)N($SiMe_3$)$_2$	1.672(4)	107.3(2)		245
Me_3SiNPN($SiMe_3$)$_2$	1.674(1)	108.4(1)		243
Acyclic Diaminophosphenium Salts				
[P(N^{i}Pr$_2$)$_2$]$GaCl_4$	1.59(1), 1.60(1)	117.0(7)		24
Mes*N(H)PN(^{i}Pr)$_2$]OTf	1.602(1)	107.8(1)		33
[P(N^{i}Pr$_2$)$_2$]$AlCl_4$	1.611(4), 1.615(4)	114.8(2)		27,28
[P(N(H)Mes*)$_2$]$GaCl_4$	1.617(3)	103.9(2)		25

Table 2.2: Comparison of P–N(Lg) bond lengths in complexes featuring inter- and intra-molecular phosphorus-nitrogen coordination. The sigma-lambda notation indicates the type of phosphorus bonding environment (not including the contribution by the ligand). Complexes are ordered by increasing *d*(P–N(Lg)). Words or letters in bold type indicate the connecting centres of the P–N(Lg) interaction.

Compound		*d*(P–N(Lg)) (Å)	Coordination, Environment	Reference
[**P**NCy_2•**DBN**$_2$](PF_6)		1.752(4), 1.766(5)	Inter, σ^1, λ^1	97
[**P**S_2•**Py**$_2$]Br	(**2.11**)	1.77(1), 1.87(1)	Inter, σ^2, λ^4	17
[**P**($N(^iPr)_2$)$_2$•**DBN**]PF_6		1.796(3)	Inter, σ^2, λ^2	97
K[**OP**$(O)_2$•NH_3]		1.800(4)	Inter, σ^3, λ^5	180
[(Mes*N)$_2$**P**•**4-DMAP**$_2$]Br		1.812(4), 1.830(4)	Inter, σ^2,λ^5	16
(Mes*N)$_2$(Br)**P**•**4-DMAP**		1.815(5)	Inter, σ^3,λ^5	16
[**P**S_2•**Py**$_2$]I	(**2.11**)	1.831(1)	Inter, σ^2, λ^4	17
[**P**(Me)S($Me_2NCH_2CH_2NMe$)]BPh_4		1.838(3)	Intra, σ^3, λ^4	197
F_5**P**•NH_3		1.842(2)	Inter, σ^5, λ^5	246
Cl_4**P**•(NC_5H_4NMe-2)		1.845(4)	Inter, σ^5,λ^5	247
P(Cl)S_2•**Py**	(**2.12**)	1.849(2)	Inter, σ^3, λ^5	186
[**P**Ph($Me_2NCH_2CH_2NMe$)]BPh_4		1.88(1)	Intra, σ^2, λ^2	248
F_5**P**•**Py**	(**2.10**)	1.885(4)	Inter, σ^5, λ^5	185
[($C_6H_4O_2$-1,2)$_2$**P**•**Dipy**]PF_6	(**2.13**)	1.896(4), 1.898(4)	Inter, σ^4, λ^4	202
Cl_4**P**(**N**MeC(Cl)NMe)		1.91(4), 1.85(6)	Inter, σ^4, λ^4	203
PS_2($C_6H_2(^tBu)_2$-4,6,CH_2NMe_2-2)		1.921(8)	Intra, σ^3, λ^5	199
[Mes*N**P**•**Qncd**]OTf	(**2.8**)	1.933(2)	Inter, σ^1, λ^3	216
[Cl**P**($MeNCH_2CH_2$)$_3$**N**)]PCl_6		1.934(8)	Intra, σ^4, λ^4	249
F_4**P**($Me_2NCH_2CH_2NMe$)		1.957(2)	Intra, σ^5, λ^5	196
[Mes*N**P**•**Py**]OTf	(**2.9**)	1.958(8)	Inter, σ^1, λ^3	215
[**P**(MeNC(O)NMe)Cl($Me_2NCH_2CH_2NMe$)]BPh_4		1.975(4)	Intra, σ^4, λ^4	250
PhF_3**P**($OC_{10}H_5$**N**-8,Me-7)		1.980(3)	Inter, σ^5,λ^5	251
P(NMe_2)F_2($Me_2NCH_2CH_2NMe$)		1.987(1)	Intra, σ^4, λ^4	252
P(Ph)F_3($OC(O)CH_2NMe_2$)		2.013(4)	Inter, σ^5, λ^5	194
Cl_5**P**•**Pyz**		2.021(5)	Inter, σ^5,λ^4	188
PS_2($C_6H_2(^tBu)_2$-4,6,**N**(Me)^{i}Pr-2)		2.023(8)	Intra, σ^3, λ^5	198
P($N(SiMe_3)AlCl_2N(SiMe_3)$)•**Qncd**	(**2.4**)	2.038(9)	Inter, σ^2, λ^3	91
[Mes*N**P**•**Dipy**]OTf	(**2.9**)	2.065(4), 2.066(4)	Inter, σ^1, λ^3	216
[**P**H(C_6H_4($CHNMe_2$)$_2$-2,6)]PF_6		2.068(4), 2.082(3)	Intra, σ^2, λ^2	212
[**P**(Ph_2)F($Me_2NCH_2CH_2NMe$)]PF_6		2.070(3)	Intra, σ^4, λ^4	253
(**P**($N(SiMe_3)AlCl_2N(SiMe_3)$)$_2$•**Tmeda**	(**2.5**)	2.110(6)	Inter, σ^2, λ^3	91
P($OPh)_3$($OC_6H_2$$^tBu$-2-Me-4-CH)$_2$**N**(Me)		2.143(3),	Intra, σ^5, λ^5	204
PPh_2($C_{10}H_6NMe_2$-8)		2.706(6), 2.729(6)[a]	Intra, σ^3, λ^3	206
P($C_{10}H_6NMe_2$-8)$_3$		2.805†, 2.844†, 2.853†	Intra, σ^3, λ^3	208
PO(OEt)$_2$($C_{10}H_6NMe_2$-8)		2.869(3)	Intra, σ^4, λ^5	47
P($C_{10}H_6CH_2NMe_2$-8)$_3$		2.999†	Intra, σ^3, λ^3	208
OP($MeNCH_2CH_2$)$_3$**N**)		3.137(3)	Intra, σ^4, λ^5	254
PPh($OC_6H_2$$^tBu$-2-Me-4-CH)$_2$**N**(Me)		3.152(3)	Intra, σ^3, λ^3	204

([a]) Value from second structurally different molecule in the asymmetric unit.

Table 2.3: Comparison of solution and solid-state isotropic $\delta(^{31}P)$ values for [Mes*NP•Lg]OTf (Lg = Py **2.7**, Qncd **2.8**, or Dipy **2.9**) with iminophosphines and acyclic diaminophosphenium salts. Compounds are listed by increasing $\delta_{soln}(^{31}P)$ values. All values in ppm.

Compound	$\delta_{soln}(^{31}P)$	$\delta_{iso}(^{31}P)$	Reference
[Mes*NP•Dipy]OTf (**2.9**)	54	67	216
Mes*NPOTf	55	52	130, 232
[Mes*NP•Py]OTf (**2.7**)	71	64	215
[Mes*NP•Qncd]OTf (**2.8**)	144	–	216
Amino-iminophosphines			
$Mes*NPN(Ph)_2$	198	144	255
$Mes*NPNMe_2$	203	182	256,119
Mes*NPN(H)^{t}Bu	210		112
$Mes*NPN(Et)_2$	225	269	256, 119
$Mes*NPN(H)CPh_3$	226		112
Mes*NPNH(Tipp)	235		256
$Mes*NPN(^iPr)_2$	268	272	256, 119
Mes*NPN(H)Mes*	272	281	240, 255
$Mes*NPN(^tBu)_2$	305		256
$Mes*NPN(SiMe_3)_2$	327		256
Acyclic Phosphenium Cations			
[Mes*N(H)PN(^{i}Pr)$_2$]OTf	261		33
$[(Et_2N)_2P]AlCl_4$	263		257
$[(Et_2N)_2P]OTf$	263		41
$[(Me_2N)_2P]AlCl_4$	264		257
$[(Mes*N(H))_2P]GaCl_4$	272	281	25
[Mes*N(H)PN(Me)$_2$]OTf	275		33
$[(Mes*N(H))_2P]OTf$	280		33
$[(^iPr_2N)_2P]BPh_4$	312		23
$[(^iPr_2N)_2P]AlCl_4$	313		27
$[(^iPr_2N)_2P]GaCl_4$	313		23
$[((Me_3Si)_2N)_2P]AlCl_4$	450		257

Chapter 3: Synthesis and Characterization of Phosphadiazonium and Iminophosphine Complexes involving an Imidazol-2-ylidene Ligand

3.1: Introduction: Overview of the Coordination Chemistry of Phosphorus involving Carbene Ligands

The coordination of chemistry of carbenes as ligands has dramatically expanded with the discovery of stable ylidenes (singlet carbenes).[258,259] At present, there is a diverse range of ylidenes, where the disubstituted carbon centre is contained in an acyclic,[260-263] saturated,[264,265] or unsaturated[258,266-269] heterocyclic framework. The majority of studies focused on coordination chemistry using carbenes as ligands, including the research presented in this chapter, use a derivatized form of imidazol-2-ylidene **3.1**, hereafter abbreviated as Im, for which a convenient synthesis has been reported.[266]

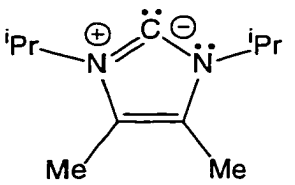

3.1

Since the time of their discovery, ylidenes such as Im, have been shown to be strongly nucleophilic and highly basic (pK_a (in DMSO) of Im•H$^+$ = 24,[270] c.f., Py•H$^+$ (in DMSO) is 3.45[219]). These two properties enable ylidenes to form complexes even with the weakest of Lewis acids. Importantly, many newly discovered ylidene complexes represent a new bonding environment for the Lewis acidic main-group element involved and are described in several comprehensive review articles.[271-273]

In contrast to the large number of reported phosphorano- and phosphino-complexes involving a nitrogen, phosphine, or chalcogen group as the Lewis basic

component, at present, only ten phosphorus-ylidene complexes have been reported, and of these, only two complexes feature a phosphorano-bonding environment; tetraflurorophenyl-phosphoranide-ylidene[274] **3.2** and diphenylselenophosphoryl-ylidene[48] **3.3**. The other types of phosphorus-ylidene complexes contain either a σ- or π-phosphino-bonding environment.

The phosphenium-ylidene chloride and tetrachloroaluminate salts **3.4** (An = Cl^- or $AlCl_4^-$)[48] are examples of compounds featuring a phosphenium cation which is stabilized through coordination and not by lone pair π-conjugation. The phosphenium-ylidene tetrachloroaluminate salt **3.4** (An = $AlCl_4^-$), has reactivity analogous to that of a tertiary σ-phosphine. For example, complex **3.4** (An = $AlCl_4^-$) is a ligand with respect to late transition metal centres MCl_3 (M = Pd or Pt), forming compounds of the type **3.5**.[275] Furthermore, complex **3.4** (An = $AlCl_4^-$) is oxidized by elemental selenium resulting in the diphenylselenophosphoryl-ylidene complex **3.3**.[48]

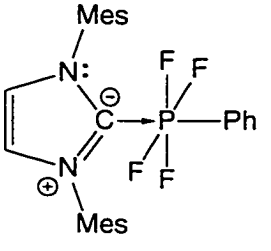

3.2

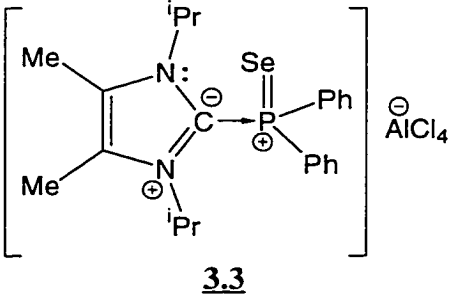

3.3

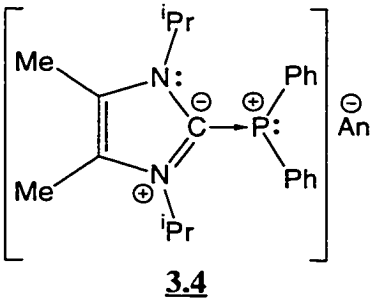

3.4

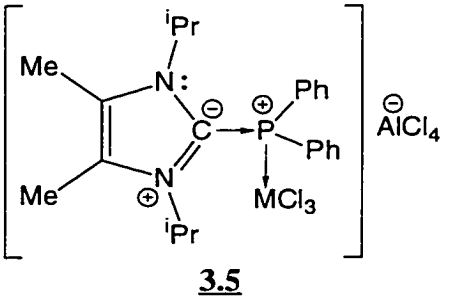

3.5

The strong nucleophilicity of ylidenes is demonstrated by their reactions with cyclic polyphosphines.[276,277] The resulting complexes **3.6** (R = Ph or R = CF_3), and **3.7** can be considered to be either phosphaiminoureas (a type of phosphaalkene), featuring a highly polarized π-P-C bond, or phosphinidene complexes **3.8**, which contain a coordinating interaction between a phosphorus and a carbene centre (Figure 3.1). Evidence in support of the phosphinidene bonding character for **3.8** (R = Ph), is provided by the synthesis and characterization of complex **3.9**, which contains two Lewis acidic borane units coordinating with a phosphinidene centre.[278] The isolation of complexes **3.6**-**3.7** compounds represent a new method for synthesizing phosphaalkenes using coordination chemistry.

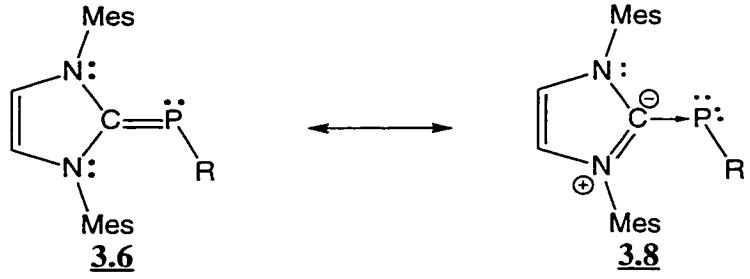

Figure 3.1: Two representative resonance structures describing the bonding in phosphaiminoureas.

Compounds containing a phosphino-diaminomethylene fragment $PC(NR_2)_2$, phosphaiminoureas **3.10** and phosphamethine cyanines **3.11**, have been isolated and

characterized prior to the discovery of phosphino-ylidene complexes.[279,280] Phosphamethine cyanines, also referred to as 2-phosphaallylic salts, can be considered examples of complexes containing a phosphorus cation coordinated by two ylidene-type ligands **3.13**, as shown in Figure 3.2.[279] The spectroscopic and structural features of phosphaiminoureas **3.10** and phosphamethine cyanines **3.12** are discussed in comparison with those of phosphorano- and phosphino-ylidene complexes in the following sections.

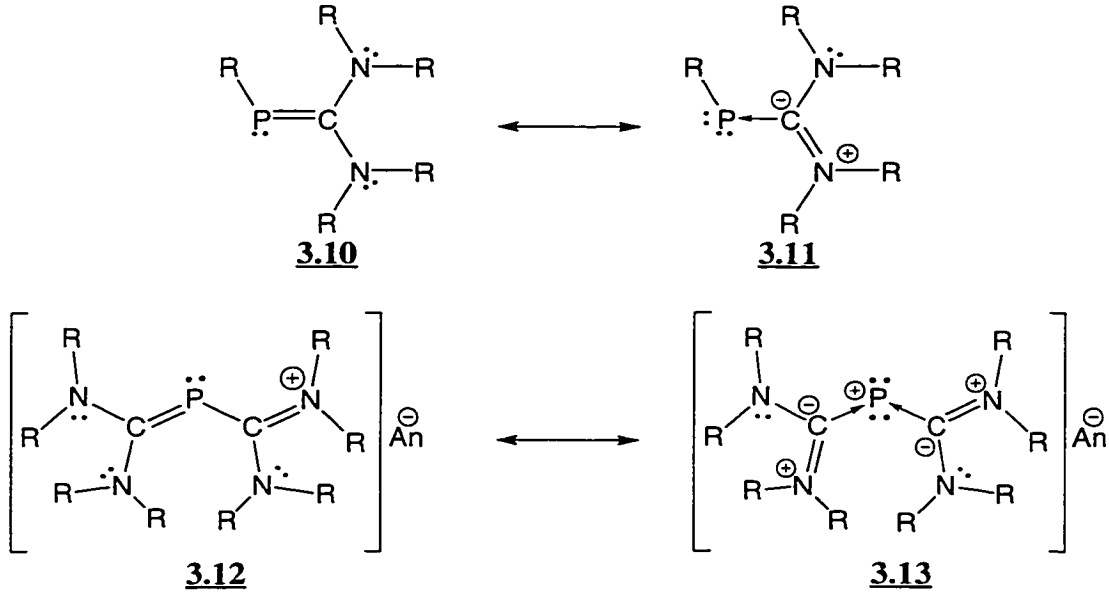

Figure 3.2: Representative resonance structures describing the bonding in phosphaiminoureas (top, **3.10**-**3.11**) and phosphamethine cyanines (bottom, **3.12**-**3.13**).

A study was preformed by the author of this thesis, to determine the reactivity of two types of Lewis acidic iminophosphines, Mes*NPCl and Mes*NPOTf, with the imidazol-2-ylidene Im, **3.1**. The *P*-aryl-iminophosphine Mes*NPPh, also was shown to be Lewis acidic, as a complex is postulated to form when combined with Im. The resulting Lewis acid-base complexes **3.14**-**3.17** represent distinctly new bonding

environment for phosphorus. Descriptions, structural and spectroscopic comparisons of these new complexes are presented in the following sections.

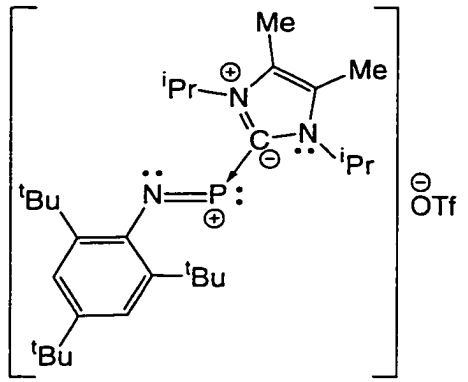

3.14

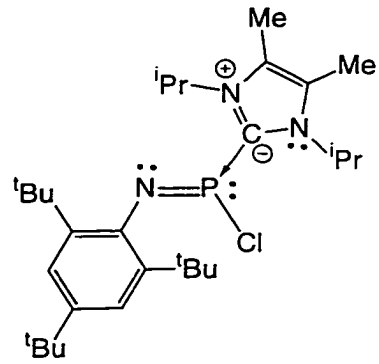

3.15

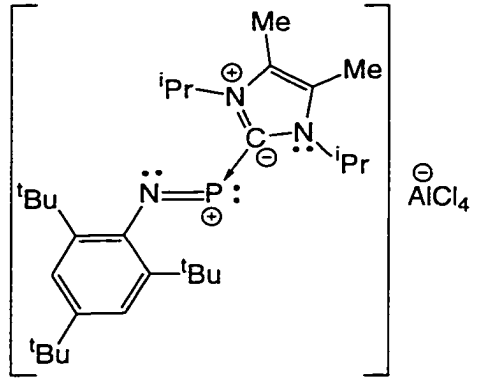

3.16

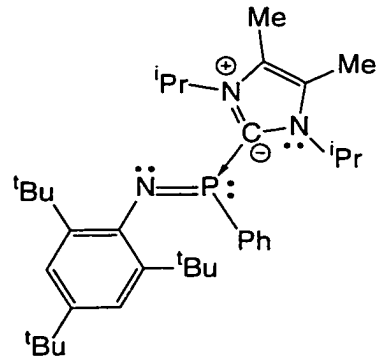

3.17

3.2: Results and Discussion

3.2.1: Synthesis of Phosphadiazonium-imidazol-2-ylidene Complexes ([Mes*NP•Im]An, where An = OTf^- (3.14) or $AlCl_4^-$ (3.16)) and Iminophosphine-imidazol-2-ylidene-Complexes (Mes*NP(R)•Im, where R = Cl (3.15) or Ph (3.17))

Complexes **3.14** and **3.15** were synthesized by the addition of imidazol-2-ylidene Im, to Mes*NPX, using a 1:1 stoichiometry.[215] For X = OTf, the solution immediately developed an intense dark purple colour, whereas for X = Cl, the solution gradually

turned orange.[215] Both complexes crystallized on removal of the solvent and were characterized using crystallography, multinuclear NMR, IR and elemental analysis.[215] 31-P NMR spectra of the reaction mixtures contained dominant signals corresponding to the complexes. However, various amounts of other phosphorus species were also present. In a separate experiment, one side product was tentatively identified, based on data from ^{31}P NMR spectroscopy, as the amino-iminophosphine Mes*NPN(H)Mes* ($\delta(^{31}P) = 268$ ppm[240]). A second side product was tentatively assigned, based on data from ^{1}H NMR spectroscopy ($\delta(^{1}H) = 8.91$ ppm) as an imidazolium salt **3.18** (An = Cl^- or OTf^-), the conjugate acid of the imidazol-2-ylidene Im **3.1**.

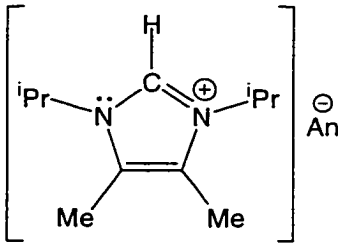

3.18

Apart from the sensitivity of complexes **3.14**-**3.15** on exposure to the atmosphere, the analytically pure isolation of these compounds depended primarily on the type of reaction solvent and rate of reagent addition. For example, when toluene is used as the reaction solvent, the addition of imidazol-2-ylidene to Mes*NPOTf resulted in a brown coloured reaction mixture. The ^{31}P NMR spectrum of this mixture showed a number of unidentified species. Reactions which involved the rapid of addition of the imidazol-2-ylidene, less than 10 minutes, resulted in increased amounts of side products, including Mes*NPN(H)Mes* and the imidazolium salt **3.18**. Optimized reaction conditions which maximized the yields of [Mes*NP•Im]OTf **3.14**, and Mes*NP(Cl)•Im **3.15**, involved the slow addition, 45 to 60 minutes, of imidazol-2-ylidene to Mes*NPX using benzene as the

reaction solvent.[215] The isolated complexes **3.14** and **3.15** were shown, by data from ^{31}P NMR spectroscopy, to be inert when redissolved in dichloromethane. Alternatively, [Mes*NP•Im]OTf can be synthesized by the addition of imidazol-2-tellurone TeIm, to Mes*NPOTf, using a 1:1 ratio, with precipitation of elemental tellurium, see Section 5.2.1. The [Mes*NP•Im]$AlCl_4$ **3.16** complex was synthesized by chloride abstraction from Mes*NP(Cl)•Im using Al_2Cl_6 in a 2:1 stoichiometry.

A bright yellow crystalline solid was isolated from the addition of imidazol-2-ylidene Im, to the light blue *P*-phenyl-iminophosphine Mes*NPPh, in a 1:1 ratio, using n-pentane as the reaction solvent. The product was shown to be polycrystalline and unsuitable for single crystal X-ray diffraction studies. Nevertheless, based on data from ^{31}P, ^{1}H, and ^{13}C NMR spectroscopy, the product is postulated to be the *P*-ylidene-*P*-phenyl-iminophosphine complex **3.17**. 31-P NMR spectra of the reaction mixture showed a broad but dominant signal for the complex accompanied by small amounts (< 5 % based on peak integration) of other unknown phosphorus containing species. Upon redissolving in dichloromethane, the Mes*NP(Ph)•Im complex **3.17** decomposed into several unidentified phosphorus containing species over a 12 hour period. Solutions of **3.17** in benzene or n-pentane exhibited thermochromic properties. Heating of the product above 60 °C changed the colour of the solution from dark yellow to a deep blue, matching the free *P*-phenyl-iminophosphine. The original colour of the solution returned upon cooling to room temperature. These observations suggest an association-disassociation equilibrium process between imidazol-2-ylidene Im, *P*-phenyl-iminophosphine, and the complex **3.17**.

3.2.2: Structural Features of the Phosphadiazonium-imidazol-2-ylidene Complex [Mes*NP•Im]OTf (3.14) and the Iminophosphine-imidazol-2-ylidene Complex Mes*NP(Cl)•Im (3.15)

The crystal structures of complexes [Mes*NP•Im]OTf **3.14** and Mes*NP(Cl)•Im **3.15**, (Figures 3.3 and 3.4) show a monodentate interaction between the central carbon of the ligand and the phosphorus centre associated with the Mes*NP unit.[215] The [Mes*NP•Im]OTf complex is composed of a cationic phosphadiazonium-ylidene unit and a triflate anion. In contrast, for the Mes*NP(Cl)•Im complex, a chlorine atom is bonded to the phosphorus centre of the Mes*NP•Im unit.[215] The crystal structures of the complexes show that the molecular units [Mes*NP•Im]OTf and Mes*NP(Cl)•Im are independent with no intermolecular interactions except for hydrogen bonding.

The P–C(Im) bond in [Mes*NP•Im]OTf **3.14** (d(P–C(Im) = 1.852(5) Å)[215] and Mes*NP(Cl)•Im **3.15** (d(P–C(Im) = 1.886(5) Å)[215] is longer than those reported for the phosphinidene-ylidene **3.6**-**3.7** (d(P–C(Im) = 1.746(6) to 1.784(2) Å), the phosphenium-ylidene **3.4** (An = $AlCl_4^-$), (d(P–C(Im) = 1.813(7) Å)[48] and the *P*-amino-*P*-aryl-phosphenium [MesPN(^{i}Pr)$_2$]$AlCl_4$ (d(P–C(Mes)) = 1.787(6) Å)[42] complexes, individual values for the phosphinidene-ylidene complexes are given in Table 3.1. The P–C(Im) bond in the tetraflurorophenylphosphoranide-ylidene complex **3.2** (d(P–C(Im) = 1.910(4) Å)[274] is significantly longer than that in [Mes*NP•Im]OTf **3.14** and Mes*NP(Cl)•Im **3.15**, which is surprising considering that phosphoranes such as PF_5Ph, are strong Lewis acids. In comparison, the P–C bonds in [Mes*NP•Im]OTf and Mes*NP(Cl)•Im are longer than those found in the phosphaiminoureas **3.10** and phosphamethine cyanines **3.12** (d(P–C(NR$_2$)$_2$) = 1.771(5) to 1.826(2) Å). Individual values for **3.10** and **3.12** are provided in Table 3.1.

For [Mes*NP•Im]OTf **3.14** and Mes*NP(Cl)•Im **3.15**, the P–C(Im) bond lengths (d(P–C(Im) = 1.852(5) Å and 1.886(5) Å, respectively)[215] are comparable or equivalent to

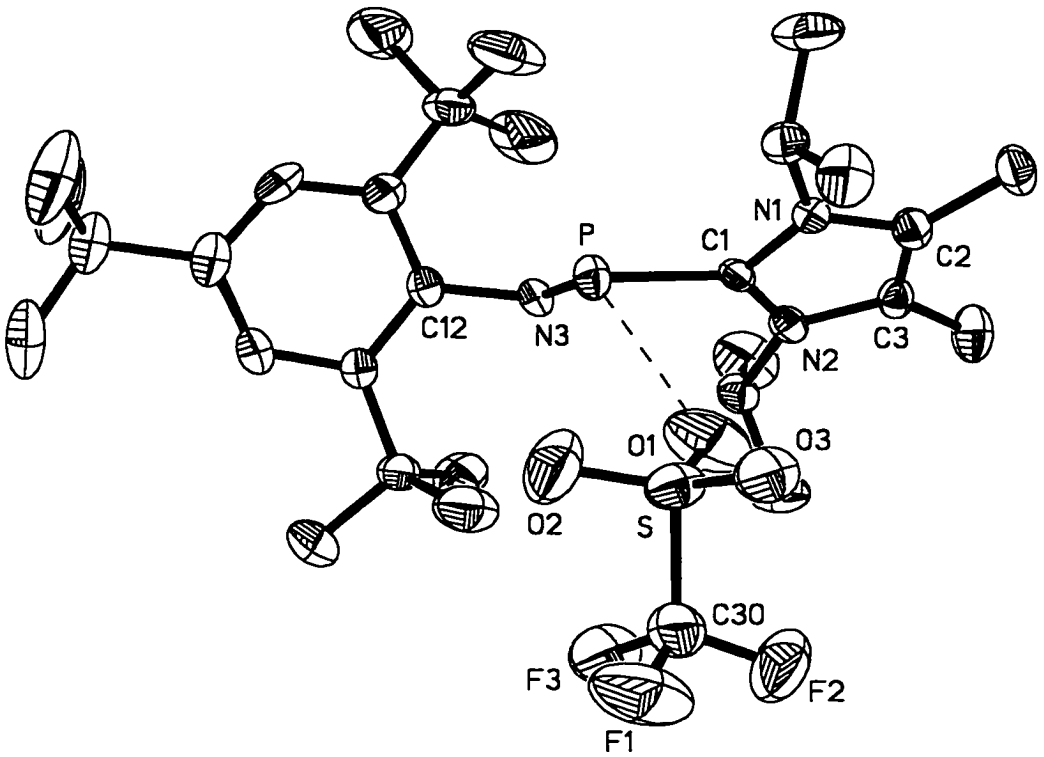

Figure 3.3: ORTEP-like view of [Mes*NP•Im]OTf **3.14**, drawn with 50% probability ellipsoids. The hydrogen atoms have been omitted for clarity. Important lengths (Å) and angles (°): P–N(3) 1.574(4), P–C(1) 1.852(5), P–O(1) 2.951(5), N(1)–C(1) 1.355(5), N(2)–C(1) 1.379(6), N(3)–C(12) 1.422(6), C(12)-N(3)-P 116.2(3), N(3)-P-C(1) 103.2(2), N(3)-P-O(1) 123.0(2), N(1)-C(1)-N(2) 107.5(4). Values reproduced from reference 215.

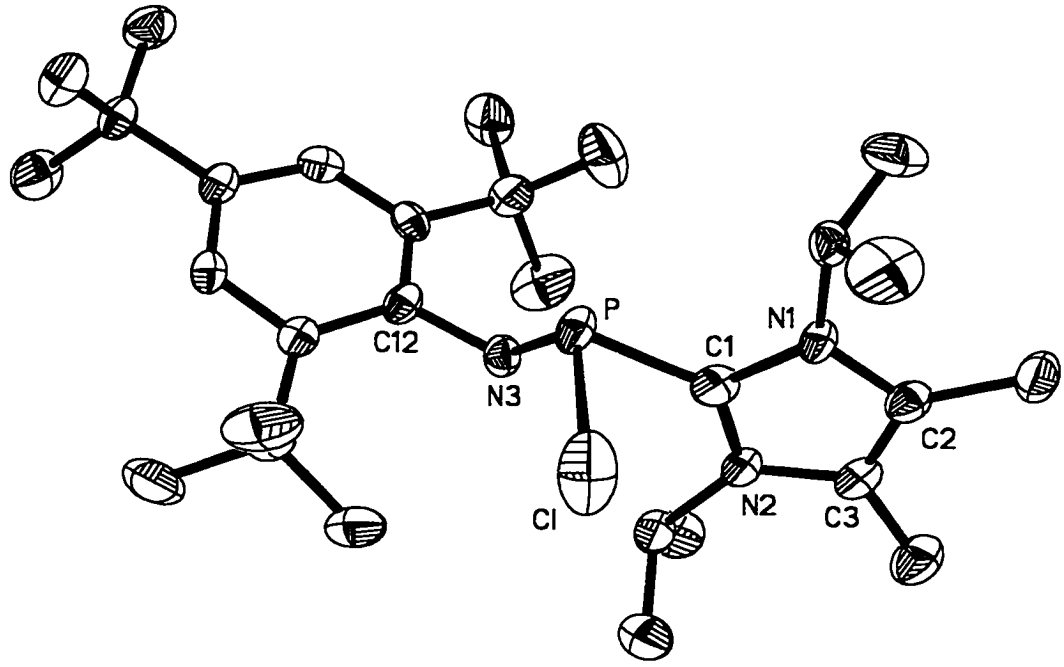

Figure 3.4: ORTEP-like view of Mes*NP(Cl)•Im **3.15**, drawn with 50% probability ellipsoids. The hydrogen atoms have been omitted for clarity. Important lengths (Å) and angles (°): P–N(3) 1.585(5), P–C(1) 1.886(5), Cl–P 2.471(2), N(1)–C(1) 1.365(7), N(2)–C(1) 1.370(7), N(3)–C(12) 1.446(7), C(12)-N(3)-P 102.2(4), N(3)-P-C(1) 101.9(2), N(3)-P-C(l) 101.9(2), N(1)-C(1)-N(2) 106.7(4). Values reproduced from reference 215.

P–C single bond values found in tertiary alkyl-phosphines (d(P–C) = 1.855[19] Å)[131] and *P*-alkyl-iminophosphines (d(P–C) = 1.837(3) to 1.883(3) Å), individual values for *P*-alkyl-iminophosphines are given in Table 3.1. In contrast, the phosphorus-carbon interactions in Cp*-iminophosphines (d(P–C(Cp*)) = 2.168(4), 2.122(4) Å, $Et_3SiNPCp^*$; 1.94(1) Å, Mes*NPCp*),[135] η^2 Cp*-phosphanylium (d(P–C(Cp*)) = 1.990(2) Å, [Cp*PNH(^{t}Bu)]$AlCl_4$)[35] and η^6 arene-phosphadiazonium complexes (d(P–C(arene) = 2.687(7) to 3.08(1) Å)[93,94,123] are considerably longer than those in [Mes*NP•Im]OTf **3.14** and Mes*NP(Cl)•Im **3.15**. Individual values for the η^6 arene-phosphadiazonium complexes are given in Table 1.3.

The (Mes*)N-P-C(Im) bond angles in [Mes*NP•Im]OTf **3.14** (103.2(2)°)[215] and Mes*NP(Cl)•Im **3.15** (101.9(2)°)[215] are similar or identical to that in Mes^*NPCEt_3 (104.7(1)°),[136] $Mes^*NPC(SiMe_3)_3$ (110.4(2)°),[281] Mes*NPCp* (106.0(4)°)[135] and those in the aminodiphenylphosphine $Mes^*N(H)PPh_2$, (99.7(1)° and 102.1(1)°[282]). However, the bond angles in **3.14** and **3.15** are smaller than that reported for the imino(methylene)phosphorane $Mes^*NP(Cl)C(SiMe_3)_2$ (130.5(2)°),[283] which features both P-C and P-N π-bonding.

The phosphorus-triflate distance in [Mes*NP•Im]OTf **3.14** (d(P–O(Tf)) = 2.951(5) Å)[215] is significantly longer than that in Mes*NPOTf (d(P–O(Tf) = 1.923(4) Å[130]). However, this distance is less than 3.30 Å (from $\Sigma\, r_w$(P) + r_w(O)). Hence, the triflate group in [Mes*NP•Im]OTf **3.14** has distinctly more ionic bonding character than in Mes*NPOTf, as suggested by the observation of equal S–O bond lengths in the triflate group of the former. A comparison of the P–O(Tf) distance and structural features associated with the triflate group in [Mes*NP•Im]OTf **3.14** with other phosphadiazonium-ligand-triflate complexes [Mes*NP•Lg]OTf, is described in Chapter 6. Other structural differences between [Mes*NP•Im]OTf **3.14** and Mes*NPOTf include

a larger (Mes*)N-P-O(Tf) bond angle in the former (123.0(2)°[215] versus 108.4(2)°[130]), and a significantly smaller (Mes*)C-N-P-O(Tf) torsion angle in [Mes*NP•Im]OTf **3.14** (112.8(3)°[215] c.f., 162(6)°[130] in Mes*NPOTf). Coordination by the imidazol-2-ylidene Im, to *P*-chloro-iminophosphine is reflected in a longer Cl–P bond in complex **3.15** (d(Cl–P) = 2.471(2) Å)[215] as compared with that reported for Mes*NPCl (d(Cl–P) = 2.142) Å[123]). This Cl–P bond length is also considerably greater than that observed in *cyclo*-chlorophosphines (d(Cl–P) = 2.314(1) Å, **3.19**; 2.416(2) Å, **3.20**)[32,54] and chloro-substituted phosphorano-bonding environments, including $Mes*NPCl_3$ (d(Cl–P) = 2.004(1), 2.017(1) Å)[151] and $Mes*NP(Cl)C(SiMe_3)_2$) **3.22**, (d(Cl–P) = 2.069(2) Å[283]). The Cl–P bond length in Mes*NP(Cl)•Im **3.15** is significantly less than 3.71 Å (from $\Sigma\, r_W$(Cl) + r_W(P)). Furthermore, the chlorine-phosphorus distance in **3.15** is less than that reported for the diazaphospholenium chloride complex **3.21**, (d(Cl–P) = 2.759(2) Å),[32] which has been suggested not to contain a formal Cl–P covalent bond.[32] Therefore, Mes*NP(Cl)•Im **3.15**, can be considered as having a formal Cl–P bond, but that the bond has a greater electrostatic component than that in Mes*NPCl. Coordination of imidazol-2-ylidene Im, to Mes*NPCl resulted in a 0.344(2) Å longer Cl–P bond, whereas for Mes*NPOTf, the P–O(Tf) distance was increased by 1.028(6) Å. This difference is attributed to greater Lewis basicity of chloride versus that of the triflate anion.[215] Other structural changes induced by the coordination of imidazol-2-ylidene Im, to Mes*NPCl includes an increase in the (Mes*)N-P-Cl bond angle (116.8(2)°, Mes*NP(Cl)•Im;[215] 112.4(2)°, Mes*NPCl[123]) and in the (Mes*)C-N-P-Cl torsion angle (110.5(4)°, Mes*NP(Cl)•Im;[215] 0°, Mes*NPCl[123]).

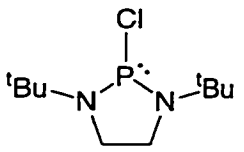

3.19

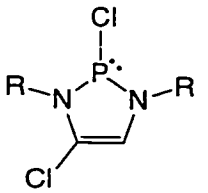

3.20

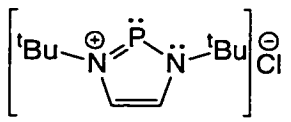

3.21

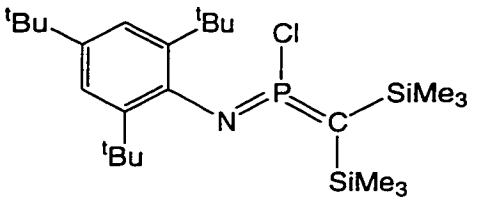

3.22

The P–N(Mes*) bond in [Mes*NP•Im]OTf **3.14** (d(P–N) = 1.574(4) Å)[215] and Mes*NP(Cl)•Im **3.15** (d(P–N) = 1.585(5) Å)[215] are significantly longer than those in Mes*NPOTf (d(P–N) = 1.467(4) Å),[130] Mes*NPCl (d(P–N) = 1.495(4) Å),[123] Mes*NPCp* (d(P–N) = 1.551(8) Å)[135] and the chloro-imino(methylene)phosphorane **3.22** (d(P–N) = 1.527(4) Å).[283] However, they are slightly longer than those reported for *P*-alkyl-iminophosphines (d(P–N) = 1.556(5) to 1.566(3) Å), individual values for *P*-alkyl-iminophosphines are given in Table 3.1. The P–N(Mes*) distances in **3.14** and **3.15** are less than the P–N(R) bond lengths observed in phosphinoamide complexes **3.23** (d(P–N) = 1.660(2) to 1.672(2) Å)[282,284] or the aminodiphenylphosphine Mes*N(H)PPh_2 (d(P–N) = 1.730(2) Å[282]). Phosphinoamides **3.23** feature a σ-phosphino-bonding environment with an amido-substituent bonded to the phosphorus centre (vide infra).[285]

The (Mes*)C-N-P bond angle in Mes*NP(Cl)•Im **3.15** (120.2(2)°)[215] is slightly larger than that in [Mes*NP•Im]OTf **3.14** (116.2(3)°),[215] but both complexes have significantly smaller (Mes*)C-N-P bond angles than those reported for Mes*NPCl (154.8(4)°),[123] Mes*NPOTf (176.4(3)°[130]). The (Mes*)C-N-P bond angles in **3.14** and **3.15** are closer or identical to those found in *P*-alkyl-iminophosphines (124.8(2)°,[136] Mes*NPCEt_3; 124.8(2)°,[281] Mes*NP$C(SiMe_3)_3$), Mes*NPCp* (125.9(6)°),[135] and the

lithium phosphinoamide [Li•OEt_2]Mes*$NPPh_2$ **3.23** (R = Mes*), (114.6(2)°[282]). The structural parameters relating to the Mes*NP unit in [Mes*NP•Im]OTf **3.14** are compared with other phosphadiazonium-ligand-triflate complexes [Mes*NP•Lg]OTf, in Chapter 6.

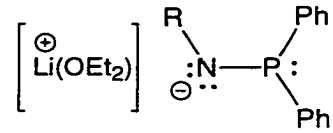

3.23

For comparison purposes, the crystal structure of the imidazol-2-ylidene **3.1**, which had not been previously reported, was determined. The structural features of the imidazol ring are identical to those found in other functionalized imidazol-2-ylidenes. The bond lengths and angles associated with the imidazol-2-ylidene unit in [Mes*NP•Im]OTf **3.14** (e.g., *d*(N–C) = 1.355(5), 1.347(6) Å)[215] and Mes*NP(Cl)•Im **3.15** (e.g., *d*(N–C) = 1.365(7), 1.370(7) Å)[215] are equivalent or close to those observed in the free ligand, (*d*(N–C) = 1.360(1) Å). The exception is a slight increase of the N-C-N bond angle in [Mes*NP•Im]OTf (107.5(4) Å)[215] and Mes*NP(Cl)•Im (106.7(4)°)[215] as compared with that in Im (102.1(1)°). This observation is consistent with complexes involving both an imidazol-2-ylidene ligand and a Lewis acidic main-group centre.

The imidazol ring of the ligand in [Mes*NP•Im]OTf **3.14** and Mes*NP(Cl)•Im **3.15** is planar (mean deviation from the plane is 0.007(3) Å and 0.009(3) Å, respectively)[215] as observed for the free ligand (0.004(2) Å). Furthermore, the central carbon and adjacent nitrogen atoms have planar geometry as indicated by the sum of the bond angles about C(1), N(1), and N(2), (Table 3.3).

The crystal structures of [Mes*NP•Im]OTf **3.14** and Mes*NP(Cl)•Im **3.15** reveal that the methyl groups of the isopropyl substituents on the ligand are pointing away from

the Mes*NP unit, a feature common in all complexes containing a 1,3-diisopropyl-4,5-dimethyl-imidazol-2-ylidene ligand. This structural arrangement probably minimizes steric interactions. In contrast, the isopropyl groups are pointing in the opposite direction in the free ligand.

The relative spatial orientation of the ylidene ligand with respect to the phosphadiazonium unit is very similar in both [Mes*NP•Im]OTf **3.14** and Mes*NP(Cl)•Im **3.15**. For example, the (Mes*)N-P-C-N and X-P-C-N(Mes*) torsion angles (X = Cl or O(Tf)) show an almost equal rotation of the ylidene ring plane (as defined by atoms C(1), C(3), N(1), and N(2)) with respect to the Mes*NP unit (Table 3.3). Furthermore, the difference ϕ, between torsion angles (Mes*)C-N-P-X and (Mes*)C-N-P-C are comparable for both complexes (ϕ = 59.6(5)° in Mes*NP(Cl)•Im; ϕ = 49.2(5)° in [Mes*NP•Im]OTf).[215] This is surprising considering the large difference in the P–X distance between Mes*NP(Cl)•Im and [Mes*NP•Im]OTf. The imidazol ring plane of the ligand is rotated 51.7(2)° in [Mes*NP•Im]OTf and 67.2(2)° in Mes*NP(Cl)•Im with respect to the aryl ring plane of the Mes* substituent.[215] The large (Mes*)C-N-P-C torsion angle in [Mes*NP•Im]OTf (162.0(4)°) and Mes*NP(Cl)•Im (170.1(3)°) shows that the Im ligand and the Mes* substituent have a *trans*-configuration across the (Im)P–N(Mes*) bond,[215] consistent with that reported for *P*-alkyl-iminophosphines.

The sum of the bond angles about the phosphorus centre in [Mes*NP•Im]OTf **3.14** ($\Sigma \angle$(P) = 301.1(3)°)[215] and Mes*NP(Cl)•Im **3.15** ($\Sigma \angle$(P) = 298.3(3)°)[215] indicate a pyramidal geometry consistent with that reported for other tertiary σ-phosphines (e.g., $\Sigma \angle$(P) = 303.5(2)°,[282] Mes*N(H)PPh_2; 308.3(2)°,[286] PPh_3) and the phosphenium-ylidene complex **3.4** (An = $AlCl_4^-$), ($\Sigma \angle$(P) = 310.1(5)°[48]).

3.2.3: Spectroscopic Properties of Phosphadiazonium-imidazol-2-ylidene Complexes ([Mes*NP•Im]An, where An = OTf^- (3.14) or $AlCl_4^-$ (3.16)) and Iminophosphine-imidazol-2-ylidene Complexes ([Mes*NP(R)•Im, where R = Cl (3.15) or Ph (3.17))

The ^{31}P NMR solution spectra show that the [Mes*NP•Im]An ($\delta(^{31}P)$ = 339 ppm, An = OTf^-;[215] 331 ppm, An = $AlCl_4^-$ **3.16**) and Mes*NP(Cl)•Im **3.15** ($\delta(^{31}P)$ = 172 ppm)[215] complexes contain a deshielded phosphorus nucleus as compared with those in the parent iminophosphines Mes*NPX ($\delta(^{31}P)$ = 135 ppm, X = Cl;[123] 55 ppm, X = OTf[130]) and the phosphadiazonium cation [Mes*NP•C_6H_5Me)]$AlCl_4$ ($\delta(^{31}P)$ = 79 ppm[130]). The $\delta(^{31}P)$ value for [Mes*NP•Im]An complexes (An = OTf^- **3.14** and $AlCl_4^-$ **3.16**) are near to those reported for *P*-alkyl-iminophosphines ($\delta(^{31}P)$ = 363 to 500 ppm), individual values for *P*-alkyl-iminophosphines are provided in Table 3.4.

The solution ^{31}P NMR spectra of Mes*NP(Ph)•Im **3.17**, show that the phosphorus nucleus is significantly shielded ($\delta(^{31}P)$ = 55 ppm, $\Delta\delta(^{31}P)$ = 355 ppm) as compared with the *P*-phenyl-iminophosphine Mes*NPPh, ($\delta(^{31}P)$ = 415 ppm[106]). Furthermore, the $\delta(^{31}P)$ value of Mes*NP(Ph)•Im **3.17**, is in the range reported for lithium phosphinoamide salts **3.23**, ($\delta(^{31}P)$ = 33 to 63 ppm),[282,284] individual values for **3.23** are provided in Table 3.4.

The broadness of the ^{31}P resonance in Mes*NP(Ph)•Im **3.17** prevented the observation of a $^1J(^{31}P,^{13}C)$ value. The $\delta(^{31}P)$ and $^1J(^{31}P,^{13}C)$ values for the [Mes*NP•Im]OTf **3.15** and Mes*NP(Cl)•Im **3.15** complexes have a notable solvent dependence (Table 3.4). Furthermore, the solid-state isotropic $\delta(^{31}P)$ values ($\delta_{iso}(^{31}P)$ = 366 ppm, [Mes*NP•Im]OTf; 193 ppm, Mes*NP(Cl)•Im) are different from those in solution ($\delta_{iso}(^{31}P)$ = 339 ppm, [Mes*NP•Im]OTf; 172 ppm, Mes*NP(Cl)•Im). Coupling constant values $^1J(^{31}P,^{13}C)$ could not be resolved from solid-state ^{31}P NMR spectra. The $^1J(^{31}P,^{13}C)$ values for [Mes*NP•Im]OTf ($^1J(^{31}P,^{13}C)$ = 132 Hz)[215] and Mes*NP(Cl)•Im ($^1J(^{31}P,^{13}C)$ = 115 Hz),[215] in solution, are larger as compared with compounds containing a

P–C double bond, such as phosphaalkenes ($^1J(^{31}P,^{13}C)$ = 115 Hz),[287] or a P–C single bond including *P*-alkyl-iminophosphines ($^1J(^{31}P,^{13}C)$ = 46 to 102 Hz), individual values are provided in Table 3.4. Trisubstituted π-phosphorano-compounds such as the *P*-chloro-imino(methylene)phosphorane **3.22** ($^1J(^{31}P,^{13}C)$ = 65 Hz)[283] and methylenephosphonium salts (e.g., $^1J(^{31}P,^{13}C)$ = 51 Hz, [^{t}Bu$_2$PCPh$_2$]AlCl$_4$),[288] which both feature P–C π-bonding, have smaller values than that in [Mes*NP•Im]OTf and Mes*NP(Cl)•Im.

In comparison, the $^1J(^{31}P,^{13}C)$ value in [Mes*NP•Im]OTf ($^1J(^{31}P,^{13}C)$ = 132 Hz)[215] and Mes*NP(Cl)•Im ($^1J(^{31}P,^{13}C)$ = 115 Hz)[215] are larger than those reported for the phosphinidene-ylidene complexes **3.6**-**3.7** ($^1J(^{31}P,^{13}C)$ = 87 to 103 Hz), individual values are given in Table 3.4. However, they are not as large as that observed for the tetraflurorophenyl-phosphoranide-ylidene **3.2**, ($^1J(^{31}P,^{13}C)$ = 306 Hz),[274] which is surprising, considering the long P–C(Im) bond in this compound (*d*(P–C(Im) = 1.910(4) Å[274]). Since there is no discernable difference in $^1J(^{31}P,^{13}C)$ values for compounds with phosphorus-carbon single or double bonds, the magnitude of this coupling constant provides no information about P–C bond order.

The ^{13}C NMR spectra showed that the central carbon nucleus associated with the ligand is shielded in the [Mes*NP•Im]OTf **3.14** ($\delta(^{13}C)$ = 153.6 ppm)[215] and Mes*NP(R)•Im ($\delta(^{13}C)$ = 146.4 ppm, R = Cl **3.15** ; 143.9 ppm, R = Ph **3.17**)[215] complexes as compared with that in the free imidazol-2-ylidene Im, ($\delta(^{13}C)$ = 207.8 ppm[270]). This is consistent with the reports of deshielded central carbon nuclei in other main-group-ylidene complexes (e.g., Cl$_2$S(O)Im $\delta(^{13}C)$ = 126.3 ppm).[289] Comparison of other $\delta(^{13}C)$ values in **3.14**, **3.15**, and **3.16** with Im, **3.1** are provided in Table 3.5.

The ^1H NMR spectra of [Mes*NP•Im]OTf **3.14** and Mes*NP(R)•Im (R = Cl **3.15** or Ph **3.17**) show that the $\delta(^1H)$ values associated with the ylidene group differ from that of the free ligand (Table 3.5). This suggests that the complexes **3.14**-**3.15**, **3.17** are

present in solution. The protons associated with the ligand of Mes*NP(Ph)•Im **3.17** are shielded and the $^{3}J(^{1}H,^{1}H)$ coupling for the isopropyl group is unresolved. The observation of phosphorus coupling to the methine protons in the isopropyl groups of the ligand suggests that phosphadiazonium-ylidene coordination in the [Mes*NP•Im]OTf **3.14** and Mes*NP(Cl)•Im **3.15** complexes is retained in solution.

Both solution ^{13}C and ^{1}H NMR spectra of [Mes*NP•Im]OTf **3.14** and Mes*NP(R)•Im (R = Cl **3.15** or Ph **3.17**) show single sets of resonances for the ligand, and suggests that either the ligand has free rotation about the P–C(Im) bond or the ligand and the Mes*NP unit are in an association-dissociation equilibrium with the complex Mes*NP•Lg. In comparison, imino(methylene)phosphoranes such as **3.22**, have anisochronous trimethylsilyl groups, which indicate that these substituents have a fixed orientation caused by P–C π-bonding.[283,290]

In general, the infrared spectra of [Mes*NP•Im]OTf **3.14** and Mes*NP(Cl)•Im **3.15**, prepared as paraffin oil mulls, were too complicated to assign peaks with specific bond stretching frequencies. However, the Cl–P bond stretching frequency in Mes*NP(Cl)•Im **3.15** is tentatively assigned at 551 cm^{-1} and is consistent with the 550 cm^{-1} value reported for **3.20**, which also has a long Cl–P bond.[54] Descriptions and comparison of the spectroscopic features associated with the triflate group in [Mes*NP•Im]OTf **3.14** is provided in Chapter 6.

The ^{27}Al NMR solution spectra of the reaction mixture containing [Mes*NP•Im]$AlCl_4$ **3.17** shows a single peak with a chemical shift of 102 ppm and a $\nu_{1/2}$ of 8 Hz. Both features are consistent with the observation of a tetrachloroaluminate anion in solution (c.f., [MesPN(^{i}Pr)$_2$]$AlCl_4$ $\delta(^{27}Al)$ = 105 ppm, $\nu_{1/2}$ = 6 Hz[42]).[291]

3.3: Conclusions: Bonding Implications for Phosphadiazonium-imidazol-2-ylidene Complexes ([Mes*NP•Im]An, where An = OTf^- (3.14) or $AlCl_4^-$ (3.16)) and Iminophosphine-imidazol-2-ylidene Complexes (Mes*NP(R)•Im, where R = Cl (3.15) or Ph (3.17))

The spectroscopic and structural data indicate that the iminophosphines, Mes*NPOTf and Mes*NPCl are Lewis acids with respect to imidazol-2-ylidenes and that coordination of this strongly Lewis basic ligand causes significant structural changes within the phosphadiazonium unit. The [Mes*NP•Im]OTf complex **3.14** is best described as a disubstituted π-phosphino-bonding environment with structural parameters similar to those found in *P*-alkyl-iminophosphines. Hence, the $Mes*NP•Im^+$ unit of **3.14** can be considered a cationic analogue of a *P*-alkyl-iminophosphine $Mes*NPCR_3$. The *P*-aryl-*P*-amino-phosphenium complex **3.24** also features a disubstituted π-phosphino-centre with a P–C σ-bond, but differs from **3.14** by having an amino rather than an imino-substituent.[42]

The Mes*NP(Cl)•Im **3.15** complex differs from [Mes*NP•Im]OTf **3.14** in that the bonding of the chlorine group results in a trisubstituted π-phosphino-centre. The shorter P–C(Im) bond in [Mes*NP•Im]OTf versus Mes*NP(Cl)•Im is perhaps due to weaker Lewis acidity of the phosphorus centre in the latter. Both Mes*NP(Cl)•Im and [Mes*NP•Dipy]OTf **2.9** represent a new bonding environment for phosphorus; an iminophosphide, which by virtue of a pair of non-bonding valence electrons on phosphorus is distinct from other trisubstituted π-phosphorano-compounds **3.25**-**3.27**.[215] Iminophosphides are characterized by having pyramidal phosphorus geometry, whereas trisubstituted π-phosphorano-compounds (e.g., phosphinoboranes[292] **3.25**, methylenephosphonium[288,293-296] **3.26**, and phosphanyl-phosphenium[297] **3.27** cations) feature a trigonal planar phosphorus centre.

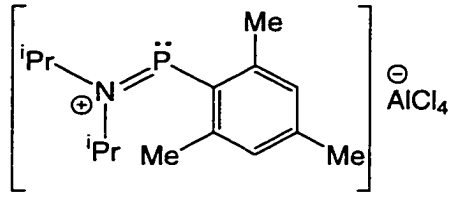

3.24

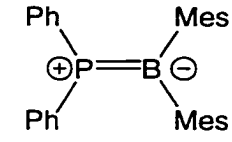

3.25

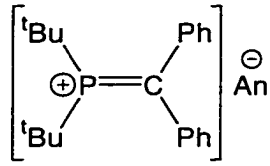

3.26

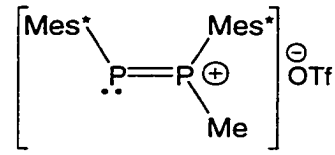

3.27

In comparison, the short P–N(Mes*) bond in [Mes*NP•Dipy]OTf **2.9**, (d(P–N) = 1.497(4) Å)[216] indicates that this complex has more phosphadiazonium-like bonding character than Mes*NP(Cl)•Im (d(P–N) = 1.585(5) Å),[215] (i.e., the Mes*NP unit has a formal P-N triple bond). Furthermore, the Mes*NP•Dipy$^+$ unit has a positive charge, whereas Mes*NP(Cl)•Im **3.14** could be argued to be a neutral compound. The lithium phosphinoamides **3.23** are considered to have a higher concentration of negative charge situated on the nitrogen rather than on the phosphorus centre as speculated for the iminophosphides.[285] Figure 3.5 illustrates the bonding character in compounds featuring a disubstituted nitrogen centre and a trisubstituted phosphorus centre $RNPR_2$. The two bonding extremes are represented by phosphinoamides and iminophosphides, respectively.

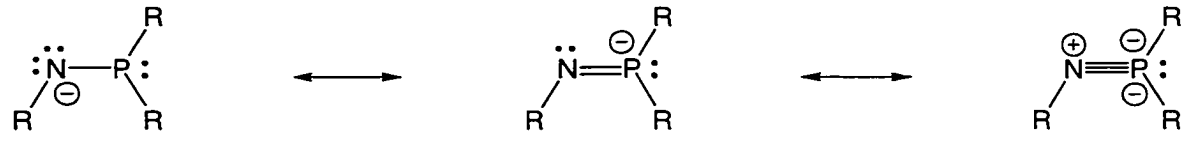

Figure 3.5: The bonding relationship of $RNPR_2$ type-compounds as represented by resonance structures. The bonding extremes are represented by phosphinoamides (left) and iminophosphides (middle and right).

Ab initio calculations show that the model compound $HNPH_2^-$, has a phosphinoamide structure with pyramidal geometry at phosphorus and a long P–N bond (d(P–N) = 1.649 Å) as compared with the iminophosphine HNPH, (d(P–N) = 1.550 Å).[298] Subsequent replacement of the hydrogen atoms on phosphorus in H_2PNH^- with electronegative substituents (i.e., fluorine) causes the model to develop iminophosphide bonding character with a shorter P–N bond (d(P–N) = 1.649 Å, $H(F)PNH^-$; 1.574 Å, F_2PNH^-). This suggests a greater π-component in the P–N bond.[298] This is consistent with experimental observations; from structural parameters, it is suggested that the lithium phosphinoamide [Li•OEt_2]Mes*$NPPh_2$ **3.23**, Mes*NP(Cl)•Im **3.15**, and [Mes*NP•Dipy]OTf **2.9** complexes represent a continuum from compounds having a phosphinoamide bonding character to those having an iminophosphide bonding character. Iminophosphide bonding character is induced by the attachment of electron-withdrawing substituents or weakly donating ligands to the phosphorus centre (i.e., chloride in **3.15**, and 2,2'-dipyridyl in **2.9**). A further example of how electron-withdrawing substituents attached to a phosphorus centre affects the nature of the P–N bond is represented by dimethyldifluorophosphine Me_2NPF_2. The crystal structure shows that the P–N bond (d(P–N) = 1.628(5) Å)[299] is short for an aminophosphine (c.f., d(P–N) = 1.730(2) Å). Moreover, the amino centre has planar geometry. Both observations are consistent with an increase in the π-component of the P–N bond.

There have been previous attempts at synthesizing iminophosphides by hydride addition,[157] methylation[300] or radical addition[301] to the *P*-amino-iminophosphine $Me_3SiNPN(SiMe_3)_2$. However, the identities of the products from these reactions were postulated solely from data obtained from NMR or ESR spectroscopy. In comparison, lithium phosphinoamide salts are synthesized by the deprotonation of an aminophosphine.[282,284] Importantly, the synthesis of the Mes*NP(Cl)•Im **3.15**,

Mes*NP(Ph)•Im **3.17**, and [Mes*NP•Dipy]OTf **2.9** complexes demonstrate that the creation of new bonding environments is viable via coordination which, is a consequence of the Lewis acidic properties of iminophosphines.

Interestingly, the *P*-chloro-imino(methylene)phosphorane **3.22** and Mes*NP(Cl)•Im **3.15** are related in that both compounds contain the Mes*NP(Cl)CR_2 unit, differing only by the substituents attached to the central carbon. However, the properties of the substituents R, directly determine the bonding character of the compound, and in particular the bonding or non-bonding nature of the valence electrons on phosphorus. For example, Mes*NP(Cl)•Im **3.15** represents a π-phosphino-bonding environment, which features a phosphorus centre with pyramidal geometry. In contrast, Mes*NP(Cl)$C(SiMe_3)_2$ **3.22**, is a π-phosphorano-compound featuring a trigonal planar phosphorus centre. The difference in bonding between Mes*NP(Cl)•Im and Mes*NP(Cl)$C(SiMe_3)_2$ can be rationalized on the basis that the central carbon of the CR_2 unit in **3.15** engages in N–C π-bonding, whereas the P–CR_2 fragment is π-bonded in **3.22**. This is supported by the observation that the N–C distances (d(N–C) = 1.365(7), 1.370(7) Å) in Mes*NP(Cl)•Im are significantly less than typical N-C single bond values (c.f., $d(N(sp^3)–C(sp^3))$ = 1.469[14] Å[131]). The effect of nitrogen-carbon lone pair π-conjugation appears to be general for all compounds with a $PC(NR_2)_2$ fragment. For example, phosphaiminoureas **3.10** compounds feature a long P–C bond with short N–C bonds, which suggest that these compounds are more appropriately described as phosphinidene-ylidene complexes **3.11**.

The synthesis of Mes*NP(Cl)•Im **3.15** demonstrates the Lewis acidic properties of Mes*NPCl. However, Mes*NPCl is amphoteric as it can also act as a Lewis base. In particular, Mes*NPCl coordinates, in a η^1 mode, to transition metal centres in low oxidation states (i.e., Rh(+1), Ni(0) and Pt(0)).[164,302,303] As a ligand, however, Mes*NPCl,

exhibits minor structural variations, in contrast to its behaviour as a Lewis acid (Figure 3.6). Similarly, the *P*-phenyliminophosphine Mes*NPPh, also has been shown to coordinate to transition metals (i.e., $Cl(Ph_3P)Rh(PhPNMes^*)_2$).[303]

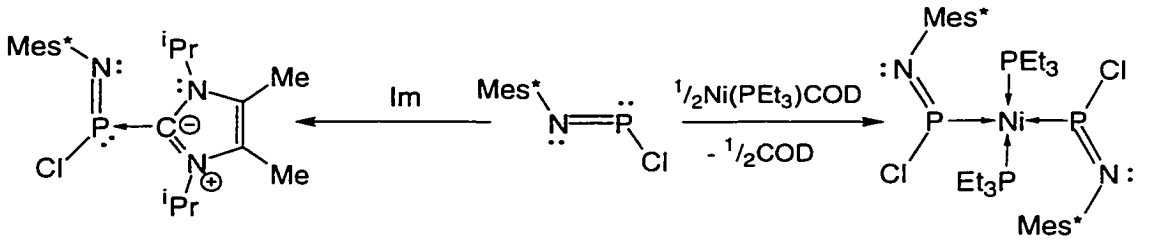

d(P–N) (Å)	1.585(5)	1.509(2)	1.498(5)
d(Cl–P) (Å)	2.471(2)	2.127(1)	2.145(3)
∠C-N-P) (°)	120.2(4)	146.4(2)	142.1(5)
∠(Cl-P-N) (°)	116.8(2)	111.47(9)	108.1(2)
Reference	215	153	164

Figure 3.6: Comparison of structural parameters for *P*-chloro-iminophosphine as a Lewis acid (left) and as a Lewis base (right).

The imidazol-2-ylidene coordination of *P*-phenyl-iminophosphine suggests that iminophosphines without an electron-withdrawing *P*-substituent can also behave as Lewis acids. The Mes*NP(Ph)•Im complex **3.17** is postulated to have a structure similar to the lithium phosphinoamides **3.23**. However, evidence of an equilibrium suggests that that the phosphorus-ylidene coordination in Mes*NP(Ph)•Im **3.17** is labile and that Mes*NPPh is a weaker Lewis acid as compared with Mes*NPCl and Mes*NPOTf. In contrast, the phosphadiazonium-ylidene interaction in $[Mes^*NP•Im]AlCl_4$ **3.16** is strong, as the complex has been shown to be stable, by ^{31}P NMR spectroscopy, for months in solution at ambient temperature. In contrast, the phosphadiazonium-triphenylphosphine complexes $[Mes^*NP•PPh_3]AlXCl_3$ (X = Cl or $OC_6H_2(^tBu)_2$-2,6,Me-4), rapidly decompose into Mes*NPCl and $Cl_2XAl•PPh_3$ on warming to room temperature.[38,95]

Table 3.1: Comparison of P–C and P–N bond lengths in [Mes*NP•Im]OTf **3.14** and Mes*NP(Cl)•Im **3.15** with selected phosphaiminoureas **3.10**, phosphamethine cyanines **3.12**, imino(methylene)phosphoranes, lithium phosphinoamides **3.23**, and other phosphorus-ylidene complexes. All values in Å.

Compound		*d*(P–N)	*d*(P–C)	Reference
Mes*NP(Cl)•Im	(**3.15**)	1.585(5)	1.886(5)	215
[Mes*NP•Im]OTf	(**3.14**)	1.574(4)	1.852(5)	215
Mes*NPCl		1.509(2)	–	124
		1.495(4)[a]	–	123
Mes*NPOTf		1.467(4)	–	130
Phosphorus-ylidene Complexes				
$F_4PhP•C(N(Mes)CH)_2$	(**3.2**)	–	1.910(4)	274
$PhP•C(N(Me)C(Me)_2$	(**3.6**)	–	1.794(3)	276
$PhP•C(N(Mes)CH)_2$	(**3.6**)	–	1.763(6)	277
$PhP•C(N(Mes)CH_2)_2$	(**3.7**)	–	1.746(4)	277
$(CF_3)P•C(N(Mes)CH)_2$	(**3.6**)	–	1.784(2)	277
$[Ph_2P•Im]AlCl_4$	(**3.4**)	–	1.813(7)	48
Imino(methylene)phosphoranes				
$Mes*NP(Cl)C(SiMe_3)_2$	(**3.22**)	1.527(4)	1.624(4)	283
$Mes*NP(Ph)C(SiMe_3)_2$		1.552(2)	1.639(3)	304
Phosphaiminoureas and Phosphamethine Cyanines				
$(C_6H_4(NMe)$-1,3-C)PCN	(**3.10**)	–	1.771(5)	305
$HPC(NMe_2)_2$	(**3.10**)	–	1.740(1)	306
$Me_3SiPC(NMe_2)NEt_2$	(**3.10**)		1.761(3)	307
$[(Me_2N)_2CPC(NMe_2)_2]ClO_4$	(**3.12**)	–	1.796(4)	308
$(Me_3Si)SC(S)PC(NMe_2)_2$	(**3.10**)		1.826(2)	309
P-Alkyl-iminophosphines and π–Coordinated Phosphadiazonium Complexes[b]				
Mes*NPCp*		1.551(8)	1.94(1)	135
$Et_3SiNPCp*$		1.533(3)	2.168(4), 2.122(4)	135
$[Mes*NP•C_6H_3Me_3$-1,3,5$]Ga_2Cl_7$		1.471(6)	2.687(4)	93
$Mes*NPC(SiMe_3)_3$		1.566(3)	1.837(3)	281
$Mes*NPCEt_3$		1.566(2)	1.870(3)	136
$^tBuNPMes*$		1.556(5)	1.836(8)	108
(FMes)NP(FMes)		1.561(2)	1.883(3)	107
Lithium Phosphinoamide Salts				
$([Li•OEt_2]PhNPPh_2)_2$	(**3.23**)	1.672(2)	1.843(2), 1.845(2)	284
$([Li•OEt_2]NpNPPh_2)_2$	(**3.23**)	1.660(2)	1.843(4), 1.846(4)	282
		1.669(2)[b]	1.848(3),[c] 1.843(4)[c]	282
$([Li•OEt_2]^iPrNPPh_2)_2$	(**3.23**)	1.659(4)	1.852(4), 1.850(4)	282
		1.666(4)[b]	1.852(4),[c] 1.861(4)[c]	282
$[Li•OEt_2]Mes*NPPh_2$	(**3.23**)	1.661(2)	1.879(3), 1.848(3)	282

([a]) Solved using a non-centrosymmetric space group. ([b]) The *d*(P–N) and *d*(P–C) values in other η^6 arene-phosphadiazonium complexes are listed in Table 1.3. ([c]) Values from a second structurally different molecule in the unit cell.

Table 3.2: Comparison of (Mes*)C-N-P and (Mes*)N-P-C bond angles in [Mes*NP•Im]OTf **3.14**, Mes*NP(Cl)•Im **3.15** with related phosphino- and phosphorano-compounds. Compounds are listed by decreasing ∠(C(Mes*)-N-P). All values in degrees.

Compound	∠(Mes*)C-N-P	∠((Mes*)N-P-C)	Reference
Mes*NPOTf	176.4(3)	–	130
Mes*NPCl	154.8(4)	–	123
	146.4(2)[a]	–	124
Mes*NP(Cl)C($SiMe_3$)$_2$ (**3.22**)	127.0(3)	130.5(2)	283
Mes*NPCp*	125.9(6)	106.0(4)	135
Mes*NPCEt_3	124.8(2)	104.7(1)	136
Mes*NPC($SiMe_3$)$_3$	120.2(2)	110.4(2)	281
[Mes*NP(Cl)•Im (**3.15**)	120.2(4)	101.9(2)	215
[Mes*NP•Im]OTf (**3.14**)	116.2(3)	103.2(2)	215
[Li•OEt_2]Mes*NPPh_2 (**3.23**)	114.6(2)	104.8(1), 111.5(1)	282
Mes*N(H)PPh_2	114.6(1)	99.7(1), 102.1(1)	282

([a]) Solved using a non-centrosymmetric space group.

Table 3.3: Comparison of torsion angles (including the torsion angle difference ϕ) and sums of bond angles ($\Sigma\angle$) in [Mes*NP•Im]OTf **3.14** and Mes*NP(Cl)•Im **3.15**. Atom numbering scheme corresponds to that used in Figures 3.3 and 3.4. All values are given in degrees and obtained from reference 215.

Parameter	Mes*NP(Cl)•Im X = Cl (**3.15**)	[Mes*NP•Im]OTf X = O (**3.14**)
N(3)-P-C(1)-N(1)	148.7(4)	148.6(4)
N(3)-P-C(1)-N(2)	-35.0(6)	-34.2(5)
X-P-C(1)-N(1)	-95.4(4)	-90.6(4)
X-P-C(1)-N(2)	80.9(5)	86.6(5)
C(X)-N(3)-P-C(1)	170.1(3)	162.0(4)
C(X)-N(3)-P-X	110.5(4)	112.8(3)
ϕ	59.6(5)	49.2(5)
$\Sigma\angle$(P)	298.3(3)	301.1(3)
$\Sigma\angle$(C(1))	360.0(7)	360.0(6)
$\Sigma\angle$(N(1))	359.8(7)	359.9(7)
$\Sigma\angle$(N(2))	360.0(7)	360.0(7)

Table 3.4: Comparison of solution and solid-state $\delta(^{31}P)$ and $^{1}J(^{31}P,^{13}C)$ values for [Mes*NP•Im]An (An = OTf^- or $AlCl_4^-$) and Mes*NP(R)•Im (R = Cl or Ph) with related phosphorus compounds.

Compound	Solution (CD_2Cl_2) $\delta(^{31}P)$ (ppm)	Solution (CD_2Cl_2) $^{1}J(^{31}P,^{13}C)$ (Hz)	Solution (C_6D_6) $\delta(^{31}P)$ (ppm)	Solution (C_6D_6) $^{1}J(^{31}P,^{13}C)$ (Hz)	Solid State (CP/MAS) $\delta_{iso}(^{31}P)$ (ppm)
Mes*NP(Ph)•Im (**3.17**)	55	[a]	57	[a]	–
Mes*NP(Cl)•Im[b] (**3.15**)	172	115	156	[a]	193
[Mes*NP•Im]$AlCl_4$ (**3.16**)	331	[a]	–	–	–
[Mes*NP•Im]OTf[b] (**3.14**)	339	132	350	162	366

Compound	Solution $\delta(^{31}P)$ (ppm)	Solution $^{1}J(^{31}P,^{13}C)$ (Hz)	Solid State (CP/MAS) $\delta_{iso}(^{31}P)$ (ppm)	Reference
Mes*NPOTf	55	-	53	130, 232
[Mes*NP•C_6H_5Me]$AlCl_4$	79	-	77	123, 310
Mes*NPCl	135	-	145	255
P-Alkyl-iminophosphines				
Mes*NPMes	455	69		14
Mes*NPAd	457	–		14
Mes*NPCH($SiMe_3$)$_2$	487	86		106
Mes*NP(^{t}Bu)	490	46	487	255
Mes*NP(^{i}Pr)	491	47		106
Mes*NPEt_3	495	53		136
Mes*NPC($SiMe_3$)$_3$	500	100		281
Cp*-Substituted Iminophosphines				
Me_3SiNPCp*	138	–		135
Mes*NPCp*	195	–	270	135
Phosphino- and Phosphorano-ylidene Complexes				
[Ph_2P(Se)•Im]$AlCl_4$ (**3.3**)	22	[a]		48
PhP•C(N(Mes)CH)$_2$ (**3.6**)	-12	87		277
PhP•C(N(Mes)CH_2)$_2$ (**3.7**)	-23	103		277
(CF_3)P•C(N(Mes)CH)$_2$ (**3.6**)	-24	101		277
[Ph_2P•Im]Cl (**3.4**)	-27	[a]		48
[Ph_2P•Im]$AlCl_4$ (**3.4**)	-27	[a]		48
PhP•C(N(Me)CMe)$_2$ (**3.6**)	-54	98		276
F_4PhP•C(N(Mes)CH)$_2$ (**3.2**)	-141	306		274

Compound	Solution $\delta(^{31}P)$ (ppm)	Solution $^{1}J(^{31}P,^{13}C)$ (Hz)	Reference
Imino(methylene)phosphoranes			
$Mes^*NP(Cl)C(SiMe_3)_2$ (**3.22**)	73	65	283
$Mes^*NP(Ph)C(SiMe_3)_2$	130	73	311
Lithium Phosphinoamide Complexes			
$([Li{\bullet}OEt_2]PhNPPh_2)_2$ (**3.23**)	33	–	284
$([Li{\bullet}OEt_2]^{i}PrNPPh_2)_2$ (**3.23**)	44	–	282
$([Li{\bullet}OEt_2]NpNPPh_2)_2$ (**3.23**)	45	–	282
$[Li{\bullet}OEt_2]Mes^*NPPh_2$ (**3.23**)	63	–	282
Phosphamethine Cyanines and Phosphaiminoureas			
$(Me_3Si)SiC(S)PC(NMe_2)_2$ (**3.10**)	145	87	309
$^{t}BuNP(NMe_2)_2$ (**3.10**)	92	73	312
$Ph(SiMe_3)NC(S)PC(NMe_2)_2$ (**3.10**)	83	72	309
$PhC(O)C(NMe_2)_2$ (**3.10**)	31	79	309
$PhNPC(NMe_2)_2$ (**3.10**)	28	67	313
$MesNP(NMe_2)_2$ (**3.10**)	9	68	313
$(Me_3Si)PC(NMe_2)_2$ (**3.10**)	-47	–	314
$HPC(NMe_2)_2$ (**3.10**)	-63	71	312
$[P((C(NMe_2)_2)_2]Cl$ (**3.12**)	-93	79	315
$[P((C(NEt_2)_2)_2]BPh_4$ (**3.12**)	-95	82	315

([a]) Not resolved. (b) Values obtained from reference 215.

Table 3.5: Comparison of $\delta(^1H)$, $\delta(^{13}C)$ values and coupling constants associated with the imidazol-2-ylidene unit in [Mes*NP•Im]OTf **3.14** and Mes*NP(R)•Im (R = Cl **3.15** or Ph **3.17**) with the free ligand Im. Chemical shifts reported in ppm. Coupling constants, if applicable, are in parentheses and reported in Hz.

Position	Mes*NP(Cl)•Im[g] **3.15**	[Mes*NP•Im]OTf[g] **3.14**	Mes*NP(Ph)•Im **3.17**	Im[f] **3.1**
$\delta(^1H)$				
$(C\underline{H}_3)_2CH$	1.66	1.63	0.61	1.47
	(7.02[c])	(7.0[a])	–	(6.41[a])
$(CH_3)_2C\underline{H}$	5.86	6.20	5.48	3.95
	(7.02[a], 0.80[b])	([c])	–	(6.41[a])
$NC(C\underline{H}_3)$	2.50	2.35	1.08	1.75
$\delta(^{13}C)$				
$(\underline{C}H_3)_2CH$	22.4	21.5	21.7	25.1
$(CH_3)_2\underline{C}H$	52.7	50.6	50.2	48.8
	(8.6[d])	(19.6[d])	–	
$NC(\underline{C}H_3)$	11.5	11.1	10.1	9.2
$N\underline{C}(\underline{C}H_3)$	132.4	127.4	127.1	121.7
$N\underline{C}N$	146.4	153.6	143.9	207.8
	(131.6[e])	(114.9[e])	–	

([a]) $^3J(^1H,^1H)$. ([b]) $^4J(^{31}P,^{13}C)$. ([c]) Cannot resolve the $^1H,^1H$ and $^{31}P,^{13}C$ coupling constants. ([d]) $^3J(^{31}P,^{13}C)$. ([e]) $^1J(^{31}P,^{13}C)$. ([f]) Measured under the conditions used to record the complexes [Mes*NP•Lg]OTf, see Section 8.1. Values except for $\delta(^{13}C)$ of $N\underline{C}N$ are similar to those reported in reference 266. The $\delta(^{13}C)$ value of $N\underline{C}N$ agrees with that reported in reference 270. ([g]) Values obtained from reference 215.

Chapter 4: Synthesis of *P*-Silyl-iminophosphines via the Coordination of Iminophosphines involving a Diaminosilylene

4.1: Introduction: Overview of Phosphorus-silylene Chemistry

Silylenes, and the other heavier group 14 ylidenes ER_2 (E = Ge, Sn, or Pb), have received far less attention in terms of chemical reaction studies than carbenes. Silylenes, analogous with carbenes have been traditionally regarded as highly reactive, transient reaction intermediates.[316] Nevertheless, the coordination chemistry of silylenes as ligands is starting to develop, due in part to the discovery of stable diaminosilylenes,[317-320] such as **4.1** and **4.2**.

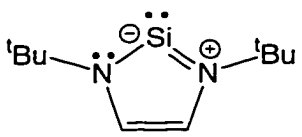

4.1

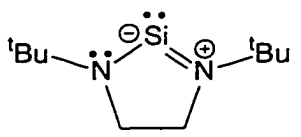

4.2

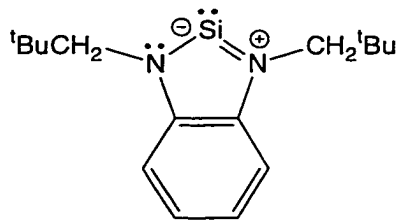

4.3

It is postulated from theoretical calculations and data from PE and ISEE spectroscopy that diaminosilylenes are stabilized through lone pair π-conjugation between the silicon and nitrogen centres.[321-323] However, a kinetically stable silylene, which does contain lone pair bearing substituents attached to the silicon centre, has been recently isolated and structurally characterized.[324] For the purposes of the research presented in this chapter, the reactivity of the diaminosilylene[317,318] **4.1**, (hereafter abbreviated as SiDAB) was investigated for which a convenient synthesis has been previously reported.

The Lewis basicity of diaminosilylenes is significantly weaker as compared with that of diaminocarbenes such as imidazol-2-yliene Im, **3.1**. Alkyl- and aryl-substituted

silylenes have Lewis acidic properties and are frequently used in the synthesis of silicon-containing heterocycles.[325] Nevertheless, diaminosilylenes have been shown capable of behaving as ligands with respect to transition metal centres and main-group Lewis acids. For example, the diaminosilylene SiDAB, forms a σ-coordination complex with trispentafluorophenylborane $B(C_6F_5)_3$ (vide infra).[326]

Few studies have examined the reactivity between silylenes and phosphorus compounds. However, it has been shown that silylenes mainly undergo insertion into halogen-phosphorus bonds.[327] The *in situ* generated silylene $^tBu_2Si$, undergoes [2+1] cycloaddition with the phosphaalkyne AdCP, forming a phosphasilirene[328] **4.4** or alternatively, the phosphadisilacyclobutene[329] **4.5** is obtained if the reacting silylene has bulky substituents (i.e., Mes_2Si). The diaminosilylene **4.3** undergoes a [1+4] cycloaddition with the tris-*tert*-butyl substituted 1,3,5-triphosphabenzene forming the bicyclic compound **4.6**.[330] However, no reaction was observed between SiDAB and elemental white phosphorus.[318]

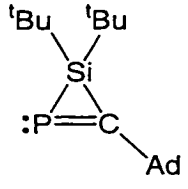

4.4

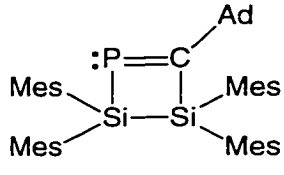

4.5

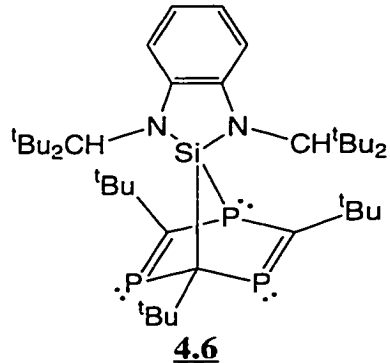

4.6

In an attempt to synthesize and characterize phosphadiazonium-complexes with a silylene as the ligand, a study was undertaken in which the Lewis acidic iminophosphines, Mes*NPOTf and Mes*NPCl, were combined in separate reactions,

with the diaminosilylene SiDAB. The reactions did not result in the formation of σ-coordination compounds [Mes*NP•Lg]OTf. Rather, the resulting compounds represent new types of *P*-functionalized iminophosphines **4.7** (X = OTf or Cl).

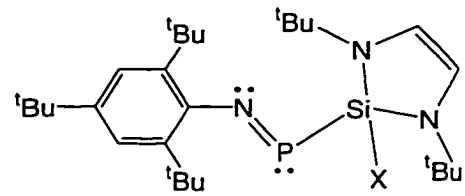

4.7

4.2: Results and Discussion

4.2.1: Synthesis of *P*-Silyl-iminophosphines Mes*NPSi(X)DAB 4.7 (where X = OTf or Cl)

The addition of diaminosilylene SiDAB, to Mes*NPOTf, in a 1:1 stoichiometry, resulted in a dark blue solution which crystallized on removal of solvent. Solution ^{1}H, ^{13}C, ^{19}F, ^{29}Si, ^{31}P NMR spectroscopy, crystallography, and elemental analysis identified the product as a *P*-silylated iminophosphine, Mes*NPSi(OTf)DAB **4.7** (X = OTf). 31-P NMR spectra of the reaction mixture showed the reaction was virtually quantitative. An analogous reaction using *P*-chloro-iminophosphine Mes*NPCl, in place of Mes*NPOTf, resulted in a dark blue oil which, by solution ^{31}P NMR spectroscopy, showed the formation of several phosphorus containing species. However, one product was postulated as Mes*NPSi(Cl)DAB **4.7** (X = Cl), based on a phosphorus chemical shift ($\delta(^{31}P)$ = 586 ppm) and a $^{1}J(^{31}P,^{29}Si)$ value (102 Hz) that are similar to those observed for Mes*NPSi(OTf)DAB **4.7** (X= OTf), ($\delta(^{31}P)$ = 566 ppm; $^{1}J(^{31}P,^{29}Si)$ = 121 Hz).

4.2.2: Structural Features of the *P*-Silyl-iminophosphine Mes*NPSi(OTf)DAB 4.7 (X = OTf)

The crystal structure of Mes*NPSi(OTf)DAB **4.7** (X = OTf), showed that the tetrasubstituted silicon centre is bonded to both the phosphorus centre of the Mes*NP unit and to an oxygen atom as part of a triflate group (Figure 4.1).

The length of the phosphorus-silicon bond in Mes*NPSi(OTf)DAB **4.7** (X = OTf), (d(P–Si) = 2.290(1) Å) is within the range reported for acyclic monosilylated phosphines (2.264[19] Å),[131] and is significantly longer than the length of a P–Si double bond such as that found in Tipp(^{t}Bu)SiPSi(^{i}Pr)$_3$ (d(P–Si) = 2.062(1) Å[331]).

The silicon-oxygen bond in Mes*NPSi(OTf)DAB **4.7** (X = OTf), (d(Si–O) = 1.772(2) Å) is longer than those reported for diaryl- or dialkyl-siloxanes (d(Si–O) = 1.626(2) Å,[332] $(Me_3Si)_2O$; 1.616(1) Å,[332] $(Ph_3Si)_2O$)). The longer Si–O bond in Mes*NPSi(OTf)DAB **4.7** (X = OTf), is probably due to the electron-withdrawing properties of the triflate group. However, the Si–O bond in Mes*NPSi(OTf)DAB (d(Si–O) = 1.772(2) Å) is shorter than that reported for transition metal complexes, which feature a triflate-silicon bond (d(Si–O) = 1.853(5) to 1.951(1) Å), individual values for the transition metal complexes are given in Table 4.1. Furthermore, the sulphur-oxygen bond in **4.7** (X = OTf), which connects to the silicon centre (d(S–O) = 1.521(2) Å), is longer than the other two S–O bonds (d(S–O) = 1.417(3), 1.409(3) Å), an observation consistent with compounds containing a covalently bonded triflate group such as Mes*NPOTf, (d(S–O) = 1.499(4), 1.409(4), 1.405(4) Å[130]). However, the S–O(Si) bond in Mes*NPSi(OTf)DAB **4.7** (X = OTf), (d(S–O) = 1.521(2) Å) is significantly longer than those reported for other compounds containing a Si-OTf unit (d(S–O) = 1.490(3) Å,[333] Ph($C_6H_4CH_2O$-2)Si(H)OTf; 1.486(1) Å,[333] Ph($C_6H_4CH_2NMe_2$-2)Si(H)OTf).

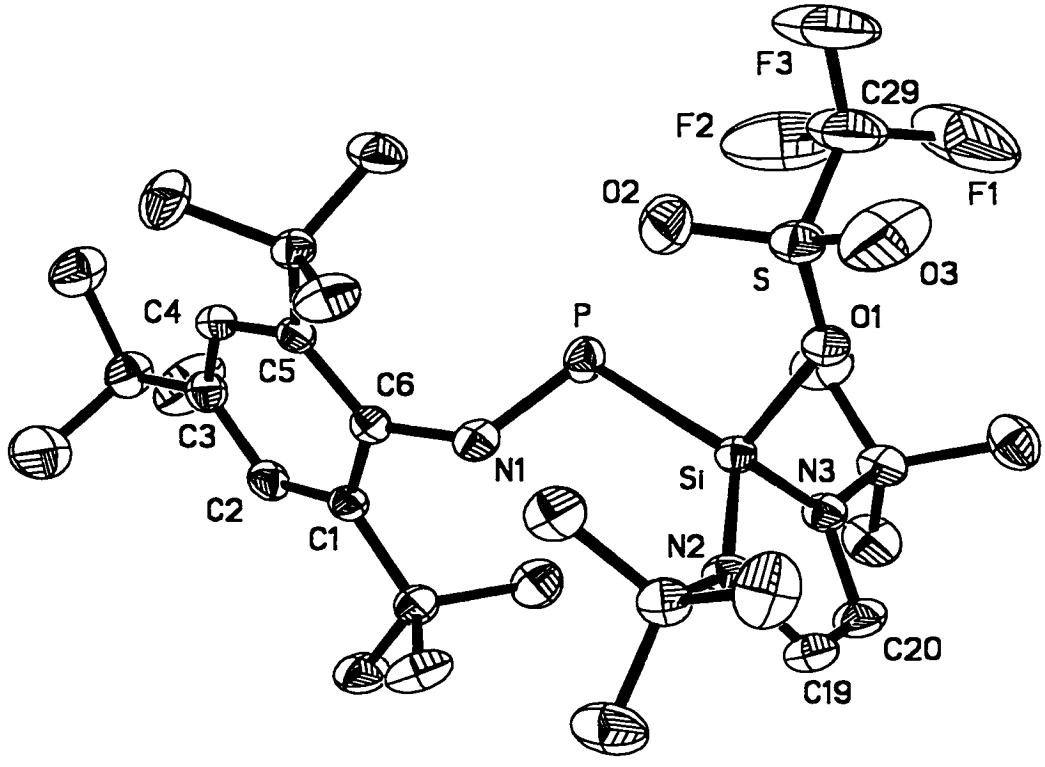

Figure 4.1: ORTEP-like view of Mes*NPSi(OTf)DAB 4.7 (X = OTf), drawn with 50% probability ellipsoids. The hydrogen atoms have been omitted for clarity. Selected bond lengths (Å) and angles (°): P–N(1) 1.578(3), P–Si 2.290(2), Si–O(1) 1.772(2), N(1)–C(6) 1.428(4), Si–N(2) 1.714(3), Si–N(3) 1.715(3), C(6)-N(1)-P 119.4(2), P-Si-N(2) 126.8(1), P-Si-N(3) 113.7(1), P-Si-O(1) 102.6(1), N(1)-Si-N(2) 95.2(1).

A direct comparison of the structural parameters of the silicon-diazasilacyclopentene unit (SiN(^{t}Bu)CHCH(^{t}Bu)N), in Mes*NPSi(OTf)DAB **4.7** (X = OTf) with those in the free diaminosilylene SiDAB, is not possible as the crystal structure of 1,3,2-diazolsilol-2-ylidene has not been solved as the result of crystal twining.[317] Nevertheless, a crystal structure has been reported for the saturated analog of SiDAB, **4.2**.[316] The Si–N bond lengths in Mes*NPSi(OTf)DAB **4.7** (X = OTf), (d(Si–N) = 1.714(3), 1.715(3) Å) are equivalent to those in the diaminosilylene **4.2**, (d(Si–N) = 1.72† Å)[316] and are similar to those reported for the diazadichlorosilacyclopentene Cl_2SiDAB **4.8**, (d(Si–N) = 1.695(3), 1.700(3) Å[317]). However, the Si–N bonds in **4.7** (X = OTf), are shorter than those found in diaminosilylene-transition metal complexes (d(Si–N) = 1.737(3) to 1.773(9) Å) and other compounds featuring a diazasilacyclopentene unit (d(Si–N) = 1.725(1) to 1.739(2) Å), individual values are provided in Table 4.2. The shorter Si–N bonds in Mes*NPSi(OTf)DAB **4.7** (X = OTf), and Cl_2SiDAB **4.8** are probably the result of an electron-withdrawing substituent attached to the silicon centre.

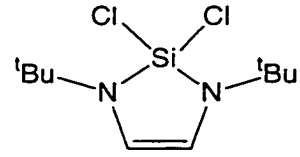

4.8

The N-Si-N bond angle in Mes*NPSi(OTf)DAB (95.2(1)°) is identical to that reported for dichlorodiazasilacyclopentene **4.8**, (95.4(1)°).[317] However, it is slightly wider than that found in the diaminosilylene **4.2**, (92.0†°),[316] and diaminosilylene-transition metal complexes (89.8(4) to 90.0(2) °), individual values are given in Table 4.2.

The nitrogen centres of the diazasilacyclopentene unit in Mes*NPSi(OTf)DAB **4.7** (X = OTf) are planar ($\Sigma \angle(N) = 359.1(3)°$ and 358.6(4)°). Hence, it is possible that there is lone pair π-conjugation between the silicon and nitrogen centres, which is also postulated to occur in the diaminosilylenes **4.1** and **4.2**.[322] It has been suggested that (σ*–p) bonding interactions between silicon and nitrogen centers causes compounds such as $N(SiMe_3)_3$ and $(Me_3Si)_2N(SiH_2Ph)$ to have planar rather than pyramidal geometry.[334] A similar bonding mechanism between the silicon and nitrogen centres may also be operative in Mes*NPSi(OTf)DAB **4.7** (X = OTf).

The diazasilacyclopentene ring (defined by atoms Si, N(1), N(2), C(2), C(3)) in Mes*NPSi(OTf)DAB **4.7** (X = OTf) is planar with a mean deviation from the plane of 0.039(3) Å. This is consistent with that reported for the free diaminosilylene **4.1**, in the gas phase as determined from an electron diffraction study.[317]

The P–N(Mes*) bond in Mes*NPSi(OTf)DAB **4.7** (X = OTf), (d(P–N) = 1.578(3) Å) is longer than that in Mes*NPOTf (d(P–N) = 1.467(2) Å),[130] the *P*-alkyl-iminophosphines, $Mes*NPCEt_3$, (d(P–N) = 1.566(2) Å),[136] and $Mes*NPC(SiMe_3)_3$ (d(P–N) = 1.556(3) Å[281]). However, the P–N(Mes*) bond length in **4.7** (X = OTf) is equivalent to that reported for the *P*-phosphino-iminophosphine $Mes*NPP(^tBu)_2$, (d(P–N) = 1.570(2) Å).[335] This experimental observation is in agreement with ab initio calculations, using the CEPA-1 level of theory with a Huzinaga basis set, which show that an iminophosphine with a strong σ-donating *P*-substituent, such as a silyl group, has a long P–N bond (d(P–N) = 1.578 Å, $FNP(SiH_3)$; 1.548 Å, HPNH).[113]

The (Mes*)C-N-P bond angle in Mes*NPSi(OTf)DAB **4.7** (X = OTf), (119.4(2)°) is significantly smaller than that in Mes*NPOTf (176.4(3)°),[130] but is similar or identical to those reported for *P*-alkyl-iminophosphines (120.2(2)°, $Mes*NPC(SiMe_3)_3$;[281] 124.8(2)°, $Mes*NPCEt_3$[136]), and that in $Mes*NPP(^tBu)_2$ (120.2(1)°).[335]

The (Mes*)N-P-Si bond angle 100.33(10)°, is smaller than the N-P-P bond angle in Mes*NPP(^{t}Bu)$_2$, 105.96(6)°,[335] but is still considered unexceptional for an iminophosphine.

The silicon centre in Mes*NPSi(OTf)DAB **4.7** (X = OTf), has a distorted tetrahedral geometry as indicated by the bond angles P-Si-O (102.6(1)°) and P-Si-N (126.8(1), 113.7(1)°). The (Mes*)C-N-P-Si torsion angle (-167.2(2)°) shows that the diazasilacyclopentene unit has a *trans*-configuration with respect to the Mes* substituent. The distance between the O(2) centre of the triflate group and phosphorus centre is 3.186(2) Å, which is slightly less than 3.30 Å (from $\Sigma\, r_w(P) + r_w(O)$). Hence, a bonding interaction between the phosphorus and oxygen centres can be considered negligible.

The crystal structure of Mes*NPSi(OTf)DAB **4.7** (X = OTf) shows there are no significant intermolecular interactions between molecules in the unit cell, except for some hydrogen bonding involving the oxygen and fluorine centres of the triflate group.

4.2.3: Spectroscopic Features of the *P*-Silyl-iminophosphines Mes*NPSi(X)DAB **4.7** (where X = Cl or OTf)

The solution ^{31}P NMR spectra of the *P*-silyl-iminophosphines Mes*NPSi(X)DAB **4.7**(X = OTf and Cl), shows that the phosphorus nucleus ($\delta(^{31}P)$ = 566 ppm, OTf; 586 ppm, Cl) in these compounds is considerably deshielded as compared with those in the parent iminophosphines Mes*NPX ($\delta(^{31}P)$ = 55 ppm, X = OTf;[130] 135 ppm, X = Cl[123]). However, the $\delta(^{31}P)$ values for **4.7** (X = OTf or Cl) are similar to those reported for *P*-alkyl-iminophosphines ($\delta(^{31}P)$ = 490 to 500 ppm) and the *P*-phosphino-iminophosphine Mes*NPP(^{t}Bu)$_2$ ($\delta(^{31}P)$ = 570 ppm),[75] but they are not as large as those reported for the *P*-arsino- and *P*-metallo-iminophosphines ($\delta(^{31}P)$ = 644 to 787 ppm), individual values are provided in Table 4.3. The substantial deshielded phosphorus nucleus in these types of

iminophosphines, including Mes*NPSi(X)DAB **4.7** (X = OTf or Cl), is attributed to the strong σ-donating ability of the *P*-substituent.[137]

The ^{31}P resonance for Mes*NPSi(X)DAB **4.7** (X = OTf or Cl), is accompanied by phosphorus-silicon coupling. The $^{1}J(^{31}P,^{29}Si)$ values (121 and 102 Hz, respectively) are large for compounds featuring a single P–Si bond ($^{1}J(^{31}P,^{29}Si)$ = 20 to 42 Hz),[336] but are small compared with phosphasilenes, which contain a P–Si double bond ($^{1}J(^{31}P,^{29}Si)$ = 149 to 203 Hz), individual values are given in Table 4.4.

The solution ^{29}Si NMR spectra of Mes*NPSi(OTf)DAB **4.7** (X = OTf) showed one doublet with a chemical shift value ($\delta(^{29}Si)$ = -46 ppm) that is significantly smaller when compared with that of the free ligand, SiDAB ($\delta(^{29}Si)$ = 78 ppm[317]). The $\delta(^{29}Si)$ value in **4.7** (X = OTf) is smaller than that observed in complexes featuring a diaminosilylene **4.1**, coordinated to a transition metal centre ($\delta(^{29}Si)$ = 21 to 139 ppm), individual values are provided in Table 4.5. However, the $\delta(^{29}Si)$ value in Mes*NPSi(OTf)DAB is typical for a tetrasubstituted diazasilacyclopentene with an electronegative substituent bonded to the silicon centre, ($\delta(^{29}Si)$ = -41 to 1 ppm), individual values are given in Table 4.5.

The solution ^{1}H and ^{13}C NMR spectra of Mes*NPSi(OTf)DAB **4.7** (X = OTf), show single sets of resonances associated with the Mes* substituent and the diazasilacyclopentene group. The resonances of the quaternary carbons of the *tert*-butyl group in the diazasilacyclopentene group exhibit coupling from both the silicon and phosphorus nuclei. The $\delta(^{1}H)$ and $\delta(^{13}C)$ values associated with the ring of the diazasilacyclopentene unit in Mes*NPSi(OTf)DAB **4.7** (X = OTf), ($\delta(^{1}H)$ = 5.58 ppm; $\delta(^{13}C)$ = 113.7 ppm) are consistent with values reported for tetrasubstituted diazasilacyclopentenes ($\delta(^{1}H)$ = 5.74 to 5.78 ppm; $\delta(^{13}C)$ = 112.6 to 113.7 ppm), individual values are given in Table 4.6. In contrast, these nuclei in the free ligand **4.1**

($\delta(^1H)$ = 6.75 ppm; $\delta(^{13}C)$ = 120.0 ppm),[318] and the diaminosilylene-transition metal complexes are deshielded; $\delta(^1H)$ = 6.59 to 6.75 ppm; $\delta(^{13}C)$ = 115.2 to 120.0 ppm), individual values are given in Table 4.6. The (^1H) and $\delta(^{13}C)$ values associated with the Mes* substituent in Mes*NPSi(OTf)DAB **4.7** (X = OTf) exhibit minor variations as compared with those in Mes*NPOTf.

Both the ^{19}F and ^{13}C NMR solution spectra of Mes*NPSi(OTf)DAB **4.7** (X = OTf) show that fluorine nuclei for the triflate group are deshielded ($\delta(^{19}F)$ = -76.5 ppm) and the trifluoromethyl carbon nucleus is shielded ($\delta(^{13}C)$ = 119.6 ppm) as compared with those in Mes*NPOTf ($\delta(^{19}F)$ = -78.5 ppm; $\delta(^{13}C)$ = 121.0 ppm),[130] and [^{n}Bu$_4$N]OTf ($\delta(^{19}F)$ = -80.0 ppm[37]). Furthermore, the fluorine nuclei in Mes*NPSi(OTf)DAB are more deshielded than those in trimethylsilyltriflate Me_3SiOTf, ($\delta(^{19}F)$ = -77.7 ppm; $\delta(^{13}C)$ = 119.1 ppm), which contains a silyl group bonded to triflate.

From comparisons of ^1H, ^{13}C, and ^{29}Si chemical shifts with other compounds containing a covalently bonded triflate group, it would appear that the molecular structure of Mes*NPSi(OTf)DAB **4.7** (X = OTf) in the solid state is the same as in solution, and that the triflate group does not dissociate from the silicon centre.

The infrared spectra of Mes*NPSi(OTf)DAB **4.7** (X = OTf), prepared as a paraffin oil mull, showed several bands corresponding to stretching frequencies of the SO_3 and CF_3 groups (1388, 1244, 1149, and 1097 cm^{-1}). Peaks were not observed in the 1270 to 1280 cm^{-1} region, which is typically where S–O stretching frequencies appear in compounds featuring a weakly coordinating triflate group.[133] Hence, the IR spectra demonstrates, as does crystallography, that the triflate group in Mes*NPSi(OTf)DAB **4.7** (X = OTf), is covalently bonded.

4.3: Conclusions: General Bonding Implications for the *P*-Silyl-iminophosphines Mes*NPSi(X)DAB 4.7 (where X = Cl or OTf)

The reactions between imidazol-2-ylidene Im, and Mes*NPX (X = Cl or OTf), resulted in σ-coordination complexes [Mes*NP•Im]OTf **3.14** and Mes*NP(Cl)•Im **3.15**, respectively. In contrast, the addition of the diaminosilylene SiDAB, to Mes*NPX (X = Cl or OTf) afforded the first examples of *P*-silyl-iminophosphines **4.7** (X = Cl or OTf). Importantly, this syntheses of **4.7** (X = OTf or Cl) demonstrates that *P*-functionalized iminophosphines can be formed through coordination chemistry with phosphorus as a Lewis acid. The reactivity between the Lewis acidic iminophosphines and SiDAB resembled that which was observed between silylenes and other phosphino-bonding environments. The formation of Mes*NPSi(X)DAB (X = Cl or OTf) can be envisaged as an insertion of the silicon centre of the diaminosilylene into a Cl–P or P–O(Tf) bond. Silylenes, including SiDAB, are known to insert into a variety of heteronuclear bonds, including Si–O, Si–H, O–H, P–X, Sn–X, and C–H.[327,337,338] A simple reaction mechanism for the formation of Mes*NPSi(X)DAB **4.7** (X = Cl or OTf), (Figure 4.2) is postulated to involve initial coordination of the diaminosilylene to the iminophosphine at the phosphorus centre, resulting in a σ-coordination complex featuring a trisubstituted silicon centre. However, this complex, an intermediate on the reaction pathway, probably converts rapidly to the *P*-silyl-iminophosphine by nucleophilic attack of the silicon centre by a chloride or triflate anion. The preference for the diaminosilylene unit to form a tetrasubstituted silicon-bonding environment is commonplace, as demonstrated by the transformation of the diaminosilylene-borane complex **4.9**. The complex converts into a tetrasubstituted diazaborosilacyclopentene **4.10** through the migration of a pentafluorophenyl group from the boron to silicon centre (Figure 4.3). The attachment of a chloride or a triflate group to the silicon atom rather than to phosphorus may reflect the lower electronegativity of silicon as compared with phosphorus (χ_{spec} of Si 1.916[6] versus

2.253[6] for P). Examples of trisubstituted silicon compounds behaving as Lewis acids, with respect to weak bases such as tetrahydrofuran and toluene, have been isolated and crystallographically characterized.[339,340]

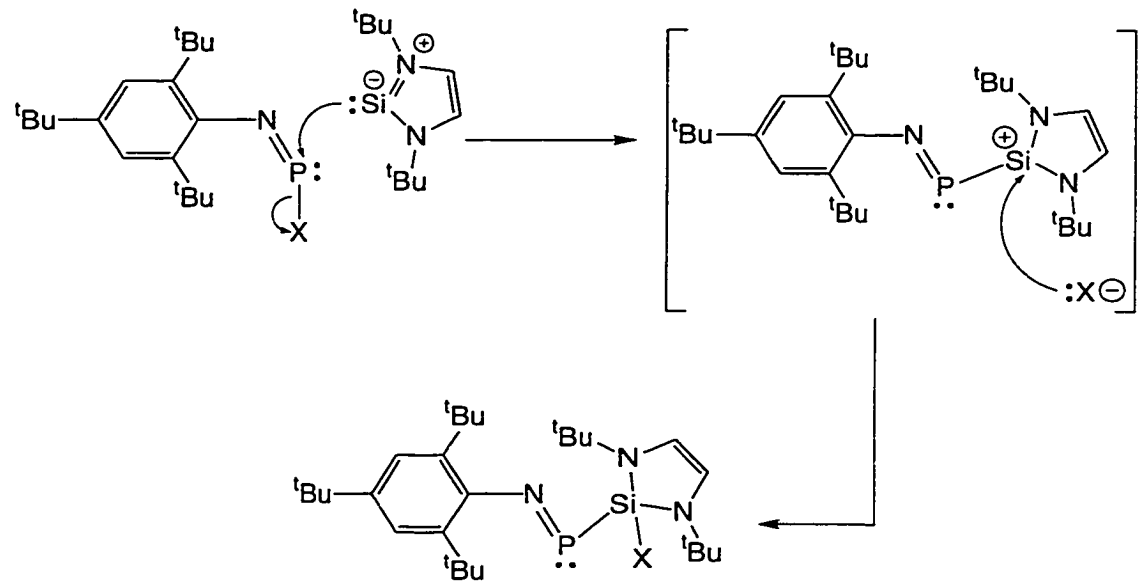

Figure 4.2: A proposed reaction mechanism for the formation of a *P*-silyl-iminophosphine Mes*NPSi(X)DAB **4.7** (X = Cl or OTf), from the addition of the diaminosilylene SiDAB, to Mes*NPX.

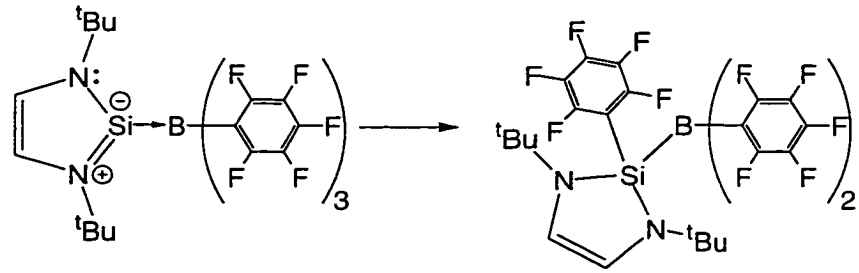

4.9 **4.10**

Figure 4.3: Transformation of the diaminosilylene-borane complex **4.9** into a diazaborosilacyclopentene **4.10**, which features a tetrasubstituted silicon centre.

Similar attempts to isolate compounds with a metal-silicon π-bond through halide abstraction were unsuccessful as the silicon centres preferentially formed compounds with tetrasubstituted bonding environments as shown by the reactions in Figure 4.4.

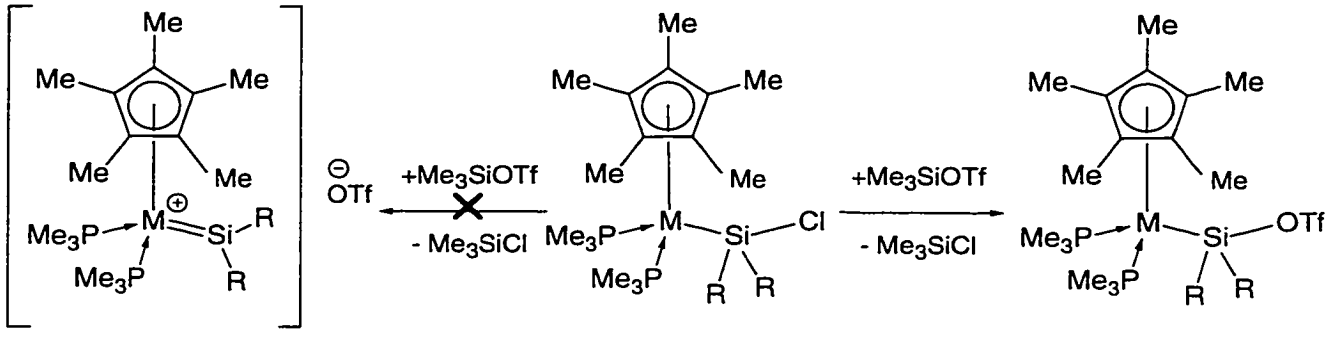

Figure 4.4: The attempted syntheses of complexes featuring a metal-silicon π-bond. However, the chlorine centre was substituted for a triflate group. M = Ru, R = Ph;[341] M = Os, R = Me.[342]

The shortness of Si–N bonds in Mes*NPSi(OTf)DAB **4.7** (X = OTf) suggests that there is Si–N π-bonding in the diazasilacyclopentene unit. The allylic silicon-nitrogen π-bonding in the free diaminosilylene SiDAB, is also probably retained in the *P*-silyl-iminophosphine Mes*NPSi(OTf)DAB **4.7** (X = OTf) (**4.11**, Figure 4.5). The hypothetical addition of OTf^- or Cl^- to the central carbon of the ylidene unit in the cationic Mes*NP•Im fragment, as found in **3.15**, would disrupt the allylic nitrogen-carbon π-bonding in the ligand. In contrast, silicon can engage in hypervalent bonding and compounds containing a tetrasubstituted π-bonded silicon centre are known.[343,344] The long P–Si bond in Mes*NPSi(OTf)DAB **4.7** (X = OTf) suggests that this compound has negligible or weak P–Si π-bonding, hence a resonance contributor with an allene-like structure **4.12**, would represent a minor component in the bonding description of **4.7** (Figure 4.5). Several factors may be responsible, including the possibility that the

resulting allene-like bonding environment **4.12**, is too unstable for phosphorus, as no donor-free bonding environments of this type have been reported.

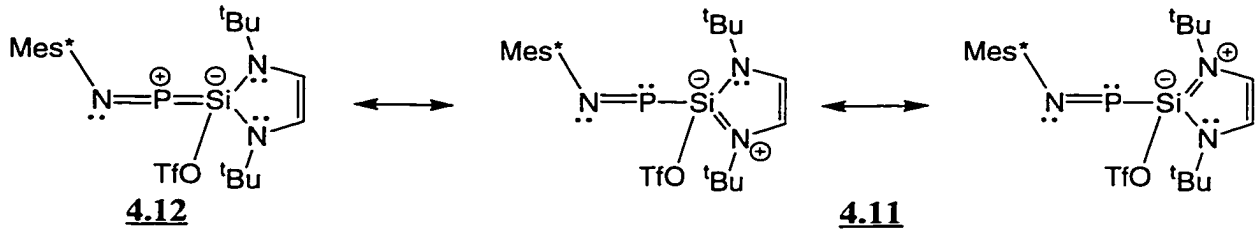

Figure 4.5: Comparison of bonding models for Mes*NPSi(OTf)DAB **4.7** (X = OTf) with P–Si or Si–N π-bonding.

Table 4.1: Comparison of Si–O and S–O bond lengths in Mes*NPSi(OTf)DAB **4.7** (X = OTf) with other compounds that contain a SiOTf or POTf fragment. Compounds are listed by increasing *d*(Si–O) values. All values in Å.

Compound	*d*(Si–O)	*d*(S–O(Si/P))	*d*(S–O)	Reference
Mes*NPOTf	–	1.499(4)	1.409(4), 1.405(4)	130
Mes*NPSi(OTf)DAB (**4.7**)	1.772(2)	1.521(2)	1.417(3), 1.409(3)	This work
$Cp^*(PMe_3)_2Si(Ph)_2OTf$	1.853(5)	–	–	341
$Ph(C_6H_4CH_2O\text{-}2)Si(H)OTf$	1.857(3)	1.490(3)	1.418(3), 1.420(3)	345
$Cp^*(PMe_3)_2OsSi(Me_2)OTf$	1.866(5)	–	–	342
$Ph(C_6H_4CH_2NMe_2\text{-}2)Si(H)OTf$	1.951(1)	1.486(1)	1.421(2), 1.422(2)	333

Table 4.2: Comparison of Si–N bond lengths and the N-Si-N bond angle in Mes*NPSi(OTf)DAB **4.7** (X = OTf) with other compounds featuring a diazasilacyclopentene unit or a diaminosilylene ligand **4.1**. Compounds are listed by increasing *d*(Si–N) values.

Compound	*d*(Si–N) (Å)	∠(N-Si-N) (°)	Reference
Cl_2SiDAB (**4.8**)	1.695(3), 1.700(3)	95.4(1)	317
Mes*NPSi(OTf)DAB (**4.7**)	1.714(3), 1.715(3)	95.2(1)	This work
$SiN(^tBu)CH_2CH_2N(^tBu)$ (**4.2**)	1.72†	92.0†	316
$O(Si(H)DAB)_2$	1.725(1), 1.739(1)	93.5(1)	318
$N_3Si(N(SiMe_3)_2)DAB$	1.728(2)	92.9(1)	340
$Ph_3CSi(THF)DAB$	1.735(3), 1.736(3)	91.8(2)	340
$S_2(SiDAB)_2$	1.735(1), 1.738(1)	93.2(1)	318
$Ni(SiDAB)_3$	1.737(3), 1.743(3)	–	346
$Se_2(SiDAB)_2$	1.739(2), 1.738(2)	93.3(1)	318
$(OC)_2Ni(SiDAB)_2$	1.743(5), 1.745(5)	90.0(2)	347
	1.745(5), 1.749(5)	89.9(2)	
$Cp_2MoSiDAB$	1.748(5)	90.0(2)	348
$Cp_2Mo(H)Si(H)DAB$	1.773(9)	89.8(4)	348

Table 4.3: Comparison of solution $\delta(^{31}P)$ values for Mes*NPSi(X)DAB **4.7** (X = Cl or OTf) with *P*-alkyl-iminophosphines, and other related *P*-substituted Mes*-iminophosphines. Compounds are listed by increasing δ values. All values in ppm.

Compound	$\delta(^{31}P)$	Reference
Mes*NPOTf	55	130
Mes*NPCl	135	123
$(Me_3Si)_2NNPP(^tBu)_2$	429	349
$Mes*NPPC(NMe_2)NEt_2$	476	149
$Mes*NPPC(NMe_2)_2$	479	149
$Mes*NP^tBu$	490	255
$Mes*NP^iPr$	491	106
$Mes*NPCEt_3$	495	136
$^iPr_3SiNPMes*$	498	135
$Mes*NPC(SiMe_3)_3$	500	281
Mes*NPSi(OTf)DAB (**4.7**)	566	This work
$Mes*NPP(^tBu)_2$	570	75
Mes*NPSi(Cl)DAB (**4.7**)	586	This work
$Mes*NPAs(^tBu)_2$	644	102
$Mes*NPFe(CO)_2Cp$	688	140
$Mes*NPRu(CO)_2Cp$	717	140
$Mes*NPW(CO)_3Cp*$	754	140
$Mes*NPFe(CO)_2Cp*$	787	140

Table 4.4: Comparison of $^1J(^{31}P,^{29}Si)$ values for Mes*NPSi(X)DAB **4.7** (X = Cl or OTf) with compounds containing a single or double phosphorus-silicon bond. Compounds are listed by increasing coupling. All values in Hz.

Compound	$^1J(^{31}P,^{29}Si)$	Reference
$(Me_3Si)PMe_2$	20	336
$(Me_3Si)PPh_2$	22	336
$(Me_3Si)_3P$	28	336
$(H_3Si)_3P$	42	336
Mes*NPSi(Cl)DAB (**4.7**)	102	This work
Mes*NPSi(OTf)DAB (**4.7**)	121	This work
$Mes*PSi(Mes)_2$	149	350
$MesPSi(Mes)_2$	149	351
$PhPSi(Tipp)_2$	151	351
$MesPSi(Tipp)_2$	152	351
$^tBuPSi(Tipp)_2$	154	351
$(^iPr)_3SiPSi(^tBu)Tipp$	161	331
$Mes*PSi(^tBu)P(Mes*)PPh_2$	203	352

Table 4.5: Comparison of solution $\delta(^{29}Si)$ values for Mes*NPSi(OTf)DAB **4.7** (X = OTf) with other compounds featuring a diazasilacyclopentene unit or a diaminosilylene ligand SiDAB, **4.1**. Compounds are listed by decreasing δ values. All values in ppm.

Compound	$\delta(^{29}Si)$	Reference
$Cp_2Mo(SiDAB)$	139	348
$Ni(SiDAB)_3$	111	346
$(OC)_2Ni(SiDAB)_2$	98	347
SiDAB (**4.1**)	78	317
$Cp_2Mo(H)Si(H)DAB$	43	348
ISi(Me)DAB	37	318
$Cp_2Mo(H)Si(OH)DAB$	36	348
$Cp_2W(H)Si(H)DAB)$	21	348
Me_2SiDAB	4	353
MeSi(Cl)DAB	1	353
$SnCl(Si(Cl)DAB)_3$	-20	338
$(Si(Cl)DAB)_2$	-33	338
HSi(Cl)DAB	-38	353
Cl_2SiDAB (**4.8**)	-41	317
$S_2(SiDAB)_2$	-45	318
Mes*NPSi(OTf)DAB (**4.7**)	-46	This work
$N_3Si(N(SiMe_3)_2)DAB$	-47	340
(DAB)SiDAB	-51	318
$O(Si(H)DAB)_2$	-58	318
$Ph_3CSi(THF)DAB$	-67	340
$Se_2(SiDAB)_2$	-68	318

Table 4.6: Comparison of $\delta(^1H)$ and $\delta(^{13}C)$ values for the for diazasilacyclopentene unit in Mes*NPSi(OTf)DAB **4.7** (X = OTf) with other compounds featuring a diazasilacyclopentene unit or a diaminosilylene **4.1** ligand. Compounds are listed by increasing δ values of the methine proton (NC**H**). All values are reported in ppm.

	$\delta(^1H)$		$\delta(^{13}C)$			
Compound	$(H_3C)_3C$	N(C**H**)	$(H_3C)_3C$	$(H_3C)_3C$	N(**C**H)	Reference
Mes*NPSi(OTf)DAB (**4.7**)	1.17	5.58	33.8	53.1	113.7	This work
Cl_2SiDAB (**4.8**)	1.24	5.74	30.4	52.6	112.6	317
ClSi(H)DAB	1.22	5.75	30.6	51.7	112.8	353
PhSi(Me)DAB	1.09	5.76	31.1	51.3	113.0	353
MeSi(Cl)DAB	1.24	5.76	30.7	51.9	112.8	353
MeSi(I)DAB	1.21	5.78	31.8	52.6	113.7	318
$Cp_2Mo(SiDAB)$	1.48	6.59	32.0	51.6	115.2	348
$Ni(SiDAB)_3$	1.54	6.60	33.5	53.8	118.2	346
$Ni(CO)_2SiDAB$	1.40	6.74	30.3	54.0	120.0	347
SiDAB (**4.1**)	1.41	6.75	30.3	54.0	120.0	317

Chapter 5: The Coordination Chemistry of the Phosphadiazonium Cation involving Tertiary Phosphine Chalcogenide and Chalcogenoimidazoline Ligands

5.1: Introduction: Overview of the Coordination Chemistry of Lewis Acidic Phosphorus Centres with Chalcogen Groups

The coordination chemistry of phosphorus as a Lewis acid has been well established from the synthesis and characterization of complexes involving a chalcogen centre as the Lewis basic component. Analogous with the phosphorus-nitrogen complexes described in Section 2.1, the majority of chalcogen-phosphorus complexes feature either a penta- or tetra-substituted phosphorano-bonding environment. For example, pentafluorophosphorane PF_5, forms complexes with tetrahydrofuran, ethers,[354] thio-, and seleno-ethers.[355] Similarly, complexes involving pentachlorophosphorane PCl_5, and a tertiary phosphorylic ligand, $OPPh_3$ or $OP(^nBu)_3$, are known.[356] Compounds of the type $[R_3PO{\bullet}P(O)X_2]X$ (X = Cl or Br), featuring a coordinated phosphoryl dihalide centre have also been isolated.[357] Many of these phosphorano-complexes have been formulated on the basis of elemental analysis and measurements of physical properties (i.e., heats of reaction, pressure-composition isotherms) or data from solution ^{19}F NMR spectroscopy.[179,358] However, knowledge of the exact nature of the chalcogen-phosphorus interaction is vague as very few of these compounds have been crystallographically characterized.

A number of compounds have been synthesized which feature intramolecular coordination between a phosphorano-centre and a Lewis basic chalcogen group, as part of a carbonyl or phosphoryl substituent. Examples include the tetrachlorophosphorano-phenylsalicylate[359] and tetrafluorophosphorano-phosphoryl complexes.[360] A series of structurally characterized phosphoryl and phosphorano-complexes which contain a sulphide R_2S, or sulphuryl R_2SO_2, bridged diphenolate substituent has been synthesized

and crystallographically characterized.[361] The phosphorus and chalcogen centres in these compounds form part of an eight-membered ring and are brought into close proximity by folding of the substituent.[362-370] Phosphorano-containing complexes containing a chelating chalcogeno-ligand have been isolated and structurally characterized. These include β-diketonate and dichalcogenocarbamate[371,372] ligands, which form complexes where the tetrasubstituted phosphorano-centre is part of a six-membered and four-membered ring, respectively.[176,373]

There are fewer examples of complexes featuring a chalcogen group coordinated to a Lewis acidic σ-phosphino-centre. However, at present, only compounds with an intramolecular σ-phosphino-chalcogen interaction are known. These include complexes with a sulphide bridged diphenolate substituent coordinated to a phosphite centre, which has been recently synthesized.[364,368] A phosphorus-oxygen interaction is often observed in σ-phosphines or σ-phosphites with a pendent carbonyl group, as part of a methylsalicylate,[374] carboxylic, or a propiophenone[375] substituent.[368] Phosphorus-oxygen interactions are also observed between the *ortho*-methoxy groups of aryl substituents attached to either a (σ^4,λ^5)-phosphorano- or (σ^3,λ^3)-phosphino-centre.[376,377] A complex with three dithiocarbamate substituents attached to a σ-phosphino-centre has been prepared.[378] The crystal structure shows that the phosphorus centre has a distorted trigonal antiprism geometry with alternating short and long sulphur-phosphorus interactions.[176,378]

In contrast to the number of complexes featuring a phosphorano- or σ-phosphino-centre coordinated by a chalcogen group, little is known about the interactions between π-phosphino-compounds and chalcogen Lewis bases. The highly reactive dichlorophosphenium cation PCl_2^+, generated from the electron ionization of PCl_3, has been shown by mass spectrometry to abstract hydroxyl groups from cyclic ethers.[379] The

diazaphospholenium triflate complex **2.19** is postulated to form a Lewis acid-base adduct with 1,4-dioxane as postulated from data obtained from ^{31}P and ^{19}F NMR spectroscopy.[37] Tetrahydrofuran and 1,4-dioxane complexes of aluminatodiiminophosphane are proposed, based on similar spans of the solid state ^{31}P chemical shielding tensor to those reported for the corresponding complexes with a nitrogen ligand **2.4**-**2.6**.[91,213] The oxidation of a *P*-phosphaseleno- or *P*-phosphathio-iminophosphine with elemental sulphur or selenium affords complexes of type **5.1** (Ch = S or Se), (Figure 5.1) which contain a phosphadiazonium cation and a dichalcogenophosphinate anion.[138] Although, the crystal structures reveal a weak interaction between the phosphadiazonium cation and anion in **5.1** (Ch = S or Se), (vide infra), data from solution ^{31}P and ^{77}Se NMR spectroscopy suggest that the cation-anion pairing in **5.1** (Ch = Se) is dissociated at room temperature.[137]

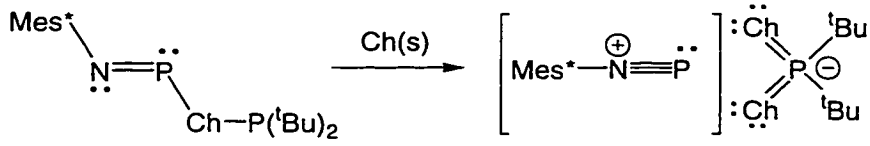

5.1

Figure 5.1: Synthesis of phosphadiazonium-dichalcogenophosphinate complexes **5.1** (Ch = S or Se) from chalcogen oxidation of the corresponding *P*-phosphachalcogeno-iminophosphine.

A study by the author of this thesis was undertaken to assess the reactivity between the Lewis acidic iminophosphine Mes*NPOTf, and a series of structurally homologous ligands, chalcogenoimidazolines **5.2** (Ch = O, S, Se, or Te), for which convenient syntheses have been reported.[266,380,381] The study was also extended to include tertiary phosphine chalcogenides, $OPPh_3$, $SPPh_3$, and $SePPh_3$. The synthesis and

characterization of the resulting complexes **5.3** (Ch = O, S, or Se), **5.4** (Ch = O or S) is described in the following sections.

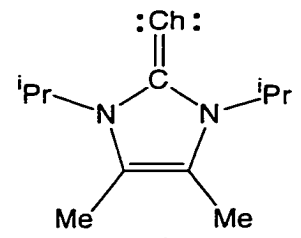

5.2

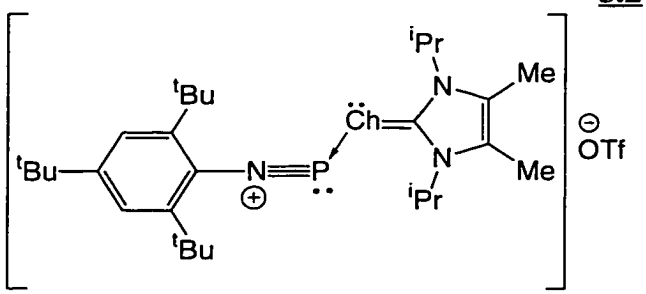

5.3

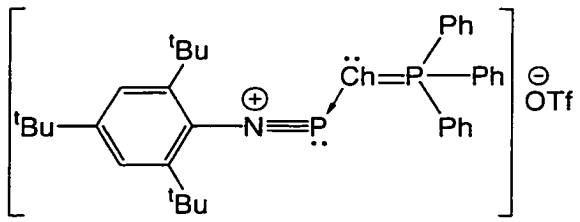

5.4

5.2: Results and Discussion

5.2.1: Synthesis of Phosphadiazonium-triflate Complexes with Chalcogeno-imidazoline (5.3) and Tertiary Phosphine Chalcogenide (5.4) Ligands

Synthesis of complexes with the general formula [Mes*NP•Lg]OTf (Lg = OIm, SIm, or SeIm) **5.3** (Ch = O, S, or Se), and $OPPh_3$ **5.4** (Ch = O), involved the addition of triphenylphosphine oxide or a chalcogenoimidazoline (abbreviated as OIm **5.2** (Ch = O), SIm **5.2** (Ch = S), or SeIm **5.2** (Ch = Se)) to Mes*NPOTf using a 1:1 stoichiometry. Crystalline material was obtained on slow removal of the solvent (benzene). Alternatively, the [Mes*NP•OIm]OTf **5.3** (Ch = O), complex precipitated out of solution upon mixing of the reagents when the reaction solvent was n-hexane. The complexes were characterized using solution ^{31}P, ^{19}F, ^{13}C, ^{1}H NMR, IR spectroscopy, and crystallography. The ^{31}P NMR spectra of the reaction mixtures showed that complexes

were formed in high yield (> 90 %, based on ^{31}P NMR signal integration). One side product in the reaction mixture of [Mes*NP•SIm]OTf **5.3** (Ch = S) was tentatively assigned as the diaminophosphenium-triflate salt [(Mes*N(H))$_2$P]OTf ($\delta(^{31}P)$ = 279 ppm[33]).

In the case of [Mes*NP•SPPh$_3$]OTf **5.4** (Ch = S), a bright red reaction mixture was observed, but solid product could not be obtained, despite various attempts using different crystallization techniques. Instead, the components of the reaction mixture crystallized out separately. Nevertheless, [Mes*NP•SPPh$_3$]OTf **5.4** (Ch = S) was characterized in solution by ^{31}P, ^{19}F, ^{13}C, and ^{1}H NMR spectroscopy. The ^{31}P and ^{13}C NMR spectra of a solution containing Mes*NPOTf with triphenylphosphine selenide, using a 1:1 stoichiometry, showed no evidence of complex formation.

The addition of imidazol-2-tellurone, hereafter abbreviated as TeIm **5.2** (Ch = Te), to Mes*NPOTf, using a 1:1 stoichiometry, resulted in a cloudy dark purple reaction mixture. A black solid speculated as being elemental tellurium, was filtered from the solution and a purple crystalline solid was obtained by slow solvent removal. The solution ^{31}P NMR spectrum of the product showed that the dominant peak ($\delta(^{31}P)$ = 336 ppm) was consistent with that assigned to the [Mes*NP•Im]OTf complex **3.14**, which is also formed directly by the addition of imidazol-2-ylidene Im, to Mes*NPOTf (see Section 3.2.1).

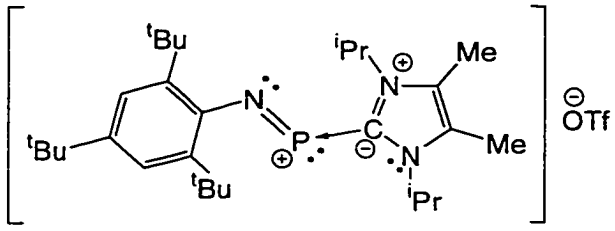

3.14

5.2.2: Structural Features of the [Mes*NP•Lg]OTf Complexes 5.3 (Ch = O, S, or Se), and 5.4 (Ch = O) where Lg is OIm, SIm, SeIm, or $OPPh_3$

The crystal structures of the phosphadiazonium-triflate complexes with chalcogen bases show that the terminal end of the chalcogenoimidazoline or triphenylphosphine oxide ligand has a monodentate bonding interaction with the phosphorus centre of the Mes*NP unit (Figures 5.2 to 5.5). Each structure is composed of a cationic phosphadiazonium-ligand unit and a triflate anion. The crystal structure of [Mes*NP•$OPPh_3$]OTf **5.4** (Ch = O), refines with two positions of 50% occupancy, for the phosphorus centre associated with the phosphadiazonium unit (Figure 5.3). The crystal structure of [Mes*NP•OIm]OTf **5.3** (Ch = O), shows the presence of a single disordered toluene molecule within the unit cell. The nearest [Mes*NP•OIm]OTf units are clustered around the toluene with the nearest [Mes*NP•OIm]OTf-toluene distances (d(O(1)–C)) equal to 3.65(1) Å. This distance is greater than 3.25 Å (from $\Sigma\, r_w(O) + r_w(C)$). Thus, it is concluded that there are no interactions between [Mes*NP•OIm]OTf and the toluene molecules. The [Mes*NP•Lg]OTf (Lg = SIm or SeIm) complexes **5.3** (Ch = S or Se), are isomorphous with unit cell parameters (e.g., space group, unit cell lengths and angles) which are similar or identical (Table 8.4).

In general, the (Mes*N)P–Ch(Lg) interaction in the [Mes*NP•Lg]OTf complexes (Lg = OIm, SIm, SeIm, or $OPPh_3$) are longer than those observed in compounds with a phosphino-bonding environment, which feature a phosphorus-chalcogen single bond. These include trischalcogeno-phosphines **5.5**, *cyclo*-triphospholanes **5.6**, and *P*-chalcogeno-iminophosphines **5.7**.

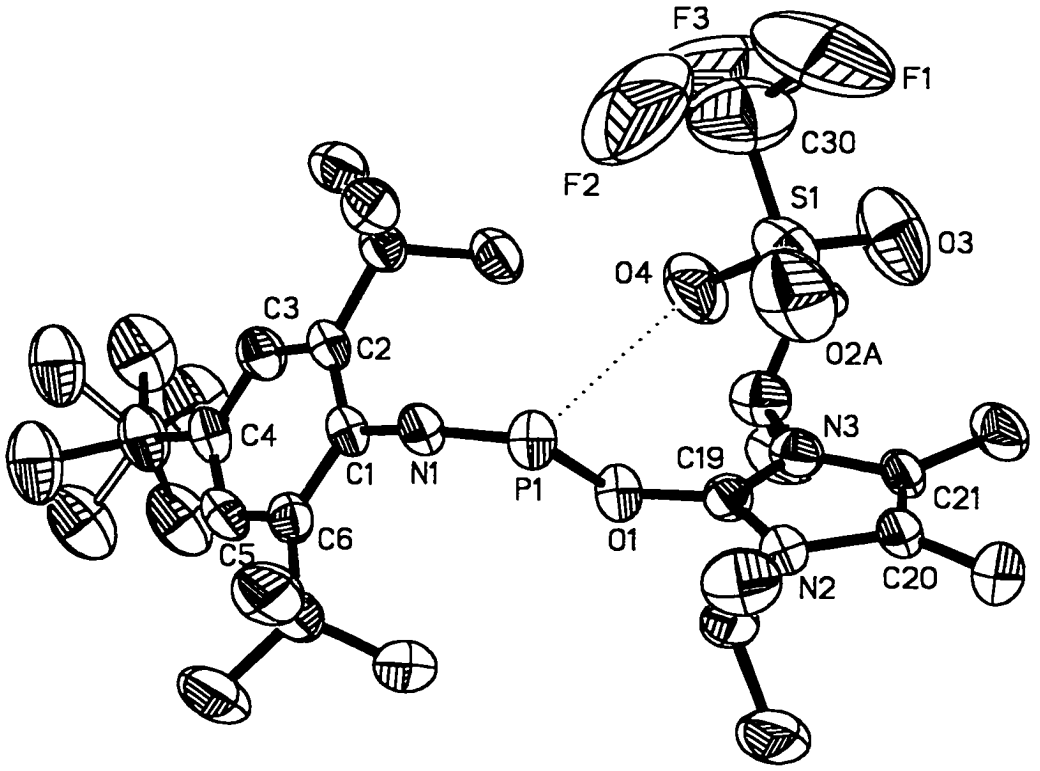

Figure 5.2: ORTEP-like view of [Mes*NP•OIm]OTf **5.3** (Ch = O), drawn with 50% probability ellipsoids. The hydrogen atoms have been omitted for clarity. The *para-tert*-butyl group of the Mes* substituent is disordered between two positions. Selected bond lengths (Å) and angles (°): P(1)–N(1) 1.494(4), P(1)–O(1) 1.773(3), O(1)–C(19) 1.342(5), N(1)–C(1) 1.404(5), N(2)–C(19) 1.330(5), N(3)–C(19) 1.336(5), P(1)–O(4) 2.775(4), N(1)-P(1)-O(1) 107.5(2), P(1)-O(1)-C(19) 120.4(3), C(1)-N(1)-P(1) 159.7(3), P(1)-O(1)-C(19) 120.5(3), O(1)-C(19)-N(2) 126.0(4), O(1)-C(19)-N(3) 123.1(4), N(2)-C(19)-N(3) 110.9(4).

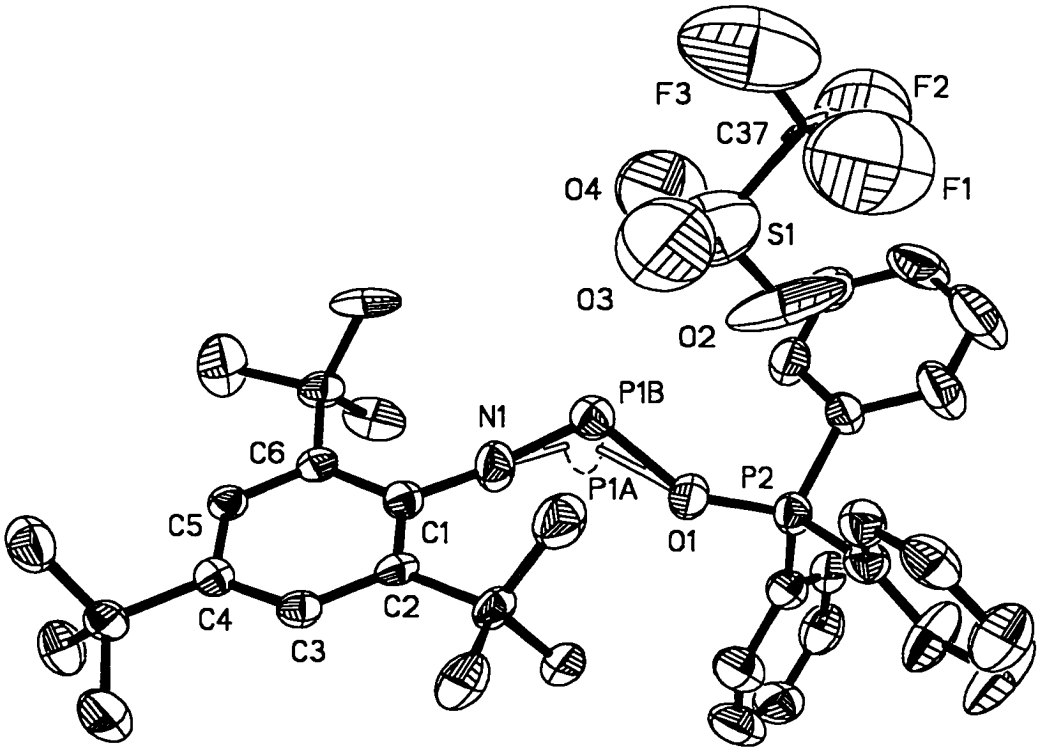

Figure 5.3: ORTEP-like view of [Mes*NP•OPPh$_3$]OTf **5.4** (Ch = O), drawn with 50% probability ellipsoids. The phosphorus centre, P(1A) and P(1B), associated with the phosphadiazonium unit is disordered between two positions. The hydrogen atoms have been omitted for clarity. Selected bond lengths (Å) and angles (°): P(1A)–P(1B) 0.60(1), P(1A)–N(1) 1.497(7), P(1B)–N(1) 1.504(7), P(1A)–O(1) 1.734(6), P(1B)–O(1) 1.746(6), N(1)–C(1) 1.396(7), P(2)–O(1) 1.563(4), C(1)-N(1)-P(1A) 165.9(5), C(1)-N(1)-P(1B) 170.0(6), N(1)-P(1A)-O(1) 108.4(4), N(1)-P(1B)-O(1) 107.5(4), P(1A)-O(1)-P(2) 138.0(3), P(1B)-O(1)-P(2) 142.2(3).

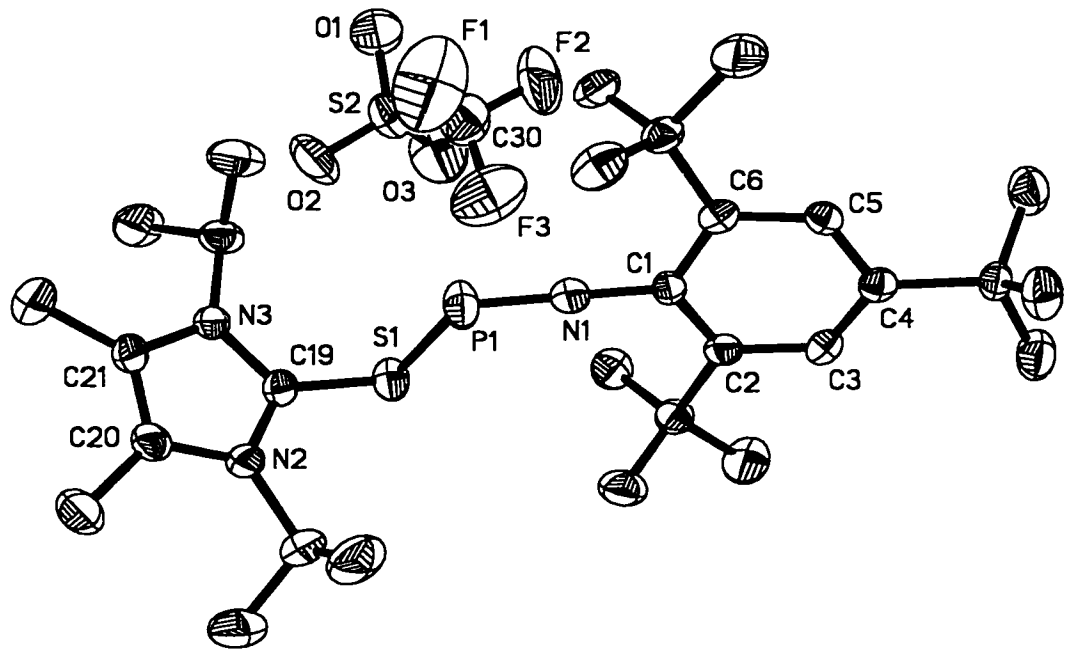

Figure 5.4: ORTEP-like view of [Mes*NP•SIm]OTf **5.3** (Ch = S), drawn with 50% probability ellipsoids. The hydrogen atoms have been omitted for clarity. Selected bond lengths (Å) and angles (°): P(1)–N(1) 1.498(2), S(1)–P(1) 2.266(1), N(1)–C(1) 1.382(3), S(1)–C(19) 1.736(3), N(2)–C(19) 1.346(3), N(3)–C(19) 1.358(3), S(1)-P(1)-N(1) 114.1(1), P(1)-N(1)-C(1) 174.4(2), P(1)-S(1)-C(19) 91.8(1), S(1)-C(19)-N(2) 125.6(2), S(1)-C(19)-N(3) 126.7(2), N(2)-C(19)-N(3) 107.5(2).

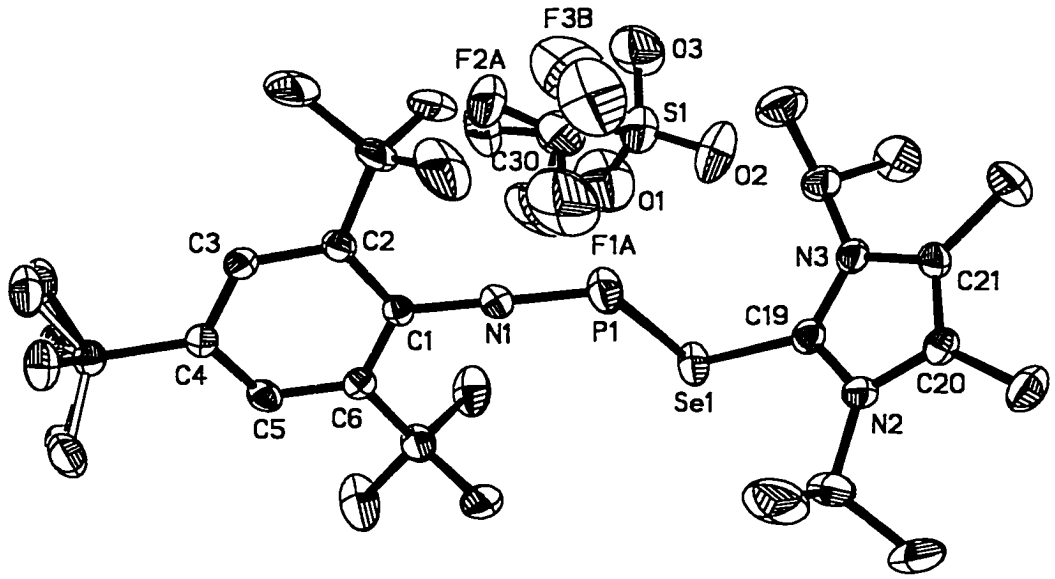

Figure 5.5: ORTEP-like view of [Mes*NP•SeIm]OTf **5.3** (Ch = Se), drawn with 50% probability ellipsoids. The hydrogen atoms have been omitted for clarity. The *para-tert*-butyl group of the Mes* substituent and the trifluoromethyl group of the triflate anion is disordered between two positions. Selected bond lengths (Å) and angles (°): P(1)–N(1) 1.500(2), Se(1)–P(1) 2.407(1), N(1)–C(1) 1.381(3), Se(1)–C(19) 1.889(3), N(2)–C(19) 1.345(3), N(3)–C(19) 1.355(3), Se(1)-P(1)-N(1) 115.4(1), P(1)-N(1)-C(1) 175.5(2), P(1)-Se(1)-C(19) 88.3(8), Se(1)-C(19)-N(2) 125.4(2), Se(1)-C(19)-N(3) 126.4(2), N(2)-C(19)-N(3) 108.1(2).

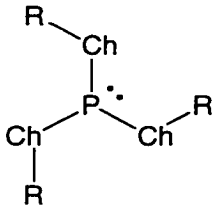

5.5

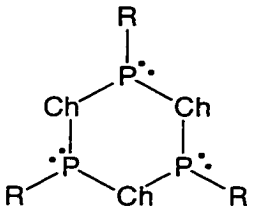

5.6

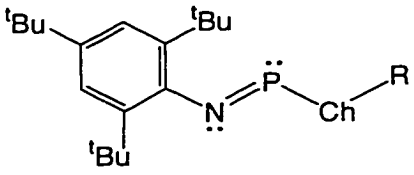

5.7

For example, the (Mes*N)P-O(Lg) bond length in [Mes*NP•OIm]OTf **5.3** (Ch = O), (d(P–O) = 1.773(3) Å) and [Mes*NP•OPPh$_3$]OTf **5.4** (Ch = O), (d(P$_A$–O) = 1.734(6) Å; d(P$_B$–O) = 1.746(6) Å) are longer than those in the σ-phosphine P(OC$_6$H$_4$(OMe)-2)$_3$ **5.5**, (d(P–O) = 1.624(4) Å)[382] and the *P*-silyloxy-, alkyloxy-, aryloxy-iminophosphines **5.7**, (d(P–O) = 1.585(3) to 1.658(1) Å), individual values for the *P*-oxy-iminophosphines are provided in Table 5.1. However, they are significantly shorter than the P–O(Tf) bond in Mes*NPOTf (d(P–O) = 1.923(3) Å[130]). For [Mes*NP•OPPh$_3$]OTf **5.4** (Ch = O), the (Mes*N)P–O(Lg) bond lengths are identical to the P–O distance in the *P*-tosyl-iminophosphine **5.7** (Ch = O, R = SO$_2$C$_6$H$_4$Me-4), (d(P–O) = 1.728(3) Å).

In comparison, the (Mes*N)P–O(Lg) bonds in [Mes*NP•OIm]OTf (d(P–O) = 1.773(3) Å) and [Mes*NP•OPPh$_3$]OTf (d(P$_A$–O) = 1.734(6) Å; d(P$_B$–O) = 1.746(6) Å) are considerably shorter than the intra or inter molecular P–O(Lg) interactions found in σ-phosphino- (σ^3,λ^3 d(P–O) = 2.652(5) to 2.823(2) Å), phosphorano- (σ^4,λ^4, σ^4,λ^5, σ^5,λ^5 d(P–O) = 1.878(4) to 2.88(1) Å) chalcogen complexes, individual values are given in Table 5.2. The exceptions are complexes which feature a σ-phosphorane centre (σ^4,λ^4) coordinated by a pentane-2,4-dionato (d(P–O) = 1.715(4) to 1.752(1) Å), a carbamato (d(P–O) = 1.778(3) to 1.901(5) A), or a phosphoryl (d(P–O) = 1.732(2) Å **5.8**)[360] chelating ligand, individual values are given in Table 5.2. It should be noted that many complexes with intramolecular interactions have long P–Ch(Lg) bonds (d(P–O) > 1.9 Å;

d(S–P > 2.3 Å), which are probably caused by the structural confinements of the substituent (i.e., ring strain). Similarly, the length of the P–Ch(Lg) interactions in the [Mes*NP•Lg]OTf complexes **5.3** and **5.4** may be limited by steric hindrance resulting from interactions between the ligand and the Mes* substituent.

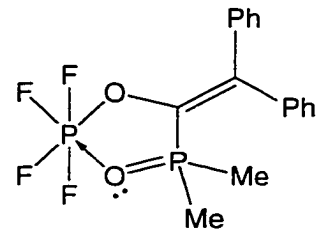

5.8

The S–P(Lg) bond length in [Mes*NP•SIm]OTf **5.3** (Ch = S) (*d*(S–P) = 2.266(1) Å) is longer than the single sulphur-phosphorus distance observed in the σ-phosphine $(PhS)_3P$ **5.5**, (*d*(S–P) = 2.122(1) Å),[383] the *cyclo*-trithio-triphospholane $(Mes*PS)_3$ **5.6**, (*d*(S–P) = 2.115(3), 2.142(3) Å),[384] and the *P*-alkyl-thio-iminophosphine Mes*NPS'Bu **5.7**, (*d*(S–P) = 2.098(1) Å[335]). However, the S–P(Lg) bond in [Mes*NP•SIm]OTf **5.3** (Ch = S), (*d*(S–P) = 2.266(1) Å) represents the shortest sulphur-phosphorus interaction known for a complex containing a Lewis acidic σ-phosphino- (σ^3,λ^3 *d*(S–P) = 2.816(2) to 2.952(9) Å) or phosphorano- (σ^4,λ^5, σ^5,λ^5 *d*(S–P) = 2.331(1) to 3.114(2) Å) centre, individual values are provided in Table 5.2.

Examples of complexes which feature both a Lewis acidic phosphorus centre and a selenium group as the Lewis basic component are extremely rare. There are no crystallographically characterized complexes with a coordination interaction between a phosphorano centre and a selenium donor. The Se(Lg)–P bond length in [Mes*NP•SeIm]OTf **5.3** (Ch = Se), (*d*(Se–P) = 2.407(1) Å) is significantly shorter than the intermolecular selenium-phosphorus distances reported for the polymeric phosphorus

selenide *catena*-$(P_4Se_4)_n$, (d(Se–P) = 3.258(1) to 3.421(1) Å[385]). However, the Se(Lg)–P interaction in [Mes*NP•SeIm]OTf **5.3** (Ch = Se) is longer than the Se–P single bond in the σ-phosphine $(PhSe)_3P$, (d(Se–P) = 2.271(2) Å[386]).

The [Mes*NP•Lg]OTf (Lg = SIm or SeIm) complexes **5.4** (Ch = S or Se) have (Lg)Ch–P(NMes*) distances (d(S–P) = 2.266(1) Å; d(Se–P) = 2.407(1) Å), which are considerably less than those reported for the [Mes*NP]$S_2P(^tBu)_2$ **5.1** (Ch = S), (d(S–P) = 2.442(2), 2.739(2) Å),[387] and [Mes*NP]$Se_2P(^tBu)_2$ **5.1** (Ch = Se), (d(Se–P) = 2.636(5), 2.788(5) Å)[138] complexes.

The (Lg)O-P-N bond angles in [Mes*NP•OIm]OTf **5.3** (Ch = O), (107.5(4)°) and [Mes*NP•$OPPh_3$]OTf **5.4** (Ch = O), (107.5(4), 108.4(4)°) are in the range reported for Mes*NPOTf (108.4(2)°),[130] *P*-alkyloxy- and *P*-aryloxy-iminophosphines (106.3(2) to 115.8(2) °), individual values are given in Table 5.1. The N-P-S(Im) bond angle in [Mes*NP•SIm]OTf **5.3** (Ch = S), (114.1(1)°) is slightly larger than that reported for the *P*-alkyl-thio-iminophosphine Mes*NPS^{t}Bu, (109.0(1)°[335]). The Se-P-N bond angle in [Mes*NP•SeIm]OTf **5.3** (Ch = Se), (115.4(1)°) is slightly larger than that in [Mes*NP•SIm]OTf (114.1(1)°). In general, the Ch-P-N bond angles in [Mes*NP•Lg]OTf (Lg = OIm, SIm, SeIm, or $OPPh_3$) are comparable regardless of the type of chalcogen ligand coordinated to the phosphadiazonium unit.

The P-O-C bond angle in [Mes*NP•OIm]OTf (120.4(3)°) is larger than the near 90° P-S-C and P-Se-C bond angles in [Mes*NP•SIm]OTf and [Mes*NP•SIm]OTf (91.8(1)° and 88.3(1)°, respectively). The smaller P-Ch-C bond angles in [Mes*NP•SIm]OTf and [Mes*NP•SeIm]OTf are probably a consequence of the inability of the valence s-orbital in heavier main-group elements such as sulphur and selenium, to engage in bonding using orbital hybridization.[4]

The phosphorus-oxygen bond of the Ph_3PO unit in [Mes*NP•$OPPh_3$]OTf **5.3** (Ch = O), (d(P–O) = 1.563(4) Å) is significantly longer than that reported for the free ligand (d(P–O) = 1.487(3) Å)[286] and other main-group and transition-metal complexes featuring a coordinating Ph_3PO molecule (d(P–O) = 1.47(2) to 1.522(3) Å), individual values are given in Table 5.3. However, the (Ph)P–O bond length in [Mes*NP•$OPPh_3$]OTf **5.3** (Ch = O), (d(P–O) = 1.563(4) Å) is comparable with that found in phosphates with single P–O bonds (d(P(O)–P(R)) = 1.558[11] Å[131]). For comparison, the phosphoryl P–O bond in **5.8** (d(P–O) = 1.555(2) Å)[360] is also quite long, but is less than that in **5.3** (Ch = O), [Mes*NP•$OPPh_3$]OTf (d(P–O) = 1.563(4) Å). All other structural parameters associated with the Ph_3PO unit in [Mes*NP•$OPPh_3$]OTf **5.3** (Ch = O), the P–C(Ph) bond lengths and the O-P-C(Ph) bond angles, are unexceptional.

The P-O-P bond angle in [Mes*NP•$OPPh_3$]OTf **5.3** (Ch = O), is considerably smaller (138.0(3)°, 142.2(3)°) as compared with the 180° O-P-E bond angles in Cl_3E•$OPPh_3$ (E = Al or Ga) complexes,[388] but it is slightly larger than the P-O-B bond angle in F_3B•$OPPh_3$ (134.5(2)°[389]). The magnitude of the P-O-E bond angle and the P–O bond length has implications for the mode of coordination adopted by the Ph_3PO ligand (vide infra).[390]

The structural parameters associated with the chalcogenoimidazoline group in the [Mes*NP•Lg]OTf (Lg = SIm or SeIm) complexes **5.3** (Ch = S or Se), were compared with those of the free ligands. The crystal structure of 1,3-diisopropyl-4,5-dimethylimidazlidin-2(*3H*)-thione SIm **5.2** (Ch = S), was determined and it shows that the compound has disordered methyl and isopropyl groups. Nevertheless, the structural features of the imidazoline ring in **5.2** (Ch = S) are identical to those reported for other derivatized imidazol-2-thiones.[391] The crystal structure of 1,3-diisopropyl-4,5-dimethylimidazlidin-2(3*H*)-selenone SeIm **5.2** (Ch = Se), has been previously

reported.[380] A crystal structure was unavailable for 1,3-diisopropyl-4,5-dimethylimidazlidin-2(3H)-one OIm, **5.2** (Ch = O) or any other type of imidazlidinone. However, crystal structures are known for tetramethylurea $OC(NMe_2)_2$[392] and related cyclic saturated ureas.[393,394]

The carbonyl bond length in [Mes*NP•OIm]OTf **5.3** (Ch = O) is significantly longer (d(O–C) = 1.342(5) Å) than that reported for tetramethyl urea $OC(NMe_2)_2$ (d(O–C) = 1.226(2) Å),[392] the cyclic urea $OC(N(H)CH_2)_2$ (d(O–C) = 1.262(4) Å)[393] and ureas coordinated to a Lewis acidic centre (d(O–C) = 1.261† to 1.302(3) Å), individual values are given in Table 5.4. However, the O–C bond length in **5.3** (Ch = O) is still considerably less than the oxygen-carbon single bond values found in dialkylethers (1.469[14] Å[131]).

The sulphur-carbon and selenium-carbon bonds in [Mes*NP•SIm]OTf **5.3** (Ch = S), (d(S–C) = 1.736(3) Å) and [Mes*NP•SeIm]OTf **5.3** (Ch = Se), (d(Se–C) = 1.889(3) Å) are longer than those observed in the free ligands (d(S–C) = 1.690(5) Å, SIm; d(Se–C) = 1.853(4) Å, SeIm[380]). However, the values are identical to those reported for the chalcogenoimidazoline-pentacarbonylchromium complexes $(OC)_5Cr$•SIm (d(S–C) = 1.737(5) Å)[395] and $(OC)_5Cr$•SeIm (d(Se–C) = 1.89(2) Å[395]). The S–C bond length in [Mes*NP•SIm]OTf (d(S–C) = 1.736(3) Å) is less than a typical single bond value (d(S–C) = 1.819[19] Å)[131]. In contrast, Cl_2(O)SIm **5.9** has a S–C distance consistent with that of a typical single bond value (d(S–C) = 1.811(3) Å),[289] and hence this compound is best described as a ylidene ligand bonded to an oxidized sulphur centre.[289] However, the Se–C bond length in [Mes*NP•SeIm]OTf (d(Se–C) = 1.889(3) Å) is within the range of single Se–C bond values (d(Se–C) = 1.970[32] Å[131]).

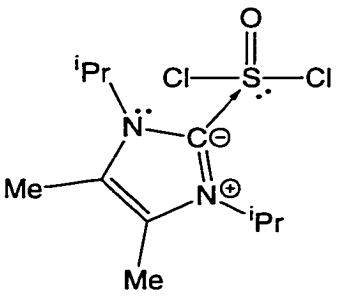

5.9

All structural parameters pertaining to the imidazoline ring, N–C, C–C bond lengths and the N-C-N bond angle, in the [Mes*NP•Lg]OTf (Lg = SIm or SeIm) complexes are equivalent or only slightly differ from those observed in the free ligands. The imidazol ring in [Mes*NP•Lg]OTf (Lg = SIm or SeIm) **5.3** (Ch = S or Se), defined by atomic centres C(19), N(1), C(20), C(21), N(2), and the chalcogen centre, occupy a common plane. The nitrogen centres associated with the imidazol ring in **5.3** (Ch = O, S, or Se) all have trigonal planar geometry. Moreover, the N–C(Im) bond lengths in [Mes*NP•OIm]OTf (*d*(N–C) = 1.330(5), 1.336(5) Å), [Mes*NP•SIm]OTf (*d*(N–C) = 1.346(3), 1.358(3) Å), and [Mes*NP•SeIm]OTf (*d*(N–C) = 1.345(3), 1355(3) Å) are less than single bond values (*d*($C(sp^3)$–$N(sp^3)$)= 1.469[14] Å),[131] but they are identical or comparable with those found in the imidazol-2-ylidene **3.1**, (*d*(N–C) = 1.360(1) Å). Hence, it is postulated that chalcogenoimidazolines **5.1**, analogous with imidazol-2-ylidenes, have lone pair π-conjugation between the nitrogen and carbon centres, which in turn directly affects the π-bonding between the chalcogen and central carbon centres (vide infra).[380,381,396,397]

The P-Ch-C-N torsion angles in [Mes*NP•SIm]OTf **5.3** (Ch = S), (-97.0(2)°, 77.4(2)°) and [Mes*NP•SeIm]OTf **5.3** (Ch = Se), (97.8(2)°, -76.3(2)°) are similar to those reported for the $(OC)_5Cr$•SeIm complex (Cr-Se-C-N, -89.0†°, 92.9†°[395]). This suggests a common coordination mode for the SIm and SeIm ligands (vide infra). In

contrast, the P-O-C-N torsion angles in [Mes*NP•OIm]OTf differ significantly (-120.4(4)°, 60.7(6)°). Both the [Mes*NP•SIm]OTf and [Mes*NP•SeIm]OTf complexes appear to have an almost identical orientation of the chalcogenoimidazoline ligand with the respect to the phosphadiazonium unit. The large N-P-Ch-C torsion angle in [Mes*NP•OIm]OTf (170.4(4)°), [Mes*NP•SIm]OTf (168.6(1)°), and [Mes*NP•SeIm]OTf (-172(1)°) shows that the carbon centre of the ligand is in a *trans*-configuration with respect to the nitrogen centre of the imino-substituent. In [Mes*NP•OIm]OTf, the ligand adopts a *cis*-configuration with respect to the Mes* substituent, (i.e., the C-N-P-O(Im) torsion angle is -5.3(10)°). In contrast, the C-N-P-S(Im) and the C-N-P-Se(Im) torsion angle in [Mes*NP•SIm]OTf (-148(2)°) and [Mes*NP•SeIm]OTf (148(3)°) are larger. These complexes have neither a *cis*- or *trans*-configuration since the (Mes*)C-N-P bond angle are close to 180° (174.4(2)° [Mes*NP•SIm]OTf; 175.5(2)° [Mes*NP•SeIm]OTf).

A comparison of the P–N(Mes*) bond length and the (Mes*)C-N-P bond angle in the [Mes*NP•Lg]OTf complexes (Lg = OIm, SIm, SeIm, or $OPPh_3$) with other phosphadiazonium-ligand-triflate compounds is presented in Chapter 6.

The methyl groups of the isopropyl substituents on the chalcogenoimidazoline ligand in [Mes*NP•Lg]OTf (Lg = OIm, SIm, and SeIm) **5.3** (Ch = O, S, or Se), are pointing away from the Mes*NP unit, which is expected to reduce internal steric strain. The structural parameters associated with the Mes* substituents in the complexes are unexceptional. However, both the [Mes*NP•OIm]OTf and [Mes*NP•SeIm]OTf complexes have a disordered *para-tert*-butyl group, which is often observed in other *N*-Mes* substituted iminophosphines.

The angle of rotation (θ) between the Mes* aryl substituent and the imidazol ring planes in the [Mes*NP•Lg]OTf complexes (Lg = OIm, SIm, or SeIm) is 49.9(2)°,

69.0(1), 70.2(1), (for definitions of θ and ω see Figure 5.6). However, in [Mes*NP•OIm]OTf, the Mes* aryl ring plane adopts an almost orthogonal orientation with respect to the plane defined by centres P, O(1) and C(19) as suggested by ω value of 83.5(2)°. In contrast, the ω value in the [Mes*NP•Lg]OTf (Lg = SIm or SeIm) complexes is considerably smaller (35.1(1)° and 31.1(1)°, respectively). This is probably due to a longer distance between the sulphur or selenium centre and the Mes* substituent (less steric crowding) whereas, since the Mes* substituent and the OIm group are *cis* with respect to each, the corresponding (Im)O-Mes* distance is shorter and the plane of the Mes* substituent is twisted to reduce steric crowding.

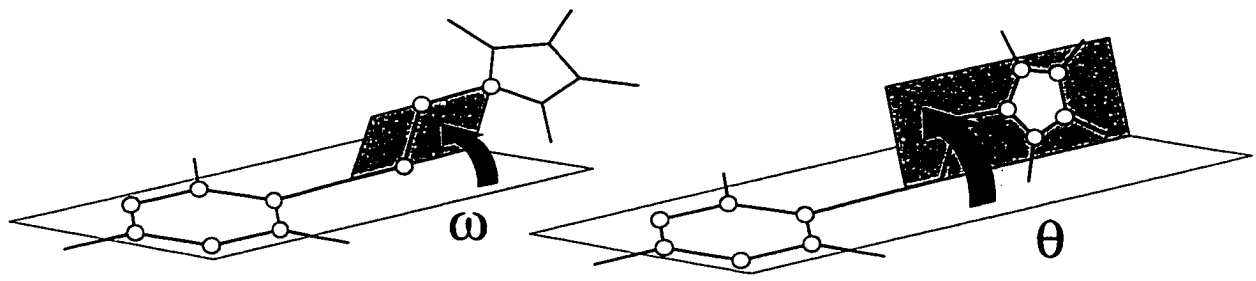

Figure 5.6: Plane angles (θ, ω) in the [Mes*NP•Lg]OTf (Lg = OIm, SIm, or SeIm) complexes. ω Represents the angle between the aryl plane of the Mes* substituent and the plane defined by the phosphorus, chalcogen and carbon C(19) centres. θ Refers to the angle between the imidazol and Mes* substituent ring planes.

With the exception of the [Mes*NP•OIm]OTf complex **5.3** (Ch = O), the triflate group in the chalcogenoimidazoline-phosphadiazonium-triflate complexes **5.3** (Ch = S or Se), have no significant interactions with the phosphorus centre of the Mes*NP unit or the chalcogen centre of the ligand. The closest cation-anion distances in these complexes are between the O(2) centre of triflate and the N(3) centre of the imidazol ring, (*d*(O–N) = 3.360(3) Å, [Mes*NP•SIm]OTf; 3.428(4) Å, [Mes*NP•SeIm]OTf). Both distances are

greater than 2.94 Å (from $\Sigma\, r_w(O) + r_w(N)$). Hence the cation-anion interactions in these complexes can be considered predominantly ionic.

The closest cation-anion distance in [Mes*NP•$OPPh_3$]OTf **5.4** (Ch = O), is between the oxygen centre of the Ph_3PO ligand and O(2) centre of the triflate group (d(O–O) = 3.49(9) Å). This distance is longer than 2.80 Å (from $\Sigma\, 2 \times r_w(O)$) and therefore, the covalent interaction is negligible. For the [Mes*NP•OIm]OTf complex **5.3** (Ch = O), a long phosphorus-oxygen interaction (d(P–O(Tf) = 2.774(4) Å) is observed, which is shorter than 3.30 Å (from $\Sigma\, r_w(P) + r_w(O)$).

The trifluoromethyl group CF_3, of the triflate anion in [Mes*NP•Lg]OTf (Lg = SIm, SeIm, or $OPPh_3$) is rotationally disordered between two positions with 50 % occupancy. Moreover, the triflate group in [Mes*NP•$OPPh_3$]OTf **5.4** (Ch = O) has additional disorder between the sulphur and carbon positions. Comparisons of the P–O(Tf) distance and structural parameters associated with the triflate group in the [Mes*NP•Lg]OTf complexes (Lg = OIm, SIm, SeIm, or $OPPh_3$) with other phosphadiazonium-ligand-triflate complexes are discussed in Chapter 6.

5.2.3: Spectroscopic Characterization of the [Mes*NP•Lg]OTf Complexes 5.3 (Ch = O, S, or Se), and 5.4 (Ch = O) where Lg is OIm, SIm, SeIm, or $OPPh_3$

Solution ^{31}P NMR spectra of the [Mes*NP•$OPPh_3$]OTf complex **5.4** (Ch = O), show that the phosphorus nucleus associated with the phosphadiazonium unit ($\delta(^{31}P)$ = 60 ppm) is only slightly deshielded as compared with that in Mes*NPOTf ($\delta(^{31}P)$ = 55 ppm[130]). However, the phosphorus nucleus in [Mes*NP•$SPPh_3$]OTf **5.4** (Ch = S), ($\delta(^{31}P)$ = 79 ppm), and [Mes*NP•OIm]OTf **5.3** (Ch = O), ($\delta(^{31}P)$ = 77 ppm) is more deshielded than that in Mes*NPOTf, and is similar or identical to those reported for the *P*-tosyl-iminophosphine Mes*$NPOSO_2C_6H_4$-Me-4 ($\delta(^{31}P)$ = 93 ppm)[130] and the

P-carboxyl-iminophosphine Mes*NPOC(O)CF_3 ($\delta(^{31}P)$ = 79 ppm[130]). In comparison, the $\delta(^{31}P)$ values of the [Mes*NP•Lg]OTf (Lg = $OPPh_3$ or OIm) complexes are less than those reported for *P*-aryloxy-, *P*-alkyloxy-, *P*-silyloxy-iminophosphines ($\delta(^{31}P)$ = 122 to 165 ppm), and the *P*-amino-*P*-aryloxy-phosphenium cation in the [Mes*N(H)POMes*]$GaCl_4$ salt ($\delta(^{31}P)$ = 296 ppm),[25] individual values are provided in Table 5.5.

The phosphorus nucleus in the *P*-thio- and *P*-seleno-iminophosphines Mes*NPS^{t}Bu ($\delta(^{31}P)$ = 320) ppm)[398] and Mes*NPSe^{t}Bu ($\delta(^{31}P)$ = 314 ppm)[102] is considerably deshielded as compared with [Mes*NP•$SPPh_3$]OTf **5.4** (Ch = S), ($\delta(^{31}P)$ = 79 ppm), [Mes*NP•SIm]OTf **5.3** (Ch = S), ($\delta(^{31}P)$ = 148 ppm), and [Mes*NP•SeIm]OTf **5.3** (Ch = S), ($\delta(^{31}P)$ = 178 ppm). The phosphorus nucleus of the phosphadiazonium unit in [Mes*NP•SeIm]OTf ($\delta(^{31}P)$ = 178 ppm) is more shielded than that in [Mes*NP]$Se_2P(^tBu)_2$ **5.1** (Ch = Se), which has a $\delta(^{31}P)$ value of 92 ppm[138] and is closer to those reported for the η^6 arene-phosphadiazonium complexes (e.g., [Mes*NP•C_6H_6]$GaCl_4$ ($\delta(^{31}P)$ = 77 ppm[93]). However, at lower temperatures (-80 °C), the phosphorus nucleus of the [Mes*NP]$Se_2P(^tBu)_2$ complex **5.1** (Ch = Se), is more deshielded ($\delta(^{31}P)$ = 116 ppm) and a $^2J(^{31}P,^{31}P)$ is observed,[137] whereas for the [Mes*NP•SeIm]OTf complex **5.3** (Ch = Se), the $\delta(^{31}P)$ value changes only slightly when measured at -90 °C ($\Delta\delta(^{31}P)$ = -10 ppm).

The phosphorus nucleus of the Ph_3PO unit in [Mes*NP•$OPPh_3$]OTf **5.4** (Ch = O), ($\delta(^{31}P)$ = 52 ppm) is deshielded with respect to that observed for the free ligand ($\delta(^{31}P)$ = 30 ppm), but the shielding is similar to that reported for group 13 halide complexes X_3E•$OPPh_3$ (X = Ga or Al), ($\delta(^{31}P)$ = 44 to 46 ppm) and [H•$OPPh_3$]HSO_4 ($\delta(^{31}P)$ = 57 ppm),[399] individual values are given in Table 5.6. However, the Ph_3PO unit in **5.4** (Ch = O) is not as deshielded as that reported for [$MeOPPh_3$]$SbCl_6$

($\delta(^{31}P)$ = 65 ppm)[400] and the triphenylphosphine oxide ligand in $Ph_3PO{\bullet}PCl_5$ ($\delta(^{31}P)$ = 67 ppm)[356] and the $[Ph_3PO{\bullet}PX_2]X$ (X = Cl or Br) complexes ($\delta(^{31}P)$ = 65 ppm),[357] which suggest that in these complexes the Ph_3PO ligand may have more phosphonium-like bonding character (i.e., PR_4^+). In contrast, the $\delta(^{31}P)$ of the Ph_3PS ligand in [Mes*NP•$SPPh_3$]OTf **5.4** (Ch = S), ($\delta(^{31}P)$ = 41 ppm) is slightly less than the value observed for the free ligand ($\delta(^{31}P)$ = 46 ppm). However, the phosphorus chemical shift of the $Ph_3PS{\bullet}AlCl_3$ complex ($\delta(^{31}P)$ = 43 ppm)[401] and $[Ph_3PS{\bullet}H]HSO_4$ ($\delta(^{31}P)$ = 43 ppm),[399] is also similar to that of the free ligand ($\delta(^{31}P)$ = 46 ppm).

The ^1H and ^{13}C chemical shifts associated with the phenyl groups of the ligand in [Mes*NP•Lg]OTf (Lg = $OPPh_3$ and $SPPh_3$) show little variation from those observed for the free ligands.

The solution ^{31}P NMR spectrum of [Mes*NP•$OPPh_3$]OTf and [Mes*NP•$SPPh_3$]OTf **5.4** (Ch = O or S), show no evidence of $^2J(^{31}P,^{31}P)$ coupling. Similarly, the ^1H and ^{13}C resonances associated with the chalcogenoimidazoline ligand in the [Mes*NP•Lg]OTf (Lg = OIm, SIm, or SeIm) complexes **5.3** (Ch = O, S, or Se) do not exhibit any evidence of coupling between the central carbon and phosphorus nuclei. Interestingly, both the [Mes*NP]$Se_2P(^tBu)_2$ **5.1** (Ch = Se) and [Mes*NP•SeIm]OTf **5.3** (Ch = Se) complexes show no evidence of selenium-phosphorus (of the phosphadiazonium unit) coupling in solution ^{31}P and ^{77}Se NMR spectra obtained at ambient temperature.[138] A variable temperature solution ^{31}P NMR study of [Mes*NP•SeIm]OTf, dissolved in CH_2Cl_2, showed that at -90 °C, no $^1J(^{77}Se,^{31}P)$ value is observed. However, the spectra did exhibit two additional signals with $\delta(^{31}P)$ values at 189 and 55 ppm, respectively. The later peak is consistent with the phosphorus chemical shift reported for Mes*NPOTf,[130] and the other peak is speculated as representing the bis-coordinated phosphadiazonium-triflate complex [Mes*NP•$(SeIm)_2$]OTf **5.10**. The

additional peaks were not present in spectra collected above -70°C. Hence, these observations suggest a rapid ligand-phosphadiazonium association-dissociation process for the [Mes*NP•SeIm]OTf complex **5.3** (Ch = Se).

The ^{1}H and ^{13}C NMR solution spectra of [Mes*NP•Lg]OTf (Lg = $OPPh_3$, $SPPh_3$, OIm, SIm, or SeIm) displays single sets of resonances corresponding to the Mes* substituent and the chalcogenoimidazoline or tertiary phosphine chalcogenide ligand.

The protons and carbon nuclei associated with the substituents (Me and ^{i}Pr) on the chalcogenoimidazoline ligand in the [Mes*NP•Lg]OTf (Lg = OIm, SIm, or SeIm) complexes showed some variations in shielding in comparison with those of the corresponding free ligand (Table 5.7). The central carbon nucleus associated with the chalcogenoimidazoline ligand in [Mes*NP•SIm]OTf **5.3** (Ch = S), ($\delta(^{13}C)$ = 129.5 ppm) and [Mes*NP•SeIm]OTf **5.3** (Ch = Se), ($\delta(^{13}C)$ = 131.1 ppm) are considerably more shielded than those in the free ligands ($\delta(^{13}C)$ = 159.5 ppm, SIm; 157.6 ppm, SeIm). This suggests a significant change in bonding character for the SIm and SeIm ligands when bonded to a phosphadiazonium cation. Furthermore, the $\delta(^{13}C)$ value for the central carbon in [Mes*NP•SIm]OTf ($\delta(^{13}C)$ = 129.5 ppm) and [Mes*NP•SeIm]OTf ($\delta(^{13}C)$ = 131.1 ppm) is similar to those found in thio- or seleno-imidazolium salts **5.9** ($\delta(^{13}C)$ = 126.4 ppm)[289] and **5.11** (Ch = Se), ($\delta(^{13}C)$ = 137.2 ppm[402]).

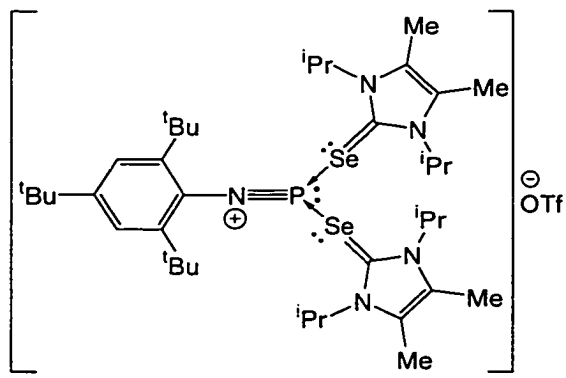

5.10

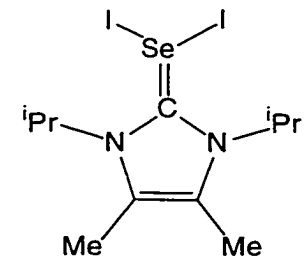

5.11

The $\delta(^1H)$ and $\delta(^{13}C)$ values associated with the Mes* substituent in [Mes*NP•Lg]OTf (Lg = OIm, SIm, or SeIm) **5.3** (Ch = O, S, or Se) complexes are comparable with those found in Mes*NPOTf. However, for the [Mes*NP•$OPPh_3$]OTf and [Mes*NP•$SPPh_3$]OTf complexes **5.4** (Ch = O or S), the ^{13}C resonances of the Mes* arene ring exhibits greater coupling with the phosphorus nucleus of the phosphadiazonium unit, further details are presented in Chapter 6.

The infrared spectra of [Mes*NP•Lg]OTf (Lg = OIm, SIm, or SeIm) **5.3** (Ch = O, S, and Se) and [Mes*NP•$OPPh_3$]OTf **5.4** (Ch = O), prepared as paraffin oil mulls, exhibit stretching frequencies for the CF_3 and SO_3 groups of the triflate anion. Spectroscopic features, including $\delta(^{19}F)$, and stretching frequencies values associated with the triflate group are discussed in comparison with other [Mes*NP•Lg]OTf complexes in Chapter 6.

The IR spectra of [Mes*NP•$OPPh_3$]OTf **5.4** (Ch = O) exhibits two (Ph)P–O stretching frequencies at 1150 and 1137 cm^{-1}, which are lower than the 1192 cm^{-1} value observed in free the ligand. However, the (Ph)P–O stretching frequencies are comparable with other complexes containing a $OPPh_3$ ligand (e.g., $Cl_3Sb(•OPPh_3)_2$, 1129 and 1137 cm^{-1}).[403,404] The lower stretching frequencies suggests a longer phosphorus-oxygen bond for the Ph_3PO ligand in [Mes*NP•$OPPh_3$]OTf **5.4** (Ch = O) and is consistent with that shown by the crystal structure. Two broad and intense peaks were observed at 944 and 925 cm^{-1}, their location and intensities are similar to reported values for P-O-P bond stretching frequencies (870 to 1025 cm^{-1}).[405]

An intense peak corresponding to the carbonyl bond stretching frequency in [Mes*NP•OIm]OTf **5.3** (Ch = O) is tentative assigned at 1555 cm^{-1}, which is lower than that in 1,3-dimethyl-2-imidazolidin-2-one (1697 cm^{-1})[406] and tetramethylurea (1650 cm^{-1} [407]). In general, the spectra were too complicated to assign the Se–C and S–C bond stretches or bends in **5.3** (Ch = S or Se). However, the IR spectra of

[Mes*NP•SIm]OTf and [Mes*NP•SeIm]OTf are similar to one another. However, as expected, the IR spectra of the [Mes*NP•OIm]OTf complex differs significantly from [Mes*NP•SIm]OTf and [Mes*NP•SeIm]OTf, which is in accordance with that shown by the crystal structures.

5.3: Conclusions: Bonding Implications for Phosphadiazonium-ligand-triflate Complexes (5.3 and 5.4) involving Tertiary Phosphine Chalcogenide or Chalcogenoimidazoline Donors

The synthesis and characterization of a homologous series of chalcogeno-phosphadiazonium-triflate complexes [Mes*NP•Lg]OTf (Lg = OIm, SIm, or SeIm) **5.3** (Ch = O, S, or Se) provides some insights into the bonding interactions between a series of main-group elements (in a common periodic group) and a π-phosphino-bonding environment. Importantly, the phosphadiazonium cation Mes^*NP^+, is shown to be capable of coordinating with chalcogen donors, ranging from small and hard oxygen (η = 6.08 eV) to large and soft selenium (η = 3.87 eV).[408] The hardness of the phosphadiazonium unit RNP^+, in terms of HSAB theory, has been calculated using ab initio methods, at the MP2/6-31G+(d) level of theory, on model compounds (η = 7.14 eV, R = H; 6.52 eV, R = Me; 4.06 eV, R = Ph)[76] and is found to be similar to Ag^+ (η = 6.96 eV)[408] and Au^+ (η = 5.6 eV[408]).

The phosphadiazonium cation Mes^*NP^+, is not as Lewis acidic as the iminosilane ^{t}BuSiNSi(^{t}Bu)$_3$, which is capable of forming coordination complexes with weak Lewis bases such as benzophenone **5.12**, (pK_a of PhC(O•H)Ph$^+$ = -6.0)[409] and tetrahydrofuran **5.13**, (pK_a of THF•H$^+$ = -2.1[410]).[99,411] Complex formation was not observed between Mes*NPOTf and benzophenone. Solutions of tetrahydrofuran readily polymerized in the presence of Mes*NPOTf. Similarly, PF_5 polymerizes tetrahydrofuran at temperatures in excess of 90 °C.[179,358]

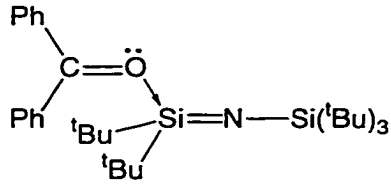

5.12

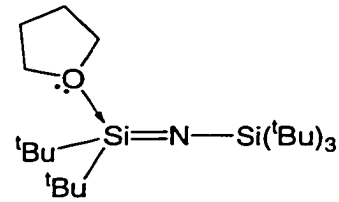

5.13

The [Mes*NP•Lg]OTf complexes (Lg = OIm, SIm, SeIm, $OPPh_3$, or $SPPh_3$) are distinct from the other phosphadiazonium-ligand-triflate complexes ([Mes*NP•PPh_3]OTf **1.44**, [Mes*NP•Py]OTf **2.7**, [Mes*NP•Qncd]OTf **2.8**, and [Mes*NP•Im]OTf **3.14**) in that the ligand undergoes structural modification when coordinated to the phosphadiazonium cation. In particular, there is an increase in the chalcogen-carbon bond length in the chalcogenoimidazoline ligand of [Mes*NP•OIm]OTf, [Mes*NP•SIm]OTf, and [Mes*NP•SeIm]OTf. Similarly, the phosphorus-oxygen bond length associated with the triphenylphosphine oxide ligand in [Mes*NP•$OPPh_3$]OTf **5.4** (Ch = O) also changes significantly.

An important structural consideration for the [Mes*NP•Lg]OTf (Lg = OIm, SIm, SeIm, or $OPPh_3$) complexes is the orientation of the ligand with respect to the phosphadiazonium unit, which has implications for the bonding in these compounds. There are three possible modes of coordination for the chalcogenoimidazoline ligand, which have C_{2v} symmetry. End-on coordination, labeled as the A_1 mode, is indicated by a linear arrangement between the carbon, chalcogen and Lewis acidic centres (i.e. the Ac-Ch-C bond angle > 160°), (Figure 5.7). Side-on coordination by a ligand to a Lewis acidic centre is indicated by a parallel or an orthogonal position of the Lewis acidic centre with respect to the plane defined by the imidazol ring, labeled as B_1 and B2, respectively (Figure 5.7). A B_1 or B_2 mode of coordination is observed in complexes featuring a small Ac-Ch-C bond angle (i.e., close to 90°). Coordination through a B_2

mode has the advantage of reduced steric interactions as the Lewis acidic centre is not in the plane of the ligand (Figure 5.7). In general, chalcogenoimidazoline ligands coordinate to a Lewis acidic centre using a B_2 mode. In contrast, the benzophenone ligand in complex **5.12**, coordinates to the silicon centre of the iminosilane through a B_1 mode.

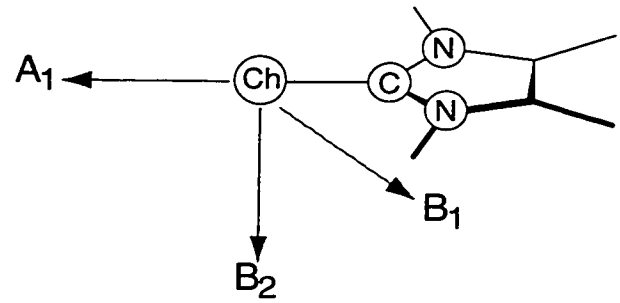

Figure 5.7: Three possible coordination modes, represented as vectors, for the chalcogenoimidazoline ligands **5.2**. The vectors represented by A_1 and B_1 are co-planar with the imidazol ring, whereas the B_2 vector is orthogonal to the imidazol ring plane.

The choice of coordination mode for different types of π-bonded chalcogen ligands is dependent on the bonding configuration within these compounds, especially the nature of the chalcogen-carbon π-bond. Alkyl- or aryl-substituted aldehydes and ketones have short O–C bonds (RC(O)H, d(O–C) = 1.192[5] Å, ν(O–C) = ~1705 cm^{-1}; RC(O)R, d(O–C) = 1.210[8] Å, ν(O–C) = ~1720 cm^{-1})[131,412] as shown by crystallography and IR spectroscopy, which suggest that these molecules have strong O–C π-bonding. In contrast, ureas have longer C–O bonds as compared with aldehydes and ketones (d(C–O) = 1.256[7] Å,[131] ν(C–O) = 1640 cm^{-1} [412]). Hence, it is postulated that ureas and imidazol-2-ones such as OIm **5.2** (Ch = O), have weaker O–C π-bonding due to inductive effects caused by electronegative nitrogen groups attached to the central carbon. Therefore, the

dipolar canonical resonance structures (e.g., **5.15**, Figure 5.8) are contributors to the valence bonding description for chalcogenoureas and chalcogenoimidazolines, whereas the contribution by this type of resonance structure for chalcogeno-ketones or -aldehydes is negligible due strong π-bonding between the chalcogen and carbon centres. Furthermore, the contributions by the dipolar resonance structures **5.15** to the overall bonding character of the chalcogenoimidazolines, increases in the order, Ch = O < S < Se < Te. This is related to the decrease in electronegativity of the chalcogen centre ({χ_{spec}}[6] O {3.61} > S {2.589} > Se {2.424} >Te {2.158}). If the dipolar resonance structures **5.15** are dominant, the non-bonding electrons on the chalcogen centre molecular occupy orbitals of A_1, B_1, and B_2 symmetry. This accounts for ability of chalcogenoureas and chalcogenoimidazolines to coordinate in a B_2 mode. However, if the **5.14** resonance structure is the major contributor to overall bonding character of the ligand, the two pairs of non-bonding electrons occupy molecular orbitals with A_1 and B_1 symmetry, and the B_2 molecular orbital is involved in π-bonding. The long chalcogen-carbon bond in the [Mes*NP•OIm]OTf (*d*(O–C) = 1.342(5) Å), [Mes*NP•SIm]OTf (*d*(S–C) = 1.736(3) Å), and [Mes*NP•SeIm]OTf (*d*(Se–C) = 1.889(3) Å), suggest greater contributions of resonance structures **5.14** to bonding description of the chalcogenoimidazoline unit in the [Mes*NP•Lg]OTf complexes (Lg = OIm, SIm, or SeIm).

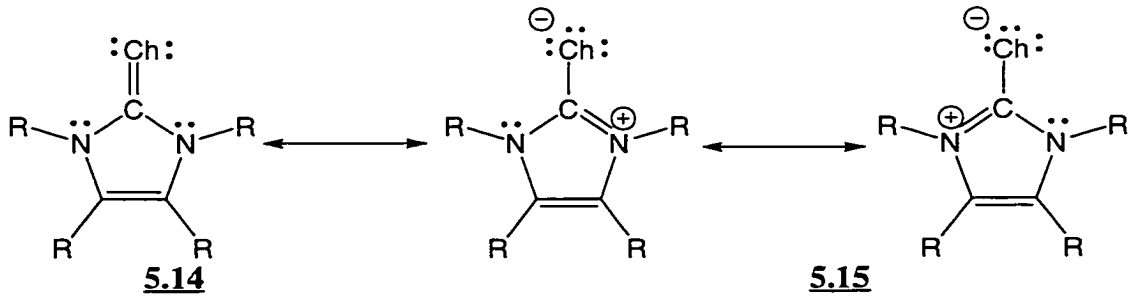

5.14 **5.15**

Figure 5.8: Resonance structures in the bonding descriptions of chalcogenoimidazolines.

Phosphorylic ligands such as $OPPh_3$ and $SPPh_3$, are known to exhibit two types of coordination modes; end-on, σ-coordination (A_1 mode), or side-on, π-coordination (E mode). The end-on coordination mode is indicated by a P-Ch-Ac bond angle in the range of 140° to 180°. If this same bond angle has a value in the range of 98° to 115°, the ligand coordinates side-on with the Lewis acidic centre. End-on coordination is usually observed for complexes featuring a oxo-phosphorylic ligand (e.g., $Ph_3P{\bullet}OAlCl_3$) in which the d-orbitals of a main-group or transition metal acceptor participate in d_π-p_π bonding with the oxygen centre.[390,413] Side-on coordination is commonly observed in thio- and seleno-phosphorylic-type ligands (e.g., $Ph_3PCh{\bullet}AlCl_3$, Ch = S or Se), but also for $Ph_3PO{\bullet}BF_3$ and [Mes*NP•$OPPh_3$]OTf. This suggests that the 3d-orbitals associated with the phosphorus centre of the Mes*NP unit in [Mes*NP•$OPPh_3$]OTf **5.4** (Ch = O) do not participate in π-bonding with the ligand.

In general, [Mes*NP•Lg]OTf (Lg = OIm, SIm, SeIm, or $OPPh_3$) complexes have structural and spectroscopic features which are distinct from those in *P*-chalcogeno-iminophosphines. However, some structural aspects (i.e., P–O(Lg), P–N(Mes*) bond length, and (Mes*)C-N-P, (Mes*)N-P-O bond angles) in [Mes*NP•OIm]OTf **5.3** (Ch = O) resemble those reported for *P*-oxy-iminophosphines. Hence, the Mes*NP•OIm^+ unit in **5.3** (Ch = O), may be considered a cationic analogue of a *P*-oxy-iminophosphine Mes*NPOR. It is interesting to note that structural aspects of the Mes*NP unit in [Mes*NP•OIm]OTf **5.3** (Ch = O), are considerably different from those in [Mes*NP•$OPPh_3$]OTf **5.4** (Ch = O), where the latter is more structurally related to the [Mes*NP•SIm]OTf and [Mes*NP•SeIm]OTf complexes **5.3** (Ch = S or Se). The Mes*NP unit in [Mes*NP•SIm]OTf and [Mes*NP•SeIm]OTf are structurally comparable, which suggests that the sulphur and selenium centres of the ligand have, as expected, similar Lewis basicities with regards to the phosphadiazonium cation.

An attempted synthesis of the [Mes*NP•TeIm]OTf complex **5.3** (Ch = Te), resulted in the formation of [Mes*NP•Im]OTf **3.14** with the precipitation of elemental tellurium. This type of reactivity is not surprising considering the instability of telluroketones, telluroureas, and imidazol-2-tellurones.[381,414,415] Transition metal complexes with imidazol-2-tellurones as ligands (e.g., TeIm•$M(CO)_5$, M = Cr, Mo, or W) are known. This suggests that tellurone ligands are stabilized through other factors, (e.g., π-back bonding) which are not present with the phosphadiazonium cation.[395] Imidazol-2-telluorones can be envisaged as masked imidazol-2-ylidenes (diaminocarbenes) as demonstrated by the conversion of complex **5.15** to a Schrock metal-alkylidene **5.16** (Figure 5.9).[414] This is also apparent from the formation of [Mes*NP•Im]OTf **3.14** from reaction between imidazol-2-tellurone TeIm, and Mes*NPOTf.

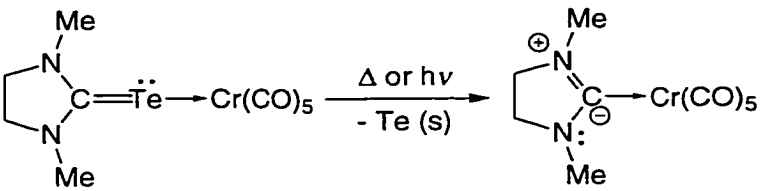

5.15 **5.16**

Figure 5.9: Conversion of a tellurourea-chromium complex **5.15** to a Schrock transition-metal complex **5.16** featuring a diaminocarbene ligand.[414]

Table 5.1: Comparison of P–Ch bond lengths and bond angles involving the chalcogen centre in [Mes*NP•Lg]OTf (Lg = OIm, SIm, SeIm, or $OPPh_3$), [Mes*NP]$Ch_2P(^tBu)_2$ (Ch = S or Se) with compounds featuring phosphorus-chalcogen single bonds. Compounds are listed by increasing *d*(P–Ch) values.

Compound	Ch	E	*d*(P–Ch) (Å)	∠(Ch-P-N) (°)	∠(P-Ch-E) (°)	Reference
$Mes^*NPOSiMe_3$	O	Si	1.585(3)	115.8(2)	155.9(2)	130
Mes^*NPO^tBu	O	C	1.601(2)	110.0(2)	126.4(2)	416
Mes*NPOMent	O	C	1.610(3)	113.1(2)	116.3(3)	139
$Mes^*NPOC(^tBu)_3$	O	C	1.615(4)	110.0(2)	135.2(3)	130
$P(OC_6H_4(OMe)\text{-}2)_3$	O	C	1.624(4)	119.1(4)	119.1(4)	382
$Mes^*NPOCH(^tBu)_2$	O	C	1.627(3)	109.3(2)	119.9(3)	130
$Mes^*NPOCH(CF_3)_2$	O	C	1.628(4)	106.3(2)	126.1(4)	141
$Mes^*NPOC_6H_4Me\text{-}2$	O	C	1.641(1)	111.8(1)	116.6(1)	129
$Mes^*NPOC_6H_2(^tBu)_2\text{-}2,6\text{-}Me\text{-}4$	O	C	1.658(1)	110.3(1)	117.4(1)	417
$Mes^*NPOSO_2C_6H_4(Me)\text{-}4$	O	S	1.728(3)	107.2(2)	123.9(2)	130
[Mes*NP•$OPPh_3$]OTf (**5.4**)	O	P	1.746(6)	108.4(4)	138.0(3)	This work
			1.734(6)[a]	107.5(4)[a]	142.2(3)[a]	
[Mes*NP•Olm]OTf (**5.3**)	O	C	1.773(3)	107.5(2)	120.4(3)	This work
Mes*NPOTf	O	S	1.923(3)	108.4(2)	121.9(2)	130
Mes^*NPS^tBu	S	C	2.098(1)	109.0(1)	102.1(1)	335
Mes^*NPS^tBu[b]	S	C	2.099(2)	109.1(1)	102.6(1)	418
$[Mes^*PS]_3$	S	P	2.115(3)	–	91.9(2)	384
			2.142(3)	–		
$(PhS)_3P$	S	C	2.122(1)	–	100.0(1)	383
[Mes*NP•Slm]OTf (**5.3**)	S	C	2.266(1)	114.1(1)	91.8(1)	This work
$[Mes^*NP]S_2P(^tBu)_2$ (**5.1**)	S	P	2.442(2)	111.7(2)	89.2(1)	387
			2.739(2)	122.5(2)	82.0(1)	
$(PhSe)_3P$	Se	C	2.271(2)	–	97.6(2)	386
[Mes*NP•SeIm]OTf (**5.3**)	Se	C	2.407(1)	115.4(1)	88.3(1)	This work
$[Mes^*NP]Se_2P(^tBu)_2$ (**5.1**)	Se	P	2.636(5)	112.6(6)	85.7(2)	138
			2.788(5)	119.6(5)	82.2(2)	

([a]) Second set of values resulting from disorder. ([b]) Molecule crystallized in a different space group.

Table 5.2: Comparison of P–Ch(Lg) bond lengths in [Mes*NP•Lg]OTf (Lg = OIm, SIm, SeIm, or $OPPh_3$) and other complexes featuring a phosphorus centre coordinated by a oxygen, sulphur, or selenium donor. 'Bonding' refers to the bonding environment of the phosphorus centre using the sigma-lambda notation and does include contributions by ligand(s). Compounds are listed by increasing *d*(P–Ch(Lg)) values. Bold letters indicate the donor and acceptor centres. All values in Å.

Compound	*d*(P–Ch(Lg))	Bonding	Reference
F_4**P**•**acac**	1.715(4), 1.723(4)	(σ^4,λ^4)	419
	1.719(4), 1.720(4)[a]		
F_4**P**(OCP(**O**)Me_2CPh_2) (**5.8**)	1.732(2)	(σ^5,λ^5)	360
[Mes*N**P**•**O**PPh_3]OTf (**5.3**)	1.734(6), 1.746(6)[b]	(σ^1,λ^3)	This work
$F(CF_3)_3$**P**•**acac**	1.746(1), 1.752(1)	(σ^4,λ^4)	373
[Mes*N**P**•**O**I**m**]OTf (**5.3**)	1.773(3)	(σ^1,λ^3)	This work
$F(CF_3)_3$**P**(**O**$_2$CNMe_2)	1.778(3), 1.832(3)	(σ^4,λ^4)	372
$Me(CF_3)_3$**P**(**O**$_2$CNMe_2)	1.808(5), 1.901(5)	(σ^4,λ^4)	371
Cl_3**P**(OC_6H_4(^{t}Bu)-2,Me-4,-6)$_2$**S**O_2	1.878(4)	(σ^5,λ^5)	363
($O_2Cl_5C_6$)OC_6F_5**P**(OC_6H_4(^{t}Bu)-2,Me-4,-6)$_2$**S**O_2	2.314(5)	(σ^5,λ^5)	366
OC_6F_5**P**(OC_6H_4(^{t}Bu)-2,Me-4,-6)$_2$**S**O_2	2.652(5)	(σ^3,λ^3)	366
Ph_2**P**(C_6H_4(C(**O**)Et)-2)	2.699(3)	(σ^3,λ^3)	375
P(C_6H_3(**O**Me)$_2$-2,6)$_3$	2.743†, 2.816†	(σ^3,λ^3)	376
OP(C_6H_3(**O**Me)$_3$-2,4,6)$_3$	2.784(4), 2.823(4)[a]	(σ^4,λ^5)	377
(OC_6H_4C(**O**)OMe-2)$_2$**P**Ph	2.788(6)	(σ^3,λ^3)	374
Ph_2**P**(CHCHC(**O**)OH)	2.823(2)	(σ^3,λ^3)	420
[Ph_2($PhCH_2$)**P**(C_6H_4**O**Me-2)]Br	2.878(14)	(σ^4,λ^4)	421
[Mes*N**P**•**SIm**]OTf (**5.3**)	2.266(1)	(σ^1,λ^3)	This work
Cl_3**P**(OC_6H_4(^{t}Bu)$_2$-2,4,-6)$_2$**S**	2.331(1)	(σ^5,λ^5)	200
(OCH_2CF_3)$_3$**P**(OC_6H_4(^{t}Bu)-2,Me-4,-6)$_2$**S**	2.363(2)	(σ^5,λ^5)	367
(OC_6F_5)$_3$**P**(OC_6H_4(^{t}Bu)-2,Me-4,-6)$_2$**S**	2.366(3)	(σ^5,λ^5)	364
($O_2C_{12}H_8$)F_3CCH_2O**P**(OC_6H_4(^{t}Bu)$_2$-2,4-6)$_2$**S**	2.373(5)	(σ^5,λ^5)	362
[Mes*N**P**]S_2P(^{t}Bu)$_2$ (**5.1**)	2.442(2), 2.739(2)	(σ^1,λ^3)	387
($O_2C_6H_3$F-3)PhO**P**(OC_6H_4(^{t}Bu)-2,Me-4,-6)$_2$**S**	2.496(2)	(σ^5,λ^5)	422
($O_2C_6Cl_5$)F_3CCH_2O**P**(OC_6H_4(^{t}Bu)-2,Me-4,-6)$_2$**S**	2.499(2)	(σ^5,λ^5)	422
($O_2C_6H_4$)PhO**P**(OC_6H_4(^{t}Bu)-2,Me-4,-6)$_2$**S**	2.509(1)	(σ^5,λ^5)	422
($O_2C_6Cl_5$)PhO**P**(OC_6H_4(^{t}Bu)-2,Me-4,-6)$_2$**S**	2.530(2), 2.594(2)[a]	(σ^5,λ^5)	422
P(S_2CNMe_2)$_3$	2.873(3), 2.982(3)[a]	(σ^3,λ^3)	378
	3.016(3), 3.014(3)[a]		
	3.016(3), 3.014(3)[a]		
OC_6F_5**P**(OC_6H_4(^{t}Bu)-2,Me-4,-6)$_2$**S**	2.876(2)	(σ^3,λ^3)	364
Cl(O)**P**(OC_6H_4(^{t}Bu)-2,Me-4,-6)$_2$**S**	3.114(2)	(σ^4,λ^5)	368
CF_3CH_2OP(O)(OC_6H_4(^{t}Bu)$_2$-2,4-6)$_2$**S**	3.166(1)	(σ^4,λ^5)	362

Compound	*d*(P–Ch(Lg))	Bonding	Reference
[Mes*NP•**SeIm**]OTf (**5.3**)	2.407(1)	(σ^1,λ^3)	This work
[Mes*N**P**]**Se**$_2$P(^{t}Bu)$_2$ (**5.1**)	2.636(5), 2.788(5)	(σ^1,λ^3)	138
catena-$(P_4Se_4)_n$	3.258(1), 3.421(1) 3.347(1)	(σ^3,λ^3)	385

([a]) Value from second structurally different molecule in the asymmetric cell.

Table 5.3: Comparison of the P–O bond length and the P-O-(E/M) bond angle for the Ph_3PO unit in some main-group and transition metal complexes as well as in the free ligand. Compounds are listed by decreasing *d*(P–O) values.

Compound	E/M (Å)	*d*(P–O) (°)	∠(P-O-(E/M))	Reference
[Mes*NP•$OPPh_3$]OTf (**5.4**)	P	1.563(4)	138.0(3) 142.2(3)[a]	This work
BF_3•$OPPh_3$	B	1.522(3)	134.5(2)	389
$AlCl_3$•$OPPh_3$	Al	1.519(4)	180[b]	401
$AlBr_3$•$OPPh_3$	Al	1.513(7)	180[b]	401
$SbCl_3$(•$OPPh_3$)$_2$	Sb	1.503(2)	141.1(1)	423
[Hg(•$OPPh_3$)]ClO_4	Hg	1.50(2)	131(1)	424
$GaCl_3$•$OPPh_3$	Ga	1.49(1)	180[b]	401
$OPPh_3$	–	1.487(3)	–	425
$Ph_3(NO_3)Sn$(•$OPPh_3$)	Sn	1.47(2)	153(1)	426

([a]) Second value resulting from disorder. ([b]) Co-planar through symmetry.

Table 5.4: Comparison of selected bond lengths and bond angles in the chalcogenoimidazoline group of [Mes*NP•Lg]OTf (Lg = OIm, SIm, or SeIm) with those in the free ligand and related transition metal or main-group complexes. Compounds are listed by increasing *d*(P–Ch) values.

Compound	*d*(O–C) (Å)	*d*(N–C) (Å)	∠(N-C-N) (°)	∠(O-C-N) (°)	∠(E-O-C) (°)	Reference
$OC(NMe_2)_2$	1.226(2)	1.371(1)	116.7(1)	121.6(1)	–	392
$OC(NMeCH_2)_2$[a]	1.24(1)	1.34(1)	109.0(6)	126, 125	–	393
$OC(N(H)CH_2)_2$	1.262(4)	1.295(4)	110.1(3)	126.8(4)	–	394
$Cl_3Al•OC(NMe_2)_2$	1.302(3)	1.330(3) 1.321(2)	1221(2)	119.7(2) 118.2(2)	132.5(2)	427
[Mes*NP•OIm]OTf (5.3)	1.342(5)	1.330(5) 1.336(5)	110.9(4)	126.0(4) 123.1(4)	120.5(3)	This work

Compound	*d*(S–C) (Å)	*d*(N–C) (Å)	*d*(C–C) (Å)	∠(S-C-N) (°)	∠(N-C-N) (°)	∠((E/M)-S-C) (°)	Reference
SIm (5.2)	1.690(5)	1.357(4)	1.359(7)	126.9(2)	106.3(4)	–	This work
[Mes*NP•SIm]OTf (5.3)	1.736(3)	1.346(3) 1.358(3)	1.362(3)	125.6(2) 126.7(2)	107.5(2)	91.8(1)	This Work
$(OC)_5Cr•SIm$	1.737(5)	1.352(6)	1.350(6)	–	107.3(5)	108.2(2)	395
$(OCl_2)SIm$ (5.9)	1.811(3)	1.334(4) 1.343(4)	1.366(5)	–	109.3(3)	111.2(2)	289

Compound	*d*(Se–C) (Å)	*d*(N–C) (Å)	*d*(C–C) (Å)	∠(Se-C-N) (°)	∠(N-C-N) (°)	∠((E/M)-Se-C) (°)	Reference
SeIm (5.2)	1.853(4)	1.357(3)	1.361(5)	126.8(1)	106.4(3)	–	380
[Mes*NP•SeIm]OTf (5.3)	1.889(3)	1.345(3) 1.355(3)	1.349(4)	125.4(2) 126.4(2)	108.1(2)	88.3(1)	This work
$(OC)_5Cr•SeIm$	1.89(2)	1.33(2) 1.34(2)	1.34(2)	–	109.6(1)	102.0(5)	395
$(I_2)SeIm$ (5.11)	1.900(4)	1.334(6) 1.344(6)	1.355(8)	–	107.9(4)	87.3(1) 88.2(1)	402

Table 5.5:Comparison of solution ^{31}P chemical shifts for [Mes*NP•Lg]OTf (Lg = OIm, SIm, SeIm, $OPPh_3$, or $SPPh_3$) with *P*-chalcogeno-iminophosphines, [Mes*NP]$Se_2P(^tBu)_2$ and related complexes. Compounds are listed by increasing δ. All values in ppm.

Compound	δ(^{31}P)	Reference
Mes*NPOTf	55	130
[Mes*NP•$OPPh_3$]OTf (5.4)	60	This work
[Mes*NP•OIm]OTf (5.3)	77	This work
[Mes*NP•$SPPh_3$]OTf (5.4)	79	This work
Mes*NPOC(O)CF_3	79	130
[Mes*NP]$Se_2P(^tBu)_2$ (5.1)	92	138
Mes*NPOS$O_2C_6H_4$-Me	93	130
Mes*NPOC$H(CF_3)_2$	122	141
Mes*NPO($C_6H_2(^tBu)_2$-2,6,Me-4)	139	428
[Mes*NP•SIm]OTf (5.3)	148	This work
Mes*NPOC$H(^tBu)_2$	149	130
Mes*NPOC$(^tBu)_3$	154	130
Mes*NPOSiMe_3	157	130
Mes*NPOC$H_2{}^tBu$	165	130
[Mes*NP•SeIm]OTf (5.3)	178	This work
Mes*NPO($C_6H_9(^iPr)$-3,Me-6)	178, (180)	139, (142)
Mes*NPS^tBu	314, (320)	102, (398)
Mes*NPSe^tBu	315	102
Mes*NPSeP$(^tBu)_2$	325	138

Table 5.6: Comparison of $\delta(^{31}P)$ value for the phosphorus centre in free and coordinated tertiary thio- and oxo-phosphine ligands. Compounds are listed by increasing δ. All values in ppm.

Compound	$\delta(^{31}P)$	Reference
$OPPh_3$	30	This work
$F_3B{\bullet}OPPh_3$	44	401
$Cl_3Al{\bullet}OPPh_3$	45	401
$Cl_3Ga{\bullet}OPPh_3$	46	401
[Mes*NP•$OPPh_3$]OTf (5.4)	52	This work
[H•$OPPh_3$]HSO_4	57	399
[MeOPPh_3]$SbCl_6$	65	400
[Cl_2(O)P•$OPPh_3$]Cl	65	357
[Br_2(O)P•$OPPh_3$]Br	65	357
$Cl_5P{\bullet}OPPh_3$	67	356
[Mes*NP•$SPPh_3$]OTf (5.4)	41	This work
$Cl_3Al{\bullet}SPPh_3$	43	388
[H•$SPPh_3$]HSO_4	43	399
$SPPh_3$	46	This work
[MeSPPh_3]$SbCl_6$	47	400

Table 5.7: Comparison of $\delta(^1H)$, $\delta(^{13}C)$ values and associated coupling constants of the chalcogenoimidazoline ligands in [Mes*NP•Lg]OTf (Lg = OIm, SIm, or SeIm) with those of in the free ligands and other derivatized chalcogenoimidazolines. Chemical shifts are reported in ppm and coupling constants in Hz.

	Lg = OIm		Lg = SIm		Lg = SeIm	
	Lg[a] 5.2	[Mes*NP•Lg]OTf 5.3 (Ch = O)	Lg[a] 5.2	[Mes*NP•Lg]OTf 5.3 (Ch = S)	Lg[a] 5.2	[Mes*NP•Lg]OTf 5.3 (Ch = Se)
$\delta(^1H)$						
$CH(C\underline{H}_3)_2$	1.61	1.33	1.58	1.34	1.60	1.41
$^3J(^1H,^1H)$	(7.02)	(6.71)	(7.02)	(6.8)	(7.02)	(7.33)
$C\underline{H}(CH_3)_2$	4.62	4.23	5.24	5.55	5.24	5.77
$^3J(^1H,^1H)$	(7.02)	(6.71)	(7.02)	([b])	(7.02)	([b])
$N(C\underline{H}_3)C$	2.29	1.97	2.41	2.09	2.46	2.18
$\delta(^{13}C)$						
$CH(\underline{C}H_3)_2$	22.3	21.4	21.7	20.7	21.6	20.6
$\underline{C}H(CH_3)_2$	50.4	51.9	53.0	49.3	54.9	51.7
$N(\underline{C}H_3)C$	10.0	9.7	11.0	10.3	11.0	10.1
$N(CH_3)\underline{C}$	128.8	113.3	128.8	121.5	128.6	123.0
$N\underline{C}(Ch)N$	148.5	152.8	129.5	159.5	131.1	157.6

([a]) Measured under the conditions described in Section 8.1. ([b]) Not resolved from spectra.

Chapter 6: Structural and Spectroscopic Comparison of the Cationic and Anionic units in Phosphadiazonium-ligand-triflate Complexes

In this chapter, common structural and spectroscopic features of the phosphadiazonium-ligand-triflate [Mes*NP•Lg]OTf complexes **1.44**, **2.8**, **2.9**, **3.14**, **5.3** (Ch = O, Se, or Se) and **5.4** (Ch = O) described in Chapters 1 through 5, are compared with one another, with related iminophosphines including Mes*NPOTf, and with complexes featuring a phosphadiazonium cation. A summary of common structural parameters for the [Mes*NP•Lg]OTf complexes is provided in Table 6.1.

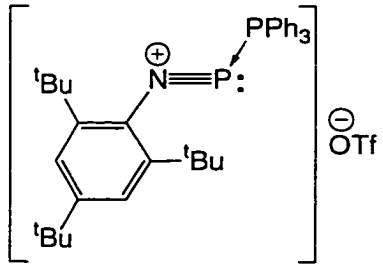

1.44

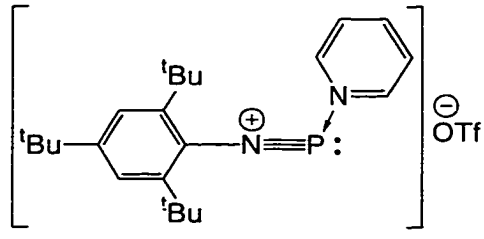

2.7

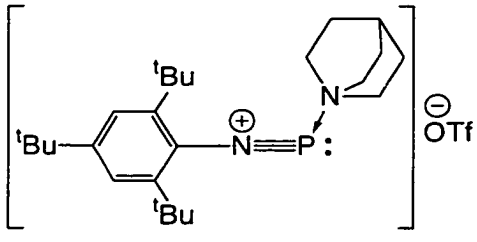

2.8

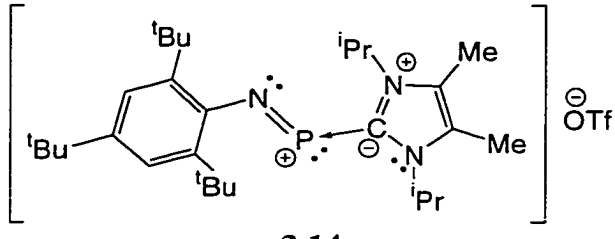

3.14

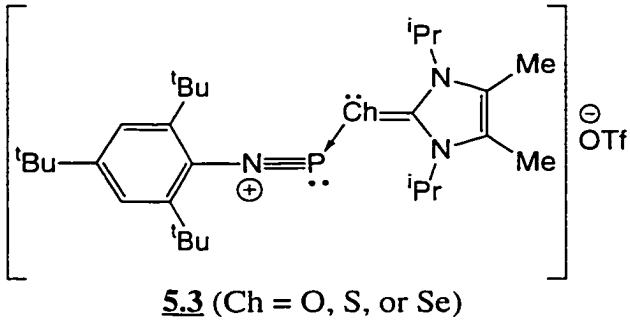

5.3 (Ch = O, S, or Se)

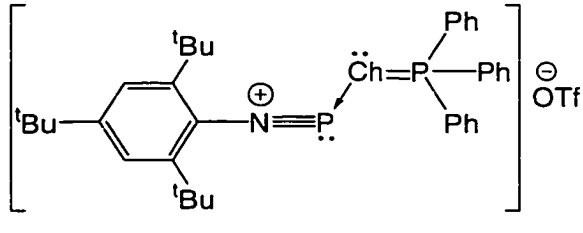

5.4 (Ch = O or S)

A feature of iminophosphines and complexes containing a phosphadiazonium cation, is the π-bonded phosphorus-nitrogen RNP unit. At present, there are over fifty different types of *N*-substituted Mes* iminophosphines which have been prepared and characterized. Importantly, crystal structures have been determined for the majority of *N*-Mes* iminophosphines (Table 6.2). Comparisons between different types of Mes*NPR compounds have revealed that the *P*-substituent directly influences a number of structural (vide infra) and spectroscopic properties including chemical shifts ($\delta(^{31}P)$,[137] $\delta(^{15}N)$,[117] $^{1}J(^{31}P,^{15}N)$[117]), and ν(P–N), I(P–N) values from vibrational spectroscopy.[429] Similarly, the structural and spectroscopic properties of the Mes*NP unit in the phosphadiazonium-ligand-triflate complexes can be compared, and conclusions drawn with respect to the nature of the phosphorus-ligand interactions.

In Chapters 2 through 5, comparisons of P–Lg bond lengths in [Mes*NP•Lg]OTf complexes with P–R bond lengths observed in iminophosphines and related phosphorus compounds were discussed. However, as a general conclusion, the phosphadiazonium-ligand interactions in [Mes*NP•Lg]OTf are longer than the phosphorus-substituent bonding in iminophosphines RNPR' and trisubstituted σ-phosphines PR_3, where the same phosphorus-element interactions are compared. To understand why the phosphorus-ligand interaction is weaker, consider the alternative bonding model for iminophosphines, which was alluded to in Chapter 1. In summary, this model suggests that an iminophosphine is composed of an interaction between a phosphadiazonium cation $Mes*NP^+$, and an anion, R^-. Evidence for this type of bonding is observed in iminophosphines with an electron-withdrawing substituent attached to phosphorus, for example, Mes*NPOTf or Mes*NPI, where the Mes*NP unit has structural and spectroscopic properties resembling those found for the phosphadiazonium cation $Mes*NP^+$, in complexes with a coordinating arene (e.g., [Mes*NP•arene]An

(An = $AlCl_4^-$, $GaCl_4^-$, or $Ga_2Cl_7^-$)). Furthermore, the bonding character of the *P*-substituent in these kinds of iminophosphines, including Mes*NPOTf and Mes*NPCp*, resemble those expected for a separated non-bonded ionic entity.[113,130] This bonding model can be extended to include the [Mes*NP•Lg]OTf-type complexes. The weaker phosphorus-ligand interaction is expected as the ligands in [Mes*NP•Lg]OTf are neutral and are weaker Lewis bases as compared with an anionic substituent R^- (e.g., Im versus $C(^tBu)_3^-$). Furthermore, the substituent-phosphorus interaction in iminophosphines is strong, partially due to an electrostatic component present between the $Mes*NP^+$ and R^- units, but this component in [Mes*NP•Lg]OTf-type complexes is weak or negligible.

The magnitudes of three important structural parameters, the P–N(Mes*), N–C(Mes*) bond lengths, and the (Mes*)C-N-P bond angle can be used to gauge the strength of interaction between a ligand or a substituent with the Mes*NP unit. The approximate range of N-P-R bond angles for iminophosphines Mes*NPR, is between 100.3(1)° (R = Si(OTf)DAB) and 118.4(3)° (R = I),[102] individual values are given in Table 6.2. A notable exception is the *P*-alkyloxy-iminophosphine $Mes*NPOC(^tBu)_3$, which has a large N-P-R angle (135.2(3)°),[130] which is probably caused by steric interactions between the $C(^tBu)_3$ and Mes* substituents.[130] In comparison, the phosphadiazonium-ligand-triflate complexes [Mes*NP•Lg]OTf (**1.44**, **2.7**, **2.8**, **3.14**, **5.3** Ch = O, S, or Se, **5.4**, Ch = O) have N-P-Lg bond angles (103.2(2)° (Lg = Im **3.14**)[215] to 115.4(1)° (Lg = SeIm **5.3** (Ch = Se)), which fit into the range observed for iminophosphines Mes*NPR. This suggests that the N-P-(R/Lg) bond angle is not generally dependent on the electronic properties of the attached ligand or substituent, but is more a consequence of the bonding properties of phosphorus (i.e., decreased participation of the 3s orbital in bonding).[3]

In contrast, the range of (Mes*)C-N-P bond angles for iminophosphines Mes*NPR, and complexes containing the phosphadiazonium cation is wide (115.3(3)° (Mes*NP(PN(SiMe$_3$)N(SiMe$_3$)$_2$))[245] to 178.7(8)° [Mes*NP•C$_6$H$_5$Me]Ga$_2$Cl$_7$)),[93] individual values are given in Table 6.2. This large range reflects the hybridization ability of the nitrogen valence 2s and 2p orbitals.[4] The majority of phosphadiazonium-ligand-triflate complexes (**1.44**, **2.7**, **5.3** (Ch = O, S, or Se), and **5.4** (Ch = O)) have large (Mes*)C-N-P bond angles which are greater than 160°. The exceptions are complexes with Lg = Qncd **2.8** (143.9(2)°),[216] or Lg = Im (116.2(3)°) **3.14**.[215] The (Mes*)C-N-P bond angle in the [Mes*NP•Lg]OTf complexes, where Lg = PPh$_3$ **1.44**, Py **2.7**, OIm **5.3**, (Ch = O), SIm **5.3** (Ch = S), SeIm **5.3** (Ch = Se), or OPPh$_3$ **5.4** (Ch = O), are comparable with those observed in iminophosphines featuring an electron-withdrawing *P*-substituent, including Mes*NPBr (159.5(4)°),[124] and Mes*NPOC$_6$H$_2$(^{t}Bu)$_2$-2,6,Me-4 (173.7(1)°[417]). In contrast, [Mes*NP•Lg]OTf complexes with Lg = Qncd **2.8** or Im **3.14**, have a (Mes*)C-N-P bond angle (143.9(2)°[216] and 116.2(3)°,[215] respectively), which is similar to those in iminophosphines with a strong π- or σ-donating *P*-substituent, for example, Mes*NPFe(CO)$_2$Cp* (119.8(9)°),[140] Mes*NPP(^{t}Bu)$_2$ (120.2(1)°),[171] and Mes*NPNMe$_2$ (140.7(4)°),[242] other examples can be found in Table 6.2.

A broad spectrum of P–N(Mes*) bond lengths is observed for iminophosphines Mes*NPR, (*d*(P–N) = 1.467(4) Å[130] (Mes*NPOTf) to 1.585(5) Å (Mes*NPN(H)Mes*[241])), individual values are provided in Table 6.2. As expected, the P–N(Mes*) bond length in these compounds is considerably less than that in σ-aminophosphines (e.g., *d*(P–N) = 1.730(2) Å,[282] (Mes*N(H)PPh$_2$); 1.732(3) Å (P(NMe$_2$)$_3$)),[430] and in phosphinoamides RNPR$_2^-$, (*d*(P–N) = 1.660(2) to 1.672(2) Å). However, compounds such as aminophosphines contain a P–N bond, which has a π-component resulting from lone pair π-conjugation from nitrogen to phosphorus.

However, the P–N π-bonding in iminophosphines and phosphadiazonium cation is considered significantly stronger (vide infra). For example, in the amino-iminophosphine Mes*NPNMe$_2$, which is postulated to have lone pair π-conjugation in the P–NMe$_2$ bond, the phosphorus-imino bond (*d*(P–N(Mes*) = 1.539(3) Å)[242] is shorter than the phosphorus-amino bond (*d*(P–N(Me$_2$) = 1.651(3) Å[242]). Nevertheless, the phosphadiazonium cation and iminophosphines featuring an electron-withdrawing *P*-substituents are speculated as having some lone pair π-conjugation between the imino-nitrogen and phosphorus centres. The P–N(Mes*) bond in Mes*NPOTf (*d*(P–N) = 1.467(4) Å)[130] and the η^6 arene-phosphadiazonium complexes (*d*(P–N) = 1.463(5) to 1.53(2) Å)[93,94,123] is shorter than that reported for diatomic phosphorus nitride PN and its cationic analogue PN^+ (*d*(P–N) = 1.4909(1) Å,[431] 1.50(1) Å,[432] respectively). This suggests that these types of iminophosphines and the phosphadiazonium cation a strong P–N π-bond (i.e., they have a formal P–N triple bond).[431] Ab initio calculations show that HNP^+ has a short P–N bond ($C_{\infty v}$ symmetry, *d*(P–N) = 1.446 Å, CISD(fc)/6-311G(df,p)) and a doubly degenerate set of π-bonding MOs. The majority of the phosphadiazonium-ligand-triflate complexes (**1.44**, **2.7**, **5.3** (Ch = O, S, or Se) and **5.4** (Ch = O)) also have a short P–N(Mes*) bond, which is less than or equal to 1.5 Å, and is comparable in length with iminophosphines that contain an electron-withdrawing *P*-substituent. For example, Mes*NPBr (*d*(P–N) = 1.498(4) Å)[124] and Mes*NPOSO$_2$C$_6$H$_4$Me-4 (*d*(P–N) = 1.492(4) Å[130]). The exceptions, [Mes*NP•Lg]OTf with Lg = Qncd **2.8** (*d*(P–N) = 1.519(2) Å)[216] or Im **3.14** (*d*(P–N) = 1.574(4) Å),[215] have a P–N(Mes*) bond length that is similar to that found in an iminophosphine with an electron-donating *P*-substituent, such as a *P*-amino-, *P*-silyl- or *P*-phosphino-iminophosphine (*d*(P–N) = 1.539(3) Å, Mes*NPNMe$_2$; 1.578(3) Å,[242] Mes*NPSi(OTf)DAB **4.7** (X = OTf); 1.570(2) Å, Mes*NPP(^{t}Bu)$_2$[171]). This suggests that

the P–N π-bonding in [Mes*NP•Qncd]OTf **2.8** and especially in [Mes*NP•Im]OTf **3.14**, is weaker than in the other [Mes*NP•Lg]OTf (**1.44**, **2.7**, **5.3** (Ch = O, S, or Se) and **5.4** (Ch = O)) and η^6 arene-phosphadiazonium complexes **1.34** . However, the P–N π-bonding in [Mes*NP•Lg]OTf, (Lg = Qncd **2.8** or Im **3.14**) is probably more closely related to the P–N π-bonding in iminophosphines with an electron-donating *P*-substituent, such as $Mes*NPNMe_2$.

The range of N–C(Mes*) bond lengths in iminophosphines Mes*NPR', and in complexes containing the phosphadiazonium cation, is narrow (*d*(N–C) = 1.398(5) Å[130] (Mes*NPOTf) to 1.445(5) Å[245] ($Mes*NPN(SiMe_3)N(SiMe_3)_2$)), individual values are provided in Table 6.2. The *d*(N–C) values in iminophosphines Mes*NPR', are similar or identical to those reported for *N,N*-disubstituted aryl-anilines $ArNR_2$, (*d*(N–C) = 1.38[3] Å)[131] and compounds featuring an aryl-substituted diazonium cation RNN^+ (*d*(N–C) = 1.394[6] Å[433]). In general, the [Mes*NP•Lg]OTf complexes (**1.44**, **2.7**, **2.8**, **5.3** (Ch = O, S, or Se) and **5.4** (Ch = O)) have N–C(Mes*) bond lengths (*d*(N–C(Mes*)) = 1.381(3) Å ([Mes*NP•SeIm]OTf **5.3** (Ch = Se)) to 1.42(1) Å[215] ([Mes*NP•Py]OTf **2.7**), which are generally in the lower range of values reported for iminophosphines. However, the N–C(Mes*) bond length in [Mes*NP•Im]OTf **3.14** (*d*(N–C(Mes*)) = 1.442(6) Å)[215] is long and identical to that reported for the σ-aminophosphine $Mes*N(H)PPh_2$ (*d*(N–C(Mes*)) = 1.431(3) Å[282]).

A plot of P–N(Mes*) bond length versus (Mes*)C-N-P bond angle for iminophosphines and [Mes*NP•Lg]An complexes (including Lg = arene), shows that short P–N bonds (less than or equal to 1.5 Å) generally correlate with large (Mes*)C-N-P bond angles (160° to 180°), (Figure 6.1). This is corroborated by the relationship between the signal intensity, *I*(P–N) of the P–N bond stretch, from Raman spectra, and the C(Mes*)-N-P bond angle.[429] Increased polarization of the P–N(Mes*) bond

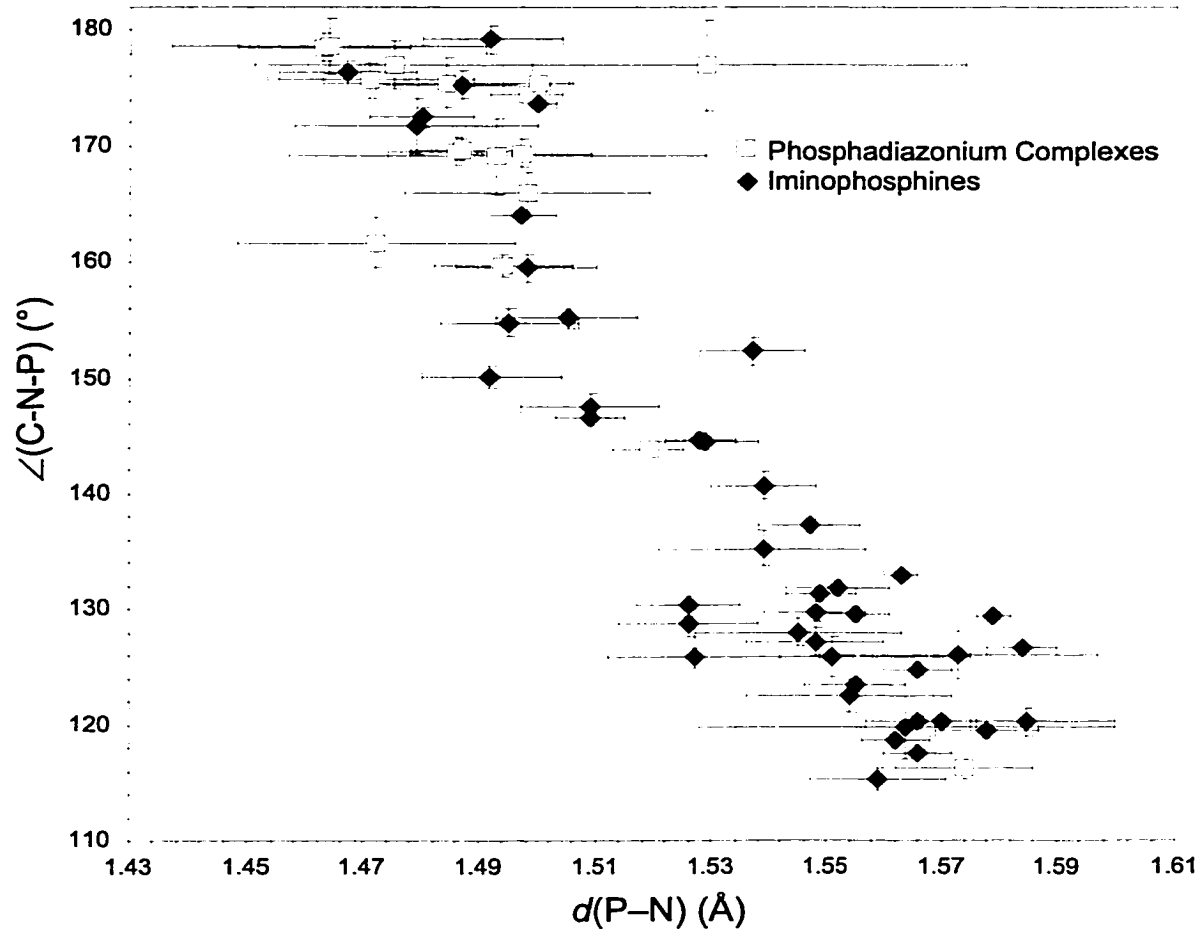

Figure 6.1: A plot of P–N(Mes*) bond length versus (Mes*)C-N-P bond angle in iminophosphines Mes*NPR, and complexes containing a Mes*NP•Lg unit. Data points represent the compounds listed in Table 6.2. Error bars are calculated using the standard error values associated with the bond lengths and angles with a 99 % confidence limit.

results in a larger *I*(P–N) value and is thought to involve π-conjugation between the PN unit and the Mes* substituent, which is maximized in systems with large (Mes*)C-N-P bond angles (~180°).[429] Iminophosphines and complexes featuring the phosphadiazonium cation, with a short N–C(Mes*) bond (less than or equal to 1.4 Å) also

have a short P–N bond (< 1.5 Å) and a large C(Mes*)-N-P bond angle (> 160°). This is opposite to that observed in diazoketones, diazoalkanes, and diazonium cations, where a short N–N bond is correlated with a long N–C bond.[433] For iminophosphines and phosphadiazonium complexes, the positive correlation between *d*(N–C) and *d*(P–N) values is probably due to a greater dipolar interaction within the PN unit than in the NN unit of RNN^{+}.[115] These structural relationships between the *d*(P–N), *d*(N–C), and ∠(C-N-P) parameters are a consequence of the *P*-, *N*-substituent σ-push-pull effect for iminophosphines described in Section 1.4.

The [Mes*NP•Lg]OTf complexes (**1.44**, **2.7**, **2.8**, **3.14**, **5.3** (Ch = O, S, or Se) and **5.4** (Ch = O)) are distinct from iminophosphines Mes*NPR, in that, the molecular structure of the former consists of an interaction between a cationic phosphadiazonium-ligand unit and an anionic triflate group. The nature of this cation-triflate interaction can provide some indication of the Lewis acidity of the phosphadiazonium unit, in particular how it is influenced by the presence of a coordinating Lewis base. The triflate group in the absence of a stronger Lewis base coordinates to the phosphadiazonium cation. The crystal structure of Mes*NPOTf reveals a covalent bonding interaction (*d*(P–O) = 1.923(3) Å)[130] between the phosphorus centre and an oxygen atom of the triflate group. In solution, the covalent nature of this compound is suggested by its high solubility in non-polar solvents such as n-hexane.

In many cases, the interaction of a ligand with the phosphadiazonium unit in Mes*NPOTf, results in a weaker phosphorus-triflate interaction or dissociation of the triflate group from the phosphorus centre. A range of P–O(Tf) distances is observed for the [Mes*NP•Lg]OTf complexes (*d*(P–O(Tf) = 2.298(4) Å[25] ([Mes*NP•PPh_3]OTf **1.44**) to 3.428(4) Å[215] ([Mes*NP•SeIm]OTf **5.3** (Ch = Se)). Two structurally distinct types of [Mes*NP•Lg]OTf complexes with a single monodentate ligand can be envisaged with

classification based on the relative amount of structural change within the ligand of the [Mes*NP•Lg]OTf complex. Compounds with type Lg^A ligands exhibit no or minor structural change when coordinating (low polarization), whereas type Lg^B ligands undergo significant structural modification (high polarization). The [Mes*NP•Lg^A]OTf complexes, (Lg^A = PPh_3 **1.44**, OIm **5.3** (Ch = O), Qncd **2.8**, Py **2.7**, and Im **3.14**) have a phosphorus-triflate distance which is less than 3.30 Å (from $\Sigma\, r_w(P) + r_w(O)$). Therefore, in the strictest sense, the triflate-phosphorus interaction has a covalent component. However, there is significant charge partition between the Mes*NP•Lg and OTf units. Therefore, a continuum of P–O(Tf) interactions in [Mes*NP•Lg^A]OTf is represented by [Mes*NP•PPh_3]OTf **1.44** and [Mes*NP•Im]OTf **3.14** (as the lower and upper limits, respectively) and that the covalent component is significant weaker in [Mes*NP•Im]OTf **3.14** than in [Mes*NP•PPh_3]OTf **1.44**. In comparison with other π-phosphino-triflate complexes, the P–O(Tf) distances in [Mes*NP•Lg^A]OTf complexes (Lg^A = PPh_3 **1.44**, OIm **5.3** (Ch = O), Qncd **2.8**, Py **2.7**, and Im **3.14**) are similar to those in the diazaphospholenium triflate complex (d(P–O(Tf) = 2.755(5) Å[36,37]). Therefore, the overall Lewis acidity of the phosphadiazonium-ligand unit Mes*NP•Lg^+ is comparable with that of a diaminophosphenium cation $P(NR_2)_2^+$, which have been shown by ab initio calculations to be weaker Lewis acids than phosphadiazonium cations RNP^+.[76,77,161] In phosphenium cations, the combination of two lone pair π-conjugation interactions results in a weakly Lewis acidic phosphorus centre. As expected, coordination of the phosphadiazonium unit Mes*NP^+, by a Lewis base reduces its Lewis acidity.

Complexes [Mes*NP•Lg^B]OTf with Lg^B = $OPPh_3$ **5.4** (Ch = O), SIm **5.3** (Ch = S), or SeIm **5.3** (Ch = Se), have a P–O(Tf) distance which is greater than 3.30 Å (from $\Sigma\, r_w(P) + r_w(O)$). In contrast to the [Mes*NP•Lg]OTf complexes featuring a Lg^A type ligand (**1.44**, **2.7**, **2.8**, **3.14**, **5.3** (Ch = O)), the shortest cation-triflate distances in the

[Mes*NP•Lg^{B}]OTf complexes (**5.4** Ch = O, **5.3** (Ch = S or Se)) are not with the phosphorus centre, but with an atomic centre associated with the ligand. These triflate-ligand interactions are also greater than the sum of van der Waals radius for the atoms involved. Hence, the Mes*NP•Lg^{+} and triflate groups in the [Mes*NP•Lg^{B}]OTf type of complex are regarded as being non-bonded with an interaction that is predominantly ionic.

In compounds with a covalently bonded triflate group, for example, Mes*NPSi(OTf)DAB and Mes*NPOTf, one S–O bond, the connecting bond, is significantly longer. Compounds that feature a non-bonded triflate group, such as Ag[OTf], have similar S–O bond lengths, thus indicating even charge distribution throughout the anion. The *d*(S–O) values for the phosphadiazonium-ligand-triflate complexes [Mes*NP•Lg]OTf are listed in Table 6.3. A longer distance between the triflate and Mes*NP•Lg^{+} units is sometimes accompanied by positional disorder in the SO_3 and CF_3 groups, resulting in less accurate S–O bond lengths. Furthermore, hydrogen bonding between the cation and triflate units can cause disproportional lengthening among the S–O bonds as observed in the triaquaoxonium triflate salt.[434] In the majority of phosphadiazonium-ligand-triflate complexes, the three sulphur-oxygen bond lengths are not equivalent. Nevertheless, a small range of S–O bond lengths (Δd(S–O)) appears related with greater Mes*NP•Lg^{+} and OTf separation (Table 6.3). For example, Mes*NPOTf has covalent bonded triflate group (*d*(P–O(Tf) = 1.923(3) Å[130]) with Δd(S–O) = 0.094(6). In contrast, [Mes*NP•Im]OTf with *d*(P–O(Tf) = 2.9 Å, has a Δd(S–O) value of 0.002(6).

IR spectra of the phosphadiazonium-ligand-triflate complexes, prepared as paraffin oil mulls, contain bands corresponding to symmetric and asymmetric ν(S–O) and ν(C–F) stretching frequencies associated with the triflate group (Table 6.4). It should be

noted, however, that due to the complexity of the spectra, the assignment of these stretching frequencies is tentative. The ν(S–O) mode (A_1 symmetry) for the [Mes*NP•Lg]OTf complexes (**1.44**, **2.7**, **2.8**, **3.14**, OIm **5.3** (Ch = O, S or Se), **5.4** (Ch = O)) has a frequency that is close or identical to that reported for silver triflate,[435] while considerably different from that observed in Mes*NPSi(OTf)DAB **4.7** (X = OTf), where the triflate group is covalently bonded to the silicon centre (see Section 4.2.2).

Solution ^{19}F NMR spectra of the phosphadiazonium-ligand-triflate complexes [Mes*NP•Lg]OTf, show identical chemical shifts (i.e., $\delta(^{19}F) = -78.6 \pm 0.5$ ppm) for fluorine nuclei associated with the triflate group. The fluorine nuclei are more shielded as compared with compounds featuring covalently bonded OTf group, such as Me_3SiOTf ($\delta(^{19}F) = -77.0$ ppm) and Mes*NPSi(OTf)DAB **4.8** (X = OTf), ($\delta(^{19}F) = -76.6$ ppm). The $\delta(^{19}F)$, $\delta(^{13}C)$ and $^1J(^{19}F,^{13}C)$ values associated with the CF_3 group in the [Mes*NP•Lg]OTf complexes are similar to those in compounds such as [^{n}Bu$_4$N]OTf ($\delta(^{19}F) = -78.3$ ppm)[36,37] for which it is established, from solution molar conductivity, that the triflate group has predominately ionic bonding character and it is dissociated.

For [Mes*NP•Lg]OTf complexes with a Lg^A-type ligand (**1.44**, **2.7**, **2.8**, **3.14**, or **5.3** (Ch = O)), the ligand and triflate group adopt a similar orientation with respect to the Mes*NP unit. This is indicated by a similar N-P-O(Tf) bond angle (111.1(2) to 123.0(2)°), N-P-Lg^A, (103.2(2) to 109.8(2)°), and Lg^A-P-O(Tf) (72.1(2) to 86.1(1) °), individual values are listed in Table 6.5. Interestingly, the Lg-P-Lg, or An-P-An bond angle in phosphadiazonium complexes featuring dual ligand- or anion-phosphorus interactions, (e.g., [Mes*NP•Dipy]OTf **2.9** (75.1(2)°),[216] [Mes*NP]Ch$_2$P(^{t}Bu)$_2$ **5.1** (77.4(1)° Ch = S; 80.6(1)° Ch = Se),[138] and Mes*NPI (88.1(1)°)[102]) are similar to the Lg^A-P-O(Tf) bond angle (111.1(2) to 123.0(2) °) in the monodentate [Mes*NP•Lg^A]OTf complexes (Table 6.5). The (Mes*)C-N-P-Lg^A and (Mes*)C-N-P-O(Tf) torsion angles in

the [Mes*NP•Lg^{A}]OTf complexes (**1.44**, **2.7**, **2.8**, **3.14**, or **5.3** (Ch = O)) are variable (9.9(5) to -175.7(3) ° and -85(1) to 112.8(3) °, respectively) and are probably dependent on steric interactions between the Mes* substituent and ligand, individual values are given in Table 6.5. Nevertheless, the difference (ϕ) between the (Mes*)C-N-P-Lg and (Mes*)C-N-P-O(Tf) torsion angles (ϕ = 80.6(1) to 86.1(1) °) are close to 90° with the exception of [Mes*NP•Im]OTf **3.14** (ϕ = 72.1(2)°), individual values are given in Table 6.5. Similarly, the ϕ values (using both (Mes*)C-N-P-Lg torsion angles) for [Mes*NP•Dipy]OTf **2.9** (ϕ = 80.6(1)°) and Mes*NPI (ϕ = 88.1(1)°) are comparable. A ϕ value of 90° was calculated for the bis-coordinated model complex $HNP(\bullet NH_3)_2^+$.[223] The value ϕ has implications for the proposed bonding model which describes the ligand-phosphadiazonium interaction in the [Mes*NP•Lg]OTf complexes (vide infra).

The stereochemistry of iminophosphines Mes*NPR and [Mes*NP•Lg]OTf complexes (**1.44**, **2.7**, **2.8**, **3.14**, **5.3** (Ch = O, S, or Se), and **5.4** (Ch = O)), as defined by the arrangement of the Mes* and ligand unit across the P–N(Mes*) bond, is either *cis* or *trans* as indicated by the (Mes*)C-N-P-(Lg/R) torsion angle. The majority of (Mes*)C-N-P-R torsion angles for iminophosphines fall into two ranges, 0° to ~13° corresponding to those compounds having a *cis*-configuration and ~160° to 180° for those having a *trans*-configuration, individual values are given in Table 6.2. However, in general, iminophosphines with an electron-withdrawing *P*-substituent and complexes containing a phosphadiazonium cation, have a wide (Mes*)C-N-P bond angle (> 170°) and a (Mes*)C-N-P-R torsion angle value that does not fit into either of the *cis*- or *trans*-ranges, for example, Mes*NPOC$_6$H$_2$(^{t}Bu)$_2$-2,6,Me-4 (86.3(8)°)[171] and Mes*NPOTf (158.4†°[130]). The [Mes*NP•OPPh$_3$]OTf **5.4** (Ch = O), [Mes*NP•SIm]OTf **5.3** (Ch = S) and [Mes*NP•SeIm]OTf **5.3** (Ch = Se) complexes have neither a *cis*- or *trans*-configuration (i.e., (Mes*)C-N-P-R is -116(2)° (123(3)°), -148(2)°, and 148(3)°,

respectively). Ab initio calculations suggest that a *trans*-configuration is preferred for an iminophosphine with a strongly σ-donating *P*-substituent, while a *cis*-configuration is observed when an electron-withdrawing *P*-substituent is present.[3,113] Similarly, phosphadiazonium-ligand-triflate complexes [Mes*NP•Lg]OTf which feature a strongly Lewis basic ligand (e.g., Lg = Qncd **2.8** and Im **3.14**) have a *trans*-configuration.

An extensive amount of solution ^{31}P NMR data has been collected on iminophosphines and related compounds. The range of $\delta(^{31}P)$ value is large, 55 to 787 ppm.[117,118,137,436,437] Consequently, $\delta(^{31}P)$ is sensitive to the electronic structure within the PN unit.[175] In some cases, it is possible to assign a *cis*- or *trans*-configuration to the iminophosphine from the magnitude of $^{1}J(^{31}P,^{15}N)$, $\delta(^{31}P)$, and $\delta(^{13}C)$ values.[117,118,438] Comparison of uv-vis, and ^{31}P NMR spectra for iminophosphines Mes*NPR show that $\delta(^{31}P)$ values and n-π* transition energies are correlated.[102,137] This suggests that the shielding of the phosphorus nucleus in iminophosphines has a high dependence on paramagnetic factors (i.e., contributions from both the ground state and excited states).[137] PE measurements show that *N*-Mes*-iminophosphines with a σ-donating *P*-substituent (e.g., alkyl or aryl group) contain a pair of non-bonding valence electrons which are higher in energy than those in iminophosphines featuring an electron-withdrawing *P*-substituent.[88] Consequently, these compounds have smaller E(n-π*) values and thus, these types of iminophosphines have a deshielded phosphorus nucleus with a $\delta(^{31}P)$ value generally in the range of 400 to 700 ppm.[137] Iminiophosphines with an electron-withdrawing *P*-substituent, such as Mes*NPOAr, Mes*NPCl, and Mes*NPOTf, have a shielded phosphorus nucleus with a $\delta(^{31}P)$ value in the range of 55 to 160 ppm.

The $\delta(^{31}P)$ values of the phosphadiazonium-ligand-triflate complexes [Mes*NP•Lg]OTf ($\delta(^{31}P)$ = 60 to 339 ppm) are greater with respect to that observed for Mes*NPOTf ($\delta(^{31}P)$ = 55 ppm),[130] but not as large as that reported for the *P*-phosphino-

iminophosphine ($\delta(^{31}P)$ = 570 ppm[75]) or other iminophosphines with a strong σ-donating substituent (i.e., $\delta(^{31}P)$ = 566 ppm for Mes*NPSi(OTf)DAB, **4.7** (X = OTf)). In general, the $\delta(^{31}P)$ values of the [Mes*NP•Lg]OTf complexes ($\delta(^{31}P)$ = 71 ppm, [Mes*NP•Py]OTf **2.7**; 144 ppm, [Mes*NP•Qncd]OTf **2.8**; 77 ppm, [Mes*NP•OIm]OTf **5.3** (Ch = O); 148 ppm, [Mes*NP•SIm]OTf **5.3** (Ch = S); 178 ppm, [Mes*NP•SeIm]OTf (Ch = Se)) complexes are nearer to those reported for iminophosphines with an electron-withdrawing *P*-substituent, such as Mes*NPCl ($\delta(^{31}P)$ = 135 ppm)[123] and Mes*NPCp* ($\delta(^{31}P)$ = 195 ppm[135]), individual values are given in Table 6.6. The [Mes*NP•Im]An (An = $AlCl_4^-$ **3.16**, and OTf^- **3.14**) complexes are unusual in that the phosphorus nucleus is highly deshielded, with $\delta(^{31}P)$ values of 331 and 339 ppm,[215] respectively. The values are closer to those reported for *P*-aryl- and *P*-alkyl-iminophosphines ($\delta(^{31}P)$ = 490 to 500 ppm[137]). The deshielded phosphorus nucleus in the [Mes*NP•Im]An (An = $AlCl_4^-$ and OTf^- **3.14**) complexes is possibly caused by the strong σ-donating ability of imidazol-2-ylidene Im.

Solid-state ^{31}P NMR spectra have been collected for a series of [Mes*NP•Lg]OTf complexes (Lg = PPh_3 **1.44**, Py **2.7**, Dipy **2.9**, and Im **3.14**), the isotropic $\delta(^{31}P)$ values and $\delta(^{31}P)$ of the principal components are provided in Table 6.7. Comparison of isotropic and solution $\delta(^{31}P)$ values show slight variations, the largest associated with the [Mes*NP•Im]OTf complex **3.14** ($\Delta\delta(^{31}P)$ = 27 ppm). Therefore, solvent effects on the phosphorus chemical shift of the [Mes*NP•Lg]OTf complexes can be considered minor and the molecular structure of the complexes is generally thought to be unaltered between solution and the solid state. The principal components of the phosphorus chemical shielding tensor (^{31}P CST) can be obtained from static solid-state NMR spectra. These same components are averaged into a single resonance in solution NMR spectra. Comparison of the principal components (δ_{11}, δ_{22}, and δ_{33}) for the [Mes*NP•Lg]OTf

complexes (Lg = PPh_3 **1.44**, Py **2.7**, Dipy **2.9**, or Im **3.14**) with those of Mes*NPOTf, reveals that the coordination of a Lewis base to the Mes*NP unit causes changes to all principal component values (Table 6.7). The largest differences in the ^{31}P CST are observed for the [Mes*NP•Im]OTf complex **3.14**, which is to be expected, based on the significant structural and spectroscopic changes caused by the strongly Lewis basic imidazol-2-ylidene. For example, the δ_{11} principal component in [Mes*NP•Im]OTf complex **3.14** has a value (δ_{11} = 915 ppm) nearer to that reported for *P*-alkyl-iminophosphines such as Mes*NP^{t}Bu (δ_{11} = 1035 ppm[255]). Previous investigations on Mes*NPOTf and other *P*-oxy- and *P*-halogeno-iminophosphines suggests that the largest contributions to shielding of the δ_{11} principal component are correlated with the magnitude of E(n-π^*).[232,255] Similarly, the ligands in the [Mes*NP•Lg]OTf complexes are expected to alter the E(n-π^*) values, thereby causing similar shielding changes to the δ_{11} principal component, as observed in iminophosphines with a strongly σ-donating *P*-substituent.

The chemical shift of the protons and carbon nuclei associated with the Mes* substituent in the [Mes*NP•Lg]OTf complexes are comparable with that observed in Mes*NPOTf. However, the magnitudes of the $^nJ(^{31}P,^{13}C)$ (n = 2 to 5), and $^5J(^{31}P,^1H)$ values are varied and appears related with the (Mes*)C-N-P bond angle. For phosphadiazonium-ligand-triflate complexes with a large (Mes*)C-N-P bond angle (> 160°), such as [Mes*NP•SIm]OTf **5.3** (Ch = S), and [Mes*NP•$OPPh_3$]OTf **5.4** (Ch = O), significant phosphorus-carbon and phosphorus-proton coupling is observed (Table 6.8). The magnitude of spin-spin coupling is increased through π-conjugation, which occurs when the π-type MOs associated with the Mes* substituent and the PN unit are brought into a linear arrangement. A similar relationship has been postulated for the

magnitude of the phosphorus-carbon couplings[439] for the Mes* substituent of the phosphaalkyne Mes*CP, which has a (Mes*)C-C-P bond angle of 177.0(1)°.[440]

In summary, the structural and spectroscopic features associated with the Mes*NP unit in the [Mes*NP•Lg]OTf complexes reveal a continuum of modifications caused by the coordination of a Lewis base. The phosphadiazonium-ligand-triflate complexes can be classified into three types. Complexes [Mes*NP•Lg^A]OTf where the ligand (Lg^A) is PPh_3 **1.44**, Py **2.7**, Qncd **2.8**, OIm **5.3** (Ch = O), or Im **3.14**. These complexes have a variable range of P–N(Mes*) bond lengths (*d*(P–N) = 1.472(8) Å to 1.574(4) Å) and (Mes*)C-N-P bond angles (116.2(3) to 169.5(4) °). The chalcogeno-phosphadiazonium-triflate complexes, [Mes*NP•Lg^B]OTf where Lg^B = $OPPh_3$ **5.4** (Ch = O), SIm **5.3** (Ch = S), and SeIm **5.3** (Ch = Se), have ionic cation-triflate interactions, and the Mes*NP unit features a short P–N(Mes*) bond (*d*(P–N) = 1.498(7) to 1.504(7) Å) with a large (Mes*)C-N-P bond angle (165.9(6) to 175.5(2) °). The ligand in the [Mes*NP•Lg^B]OTf complexes exhibits significantly moew structural and spectroscopic changes than those in a [Mes*NP•Lg^A]OTf-type complex. A third type of complex features two phosphorus-ligand interactions and an ionic cation-anion interaction. At present the only example is [Mes*NP•Dipy]OTf **2.9**.

In the [Mes*NP•Lg^A]OTf complexes PPh_3 **1.44**, Py **2.7**, Qncd **2.8**, OIm **5.3** (Ch = O), or Im **3.14**, ligand (Lg^A) basicity appears significantly to influence and determine structural and spectroscopic parameters associated with the Mes*NP unit. Furthermore, the P–O(Tf) distance appears to be related to ligand basicity. A comparison of structural characteristics and $\delta(^{31}P)$ for the [Mes*NP•Lg^A]OTf complexes with ligand basicity , as inferred from the relative pK_a of the conjugate acid is provided in Table 6.9. The structural observations indicate that strongly basic ligands (larger pK_a) cause greater structural and spectroscopic modification, where Im > Qncd > Py > PPh_3. This is similar

to the relationship between the π-basicity of the arene, the P–Lg, and P–An distances in the η^6 arene-phosphadiazonium complexes (see Section 1.4).[93,94] The triphenylphosphine ligand has only a minor influence on structural aspects of the Mes*NP unit in [Mes*NP•PPh_3]OTf **1.44**, whereas the imidazol-2-ylidene Im, has the highest basicity of the ligands examined, causes the greatest structural and spectroscopic changes within the Mes*NP unit of **3.14**. Many structural and spectroscopic features of the Mes*NP•Im^+ unit in **3.14** resemble those found in *P*-aryl- or *P*-alkyl-iminophosphines. Therefore, as the substituent σ-push-pull effect operates in iminophosphines Mes*NPR, a "ligand σ-push effect" can be envisaged for the phosphadiazonium-ligand-triflate complexes, where the coordination of a strongly basic ligand to phosphadiazonium cation $Mes*NP^+$ results in a [Mes*NP•Lg]OTf complex with a long P–N(Mes*) bond and a small (Mes*)C-N-P bond angle, for example [Mes*NP•Im]OTf **3.14**. Furthermore, the effect is cumulative, that is, the addition of two or more strongly donating ligands or substituents significantly increases P–N bond length and decreases the (Mes*)C-N-P. These structural relationships are due to the atomic properties of nitrogen and the π-bonding interaction between the imino-substituent and phosphorus centre. Analogous behaviour has been observed in systems with Si–N π-bonding such as iminosilanes.[99,441-443]

A simple bonding model can be envisaged for the phosphadiazonium-ligand-triflate complexes [Mes*NP•Lg]OTf. The phosphadiazonium cation has, assuming $C_{\infty v}$ symmetry, a doubly degenerate HOMO and LUMO of π- and π*-character, respectively. Ab initio calculations show that two ligands (NH_3) can interact with the LUMO of the HNP^+ cation.[223] Since the two π*-molecular orbitals are orthogonal with respect to each other, (Figure 6.2) the NH_3 ligands are also orthogonally orientated (i.e., the difference (ϕ) between both H-N-P-N(Lg) torsion angle is 90°).[223] Thus, according to this proposed bonding model, in [Mes*NP•Dipy]OTf, the σ-type doubly degenerate HOMO of the 2,2'-

dipyridyl ligand interacts with both π*-molecular orbitals, the LUMO of Mes*NP$^+$ (Figure 6.2). This bonding model is also applicable to the [Mes*NP•Lg]OTf complexes featuring a monodentate ligand, such as [Mes*NP•Py]OTf **2.7** or [Mes*NP•Im]OTf **3.14**. However, in this case, the primary ligand (e.g., Py or Im) interacts with one of the two degenerate MO of the LUMO, and a σ-type MO associated with the triflate group, (where OTf is envisaged as the second, weaker Lewis basic ligand), interacts with the other degenerate π*-type MO (Figure 6.2). This accounts for the almost orthogonal positioning (ϕ = ~ 85°) of the ligand and triflate groups in [Mes*NP•Lg]OTf complexes **1.44**, **2.7**, **2.8**, **3.14**, **5.3** (Ch = O).

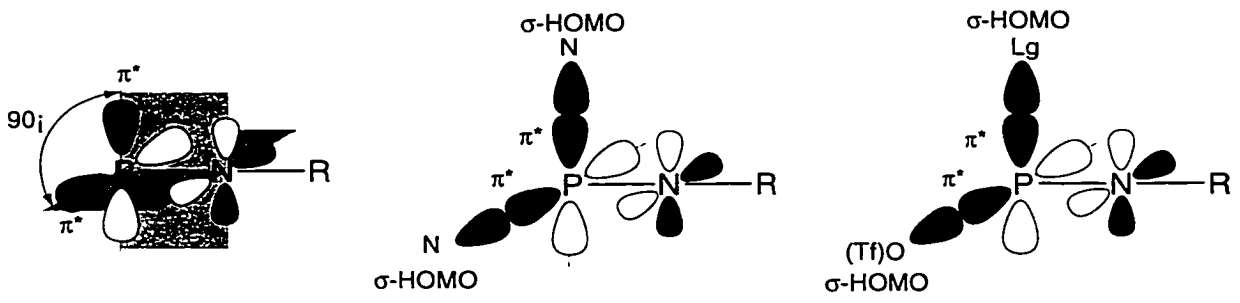

Figure 6.2: Bonding models for the phosphadiazonium cation and phosphadiazonium-ligand complexes. The LUMO of the phosphadiazonium cation (left) is composed of a doubly degenerate set of π*-MOs, which are orthogonal. The ligands, with σ-type HOMOs, interact with the π*-LUMO of the phosphadiazonium cation (middle and right).

The observation of a phosphorus-triflate interaction in [Mes*NP•Lg^A]OTf-type complexes where Lg^A = PPh_3, Py, Qncd, OIm, or Im, suggests that the highest concentration of positive charge is situated on the phosphorus centre, which is similar to the charge distribution in phosphenium cations as shown by ab initio calculations.[76] In contrast, the [Mes*NP•Lg^B]OTf-type complexes where Lg^B = $OPPh_3$ **5.4** (Ch = O), SIm

5.4 (Ch = S), or SeIm **5.4** (Ch = Se), are postulated to have a more even charge distribution over the entire phosphadiazonium-ligand unit Mes*NP•Lg^{+}.

The [Mes*NP•Lg^{B}]OTf complexes (Lg^{B} = SIm or SeIm) are unusual in that they feature a deshielded phosphorus nucleus despite having a Mes*NP unit which has a short P–N(Mes*) bond and a large (Mes*)C-N-P bond angle. This suggests that the structural features of the Mes*NP unit in the [Mes*NP•Lg]OTf are not correlated with shielding of the phosphorus nucleus, and that other factors, such the energy difference between the HOMO and LUMO, are involved. Solid-state ^{31}P NMR experiments on these complexes would be instructive. Solution ^{31}P NMR spectroscopy cannot reliably distinguish between the two types of [Mes*NP•Lg]OTf complexes. However, solid-state ^{31}P NMR spectra may provide insights into the molecular structure of phosphadiazonium-ligand complexes that cannot be structurally characterized using crystallography.

Table 6.1: Comparison of bond lengths and angles of the Mes*NP fragment in the phosphadiazonium-ligand-triflate complexes [Mes*NP•Lg]OTf, and Mes*NPOTf. Compounds are listed by increasing *d*(P–N) values.

Complex	*d*(P–N) (Å)	*d*(N–C(Mes*)) (Å)	*d*(P–Lg) (Å)	∠((Mes*)C-N-P) (°)	∠(N-P-Lg) (°)	*d*(P–O(Tf)) (Å)	∠(N-P-O(Tf)) (°)	C(Mes*)-N-P-Lg (°)
Mes*NP•OTf[a]	1.467(4)	1.398(5)		176.4(3)	–	1.923(3)	121.9(2)	–
[Mes*NP•Py]OTf[b] (**2.7**)	1.472(8)	1.42(1)	1.958(8)	161.7(7)	107.8(4)	2.712(7) 3.064(7)	113.6(2) 128.8(2)	-12(2)
[Mes*NP•PPh_3]OTf[c] (**1.44**)	1.486(4)	1.404(6)	2.625(2)	169.5(4)	109.8(2)	2.298(4)	111.1(2)	9.9(5)
[Mes*NP•OIm]OTf (**5.3** Ch = O)	1.494(4)	1.404(5)	1.773(3)	159.7(3)	107.5(2)	2.774(4)	85(1)	-5(1)
[Mes*NP•Dipy]OTf[d] (**2.9**)	1.497(4)	1.401(6)	2.065(4) 2.066(4)	169.4(4)	106.3(2) 113.0(2)	–	–	-28.2(2) -108.6(2)
[Mes*NP•SIm]OTf (**5.3** Ch = S)	1.498(2)	1.382(3)	2.266(1)	174.4(2)	114.1(1)	–	–	-148(2)
[Mes*NP•$OPPh_3$]OTf[c] (**5.4** Ch = O)	1.498(7) 1.504(7)	1.396(7)	1.734(6) 1.746(6)	165.9(5) 170.5(6)	108.4(4) 107.0(6)	–	–	-116(2) 124(3)
[Mes*NP•SeIm]OTf (**5.3** Ch = Se)	1.500(2)	1.381(3)	2.407(1)	175.5(2)	115.4(1)	–	–	148(3)
[Mes*NP•Qncd]OTf[d] (**2.8**)	1.519(2)	1.415(3)	1.933(2)	143.9(2)	103.7(1)	2.697(3)	112.5(1)	-175.7(3)
[Mes*NP•Im]OTf[c] (**3.14**)	1.574(4)	1.442(6)	1.852(5)	116.2(3)	103.2(2)	2.952(5)	123.0(2)	-170.1(3)

([a]) Reproduced from reference 130. ([b]) Reproduced from reference 215. ([c]) Reproduced from reference 25. ([d]) Reproduced from reference 216. ([e]) Second set of values resulting from disorder.

Table 6.2: Comparison of relevant bond lengths and angles of the Mes*NP unit in iminophosphines Mes*NPR, complexes containing the phosphadiazonium cation Mes*NP$^+$, and 1,3,5-triaza-2,4-diphospha-1,4-pentadienes (Mes*NP)$_2$NR. Compounds are listed in order of increasing *d*(P–N(Mes*)).

Compound	*d*(P–N) (Å)	*d*(N–C) (Å)	∠(C-N-P) (°)	∠(N-P-(Lg/R)) (°)	(Mes*)C-P-N-(Lg/R) (°)	Ref.
[Mes*NP•C_6H_6]Ga_2Cl_7	1.463(5)	1.396(7)	178.5(4)	–	–	93
[Mes*NP•C_6H_5Me]Ga_2Cl_7	1.464(9)	1.39(1)	178.7(8)	–	–	93
Mes*NPOTf	1.467(4)	1.398(5)	176.4(3)	108.4(2)	158.4†	130
[Mes*NP•C_6H_3(Me)$_3$-1,3,5]Ga_2Cl_7	1.471(6)	1.395(8)	175.7(5)	–	–	93
[Mes*NP•Py]OTf (2.7)	1.472(8)	1.42(1)	161.7(7)	107.8(4)	-12(2)	215
[Mes*NP•C_6H_5Me]$AlCl_4$	1.475(8)	1.41(1)	177.0(7)	–	–	123
Mes*NPI	1.479(7)	1.40(1)	171.8(8)	118.4(3)	130(3)	444
Mes*NPI	1.480(3)	–	172.5(3)	118.0(1)	-140(2)	102
[Mes*NP•C_6H_6]$GaCl_4$	1.484(7)	1.39(1)	175.5(7)	–	–	93
[Mes*NP•PPh_3]OTf (1.44)	1.486(4)	1.404(6)	169.5(4)	109.8(2)	9.9(5)	25
Mes*NPOC^{t}Bu$_3$	1.487(5)	1.403(6)	175.3(4)	135.2(3)	12.9†	130
[Mes*NP]S_2P(^{t}Bu)$_2$	1.487(3)	139.3(5)	169.7(3)	111.7(2)	-10†	387
				122.5(2)		
[Mes*NP]Se_2P(^{t}Bu)$_2$	1.49(1)	1.40(2)	169(1)	112.6(6)	-23.6(6)	138
Mes*NPOCH$_2$^{t}Bu$_2$	1.492(4)	1.400(7)	179.2(4)	109.3(2)	0.0†	130
Mes*NPOSO$_2$$C_6H_4$Me-4	1.492(4)	1.414(6)	150.1(3)	107.2(2)	-2.9†	130
				119.6(5)	-115.2(6)	
[Mes*NP•OIm]OTf (5.3 Ch = O)	1.494(4)	1.404(5)	159.7(3)	107.5(2)	-5(1)	This work
Mes*NPCl	1.495(4)	1.402(6)	154.8(4)	112.4(2)	0[a]	123
Mes*NPOC$_6$$H_4$Me-2	1.497(2)	1.401(2)	164.1(1)	116.6(1)	-86.3(8)	129
[Mes*NP•Dipy]OTf (2.9)	1.497(4)	1.401(6)	169.4(4)	106.3(2)	-28.2(2)	216
				113.0(2)	-108.6(2)	
[Mes*NP•$OPPh_3$]OTf[b] (5.4 Ch = O)	1.497(7)	1.396(7)	165.9(6)	108.4(4)	-116(2)	This work
	1.504(7)		170.0(6)	107.5(4)	124(3)	
[Mes*NP•SIm]OTf (5.3 Ch = S)	1.498(2)	1.382(3)	174.4(2)	114.2(1)	-148(2)	This work
Mes*NPBr	1.498(4)	1.400(5)	159.5(4)	113.6(2)	0[a]	124
[Mes*NP•SeIm]OTf (5.3 Ch = Se)	1.500(2)	1.381(3)	175.5(2)	115.4(1)	148(3)	This work
Mes*NPOC$_6$$H_2(^{t}Bu)_2$-2,6,Me-4	1.500(1)	1.395(2)	173.7(1)	117.4(1)	86.3(8)	417
Mes*NPOMent	1.505(4)	1.403(6)	155.2(3)	113.1(2)	1.8(9)	139
(Mes*NP)$_2$N(Ad)	1.509(4)	1.405(7)	147.5(4)	116.6(2)	–	112
	1.543(4)	1.432(6)	129.2(3)	115.1(2)	–	
Mes*NPCl	1.509(2)	1.423(4)	146.5(2)	111.4(1)	-1.3(8)	153
[Mes*NP•Qncd]OTf (2.8)	1.519(2)	1.415(3)	143.9(2)	103.7(1)	-175.7(3)	216
Mes*NPOCH(CF$_3$)$_2$	1.526(4)	1.419(6)	128.8(4)	106.3(2)	0[a]	141
(Mes*NP)$_2$N(^{t}Bu)	1.526(3)	1.411(4)	130.3(3)	105.8(2)	–	112
	1.531(3)	1.417(5)	124.4(2)	109.0(2)	–	
(Mes*NP)$_2$N^{t}Bu	1.527(5)	1.428(6)	125.8(3)	109.4(2)	–	111
	1.529(4)	1.440(6)	120.3(3)	109.4(2)		
Mes*NPO^{t}Bu	1.528(2)	–	144.7(2)	110.0(2)	0[a]	416
Mes*NPOSiMe$_3$	1.529(3)	1.405(3)	144.4(2)	115.8(2)	-1.3†	130
[Mes*NP•C_6H_5Me]$GaCl_4$	1.53(2)	1.39(2)	177(1)	–	–	93
Mes*NPN(Mes*)PMeSi(SiMe$_3$)$_2$	1.537(3)	1.458(5)	152.3(4)	111.2(2)	-153.6(4)	147
Mes*NPN(Mes*)P(NCPh$_2$)$_2$	1.539(6)	1.437(8)	135.2(5)	107.4(3)	178.6(6)	147
Mes*NPNMe$_2$	1.539(3)	1.418(4)	140.7(4)	115.9(3)	-4.9(7)	242

Compound	*d*(P–N) (Å)	*d*(N–C) (Å)	∠(C-N-P) (°)	∠(N-P-(Lg/R)) (°)	(Mes*)C-P-N-(Lg/R) (°)	Ref.
Mes*NPN(H)^{t}Bu	1.545(6)	1.436(8)	128.0(4)	110.4(3)	0[a]	112
Mes*NPNFln	1.547(3)	1.415(5)	137.2(2)	114.6(2)	1.8(4)	144
Mes*NPN(H)CPh$_3$	1.548(4)	1.427(6)	127.2(4)	–	–	112
Mes*NPNPH(N^{i}Pr$_2$)$_2$	1.548(3)	1.415(5)	129.8(3)	112.7(2)	–	110
Mes*NPS^{t}Bu	1.549(2)	1.420(2)	131.3(2)	109.0(1)	1.5(2)	108
Mes*NPCp*	1.551(8)	1.43(1)	125.9(6)	106.0(4)	178.7(7)	135
Mes*NPS^{t}Bu[b]	1.552(3)	1.421(4)	131.8(2)	109.1(1)	0[a]	418
(Mes*NP)$_2$NMes	1.554(6)	1.406(8)	122.5(5)	104.8(3)	–	112
	1.537(7)	1.44(1)	121.4(4)	114.7(3)	–	
Mes*NPNC^{t}Bu$_2$	1.555(3)	1.421(4)	123.4(2)	107.3(1)	-175.6(3)	144
Mes*NPN^{i}Pr$_2$	1.555(2)	1.404(3)	129.6(2)	105.6(1)	179.9(3)	242
Mes*NPN(SiMe$_3$)N(SiMe$_3$)$_2$	1.559(4)	1.445(5)	115.3(3)	107.3(2)	–	245
Mes*NPFeCp*(CO)$_2$	1.56(1)	1.408(7)	119.8(9)	115.4(5)	0[a]	140
[Mes*NPNPN(Cy)$_2$]$_2$	1.562(2)	1.423(3)	118.6(2)	107.1(1)	–	110
Mes*NPNPPh$_3$	1.563(1)	1.413(2)	132.9(1)	112.4(1)	3.4(2)	148
Mes*NPCEt$_3$	1.566(2)	1.425(3)	124.8(2)	104.7(1)	177.9(2)	136
Mes*NPN(SiMe$_3$)$_2$	1.566(2)	1.429(2)	117.6(1)	109.3(1)	177.6(2)	244
Mes*NPC(SiMe$_3$)$_3$	1.566(3)	1.429(4)	120.2(2)	110.4(2)	178.7(2)	281
Mes*NPP^{t}Bu$_2$	1.570(2)	1.427(2)	120.2(1)	106.0(1)	165.1(2)	171
Mes*NPN(H)Mes*	1.573(8)	1.48(1)	126.1(7)	103.8(5)	–	240
[Mes*NP•Im]OTf (**3.14**)	1.574(4)	1.442(6)	116.2(3)	103.2(2)	-170.1(3)	215
Mes*NPSi(OTf)Im (**4.7** X =OTf)	1.578(3)	1.428(4)	119.4(2)	100.3(1)	-167.2(2)	This work
Mes*NPTMP	1.579(1)	1.402(2)	129.4(1)	105.0(2)	-179.1(2)	241
Mes*NPN(H)Mes*	1.584(2)	1.426(2)	126.6(1)	104.0(1)	-176.3(2)	241
Mes*NP(Cl)•Im (**3.15**)	1.585(5)	1.446(7)	120.2(4)	101.9(2)	-162.0(4)	215
[Li•OEt$_2$]Mes*NPPh$_2$	1.661(2)	1.442(3)	114.6(2)	111.5(1)	114.0(2)	282
				104.8(1)	-146.2(2)	
Mes*N(H)PPh$_2$	1.730(2)	1.431(3)	99.7(1)	99.7(1)	175.7(2)	282
				102.1(1)	-80.0(2)	

([a]) Co-planar through symmetry. ([b]) Crystallized in a different space group.

Table 6.3: Comparison of S–O bond lengths in the phosphadiazonium-ligand-triflate complexes [Mes*NP•Lg]OTf with compounds that have a covalent bonded or anionic triflate group. The difference between the longest and shortest S–O bond is represented by Δd(S–O). All values in Å.

Compound	E	d(E–O(Tf))	d(S–O(E))	d(S–O)	Δd(S–O)	Reference
Mes*NPSi(OTf)DAB (**4.7**)	Si	1.772(2)	1.521(2)	1.409(3), 1.417(3)	0.112(4)	This work
Mes*NPOTf	P	1.923(3)	1.499(5)	1.405(4), 1.409(5)	0.094(6)	130
[Mes*NP•PPh_3]OTf (**1.44**)	P	2.298(4)	1.467(4)	1.427(5), 1.428(4)	0.040(6)	25
[Mes*NP•Qncd]OTf (**2.8**)	P	2.697(3)	1.414(3)	1.426(3), 1.432(3)	0.018(4)	216
[Mes*NP•Py]OTf (**2.7**)	P	2.712(7)[a]	1.433(7)	1.441(7), 1.441(7)	0.008(10)	215
[Mes*NP•OIm]OTf (**5.3**)	P	2.775(4)	1.417(4)	1.434(4), 1.437(4)	0.020(6)	This work
[Mes*NP•Im]OTf (**3.14**)	P	2.951(5)	1.440(4)	1.438(4), 1.438(4)	0.002(6)	215
[Mes*NP•Dipy]OTf (**2.9**)	N	3.208(6)	1.416(4)	1.421(4), 1.425(4)	0.009(6)	216
[Mes*NP•SIm]OTf (**5.3**)	N	3.360(3)	1.450(3)	1.422(2), 1.428(2)	0.028(4)	This work
[Mes*NP•SeIm]OTf (**5.3**)	N	3.428(4)	1.431(3)	1.426(3), 1.426(3)	0.005(4)	This work
[(^{n}Bu)$_4$N]OTf	–	–	1.437(4)	1.431(4), 1.433(4)	0.006(6)	445
$[H_9O_4]$OTf	H	2.502(2)	1.435(1)	1.447(1), 1.450(1)	0.015(1)	434

([a]) Shortest P–O(Tf) interaction.

Table 6.4: Comparison of stretching frequencies associated with the CF_3 and SO_3 groups of the triflate units in the [Mes*NP•Lg]OTf complexes and other compounds containing a triflate group. All values in cm^{-1}.

Compound	$\nu(SO_3(E))$[a]	$\nu(SO_3(A_1))$[a]	$\nu(CF_3\ (A_1))$[a]	$\nu(CF_3(E))$[a]	Reference
[Ag]OTf	1270	1043	1237	1167	435
Mes*NPSi(OTf)DAB (**4.7**)	1388	1097	1244	1149	This work
Mes*NPOTf	1261	1022	1235	1193	429
[Mes*NP•Qncd]OTf (**2.8**)	1278	1026	1241	1163	216
[Mes*NP•Im]OTf (**3.14**)	1280	1026	1246	1159	215
[Mes*NP•OIm]OTf (**5.3**)	1272	1028	1221	1153	This work
[Mes*NP•SIm]OTf (**5.3**)	1265	1030	1265	1149	This work
[Mes*NP•SeIm]OTf (**5.3**)	1266	1031	1266	1147	This work
[Mes*NP•$OPPh_3$]OTf (**5.4**)	1266	1031	1266	1150	This work
[Mes*NP•Dipy]OTf (**2.9**)	1275	1031	1226	1160	216
[Mes*NP•Py]OTf (**2.7**)	1288	1024	1223	1161	215
[Mes*NP•PPh_3]OTf (**1.44**)	1260	1030	1231	1170	25

([a]) Vibrational mode assignments based on the assumption that the CF_3 and SO_3 groups have C_{3v} symmetry.

Table 6.5: Comparison of the Lg-P-O(Tf) bond angle and torsion angles in [Mes*NP•Lg]OTf and selected complexes featuring the phosphadiazonium cation Mes*NP. Angle ϕ represents the difference between the (Mes*)C-N-P-Lg and (Mes*)C-N-P-O(Tf) torsion angles (or the difference between both (Mes*)C-N-P-Lg torsion angle in complexes with dual ligand- or anion-phosphorus interactions). All values in degrees.

Compound	∠(Lg-P-O(Tf)) ∠(Lg-P-Lg)	C-N-P-Lg	C-N-P-O(Tf) (C-N-P-Lg)	ϕ	Reference
[Mes*NP•OIm]OTf (**5.3**)	80.6(1)	-5(1)	-85(1)	90(1)	This work
[Mes*NP•PPh_3]OTf (**1.44**)	85.0(4)	9.9(3)	102(4)	92(5)	25
[Mes*NP•Py]OTf[a] (**2.7**)	85.8(2)	-12(2)	105.5(2)	93.5(3)	215
[Mes*NP•Qncd]OTf (**2.8**)	86.1(1)	-175.7(3)	92.9(3)	91.4(4)	216
[Mes*NP•Im]OTf (**3.14**)	72.1(2)	-170.1(3)	112.8(3)	77.1(4)	215
[Mes*NP•Dipy]OTf (**2.9**)	75.1(2)	-108.6(2)	-28.2(2)	80.4(3)	216
Mes*NPI	88.1(1)	130(3)	-30(4)	100(5)	444
[Mes*NP]$S_2P(^tBu)_2$	77.4(1)	-10†	-99†	-89	387
[Mes*NP]$Se_2P(^tBu)_2$	80.6(1)	-115.2(6)	-23.6(6)	91.6(8)	138

([a]) Value from shortest P–O(Tf) interaction.

Table 6.6: Comparison of solution $\delta(^{31}P)$ values for the phosphadiazonium-ligand-triflate complexes [Mes*NP•Lg]OTf with those observed for [Mes*NP•Lg]ECl_4 (E = Al or Ga; Lg = Arene, PPh_3, or Im) and complexes featuring the phosphadiazonium cation. Unless otherwise indicated, the values were obtained from spectra where the compound was redissolved in d_2-dichloromethane at 25 °C. Compounds are listed in increasing δ values. All values in ppm.

Compound	$\delta(^{31}P)$	Reference
[Mes*NP•Dipy]OTf (**2.9**)	54	216
Mes*NPOTf	55	130
[Mes*NP•$OPPh_3$]OTf (**5.4** Ch = O)	60	This work
[Mes*NP•Py]OTf	71	215
[Mes*NP]$GaCl_4$	76	93
[Mes*NP•C_6H_6]$GaCl_4$	76	93
[Mes*NP•MeC_6H_5]$GaCl_4$	76	93
[Mes*NP]((Ar)$AlCl_3$)	77	33
[Mes*NP•OIm]OTf (**5.3** Ch = O)	77	This work
[Mes*NP•$SPPh_3$]OTf (**5.4** Ch = O)	79	This work
[Mes*NP•MeC_6H_5]$AlCl_4$	79	123
[Mes*NP•PPh_3]((Ar)$AlCl_3$)[b]	84	33
[Mes*NP•PPh_3]$AlCl_4$[b]	87	38
[Mes*NP•$Me_3C_6H_3$]Ga_2Cl_7	91	93
[Mes*NP]$Se_2P(^tBu)_2$[a]	92	138
[Mes*NP•C_6H_6]Ga_2Cl_7	93	93
[Mes*NP•MeC_6H_5]Ga_2Cl_7	95	93
[Mes*NP]$Se_2P(^tBu)_2$[a,c]	116	138
[Mes*NP•Qncd]OTf (**2.8**)	144	216
[Mes*NP•SIm]OTf (**5.3** Ch = S)	148	This work
[Mes*NP•SeIm]OTf (**5.3** Ch = Se)	178	This work
[Mes*NP•Im]$AlCl_4$ (**3.17**)	331	This work
[Mes*NP•Im]OTf (**3.14**)	339	215

Ar = $C_6H_2(^tBu)_2$-2,6-Me-4. ([a]) Compound redissolved in C_6D_6. ([b]) Complex decomposes at higher temperature. ([c]) Value obtained from spectra collected at -80 °C.

Table 6.7: Comparison of principal components of the ^{31}P chemical shift tensor for phosphadiazonium-ligand-triflate complexes [Mes*NP•Lg]OTf with iminophosphines Mes*NPR, as determined by solid-state NMR spectroscopy. $\Delta\delta$ Represents the difference in chemical shift value between the complex and that reported for Mes*NPOTf. All values in ppm.

Compound	δ_{iso}	δ_{soln}	δ_{11}	$\Delta\delta_{11}$	δ_{22}	$\Delta\delta_{22}$	δ_{33}	$\Delta\delta_{33}$	Reference
Mes*NPOTf	53	55	235	–	199	–	-276	–	232
[Mes*NP•Dipy]OTf (**2.9**)	65	54	250	+15	196	-3	-251	+25	This work
[Mes*NP•Py]OTf (**2.7**)	67	71	338	+103	146	-53	-282	-6	This work
[Mes*NP•PPh_3]OTf (**1.44**)	71	–	307	+72	174	-25	-269	+7	172,25
[Mes*NP•Im]OTf (**3.14**)	366	339	915	+680	128	-71	55	-221	This work
Mes*NPCl	146	135	45		129		-140		255
Mes*NPBr	400	140	400		125		-104		255
Mes*NPI	100	218	276		192		-167		255
Mes*NP(^{t}Bu)	487	482	1035		297		130		255
Mes*NPN(H)Mes*	281	272	628		124		90		255

Table 6.8: Comparison of $^2J(^{31}P,^{13}C)$ and $^5J(^{31}P,^1H)$ coupling constants for the Mes* substituent with the (Mes*)C-N-P bond angle in the phosphadiazonium-ligand-triflate complexes [Mes*NP•Lg]OTf. Compounds are listed by decreasing (Mes*)N-C-P bond angles.

Compound	$^2J(^{31}P,^{13}C)$ (Hz)	$^5J(^{31}P,^1H)$ (Hz)	∠((Mes*)C-N-P) (°)
Mes*NPOTf[a]	44.6	1.2	176.4(3)
[Mes*NP•$SPPh_3$]OTf (**5.4** Ch = S)	43.4	1.8	([h])
[Mes*NP•$OPPh_3$]OTf (**5.4** Ch = O)	40.1	1.5	176.1(4)
[Mes*NP•SeIm]OTf (**5.3** Ch = Se)	32.5	1.5	175.5(2)
[Mes*NP•SIm]OTf (**5.3** Ch = S)	41.5	1.5	174.4(2)
[Mes*NP•Dipy]OTf[c] (**2.9**)	46.7	1.8	169.4(4)
[Mes*NP•Py]OTf[d] (**2.7**)	39.1	1.8	161.7(7)
[Mes*NP•OIm]OTf (**5.3** Ch = O)	39.0	1.2	159.4(3)
[Mes*NP•Qncd]OTf[c] (**2.8**)	26.2	1.5	143.9(2)
[Mes*NP•Im]OTf[d] (**3.14**)	11.5	0.8	116.2(3)

([a]) Reproduced from reference 130. ([h]) Crystal structure could not be obtained.
([c]) Reproduced from reference 216. ([d]) Reproduced from reference 215.

Table 6.9: Comparison of ligand basicity, as inferred from pK_a of the conjugate acid, with structural parameters and $\delta(^{31}P)$ values in the phosphadiazonium-ligand-triflate complexes [Mes*NP•Lg]OTf, where the d(P–O(Tf)) value is less than 3.30 Å. Compounds are listed by increasing pK_a.

[Mes*NP•Lg]OTf Lg =	pK_a (DMSO)	d(P–N(Mes*)) (Å)	d(P–O(Tf)) (Å)	∠((Mes*)C-N-P) (°)	$\delta(^{31}P)$ (ppm)	Reference
PPh_3 (**1.44**)	2.7[a]	1.486(4)	2.298(4)	169.5(4)	([b])	25, 96
Py (**2.7**)	5.8	1.472(8)	2.712(7)[c]	161.7(7)	71	215 ,219
Qncd (**2.8**)	9.8	1.519(2)	2.697(3)	143.9(2)	144	216 ,218
Im (**3.14**)	24	1.574(4)	2.952(5)	116.2(3)	338	215, 270

([a]) Measured in ethanol-acetone solution. ([b]) Complex not formed in solution. ([c]) Value from shortest P–O(Tf) interaction.

Chapter 7: Conclusions and Proposals for Future Work

7.1: Summary and Conclusions

From the first isolations of complexes featuring a phosphadiazonium cation Mes*NP$^+$, this molecular unit has shown an ability to form Lewis acid-base complexes (i.e., π-type complexes with arenes[93,94] and a σ-type complex with triphenylphosphine).[25,33,38] The new [Mes*NP•Lg]OTf complexes (Lg = Py **2.7**, Qncd **2.8**, Dipy **2.9**, Im **3.14**, OIm **5.3** (Ch = O), SIm **5.3** (Ch = S), SeIm **5.3** (Ch = Se), $OPPh_3$ **5.4** (Ch = O), and $SPPh_3$ **5.4** (Ch = S)) reported in thesis represent further exploration into the coordination chemistry of the phosphadiazonium cation Mes*NP$^+$, as an Lewis acid. This investigation was extended to include iminophosphines such as Mes*NPCl and Mes*NPPh, which have also been shown to be Lewis acids. Furthermore, it can be concluded that iminophosphines are amphoteric, that is, they are capable of behaving as Lewis acids or Lewis bases under appropriate conditions. Importantly, the synthesis of phosphadiazonium-, and iminophosphine-ligand complexes establishes coordination chemistry as a viable and direct method for the creation of phosphorus-element bonds and new bonding environments for phosphorus.

The phosphadiazonium-ligand-triflate complexes [Mes*NP•Lg]OTf represent a new form of π-phosphino-bonding environment, which are precluded from classification as either iminophosphines or phosphenium cations. However, they possess characteristics of both (i.e., the cation-anion ionic relationship found in phosphenium salts and the same Mes*NP unit found in iminophosphines). The coordination of a Lewis base to the Mes*NP unit in the [Mes*NP•Lg]OTf complexes causes similar structural and spectroscopic changes as observed in different *P*-substituted iminophosphines. The ligands in this study represented a cross-section of available main-group Lewis bases, each with varying degrees of basicities and polarizabilities. The formation of stable

complexes with a wide range of ligand types demonstrates the versatile coordination nature of the phosphadiazonium cation Mes*NP$^+$. The observed structure of [Mes*NP•Dipy]OTf **2.9** proves conclusively that the phosphadiazonium cation can interact with a single ligand feature multiple donor sites. Diverse coordination behaviour is known for pentasubstituted phosphoranes, such as PF_5, but is not yet fully demonstrated for any other type of π-phosphino-bonding environment, except for now, the phosphadiazonium cation Mes*NP$^+$.

Finally, the research presented in this thesis has contributed to a growing body of experimental evidence, which shows that a phosphorus centre with a pair of non-bonding valence electrons, a phosphino-bonding environment, can behave as a Lewis acid. Lewis acidity has traditionally been associated with transition metals and heavier main-group elements. However, isolation of [Mes*NP•Lg]OTf and related complexes (e.g., Mes*NP(Cl)•Im **3.14**) help to bridge and extend concepts regarding the Lewis acidic aspects of coordination to phosphorus. For example, complexes such as [Mes*NP•Dipy]OTf **2.9**, can be envisaged as an all main-group analogue of alkylidenes (e.g., **7.1**),[446] and imido-substituted transition metal complexes (e.g., **7.2**).[447]

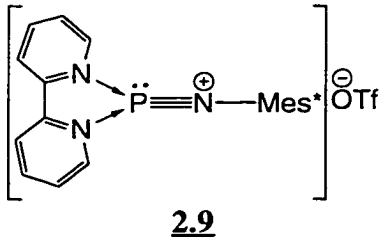

2.9

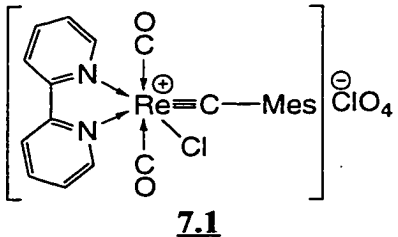

7.1

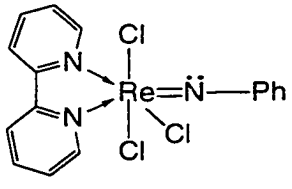

7.2

7.2: Possible Avenues of Exploration Regarding the Chemistry of Iminophosphines, the Phosphadiazonium Cation, and other types of π-Phosphino-compounds

The coordination behaviour of Mes*NPOTf as a Lewis acid, should be further exploited in the isolation of [Mes*NP•Lg_n]OTf complexes with multiple monodentate ligands ($n > 1$). For example, the isolation of [Mes*NP•$(Py)_2$]OTf would serve as a useful comparison with [Mes*NP•Dipy]OTf **2.9**, in terms of spectroscopy, structural features, and chemical reactivity. In particular, to determine if [Mes*NP•Dipy]OTf **2.9** has greater stability as compared with [Mes*NP•$(Py)_2$]OTf as postulated by the chelate effect. Other complexes involving the phosphadiazonium cation may be isolated using chelating ligands such as β-diketonate, chalcogenocarbamates Ch_2CNMe_2 (Ch = O, S and Se), or the other types of bi- or poly-functional molecules listed in reference 448. These compounds could conceivably be formulated as complexes containing a phosphadiazonium cation $Mes*NP^+$, coordinated by a chelating ligand **7.3** (R = Me), or iminophosphines featuring intramolecular coordination **7.4** (R = Me). Moreover, it would be interesting to determine if the preference for either **7.3** or **7.4** could be switched by altering the functional groups on the ligand. For example, using a β-diketonate ligand that has electron-withdrawing (e.g., **7.3**-**7.4** R = CF_3) or electron-donating (e.g., **7.3**-**7.4** R = NMe_2) groups. For β-diketonate-type ligands, there is a third possibility where attachment to the phosphorus centre occurs through the β-carbon position, as is occasionally observed in transition metal complexes.

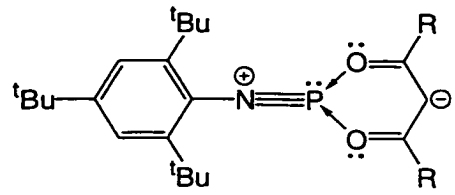

7.3

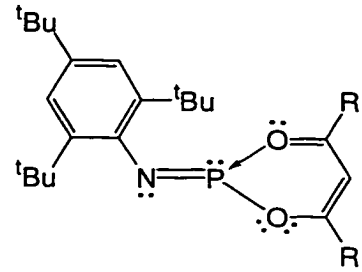

7.4

To assess the maximum coordination limit of the phosphadiazonium cation, multidentate ligands such as 2,2',6',2''-terpyridyl, phorphyrins, phthalocyanins, 2,2-diphosphinines, cryptans, oxo-, or thio-crown-ethers should be reacted with Mes*NPOTf. Diazonium-crown-ether complexes have been isolated and characterized through crystallography.[449,450] Hence, analogous crown-ether complexes involving the phosphadiazonium cation should also be possible.

Compounds such as triphenylarsine, triphenylstibine, and benzophenone are weakly basic ligands, showing no evidence of complex formation upon addition to solutions containing Mes*NPOTf. Forming [Mes*NP•Lg]OTf adducts with these types of ligands and weak Lewis bases in general, would require increasing the Lewis acidity of the phosphadiazonium cation. This might be accomplished through the attachment of an electron-withdrawing *N*-substituent in place of Mes*, provided that the substituent has adequate steric bulk to prevent dimerization of the RNP^+ unit. However, an alternative method involves the use of anions that are less basic than triflate, such as tetrakispentafluorophenylborate $B(C_6F_5)_4^-$. This synthetic methodology is analogous to the preparation of strongly Lewis acidic organometallic cations using weakly coordinating anions.[51,451]

There is preliminary evidence to suggest that iminophosphines, such as Mes*NPPh, have Lewis acidic properties and form iminophosphide complexes, but only

with highly Lewis basic ligands such as imidazol-2-ylidenes. In order to further investigate the coordination chemistry of iminophosphines as Lewis acids, compounds with greater Lewis acidity are required. Such an iminophosphine Mes*NPR could be prepared through the attachment of a strongly electron-withdrawing *P*-substituent (e.g., R = CF_3, $CH(CF_3)_2$, or FMes). An iminophosphine **7.5** with electron-withdrawing substituents attached to both the phosphorus and nitrogen centres has been previously reported.[107] These substituents offer the additional advantage that the phosphorus-carbon bond is more resistant towards cleavage than iminophosphines containing P–X (X = halogen) or P–O(R) bonds, where R is an alkyl, aryl, or organosulphonyl group.

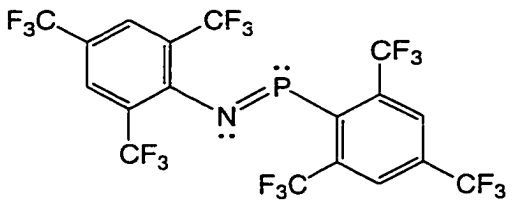

7.5

The strength of the ligand-phosphorus interaction in [Mes*NP•Lg]OTf has been related with structural changes in the phosphadiazonium unit. However, another method of evaluating this interaction involves performing a series of ligand substitution reactions. The series of ligands should be chosen such that various steric and basicity properties can be tested. For example, the basicity constants and steric parameters of a wide range of tertiary alkyl and aryl phosphine have been determined.[66] Ligand exchange could be monitored by changes to the $\delta(^{31}P)$ values and compared with those of previously isolated complexes. There is also the possibility that mixed bis- or poly-coordinated phosphadiazonium-ligand-triflate complexes could be isolated.

The phosphadiazonium-ligand-triflate complexes have potential as precursors for the syntheses of new types of phosphorus bonding environments. A number of iminophosphines, including Mes*NPCl and Mes*NPPh, are ligands with respect to transition metal centres. It is reasonable to expect that the basicity of the [Mes*NP•Lg]OTf and Mes*NP(R)•Lg complexes is greater than that of the parent compounds Mes*NPOTf and Mes*NPR. Hence, these complexes may have potential application as ligands. For example, the recently isolated phosphenium-imidazol-2-ylidene complex $[Ph_2P•Im]AlCl_4$,[48] has been shown to coordinate to both Pd and Pt centres.[275] The resulting complexes would represent examples of in-series coordination complexes **7.6** and **7.7**. Through the attachment of different ligands to the phosphorus centre of phosphadiazonium cations or iminophosphines, it may be possible to change or "tune" the donor properties of the resulting complexes for use with specific Lewis acids, in the same way that phosphines with different Lewis basicity are used to alter the catalytic reactivity of transition metals centres.[452] The [Mes*NP•Lg]OTf and Mes*NP(R)•Lg complexes offer one advantage over $[Ph_2P•Im]AlCl_4$ as ligands, in that the former compounds have a P–N π-bond. With phosphadiazonium- or iminophosphine-ligand complexes, there is the potential for 1,3-migration of a hydrogen or a trimethylsilyl group from the transition metal centre, and hence forming a phosphorus-metal π-bond. This method would provide a facile route, via coordination, for the synthesis of complexes with phosphorus-metal π-bonding, which at present requires a one or two step process with some form of abstraction and by-product removal.

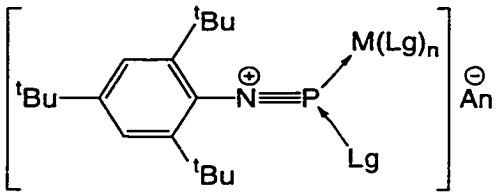

7.6

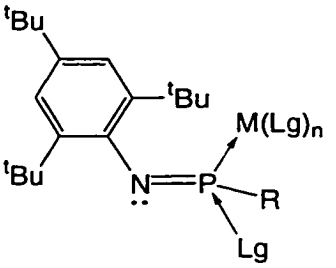

7.7

The phosphadiazonium cation Mes*NP$^+$, has shown the ability to be coordinated by a variety of different ligands. However, assessment of its Lewis acidity with other types of π-phosphino-bonding environments would provide insights into the molecular bonding of these compounds. Already, triphenylphosphine complexes involving the methylenediylphosphenium $(Me_3Si)_2CP^+$, and the diphosphonium Mes*PP$^+$, cation are known.[92,453] One advantage of studying the coordination chemistry of the phosphadiazonium cation is the facile preparation and stability of Mes*NPOTf. However, the analogous precursors of other π-phosphino-bonding environments (e.g., Mes*PPOTf and $(Me_3Si)_2CPOTf$) are unknown or too highly reactive for manipulation. Nevertheless, donor-stabilized complexes have been prepared. Through ligand exchange reactions, new complexes could be isolated, characterized and compared with the corresponding phosphadiazonium-ligand complex. For example, [Mes*PP•P$(NMe_2)_3$]BPh_4 was prepared by displacement of the triphenylphosphine ligand from [Mes*PP•PPh_3]BPh_4 using P$(NMe_2)_3$.[453]

Clearly, these possible avenues of study represent only a minor fraction of the potentially rich and diverse chemistry of the phosphadiazonium cation, iminophosphines, and their related coordination complexes.

Chapter 8: Experimental Procedures

8.1: Techniques for the Handling of Air and Moisture Sensitive Substances

Synthesis, manipulation and storage of the compounds described in this thesis were performed using an inert gas atmosphere (N_2 or Ar) or in a reduced pressure environment, unless otherwise indicated. Schlenk techniques were primarily used in the synthesis of starting materials and in sample recrystallization. Specific descriptions of Schlenk equipment and techniques are documented in references 454-456. Reactions performed in reduced pressure environments required specialized glassware with design specifications and handling procedures, which have been previously described.[152,457] Solvents and liquid reagents were transferred by reduced pressure distillation, or in the case of low volatility solvents, b.p. greater than 150 °C at 1 atm, performed using a needle and syringe. Solvent volumes are approximate. All glassware was flamed dried and cooled to room temperature under dynamic vacuum (10^{-3} torr) prior to use. Solids were manipulated in a glove box with a nitrogen atmosphere (Braun, O_2, $H_2O < 0.1$ ppm) and stored in sealed glass tubes. Reactive solid reagents such as 1,3-diisopropyl-4,5-dimethyl-imidazol-2-ylidene, were flame sealed in glass tubes under static vacuum and stored at -30 °C. Solvents were purified by standard distillation techniques[458] and were degassed using three freeze-pump-thaw cycles prior to use. Benzene and n-hexane were set to reflux over potassium, while toluene was dried using sodium. n-Pentane was dried by reflux over sodium-benzophenone with 5 % tetraethylene glycol dimethyl ether. Dichloromethane was distilled over calcium hydride, phosphorus oxide and again over calcium hydride. d_6-Benzene was dried over a 2:1 ratio of sodium-potassium alloy and d_2-dichloromethane was dried over calcium hydride. The following compounds were synthesized according to literature procedures; trifluoromethylsulfonyloxy-(2,4,6-tri-*tert*-butylphenylimino)phosphine[130] (Mes*NPOTf),

chloro-(2,4,6-tri-*tert*-butylphenylimino)phosphine[152] (Mes*NPCl), phenyl-(2,4,6-tri-*tert*-butylphenyl-imino)phosphine[106] (Mes*NPPh), 1,3-diisopropyl-4,5-dimethyl-imidazol-2-ylidene[266] (Im), 1,3-di-*tert*-butyl-2,3-dihydro-1*H*-1,3,2-diazolsilol-2-ylidene[318] (SiDAB), 1,3-diisopropyl-urea[459] ($(^{i}PrN(H))_2CO$), 1,3-diisopropyl-4,5-dimethylimidazole-2(3*H*)-thione[266] (SIm), 1,3-diisopropyl-4,5-dimethylimidazole-2(3*H*)-selenone[380] (SeIm), 1,3-diisopropyl-4,5-dimethylimidazole-2(3*H*)-tellurone[381] (TeIm). 2,2'-Dipyridyl (98 %, Aldrich), 3-hydroxy-2-butanone (Aldrich), aluminum trichloride (99.99 %, Aldrich), and 1-hexanol (Aldrich) were used as received. Pyridine (99 %, Aldrich) was purified by distillation from potassium hydroxide and subsequently set to reflux over calcium hydride. Triphenylphosphine oxide (Aldrich), and triphenylphosphine sulphide (Aldrich) were recrystallized from n-hexane. 1-Azabicyclo[2.2.2]-octane (Qncd) was obtained from the treatment of 1-azoniabicyclo[2.2.2]-octane chloride ([Qncd•H^+]Cl), (Aldrich) with an aqueous 1.0 M sodium hydroxide solution followed by extraction using diethyl ether. After removal of the solvent, the product was sublimed under static vacuum. The purity of all starting materials was accessed using NMR, IR spectroscopy, or gas-liquid chromatography.

Caution! The toxicity of the compounds described in this thesis are unknown. Therefore, all products should be treated as potentially toxic and carcinogenic. Extreme care should be employed at all times during handling. A brief survey of the hazards associated with phosphorus compounds is available.[61,460] The toxicity of the solvents and some of the starting materials has been documented.[461] Any glassware that retains a reduced pressure atmosphere may implode if damaged or improperly handled.

Samples for analysis by solution NMR spectroscopy were prepared in 5 mm or 10 mm (o.d.) flame-sealed Pyrex glass tubes. Chemical shifts are reported in ppm relative to a reference standard (100 % $(CH_3)_4Si$ (^1H, ^{13}C, ^{29}Si), 10 % CF_3Cl (^{19}F), $[Al(H_2O)_6]NO_3$ (^{27}Al), 85 % H_3PO_4 (^{31}P), 98 % H_2SeO_4 (^{77}Se)). Both ^1H and ^{13}C NMR spectra were calibrated to an internal reference signal (^1H: $CHDCl_2$, 5.32 ppm; C_6D_5H, 7.16 ppm. ^{13}C: CD_2Cl_2, 54.0 ppm; C_6D_6, 128.5 ppm). The multiplicity of the peak is reported after the chemical shift. Multiplicity labeled as "s" or "d" indicate singlets or doublets coupled with small intensity satellite peaks that arise from splitting with other spin $^1/_2$ nuclei in low natural abundance. Solution ^1H, ^{13}C, ^{19}F, and ^{31}P NMR spectra were collected on a Bruker AC-250 NMR spectrometer. 27-Al, ^{29}Si, and ^{77}Se NMR spectra were recorded on a Bruker AMX-400 NMR spectrometer by Dr. Michael D. Lumsden of the Atlantic Regional Magnetic Resonance Centre, Department of Chemistry, Dalhousie University, Halifax, NS. Unless otherwise indicated, all solution NMR spectra were obtained at 25 °C using CD_2Cl_2 as the solvent. Coupling constants from second order ^1H NMR spectra ([Mes*NP•Py]OTf **2.7**) were obtained through iteration using the gNMR software package[462] and assistance from Dr. Bruce T. Grindley, Department of Chemistry, Dalhousie University, NS. Solid state NMR spectra were acquired using a Chemagnetics CMX Infinity spectrometer or a Bruker MSL 200 spectrometer, both instruments have a field strength of 4.7 T (200 MHz). Spectra collection and analysis were performed by Miss Myrlene Gee, Department of Chemistry, University of Alberta, AB. For measured samples, both stationary and magic-angle spinning (MAS) spectra were collected. MAS spectra were obtained using cross polarization between ^1H and ^{31}P nuclei under Hartmann-Hahn matching conditions. Solid state spectra were collected on powdered samples from ground crystalline solids packed into zirconium oxide rotors and fitted with Kel-F or Vespel caps (4 mm or 7 mm o.d.). The samples showed no evidence of

decomposition during the acquisition process. The ^{31}P chemical shift tensors (obtained from the first derivative of the line shape of the static spectra) are reported as three principal components (δ_{11}, δ_{22}, and δ_{33}) where δ_{11} and δ_{33} represents the most deshielded and shielded components respectively.[463] 31-P isotropic chemical shifts (δ_{iso}) obtained from CP/MAS spectra are also reported. All solid state NMR chemical shifts are reported in ppm and referenced with respect to 85 % H_3PO_4 by setting the isotropic peak of solid ammonium dihydrogen orthophosphate ($NH_4PH_2O_4$) to 0.81 ppm. Parameters from stationary spectra were obtained by simulation of actual spectra using the WSOLIDS program.[464]

Melting points were recorded using a Fisher-Johns apparatus and the reported values are uncorrected. Infrared spectra were collected on samples prepared as paraffin oil mulls on cesium iodide plates using a Nicolet 510P FT-IR spectrometer. Peaks from vibrational spectra are reported in wave numbers (cm^{-1}) followed by a ranked intensity in parentheses, where a value of one corresponds to the most intense peak in the spectrum. Elemental analyses were performed by Beller Laboratories in Göttingen, Germany. Samples for elemental analysis were dried under dynamic vacuum (4 to 6 hours) and sealed in glass tubes.

8.2: Crystallization Techniques and Crystal Mounting Details

The primary method of growing crystals for single crystal X-ray diffraction studies was slow liquid-liquid diffusion.[465] In a typical procedure, 30 to 50 mg of sample was placed in the bottom of a 150 mm (14 mm o.d.) glass tube which was sealed using a Teflon or glass stopcock. The crystallization vessel was evacuated and a small amount of solvent (2 to 4 mL) was added to completely dissolve the solid. A second solvent (60 to 100 mL) was slowly layered on top of the solution using a needle and syringe whilst

maintaining a flow of inert gas. The compound must be either insoluble or only slightly soluble in the second solvent and its density must be less than the first solvent. The apparatus was left undisturbed for several weeks at room temperature or at a lower temperature (0 °C or -30 °C) during which the solvents slowly diffuse together and crystals develop, usually at interface of the two solvents. After sufficient quantities of crystals were deposited, the solution was carefully removed using a needle and syringe. For crystals that rapidly lost solvent, the samples were coated with oil (perfluorpolyether 216 purchased from Riedel-de Haën) immediately after removal of the solution.

Alternatively, crystals were obtained by slow evaporation (1 to 3 days) of a solution composed of the compound dissolved in a mixture of two solvents. In a typical procedure, 50 to 100 mg of sample was placed in one compartment of a two-chamber reaction vessel and solvent (10 mL) was added to dissolve the solid. Subsequently, 15 to 20 mL of a solvent for which the compound is insoluble, was added to the solution. The empty chamber was placed under a stream of cold water or over a dewar filled with liquid nitrogen to affect the transfer of solvent. After a sufficient amount of crystals had been deposited, solvent evaporation was halted to ensure that 2 to 5 mL of the mother liquor was retained with the crystals. The mother liquor was decanted away from the crystals and discarded. The crystals were washed several times with a solvent, which does not dissolve the product. The reaction apparatus was positioned as to allow the solvent or solution to drain. Dynamic vacuum was not applied to samples for X-ray diffraction studies, as some crystals contained solvent molecules and when exposed to vacuum, dried and formed amorphous powders.

Two different mounting procedures were employed for single crystal X-ray diffraction studies. Crystals were placed inside capillaries (< 1.00 mm o.d.) and flame sealed. The capillary was then glued to a metal pin and mounted on a goniometer head.

Alternatively, for samples measured using diffractometers equipped with CCD detectors and low temperature setups, a single crystal was coated with oil and frozen (ca. -80 °C) to the end of a glass capillary and attached to a goniometer head. Single crystal X-ray diffraction studies were collected using several diffractometers: Rigaku AFC5R equipped with a rotating anode source (TSC), a Siemens P4 fitted with Bruker AXS SMART CCD detector (ALR), Bruker 1KCCD (HAJ) and Bruker P4/RA (P4 four-circle) equipped with a rotating anode generator and a SMART 1000 CCD detector (RM).

Unit cell determination and data collection on all structures were performed using graphite-monochromated radiation (diffractometer, radiation source and wavelength indicated in Tables 8.1 to 8.5). Data collection and structure solutions were performed by Dr. T. Stanley Cameron (DALX), Miss Katherine N. Robertson (DALX), Dr. Daren J. LeBlanc of the Department of Chemistry, Dalhousie University, Halifax, NS, Dr. Thomas E. Concolino, Dr. Kin-Chung Lam of the Department of Chemistry, University of Delaware, Newark, DE. and Dr. Robert Macdonald of the Department of Chemistry, University of Alberta, Edmonton, AB.

Crystallographic details not listed in thesis are available upon request from Dr. Neil Burford of the Department of Chemistry, Dalhousie University, Halifax, NS, Canada, B3H 4J3. E-mail: burford@is.dal.ca.

8.3: Specific Synthetic Procedures

The optimized reaction procedures and spectroscopic characterization data for the new compounds (**2.7**, **2.8**, **2.9**, **3.14**-**17**, **4.7**, **5.3**, and **5.4**) presented in this thesis are described in the following sections. Spectroscopic data for reaction mixtures, along with relevant synthetic details, if available, are also provided. For NMR spectra of reaction mixtures, the identity and relative amount of species is given in brackets after the $\delta(^{31}P)$

values. For compounds that have been characterized by single crystal X-ray diffraction studies, relevant crystallographic information is provided in Tables 8.1 to 8.5.

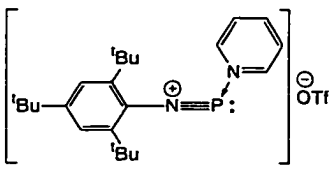

2.7

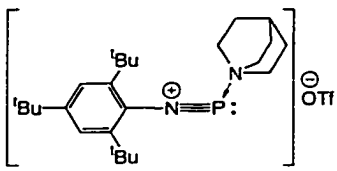

2.8

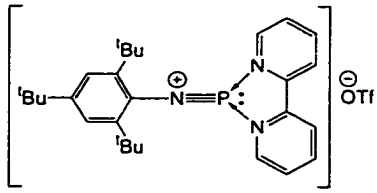

2.9

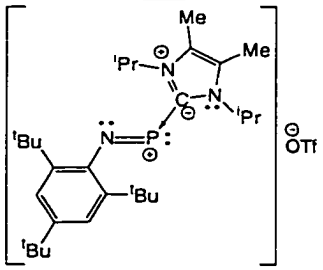

3.14

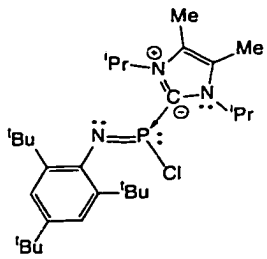

3.15

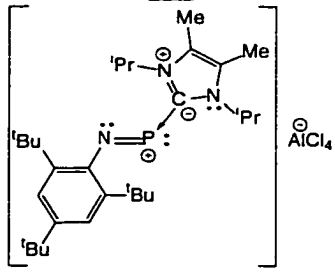

3.16

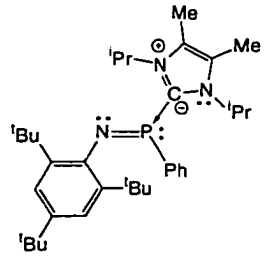

3.17

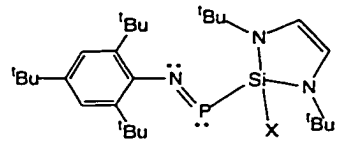

4.7 (X = OTf or Cl)

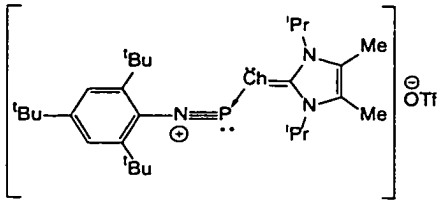

5.3 (Ch = O, S, or Se)

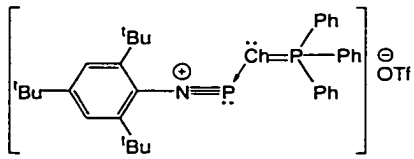

5.4 (Ch = O, or S)

8.3.1: **[Mes*NP•Py]OTf (2.7)**, 1-[(2,4,6-Tri-*tert*-butylphenylimino)phosphino]-pyridinium Trifluoromethanesulphonate

A solution of pyridine (0.13 g, 1.64 mmol) in benzene (4 mL) was added to a stirred solution of Mes*NPOTf, trifluoromethylsulfonyloxy-(2,4,6-tri-*tert*-butylphenylimino)phosphine (0.30 g, 0.69 mmol) in benzene (10 mL) over a period of 30 minutes. A red-orange solution was immediately observed followed by precipitation of red solid. The reaction mixture was stirred for 1 hour. Additional benzene (15 mL) was added and the solution was decanted. Solvent was removed *in vacuo* (overnight) to a volume of 5 mL, giving red-orange crystals. The solution was decanted from the crystals and discarded. The crystals were washed 4 times with 5 mL portions of n-hexane, dried under dynamic vacuum and characterized as $C_{24}H_{34}F_3N_2O_3PS_1$, (0.11 g, 0.22 mmol, 31 %), m.p. 118 to 120 °C.

Elemental analysis: Calculated: C, 55.59 %, H, 6.61 %, N, 5.40 %.

Found: C, 55.04 %, H, 6.95 %, N, 5.42 %.

IR: 1611(16), 1597(27), 1540(28), 1496(13), 1481(9), 1415(23), 1397(21), 1362(11), 1288(2), 1265(10), 1234(1), 1223(5), 1211(13), 1167(7) 1161(6), 1039(12), 1024(3), 1008(8), 928(29), 887(25), 880(24), 771(15), 758(19), 692(18), 651(17), 638(4), 576(26), 520(20), 515(22), 429(31), 379(30).

NMR solution: The resonances associated with the pyridinium group were simulated as a second order AA'MM'X pattern. $\delta(^1H)$ 1.34 (s, 9H, *p*-(C$\underline{H}_3$)$_3$C), 1.36 (s, 18H, *o*-(C$\underline{H}_3$)$_3$C), 7.41 (d, $^5J(^{31}P,^1H)$ = 1.8 Hz, 2H, *m*-C$\underline{H}$(Mes*)), 7.88 (m, $^3J(^1H(m),^1H(p))$ = 7.66 Hz, $^3J(^1H(o),^1H(m))$ = 5.45 Hz, $^4J(^1H(m),^1H(m'))$ = 1.43 Hz, $^5J(^1H(o),^1H(m')$ = 0.84 Hz, 2H, *m*,*m'*-C$\underline{H}$), 8.35 (tt, $^3J(^1H(m),^1H(p))$ = 7.66 Hz, $^4J(^1H(o),^1H(p))$ = 1.56 Hz, 1H, *p*-C$\underline{H}$), 8.82 (m, $^3J(^1H(o),^1H(m)$ = 5.45 Hz, $^4J(^1H(o),^1H(o'))$ = 0 Hz, 2H, *o*,*o'*-C$\underline{H}$); $\delta(^{13}C\{^1H\})$ 30.6 (s, *o*-(C$\underline{H}_3$)$_3$C), 31.4 (s, *p*-(C$\underline{H}_3$)$_3$C), 35.2 (s, *p*-(CH$_3$)$_3$C$\underline{}$), 36.0 (s, *o*-(CH$_3$)$_3$C$\underline{}$), 122.8 (s,

m-CH(Mes*)), 121.0 (q, $^{1}J(^{19}F,^{13}C)$ = 320.0 Hz, $\underline{C}F_3$), 126.4 (s, *m*-CH), 135.4 (d, $^{2}J(^{31}P,^{13}C)$ = 39.1 Hz, *i*-CNP), 140.4 (s, *o*-$(CH_3)_3C\underline{C}$), 140.5 (s, *p*-CH), 145.5 (s, *o*-CH), 148.0 (s, *p*-$(CH_3)_3C\underline{C}$); $\delta(^{19}F\{^{1}H\})$ -78.9 ("s", $^{1}J(^{19}F, ^{13}C)$ = 320.4 Hz); $\delta(^{31}P\{^{1}H\})$ 71 (s).

NMR solid state: $\delta_{iso}(^{31}P)$ 65, δ_{11} 250, δ_{22} 196, δ_{33} -251.

Reaction mixture: $^{31}P\{^{1}H\}$ NMR spectra of the reaction mixtures, prepared in CH_2Cl_2, showed a dominant signal, $\delta(^{31}P)$ = 74 ppm (91 %, [Mes*NP•Py]OTf), and a minor signal with $\delta(^{31}P)$ = 136 ppm (9 %, tentatively assigned as Mes*NPCl from the literature value[123]).

Crystallography: Crystals for X-ray diffraction analysis were obtained by slow solvent evaporation (1 day) of the product dissolved in a 1:1 mixture (30 mL) of dichloromethane and n-hexane. Crystallographic details are provided in Table 8.1.

8.3.2: [Mes*NP•Qncd]OTf (2.8), 1-[(2,4,6-Tri-*tert*-butylphenylimino)phosphino]-1-azoniabicyclo[2.2.2]octane Trifluoromethanesulphonate

A solution of 1-azabicyclo[2.2.2]octane (0.063 g, 0.57 mmol) in benzene (15 mL) was added to stirred solution of Mes*NPOTf, trifluoromethylsulfonyloxy-(2,4,6-tri-*tert*-butylphenylimino)phosphine (0.25 g, 0.57 mmol) in benzene (20 mL) over a period of 15 minutes. A red solution was immediately observed followed by precipitation of purple-red solid. After the reaction mixture was stirred (1 hour), the solution was decanted and discarded. The solid was washed twice with 5 mL portions of benzene, dried under dynamic vacuum and characterized as $C_{26}H_{42}F_3N_2O_3PS$ (0.67 g, 0.12 mmol, 22 %), m.p. 176 to 178 °C.

Elemental analysis: Calculated: C, 56.71 %, H, 7.69 %, N, 5.09 %.

Found: C, 57.10 %, H, 8.38 %, N, 5.12 %.

IR: 1600(18), 1417(12), 1365(4), 1339(11), 1278(6), 1257(5), 1241(3), 1226(7), 1163(8), 1147(9), 1026(1), 1005(14), 966(15), 923(19), 891(20), 877(17), 833(21), 786(24), 763(13), 752(10), 680(25), 637(2), 571(22), 550(23), 516(16), 450(26).

NMR solution: $\delta(^1H)$ 1.31 (s, 9H, *p*-($C\underline{H}_3)_3C$), 1.47 (s, 18H, *o*-($C\underline{H}_3)_3C$), 1.98 (m, 6H, $HC(C\underline{H}_2)_3$), 2.16 (sept, $^3J(^1H,^1H)$ = 3.35 Hz, 1H, $\underline{H}C(CH_2)_3$), 3.43 (m, 6H, $(C\underline{H}_2)_3N$), 7.40 (d, $^5J(^{31}P,^1H)$ = 1.53 Hz, 2H, *m*-C$\underline{H}$); $\delta(^{13}C\{^1H\})$ 20.8 (s, $H\underline{C}(CH_2)_3$), 24.6 (s, $HC(\underline{C}H_2)_3$), 31.4 (s, *o*-($\underline{C}H_3)_3C$), 31.5 (s, *p*-($\underline{C}H_3)_3C$), 35.5 (s, *p*-$(CH_3)_3\underline{C}$), 36.5 (s, *o*-$(CH_3)_3\underline{C}$), 48.1 (s, $N(\underline{C}H_2)_3$), 121.3 (q, $^1J(^{19}F,^{13}C)$ = 319 Hz, $\underline{C}F_3$), 123.2 (s, *m*-CH), 136.9 (d, $^2J(^{31}P,^{13}C)$ = 26.2, *i*-$\underline{C}$NP), 140.4 (d, $^3J(^{31}P, ^{13}C)$ = 8.1 Hz, *o*-$(CH_3)_3C\underline{C}$), 150.0 (s, *p*-$(CH_3)_3C\underline{C}$); $\delta(^{19}F\{^1H\})$ -78.8 ("s", $^1J(^{19}F,^{13}C)$ = 319 Hz); $\delta(^{31}P\{^1H\})$ 144 (s).

Reaction mixture: $^{31}P\{^1H\}$ NMR spectra of the reaction mixtures, prepared in CH_2Cl_2, showed a dominant signal, $\delta(^{31}P)$ = 144 ppm (97 %, [Mes*NP•Qncd]OTf), and a minor signal with $\delta(^{31}P)$ = 137 ppm (3 %, tentatively assigned as Mes*NPCl from the literature value[123]).

Crystallography: Crystals for X-ray diffraction analysis were obtained by liquid-liquid diffusion using dichloromethane and n-hexane. Crystallographic details are provided in Table 8.2.

8.3.3: [Mes*NP•Dipy]OTf (2.9), 1,1'-[(2,4,6-Tri-*tert*-butylphenylimino)phosphino]-2,2'-dipyridinium Trifluoromethanesulphonate

A solution of 2,2'-dipyridyl (0.084 g, 0.54 mmol) in benzene (15 mL) was added to a stirred solution of Mes*NPOTf, trifluoromethylsulfonyloxy-(2,4,6-tri-*tert*-butylphenylimino)phosphine (0.25 mg, 0.57 mmol) in benzene (25 mL) over a period of 5 minutes. A red-orange solution was immediately observed followed by precipitation of dark orange solid. After the reaction mixture was stirred (1 hour), the solution was

decanted and discarded. The solid was washed 3 times with 5 mL portions of n-hexane, and dried under dynamic vacuum. The product was characterized as $C_{29}H_{37}F_3N_3O_3PS$ (0.29 mg, 0.48 mmol, 84 %), m.p. 201°C.

Elemental analysis: The presence of dichloromethane solvate has precluded accurate determination.

IR: 1602(14), 1587(33), 1575(35), 1564(36), 1540(34), 1491(8), 1446(5), 1392(18), 1364(15), 1335(28), 1314(16), 1280(2), 1275(3), 1256(4), 1226(11), 1200(22), 1160(7), 1151(9), 1102(30), 1068(26), 1055(23), 1032(1), 1014(10), 964(32), 887(25), 880(21), 812(27), 778(12), 768(17), 755(20), 747(29), 651(13), 639(6), 574(24), 546(40), 518(19), 458(31), 426(38), 419(39), 354(37).

NMR solution: (Protons and carbon nuclei of the 2,2'-dipyridyl ligand are labeled according to scheme shown in Figure 2.5) $\delta(^1H)$ 1.27 (s, 9H, *p*-(C$\underline{H}_3$)$_3$C), 1.31 (s, 18H, *o*-(C$\underline{H}_3$)$_3$C), 7.31 (d, $^5J(^{31}P,^1H)$ = 1.83 Hz, 2H, *m*-C$\underline{H}$), 7.99 (m, $^3J(^1H,^1H)$ = 6.95 Hz, $^3J(^1H,^1H)$ = 5.38 Hz, $^4J(^1H,^1H)$ = 1.92 Hz, 2H, 5,5'-C$\underline{H}$), 8.54 (m, $^3J(^1H,^1H)$ = 6.95 Hz, $^3J(^1H,^1H)$ = 8.07, 2H, 4,4'-C$\underline{H}$), 8.88 (br. d, $^3J(^1H,^1H)$ = 8.07 Hz, 2H, 3,3'-C$\underline{H}$), 8.99 (ddd, $^3J(^1H,^1H)$ = 5.38 Hz, $^5J(^1H,^1H)$ = 0.84 Hz, $^4J(^1H,^1H)$ = 1.52, 2H, 6,6'-C$\underline{H}$); $\delta(^{13}C\{^1H\})$ 30.1 (s, *o*-($\underline{C}H_3$)$_3$C), 31.4 (s, *p*-($\underline{C}H_3$)$_3$C), 35.3 (s, *p*-(CH$_3$)$_3\underline{C}$), 35.8 (s, *o*- (CH$_3$)$_3\underline{C}$), 121.2 (q, $^1J(^{19}F,^{13}C)$ = 320 Hz, $\underline{C}F_3$), 122.3 (s, 3,3'-$\underline{C}$H), 122.6 (s, *m*-$\underline{C}$H), 123.9 (s, 5,5'-$\underline{C}$H), 128.5 (s, 4,4'-$\underline{C}$H), 133.9 (d, $^3J(^{31}P,^{13}C)$ = 46.7 Hz, *i*-$\underline{C}$NP), 144.6 (s, 6,6'-$\underline{C}$H), 145.2 (s, 2,2'-N$\underline{C}\underline{C}$N) 145.5 (d, $^3J(^{31}P,^{13}C)$ = 14.3 Hz, *o*-(CH$_3$)$_3$C$\underline{C}$), 148.6 (d, $^5J(^{31}P,^{13}C)$ = 4.3 Hz, *p*-(CH$_3$)$_3$C$\underline{C}$); $\delta(^{19}F\{^1H\})$ -78.8 ("s", $^1J(^{19}F,^{13}C)$ = 320 Hz); $\delta(^{31}P\{^1H\})$ 54 (s).

NMR solid state: $\delta_{iso}(^{31}P)$ 67, δ_{11} 338, δ_{22} 146, δ_{33} -282.

Reaction mixture: $^{31}P\{^1H\}$ NMR spectra of the reaction mixtures, prepared in CH_2Cl_2, showed a dominant signal, $\delta(^{31}P)$ = 54 ppm (98 %, [Mes*NP•Dipy]OTf), and a minor

signal with $\delta(^{31}P)$ = 279 ppm (2 %, tentatively assigned as $[(Mes^*N(H))_2P]OTf$ from the literature value[35]).

Crystallography: Crystals for X-ray diffraction analysis were obtained by liquid-liquid diffusion using dichloromethane and n-hexane. The crystal structure shows the presence of a single disordered dichloromethane solvate in the unit cell. Crystallographic details are provided in Table 8.2.

8.3.4: **[Mes*NP•Im]OTf (3.14)**, 1,3-Diisopropyl-4,5-dimethyl-2-[(2,4,6-tri-*tert*-butylphenylimino)phosphino]-1*H*-imidazolium Trifluoromethanesulphonate

A solution of 1,3-diisopropyl-4,5-dimethylimidazol-2-ylidene (Im) (0.13 g, 0.70 mmol) in benzene (7 mL) was added to a stirred solution of Mes*NPOTf, trifluoromethylsulfonyloxy-(2,4,6-tri-*tert*-butylphenylimino)phosphine (0.31 g, 0.70 mmol) in benzene (11 mL) over a period of 1 hour. A dark purple solution was immediately observed and the reaction mixture was stirred (1 hour). The solvent was removed *in vacuo* (overnight) to a volume of 3 mL, giving dark-purple crystals. The solution was decanted and discarded. The crystals were washed 3 times with 5 mL portions of benzene, dried under static vacuum and characterized as $C_{30}H_{49}F_3N_3O_3PS$, (0.16 mg, 0.26 mmol, 37 %), m.p. 145 °C.

Elemental analysis: Calculated: C, 58.14 %, H, 7.97 %, N, 6.78 %.

Found: C, 58.20 %, H, 7.82 %, N, 6.85 %.

IR: 1610(21), 1596(27), 1419(9), 1280(1), 1246(2), 1229(5) 1221(6), 1159(8), 1147(7), 1122(10), 1090(14), 1026(4), 934(22), 909(18), 889(20), 877(15), 847(26), 795(12), 754(16), 637(3), 628(13), 572(17), 549(19), 517(11), 499(24), 451(25), 400(23), 346(28).

NMR solution: $\delta(^1H)$ 1.34 (s, 9H, *p*-$(C\underline{H}_3)_3C$), 1.39 (s, 18H, *o*-$(C\underline{H}_3)_3C$), 1.66 (d, $^3J(^1H,^1H)$ = 7.02 Hz, 12H, $CH(C\underline{H}_3)_2$), 2.50 (s, 6H, $C(C\underline{H}_3)N$), 5.86 (dsp, $^3J(^1H,^1H)$ =

7.02 Hz, $^{5}J(^{31}P,^{1}H)$ = 0.80 Hz, 2H, C<u>H</u>$(CH_3)_2$), 7.46 (d, $^{5}J(^{31}P,^{1}H)$ = 0.92, 2H, *m*-C<u>H</u>); $\delta(^{13}C\{^{1}H\})$ 11.5 (s, C(<u>C</u>H_3)N), 22.4 (s, CH(<u>C</u>$H_3)_2$), 31.7 (s, *p*-(<u>C</u>$H_3)_3$C), 33.4 (s, *o*-(<u>C</u>$H_3)_3$C), 35.2 (s, *p*-$(CH_3)_3$<u>C</u>), 36.7 (s, *o*-$(CH_3)_3$<u>C</u>), 52.7 (d, $^{4}J(^{31}P,^{13}C)$ = 8.6 Hz, <u>C</u>H$(CH_3)_2$), 121.0 (q, $^{1}J(^{19}F, ^{13}C)$ = 321 Hz, <u>C</u>F_3), 123.1 (s, *m*-C<u>H</u>), 132.4 (s, <u>C</u>(CH_3)N), 136.1 (d, $^{2}J(^{31}P,^{13}C)$ = 11.5 Hz, *i*-<u>C</u>NP), 142.5 (d, $^{3}J(^{31}P,^{13}C)$ = 6.4 Hz, *o*-$(CH_3)_3$C<u>C</u>), 146.4 (d, $^{1}J(^{31}P,^{13}C)$ = 131.6 Hz, NP<u>C</u>) 147.7 (d, $^{5}J(^{31}P,^{13}C)$ = 1.9 Hz, *p*-$(CH_3)_3$C<u>C</u>); $\delta(^{19}F\{^{1}H\})$ -78.6 (s, $^{1}J(^{19}F,^{13}C)$ = 321 Hz, C<u>F</u>$_3$); $\delta(^{31}P\{^{1}H\})$ 339 ("s", $^{1}J(^{31}P,^{13}C)$ = 131.6 Hz).

NMR solid state: $\delta_{iso}(^{31}P)$ 366, δ_{11} 915, δ_{22} 128, δ_{33} 55.

Reaction mixture: NMR identification of the side product Mes*NPNH(Mes*): A solution of 1,3-diisopropyl-4,5-dimethylimidazol-2-ylidene (Im) (0.13 g, 0.69 mmol) in benzene (15 mL) was added to a stirred solution of Mes*NPOTf, trifluoromethylsulfonyloxy-(2,4,6-tri-*tert*-butylphenylimino)phosphine (0.29 g, 0.67 mmol) in benzene (11 mL) over a period of 5 min. The solvent was completely removed *in vacuo* (3 hours) giving dark purple oil. n-Hexane (30 mL) was added to the oil resulting in a red solution and purple solid. The solution was decanted into a 5 mm (o.d.) NMR tube, the volume of the solvent was reduced to 2 mL *in vacuo* and the tube was flame sealed. $^{31}P\{^{1}H\}$ NMR spectra showed 7 peaks with $\delta(^{31}P)$ = 308 ppm (9 %), 279 ppm (4 %) 268 ppm (51%, tentatively assigned as Mes*NPN(H)Mes* based on the literature value[240]), 146 ppm (2 %), 136 ppm (7 %), 128 ppm (13 %), 90 ppm (5 %), 10 ppm (10 %). The $^{31}P\{^{1}H\}$ spectra of the isolated [Mes*NP•Im]OTf product has occasionally reveal a small peak with $\delta(^{31}P)$ = -8 ppm. The ^{1}H spectra has shown a peak with $\delta(^{1}H)$ = 8.85 ppm, which is tentatively assigned as the imidazolium salt **<u>3.18</u>** (X = OTf) based on the literature value[258]). $^{31}P\{^{1}H\}$ spectra of the reaction mixture, prepared in toluene, showed three signals with $\delta(^{31}P)$ = 347 ppm (33 %), 307 ppm (39 %) and

279 ppm (28 % tentatively assigned as $[(Mes*N(H))_2P]OTf$ based on the literature value[33]).

Crystallography: Crystals for X-ray diffraction analysis were obtained by liquid-liquid diffusion using benzene and n-hexane. Crystallographic details are provided in Table 8.2.

8.3.5: Mes*NP(Cl)•Im (3.15), 1,3-Diisopropyl-4,5-dimethyl-2-[(2,4,6-tri-*tert*-butylphenyl-imino)chlorophosphino]-1*H*-imidazol

A solution of 1,3-diisopropyl-4,5-dimethylimidazol-2-ylidene (Im) (0.16 g, 0.89 mmol) in benzene (9 mL) was added to a stirred solution of Mes*NPCl, chloro-(2,4,6-tri-*tert*-butylphenylimino)phosphine (0.30 g, 0.92 mmol) in benzene (13 mL) over a period of 45 minutes. A darker orange solution was immediately observed. The reaction mixture was stirred (1 hour) and the solvent was removed *in vacuo* (overnight) to a volume of 5 mL, giving bright orange crystals. The solution was decanted and discarded. The crystals were washed twice with 5 mL portions of benzene, dried under static vacuum and characterized as $C_{29}H_{49}ClN_3P$, (0.11 g, 0.22 mmol, 25 %), m.p. 177 to 178 °C.

Elemental Analysis: Calculated: C, 68.82 %, H, 9.76 %, N, 8.30 %.

Found: C, 69.08 %, H, 9.82 %, N, 8.36 %.

IR: 1623(27), 1596(39), 1414(1), 1391(5), 1367(6), 1360(4), 1352(10), 1321(26), 1286(15), 1260(2), 1251(3), 1240(7), 1213(8), 1188(13), 1172(20), 1155(22), 1138(16), 1124(9), 1115(14), 1083(19), 1020(21), 951(32), 935(31), 922(34), 905(23), 887(28), 877(11), 793(12), 783(29), 772(25), 756(24), 708(37), 692(18), 673(38), 655(40), 642(35), 551(30), 514(33), 497(36), 400(17)

NMR solution: $\delta(^1H)$ 1.31 (s, 9H, *p*-C(C<u>H</u>$_3$)$_3$), 1.42 (s, 18H, *o*-C(C<u>H</u>$_3$)$_3$), 1.63 (d, $^3J(^1H,^1H)$ = 7.0 Hz, 12H, CH(C<u>H</u>$_3$)$_2$), 2.35 (s, 6H, CC(C<u>H</u>$_3$)N), 6.20 (m, 2H, C<u>H</u>(CH$_3$)$_2$), 7.29 (d, $^5J(^{31}P,^1H)$ = 1.51 Hz, 2H, *m*-C<u>H</u>); $\delta(^{13}C\{1H\})$ 11.1 (s, C(<u>C</u>H$_3$)N), 21.5 (s, CH(<u>C</u>H$_3$)$_2$), 32.0 (s, *p*-C(<u>C</u>H$_3$)$_3$), 33.0 (s, *o*-C(<u>C</u>H$_3$)$_3$), 34.8 (s, *p*-<u>C</u>(CH$_3$)$_3$), 36.6 (s, *o*-<u>C</u>(CH$_3$)$_3$), 50.6 (d, $^4J(^{31}P,^{13}C)$ = 19.6 Hz, <u>C</u>H(CH$_3$)$_2$, 122.4 (s, *m*-<u>C</u>H), 127.4 (s, <u>C</u>(CH$_3$)N), 139.5 (d, $^4J(^{31}P,^{13}C)$ = 11.9 Hz, *o*-<u>C</u>C(CH$_3$)$_3$), 140.6 (s, *p*-<u>C</u>C(CH$_3$)$_3$), 147.3 (d, $^2J(^{31}P,^{13}C)$ = 25.3 Hz, *i*-<u>C</u>NP), 153.6 (d, $^1J(^{31}P,^{13}C)$ = 114.9 Hz, NP<u>C</u>); $\delta(^{31}P\{^1H\})$ 172 ("s", $^1J(^{31}P,^{13}C)$ = 114.9 Hz).

NMR solid state: $\delta_{iso}(^{31}P)$ 193, δ_{11} 554, δ_{22} 122, δ_{33} -96.

Reaction mixture: $^{31}P\{^1H\}$ NMR spectra of the reaction mixtures, prepared in C_6H_6, showed a signal at 156 ppm (72 %, Mes*NP(Cl)•Im), and signals at 136 ppm (19 %, tentatively assigned as Mes*NPCl based on the literature value[123]), 130 ppm (9 %). The ^1H spectra of the isolated Mes*NP(Cl)•Im product has occasionally reveal a small peak with $\delta(^1H)$ = 8.62 ppm, which is tentatively assigned as the imidazolium salt **<u>3.18</u>** (X = Cl) based on the literature value[258]).

Crystallography: Crystals for X-ray diffraction analysis were obtained by liquid-liquid diffusion using benzene and n-hexane. Crystallographic details are provided in Table 8.3.

8.3.6: Identification by Solution NMR of [Mes*NP•Im]AlCl$_4$ (<u>3.16</u>), 1,3-Diisopropyl-4,5-dimethyl-2-[(2,4,6-tri-*tert*-butylphenylimino)phosphino]-1*H*-imidazolium Tetrachloroaluminate

In a 10 mm (o.d.) NMR tube, 1,3-diisopropyl-4,5-dimethyl-2-[(2,4,6-tri-*tert*-butylphenyl-imino)chlorophosphino]-1*H*-imidazol (Mes*NP(Cl)•Im) (0.16 g, 0.32 mmol) was combined with trialuminum hexachloride (Al_2Cl_6) (0.042 g, 0.16 mmol). The NMR

tube was evacuated and dichloromethane (5 mL) was added to the solid reaction mixture. Upon warming to room temperature, a dark blue solution was obtained. The NMR tube was flamed sealed and the NMR spectra were collected within one week of preparation. **NMR solution**: $\delta(^{31}P\{^{1}H\})$ 331 (s); $\delta(^{27}Al\{^{1}H\})$ 102.4 (s, $\nu_{1/2}$ = 8.1 Hz).

8.3.7: **Mes*NP(Ph)•Im (3.17)**, 1,3-Diisopropyl-4,5-dimethyl-2-[(2,4,6-tri-*tert*-butylphenyl-imino)phenylphosphino)-1*H*-imidazol

A solution of 1,3-diisopropyl-4,5-dimethylimidazol-2-ylidene (Im) (0.055 g, 0.31 mmol) in n-hexane (20 mL) was added to a stirred solution of Mes*NPPh, phenyl-(2,4,6-tri-*tert*-butylphenylimino)phosphine (0.10 g, 0.28 mmol) in n-hexane (15 mL) over a period of 15 minutes. A dark yellow solution was immediately observed and the reaction mixture was stirred (1 hour). Afterwards the solvent was removed *in vacuo* (4 days) to a volume of 10 mL, giving bright yellow solid. The solution was decanted and discarded. The solid was washed twice with 5 mL portions of n-hexane and dried under static vacuum. From solution NMR spectroscopy, the product is speculated to be $C_{35}H_{54}N_3P$ (0.068 g, 0.12 mmol, 45 %).

NMR solution (in C_6D_6): $\delta(^{1}H)$ 0.61 (m, 12H, $CH(C\underline{H}_3)_2$), 1.08 (s, 6H, $CC(C\underline{H}_3)N$), 1.24 (s, 9H, *p*-$(C\underline{H}_3)_3C$), 1.54 (s, 18H, *o*-$(C\underline{H}_3)_3C$)), 5.48 (s, 2H, $CH(C\underline{H}_3)_2$), 6.80 to 7.04 (m, 3H, *m*-, *p*-C<u>H</u>(Ph), 7.37 (d, $^{5}J(^{31}P,^{1}H)$ = 1.22 Hz, 2H, *m*-C<u>H</u>(Mes*)), 7.71 (m, 2H, *o*-C<u>H</u>(Ph)); $\delta(^{13}C\{^{1}H\})$ 10.1 (s, $C(\underline{C}H_3)N$), 21.7 (s, $CH(\underline{C}H_3)_2$), 32.7 (s, *p*-$(\underline{C}H_3)_3C$), 33.4 (d, $^{5}J(^{31}P,^{13}C)$ = 4.3 Hz, *o*-$(\underline{C}H_3)_3C$), 34.9 (s, *p*-$(CH_3)_3\underline{C}$)), 37.3 (d, $^{4}J(^{31}P,^{13}C)$ = 1.4 Hz, *o*-$(CH_3)_3\underline{C}$)), 50.2 (s, $\underline{C}H(CH_3)_2$), 121.5 (d, $^{3}J(^{31}P,^{13}C)$ = 2.4 Hz, *m*-<u>C</u>H(Ph)), 124.9 (s, *m*-<u>C</u>H(Mes*)), 127.1 (s, $\underline{C}(CH_3)N$), 128.1 (d, $^{2}J(^{31}P,^{13}C)$ = 25.8 Hz, *i*-NP<u>C</u>(Mes*)), 131.4 (d, $^{2}J(^{31}P,^{13}C)$ = 20.5 Hz, *o*-<u>C</u>H), 136.7 (s, *p*-<u>C</u>H), 143.9 (m, NP<u>C</u>(Im)), 149.6 (d, $^{3}J(^{31}P,^{13}C)$ =

9.1 Hz, *o*-$\underline{C}C(CH_3)_3$), 157.3 (d, $^5J(^{31}P,^{13}C)$ = 2.1 Hz, *p*-$\underline{C}C(CH_3)_3$), 159.3 (d, $^1J(^{31}P,^{13}C)$ = 33.9 Hz, *i*-$\underline{C}$(Ph)PN); $\delta(^{31}P\{^1H\})$ 57 (s).

Reaction mixture: $^{31}P\{^1H\}$ NMR spectra of the reaction mixtures, prepared in C_6H_6, showed a dominant signal, $\delta(^{31}P)$ = 56 ppm (78 %, Mes*NP(Ph)•Im), and other signals with $\delta(^{31}P)$ = 47 ppm (12 %) and -18 ppm (10 %).

Crystallography: The solid was shown by single crystal X-ray diffraction analysis to be polycrystalline and a molecular structure could not be determined.

8.3.8: Mes*NPSi(OTf)DAB (4.7 (X = OTf)), 1,3-Di-*tert*-butyl-2-(2,4,6-tri-*tert*-butylphenylimino)-phosphino)-2,3-dihydro-1*H*-1,3,2-diazasilol-2-yl Trifluoromethanesulphonate

A solution of 1,3-di-*tert*-butyl-2,3-dihydro-1*H*-1,3,2-diazolsilol-2-ylidene (SiDAB) (0.16 g, 0.80 mmol) in toluene (15 mL) was added to a stirred solution of Mes*NPOTf, trifluoromethylsulfonyloxy-(2,4,6-tri-*tert*-butylphenylimino)phosphine (0.36 g, 0.81 mmol) in toluene (20 mL) over a period of 20 minutes. Immediately, a dark blue solution was observed. After stirring the reaction mixture (1 hour), the solvent was completely removed *in vacuo* and n-hexane (20 mL) was added to the dark blue residue. The solution was filtered through a fine frit and the solvent completely removed *in vacuo*. The dark blue solid was recrystallized twice from n-hexane, dried under dynamic vacuum and characterized as $C_{29}H_{49}F_3N_3O_3PSSi$ (0.19 g, 0.30 mmol, 38 %), m.p. 118 to 125 °C.

Elemental Analysis. Calculated: C, 54.78%, H, 7.77 %, N, 6.61 %.
Found: C, 54.24 %, H, 7.84 %, N, 6.67 %.

IR: 1595(25), 1388(2), 1368(6), 1349(15), 1263(9), 1244(8), 1211(1), 1149(4), 1121(17), 1113(12), 1097(7), 1058(16), 1030(14), 1009(13), 931(3), 924(5), 885(20), 879(18),

814(22), 768(21), 755(19), 687(23), 630(11), 622(10), 576(29), 568(28), 544(26), 528(31), 511(27), 488(24), 434(30), 409(32), 375(33), 333(34).

NMR solution (in C_6D_6): $\delta(^1H)$ 1.13 (s, 9H, *p*-C(C$\underline{H}_3)_3$), 1.15 (s, 18H, *o*-C(C$\underline{H}_3)_3$), 1.17 (s, 18H, NC(C$\underline{H}_3)_3$), 5.58 ("s", $^3J(^{29}Si,^1H)$ = 7.94 Hz, 2H, NC$\underline{H}$), 7.60 (s, 2H, *m*-C$\underline{H}$); $^{13}C\{^1H\}$ 31.6 (d, $^4J(^{31}P,^{13}C)$ = 2.9 Hz, *o*-C($\underline{C}H_3)_3$), 32.1 (s, *p*-C($\underline{C}H_3)_3$), 33.8 ("d", $^4J(^{31}P,^{13}C)$ = 2.8 Hz, $^3J(^{29}Si,^{13}C)$ = 75.5 Hz, NC($\underline{C}H_3)_3$), 35.1 (s, *p*-$\underline{C}(CH_3)_3$), 37.0 (s, *o*-$\underline{C}(CH_3)_3$), 53.1 ("s", $^3J(^{29}Si,^{13}C)$ = 20.0 Hz, N$\underline{C}(CH_3)_3$), 113.7 (s, N$\underline{C}$H), 119.6 (q, $^1J(^{19}F,^{13}C)$ = 318 Hz, S$\underline{C}F_3$), 123.0 (s, *m*-CH), 134.3 (d, $^2J(^{31}P,^{13}C)$ = 12.4 Hz, *i*-$\underline{C}$NP), 146.3 (s, *p*-$\underline{C}C(CH_3)_3$), 157.1 (d, $^3J(^{31}P,^{13}C)$ = 8.6 Hz, *o*-$\underline{C}C(CH_3)_3$); $\delta(^{19}F\{^1H\})$ -76.5 ("s", $^1J(^{19}F,^{13}C)$ = 318 Hz); $\delta(^{29}Si\{^1H\})$ (in C_6H_6) -46.1 (d, $^1J(^{31}P,^{29}Si)$ = 121 Hz); $\delta(^{31}P\{^1H\})$ (in C_6D_6) 566 ("s", $^1J(^{31}P,^{29}Si)$ = 121 Hz).

Reaction mixture: $^{31}P\{^1H\}$ NMR spectra of the reaction mixtures, prepared in C_6H_6, showed a dominant signal, $\delta(^{31}P)$ = 566 ppm (93 %, Mes*NPSi(OTf)DAB), and other minor signals with $\delta(^{31}P)$ = -28 ppm (3 %), -148 ppm (4 %).

Crystallography: Crystals for X-ray diffraction analysis were obtained by solvent evaporation (1 day) of the product dissolved in n-hexane (15 mL). Crystallographic details are provided in Table 8.3.

8.3.9: Identification by Solution NMR of Mes*NPSi(Cl)DAB (4.7 (X = Cl)), 1,3-Di-*tert*-butyl-2-(2,4,6-tri-*tert*-butylphenylimino)phosphino)-2,3-dihydro-1*H*-1,3,2-diazasilol-2-yl Chloride

A solution of 1,3-di-tert-butyl-2,3-dihydro-1*H*-1,3,2-diazolsilol-2-ylidene (SiDAB) (0.089 g, 0.45 mmol) in toluene (10 mL) was added to a stirred -40 °C solution of Mes*NPCl, chloro-(2,4,6-tri-*tert*-butylphenylimino)phosphine (0.16 g, 0.48 mmol) in toluene (15 mL) over a period of 45 minutes. Immediately, a dark blue solution was

observed. After stirring the reaction mixture (2 hours), the solvent was completely removed *in vacuo*. The dark purple residue was dissolved with n-hexane (15 mL) and filtered through a fine frit. The solvent was completely removed *in vacuo* to give a mixture of dark blue and yellow solids, which could not be separated. The reaction mixture was characterized using ^{31}P NMR spectroscopy, one component is postulated to be $C_{28}H_{49}ClN_3PSi$.

NMR solution (in C_6H_6): $\delta(^{31}P\{^1H\})$ 586 ("s", $^1J(^{31}P,^{29}Si)$ = 102 Hz).

Reaction mixture: $^{31}P\{^1H\}$ NMR spectra of the reaction mixtures, prepared in C_6H_6, showed a dominant signal, $\delta(^{31}P)$ = 586 ppm (86 %, Mes*NPSi(Cl)DAB), and other minor signals with $\delta(^{31}P)$ = 137 ppm (9 %, tentatively assigned as Mes*NPCl), 94 ppm (4 %).

8.3.10: **OIm** (**5.2** (Ch = O)), 1,3-Diisopropyl-4,5-dimethyl-1,3-dihydro-2*H*-imidazol-2-one

The synthesis was performed without special precautions (exclusion of air and moisture) and is modification of the procedure used for the preparation of 1,3-diisopropyl-4,5-dimethylimidazole-2(3*H*)-thione[266] (SIm). To a 25 mL round bottom flask, 1,3-diisopropylurea (0.96 g, 6.7 mmol) was combined with 3-hydroxy-2-butanone (0.61 mg, 6.9 mmol) and 1-hexanol (10 mL). The reaction mixture was refluxed for 12 hours at 150 °C. After cooling to room temperature, the solvent was distilled off under reduced pressure (6 torr). The brown residue was extracted with n-hexane (15 mL) and removed under reduced pressure (4.5 torr). The off white solid was further purified by sublimation under static vacuum. The product was characterized using NMR spectroscopy as $C_{11}H_{20}N_2O$ (0.39 mg, 2.0 mmol, 30 %). Further characterization is in progress.

NMR solution: δ(^{1}H) 1.33 (d, ^{3}J(^{1}H,^{1}H) = 6.71 Hz, 12H, CH(C$\underline{H}_3$)$_2$), 1.97 (s, 6H, C(C$\underline{H}_3$)N), 4.23 (sept, ^{3}J(^{1}H,^{1}H) = 6.71 Hz, 2H, C$\underline{H}$(CH$_3$)$_2$); δ(^{13}C{^{1}H}) 9.70 (s, C(C$\underline{H}_3$)N), 21.38 (s, CH(C$\underline{H}_3$)$_2$), 41.85 (s, C$\underline{H}$(CH$_3$)$_2$), 113.28 (s, C$\underline{(}$CH$_3$)N), 152.82 (s, N$\underline{C}$ON).

8.3.11: **[Mes*NP•OIm]OTf** (**5.3** (Ch = O)), 1,3-Diisopropyl-4,5-dimethyl-2-{[(2,4,6-tri-*tert*-butyl-phenylimino)phosphino]oxy}-1*H*-imidazolium Trifluoromethanesulphonate

A solution of 1,3-diisopropyl-4,5-dimethyl-1,3-dihydro-2*H*-imidazol-2-one (0.11 g, 0.57 mmol) in benzene (10 mL) was added to a stirred solution of Mes*NPOTf, trifluoromethylsulfonyloxy-(2,4,6-tri-*tert*-butylphenylimino)phosphine (0.25 g, 0.57 mmol) in benzene (30 mL) over a period of 20 minutes. The orange colour of solution remained unchanged after stirring (1 hour). The solvent was removed *in vacuo* overnight, leaving orange-red oil, to which n-hexane (10 mL) was added and orange solid precipitated. The solution was decanted and discarded. The solid was washed twice with 5 mL portions of n-hexane, dried under dynamic vacuum and characterized as $C_{30}H_{49}F_3N_3O_4PS$ (0.28 g, 0.42 mmol, 74 %), m.p. 129.6 to 130.7 °C.

Elemental analysis: In progress.

IR: 1645(31), 1599(23), 1554(7), 1497(6), 1484(9), 1395(12), 1366(8), 1315(14), 1272(2), 1261(3), 1221(10), 1199(11), 1172(16), 1153(4), 1114(15), 1098(22), 1066(26), 1028(5), 1003(19), 925(24), 906(17), 879(20), 872(21), 774(32), 764(30), 753(27), 675(29), 652(13), 637(1), 572(25), 550(33), 516(18), 411(28), 360(34), 348(37), 315(35), 276(36).

NMR solution: δ(^{1}H) 1.30 (s, 9H, *p*-(C$\underline{H}_3$)$_3$C), 1.53 (s, 18H, *o*-(C$\underline{H}_3$)$_3$C), 1.61 (d, ^{3}J(^{1}H,^{1}H) = 7.02 Hz, 6H, CH(C$\underline{H}_3$)$_2$), 2.29 (s, 6H, C(C$\underline{H}_3$)N), 4.62 (sept, ^{3}J(^{1}H,^{1}H) =

7.02 Hz, 2H, C<u>H</u>$(CH_3)_2$), 7.45 (d, $^5J(^{31}P,^1H)$ = 1.24 Hz); $\delta(^{13}C\{^1H\})$ 10.0 (s, C(<u>C</u>H_3)N), 22.3 (s, CH(<u>C</u>$H_3)_2$), 30.2 (s, *o*-(<u>C</u>$H_3)_3$C), 31.4 (s, *p*-(<u>C</u>$H_3)_3$C), 34.1 (s, *p*-$(CH_3)_3$<u>C</u>), 36.3 (s, *o*-$(CH_3)_3$<u>C</u>), 50.4 (s, <u>C</u>H$(CH_3)_2$), 121.4 (q, $^1J(^{19}F,^{13}C)$ = 319 Hz, <u>C</u>F_3), 123.1 (s, *m*-<u>C</u>H), 128.8 (s, <u>C</u>(CH_3)N), 135.3 (d, $^2J(^{31}P,^{13}C)$ = 39 Hz, *i*-<u>C</u>NP), 141.7 (s, PO<u>C</u>), 148.5 (d, $^3J(^{31}P,^{13}C)$ = 10.5 Hz, *o*-$(CH_3)_3$C<u>C</u>), 153.5 (d, $^5J(^{31}P,^{13}C)$ = 0.7 Hz, *p*-$(CH_3)_3$C<u>C</u>); $\delta(^{19}F\{^1H\})$ -78.8 ("s", $^1J(^{19}F,^{13}C)$ = 319 Hz); $\delta(^{31}P\{^1H\})$ 77 (s).

Reaction mixture: $^{31}P\{^1H\}$ NMR spectra of the reaction mixtures, prepared in CH_2Cl_2, showed a dominant signal, $\delta(^{31}P)$ = 77 ppm (87 %, [Mes*NP•OIm]OTf), and minor signals with $\delta(^{31}P)$ = 131 ppm (3 %), 142 ppm (6 %), 279 (4 %, tentatively assigned as [Mes*N(H))$_2$P]OTf based on the literature value[33]).

Crystallography: Crystals for X-ray diffraction anaiysis were obtained by liquid-liquid diffusion at -30 °C using toluene and n-hexane. The crystal structure shows the inclusion of disordered toluene solvate molecules in the unit cell. Crystallographic details are provided in Table 8.4.

8.3.12: **[Mes*NP•SIm]OTf** (<u>5.3</u> (Ch = S)), 1,3-Diisopropyl-4,5-dimethyl-2-{[(2,4,6-tri-*tert*-butylphenylimino)phosphino]thio}-1*H*-imidazolium Trifluoromethanesulphonate

A solution of 1,3-diisopropyl-4,5-dimethylimidazole-2(3*H*)-thione (0.12 g, 0.57 mmol) in benzene (10 mL) was added to a stirred solution of a Mes*NPOTf, trifluoromethylsulfonyloxy-(2,4,6-tri-*tert*-butylphenylimino)phosphine (0.25 g, 0.57 mmol) in benzene (20 mL) over a period of 35 minutes. A red solution was immediately observed. The reaction mixture was stirred (1 hour) and the solvent was removed *in vauco* (overnight) to a volume of 5 mL, giving a red solid. The solution was decanted and discarded. The solid was washed twice with 5 mL portions of n-hexane,

dried under dynamic vacuum and characterized as $C_{30}H_{49}F_3N_3O_3PS_2$, (0.30 g, 0.45 mmol, 80 %), m.p. 159.4 to 160.7 °C.

IR: 1622(20), 1598(11), 1418(7), 1394(8), 1265(1), 1233(6), 1223(5), 1149(4), 1114(9), 1092(10), 1061(15), 1030(2), 978(12), 907(17), 885(16), 802(25), 775(21), 764(18), 759(19), 751(13), 689(26), 674(29), 651(24), 637(3), 580(27), 572(23), 559(31), 550(30), 543(32), 517(14), 484(34), 460(33), 373(22), 325(28).

Elemental analysis: In progress.

NMR solution: $\delta(^1H)$ 1.34 (s, 9H, *p*-(C$\underline{H}_3$)$_3$C), 1.46 (s, 18H, *o*-(C$\underline{H}_3$)$_3$C), 1.58 (d, $^3J(^1H,^1H)$ = 7.02 Hz, 6H, CH(C$\underline{H}_3$)$_2$), 2.41 (s, 6H, C(C$\underline{H}_3$)N), 5.24 (sept, $^3J(^1H,^1H)$ = 7.02 Hz, 2H, C$\underline{H}$(CH$_3$)$_2$), 7.45 (d, $^5J(^{31}P, ^1H)$ = 1.51 Hz); $\delta(^{13}C\{^1H\})$ 11.0 (s, C($\underline{C}$H$_3$)N), 21.7 (s, CH($\underline{C}$H$_3$)$_2$), 30.6 (d, $^5J(^{31}P,^{13}C)$ = 2.4 Hz, *o*-($\underline{C}$H$_3$)$_3$C), 31.4 (s, *p*-($\underline{C}$H$_3$)$_3$C), 34.0 (d, $^4J(^{31}P,^{13}C)$ = 2.9 Hz , *o*-(CH$_3$)$_3\underline{C}$), 36.4 (d, $^6J(^{31}P,^{13}C)$ = 1.4 Hz, *p*-(CH$_3$)$_3\underline{C}$), 53.0 (s, $\underline{C}$H(CH$_3$)$_2$), 121.5 (q, $^1J(^{19}F, ^{13}C)$ = 319 Hz, $\underline{C}$F$_3$), 123.1 (d, $^4J(^{31}P,^{13}C)$ = 2.9 Hz) *m*-$\underline{C}$H), 128.8 (s, $\underline{C}$(CH$_3$)N), 129.5 (s, PS$\underline{C}$), 137.8 (d, $^2J(^{31}P,^{13}C)$ = 41.5 Hz, *i*-$\underline{C}$NP), 145.2 (d, $^3J(^{31}P,^{13}C)$ = 12.4 Hz, *o*-(CH$_3$)$_3$C$\underline{C}$), 153.2 (d, $^5J(^{31}P,^{13}C)$ = 6.7 Hz, *p*-(CH$_3$)$_3$C$\underline{C}$); $\delta(^{19}F\{^1H\})$ -78.7 ("s", $^1J(^{19}F,^{13}C)$ = 319 Hz);$\delta(^{31}P\{^1H\})$ 148 (s).

Reaction mixture: $^{31}P\{^1H\}$ NMR spectra of the reaction mixtures, prepared in CH_2Cl_2, showed a dominant signal, $\delta(^{31}P)$ = 148 ppm (92 %, [Mes*NP•SIm]OTf), and a minor signal with $\delta(^{31}P)$ = 279 ppm (8 %, tentatively assigned as [(Mes*NH)$_2$P]OTf based on literature value[33]).

Crystallography: Crystals for X-ray diffraction studies were obtained by liquid-liquid diffusion using dichloromethane and n-hexane. Crystallographic details are provided in Table 8.4.

8.3.13: **[Mes*NP•SeIm]OTf** (5.3 (Ch = Se)), 1,3-Diisopropyl-4,5-dimethyl-2-{[(2,4,6-tri-*tert*-butyl-phenylimino)phosphino]seleno}-1*H*-imidazolium Trifluoromethanesulphonate

A solution of 1,3-diisopropyl-4,5-dimethylimidazole-2(3*H*)-selenone (0.15 g, 0.59 mmol) in benzene (15 mL) was added to a stirred solution of Mes*NPOTf, trifluoromethylsulfonyloxy-(2,4,6-tri-*tert*-butylphenylimino)phosphine (0.25 g, 0.58 mmol) in benzene (30 mL) over a period of 25 minutes. Immediately, a red solution was observed. The reaction mixture was stirred (1 hour) and the solvent was removed *in vacuo* (overnight) to a volume of 5 mL, giving red crystals. The solution was decanted and discarded. The crystals were washed twice with 5 mL portions of benzene, dried under dynamic vacuum and characterized as $C_{30}H_{49}F_3N_3O_3PSSe$, (0.21 mg, 0.30 mmol, 51 %), m.p. 139.6 to 142.3 °C.

Elemental analysis: In progress.

IR: 1618(15), 1597(10), 1557(29), 1541(24), 1413(7), 1393(8), 1364(5), 1266(1), 1222(6), 1147(4), 1112(9), 1083(14), 1060(20), 1031(3), 973(17), 928(22), 904(18), 885(11), 776(19), 752(13), 687(30), 676(28), 658(32), 638(2), 629(12), 571(21), 541(31), 517(16), 485(33), 357(23), 352(27), 316(25), 280(26).

NMR solution: $\delta(^1H)$ 1.34 (s, 9H, *p*-(C$\underline{H}_3$)$_3$C), 1.44 (s, 18H, *o*-(C$\underline{H}_3$)$_3$C), 1.60 (d, $^3J(^1H,^1H)$ = 7.02 Hz, 6H, CH(C$\underline{H}_3$)$_2$), 2.46 (s, 6H, C(C$\underline{H}_3$)N), 5.24 (m, $^3J(^1H,^1H)$ = 7.02 Hz, 2H, C$\underline{H}$(CH$_3$)$_2$), 7.45 (d, $^5J(^{31}P,^1H)$ = 1.53 Hz); $\delta(^{13}C\{^1H\})$ 11.0 (s, C($\underline{C}$H$_3$)N), 21.6 (s, CH($\underline{C}$H$_3$)$_2$), 30.4 (s, *o*-($\underline{C}$H$_3$)$_3$C), 31.1 (s, *p*-($\underline{C}$H$_3$)$_3$C), 35.9 (s, *p*-(CH$_3$)$_3\underline{C}$), 36.2 (s, *o*-(CH$_3$)$_3\underline{C}$), 54.9 (s, $\underline{C}$H(CH$_3$)$_2$), 121.3 (q, $^1J(^{19}F,^{13}C)$ = 321 Hz, $\underline{C}$F$_3$), 128.6 (s, $\underline{C}$(CH$_3$)N), 123.1 (s, *m*-$\underline{C}$H), 138.0 (d, $^2J(^{31}P,^{13}C)$ = 32.5 Hz, *i*-$\underline{C}$NP), 131.1 (s, PSe$\underline{C}$), 145.2 (d, $^3J(^{31}P,^{13}C)$ = 12.4 Hz, *o*-(CH$_3$)$_3$C$\underline{C}$), 154.0 (d, $^5J(^{31}P,^{13}C)$ = 6.7 Hz, *p*-(CH$_3$)$_3$C$\underline{C}$);

$\delta(^{19}F\{^1H\})$ -78.8 ("s", $^1J(^{19}F,^{13}C)$ = 321 Hz, C<u>F</u>$_3$); $\delta(^{31}P\{^1H\})$ 178 (br. s, N<u>P</u>Se); $\delta(^{77}Se\{^1H\})$ no signal.

Crystallography: Crystals for X-ray diffraction analysis were obtained by liquid-liquid diffusion using dichloromethane and n-hexane. Crystallographic details are provided in Table 8.4.

8.3.14: **[Mes*NP•Im]OTf (<u>3.14</u>)**, From the reaction between Mes*NPOTf, (*P*-trifluoromethyl-sulfonyloxy, *P*-(2,4,6-tri-*tert*-butylphenylimino)phosphine) and TeIm (1,3-diisopropyl-4,5-dimethylimidazole-2(3*H*)-tellurone)

The reaction was performed in the exclusion of light. A solution of 1,3-diisopropyl-4,5-dimethylimidazole-2(3*H*)-tellurone, TeIm (0.093 g, 0.30 mmol) in benzene (25 mL) was added to a stirred solution of Mes*NPOTf, trifluoromethylsulfonyloxy-(2,4,6-tri-*tert*-butylphenylimino)phosphine (0.13 mg, 0.31 mmol) dissolved in benzene (20 mL) over a period of 1 hour. Immediately a light green solution was observed. The reaction mixture was stirred (1 hour) during which the solution became cloudy with a dark purple colour. The reaction mixture was filtered through a fine frit to give a purple solution and black precipitate. The solvent was removed *in vacuo* (overnight) to volume of 5 mL, giving purple crystals. The solution was decanted and discarded. The crystals were dried under dynamic vacuum and characterized using solution ^{31}P NMR as $C_{30}H_{49}F_3N_3O_3PS$ (0.074 g. 0.12 mmol, 39 %).

NMR solution (in C_6D_6): $\delta(^{31}P\{^1H\})$ 350 (s).

8.3.15: **[Mes*NP•OPPh$_3$]OTf** (**5.4** (Ch = O)), 1,1,1-Triphenyl-3-(2,4,6-tri-*tert*-butylphenylimino)-diphosphoxan-1-ium Trifluoromethanesulphonate

A solution of triphenylphosphine oxide (0.073 g, 0.26 mmol) in benzene (16 mL) was added to a stirred solution of Mes*NPOTf, trifluoromethylsulfonyloxy-(2,4,6-tri-*tert*-butylphenylimino)phosphine (0.12 g, 0.27 mmol) in benzene (25 mL) over a period of 5 minutes. After the reaction mixture was stirred (30 minutes), solvent was removed *in vacuo* (overnight) leaving orange-red oil. The oil was washed 4 times with 5 mL portions of n-hexane until an orange solid precipitated. The most of solid was dissolved in benzene (10 mL) and the solution decanted. The solvent was removed *in vacuo* (overnight) to a volume of 2 mL, giving dark orange crystals. The solution was decanted and discarded. The crystals were washed twice with 5 mL portions of n-hexane, dried under dynamic vacuum and characterized as $C_{37}H_{44}F_3NO_4P_2S$, (0.13 g, 0.17 mmol, 66 %), m.p. 162.2 to 163.1 °C.

Elemental analysis: In progress.

IR: 1598(25), 1589(29), 1559(37), 1540(36), 1441(1), 1365(10), 1341(26), 1281(5), 1266(3), 1221(15), 1187(28), 1150(12), 1138(13), 1122(6), 1111(11), 1067(33), 1031(4), 997(23), 938(9), 922(8), 883(18), 774(30), 751(17), 730(7), 691(16), 657(35), 638(2), 615(27), 571(20), 559(19), 536(14), 517(21), 463(24), 440(22), 419(31), 383(32), 273(34).

NMR solution: $\delta(^1H)$ 1.34 (s, 9H, *p*-(C$\underline{H}_3$)$_3$C), 1.43 (s, 18H, *o*-(C$\underline{H}_3$)$_3$C), 7.41 (d, $^5J(^{31}P,^1H)$ = 1.52 Hz, 2H, *m*-C$\underline{H}$(Mes*)), 7.67 to 7.95 (m, 15H, *o*-, *m*-, *p*-C$\underline{H}$(Ph)); $\delta(^{13}C\{^1H\})$ 30.2 (d, $^5J(^{31}P,^{13}C)$ = 2.9 Hz, *o*-(C$\underline{H}_3$)$_3$C), 31.4 (s, *p*-(C$\underline{H}_3$)$_3$C), 35.8 (s, *p*-(CH$_3$)$_3$C$\underline{}$), 36.3 (s, *o*-(CH$_3$)$_3$C$\underline{}$), 121.8 (q, $^1J(^{19}F,^{13}C)$ = 321 Hz, C$\underline{F}_3$), 122.5 (d, $^1J(^{31}P,^{13}C)$ = 104.3 Hz, *i*-C$\underline{}$PO), 123.2 (d, $^4J(^{31}P,^{13}C)$ = 2.4 Hz, *m*-C$\underline{H}$(Mes*)), 130.8 (d, $^3J(^{31}P,^{13}C)$ = 13.4 Hz, *o*-C$\underline{H}$(Ph)), 133.6 (d, $^3J(^{31}P,^{13}C)$ = 11.4 Hz, *m*-C$\underline{H}$(Ph)), 135.3 (d, $^2J(^{31}P,^{13}C)$ =

40.1 Hz, *i*-CNP), 136.5 (s, *p*-CH(Ph)), 147.0 (d, $^3J(^{31}P,^{13}C)$ = 10.5 Hz, *o*-$(CH_3)_3CC$), 152.50 (d, $^5J(^{31}P,^{13}C)$ = 6.68 Hz, *p*-$(CH_3)_3CC$); $\delta(^{19}F\{^1H\})$ -78.7 ("s", $^1J(^{19}F,^{13}C)$ = 321 Hz); $\delta(^{31}P\{^1H\})$ 52 ("s", OPC, $^1J(^{31}P,^{13}C)$ = 104 Hz), 60 (s, NPO).

Reaction mixture: $^{31}P\{^1H\}$ NMR spectra of the reaction mixtures, prepared in CH_2Cl_2, showed two dominant signals, $\delta(^{31}P)$ = 52 ppm, 53 ppm ([Mes*NP•$OPPh_3$]OTf), and a minor signal with $\delta(^{31}P)$ = 279 ppm (87%, tentatively assigned as [$(Mes*N(H))_2P$]OTf based on literature value[33]).

Crystallography: Crystals for X-ray diffraction analysis were obtained by liquid-liquid diffusion using dichloromethane and n-hexane. Crystallographic details are provided in Table 8.3.

8.3.16: Solution NMR Characterization of [Mes*NP•$SPPh_3$]OTf (5.4 (Ch = S)), 1,1,1-Triphenyl-3-(2,4,6-tri-*tert*-butylphenylimino)diphosphthian-1-ium Trifluoromethanesulphonate

In a 5 mm (o.d.) NMR tube, Mes*NPOTf, trifluoromethylsulfonyloxy-(2,4,6-tri-*tert*-butylphenylimino)phosphine (0.050 g, 0.11 mmol) was combined with triphenylphosphine sulphide (0.034 g, 0.12 mmol). The NMR tube was evacuated and d_2-dichloromethane (1.2 mL) was added to the solid reaction mixture. Upon warming to room temperature, a dark red solution was obtained. The NMR tube was flamed sealed and the NMR spectra where collected within 1 day of preparation.

NMR solution: $\delta(^1H)$ 1.35 (s, 9H, *p*-$(CH_3)_3C$), 1.46 (s, 18H, *o*-$(CH_3)_3C$), 7.45 (d, $^5J(^{31}P,^1H)$ = 1.84 Hz, 2H, *m*-CH(Mes*)), 7.57 to 7.82 (m, 15H, *o*-, *m*-, *p*-CH(Ph)); $\delta(^{13}C\{^1H\})$ 30.4 (d, $^5J(^{31}P,^{13}C)$ = 2.4 Hz, *o*-$(CH_3)_3C$), 31.3 (s, *p*-$(CH_3)_3C$), 36.1 (d, $^6J(^{31}P,^{13}C)$ = 0.5 Hz, *p*-$(CH_3)_3C$), 36.4 (d, $^4J(^{31}P,^{13}C)$ = 1.4 Hz, *o*-$(CH_3)_3C$), 120.8 (q, $^1J(^{19}F,^{13}C)$ = 318 Hz, CF_3), 123.2 (d, $^4J(^{31}P,^{13}C)$ = 2.4 Hz, *m*-CH(Mes*)), 127.2 (d,

$^{1}J(^{31}P,^{13}C)$ = 85.4 Hz, *i*-CPS), 130.0 (d, $^{3}J(^{31}P,^{13}C)$ = 13.4 Hz, *o*-CH(Ph)), 133.3 (d, $^{3}J(^{31}P,^{13}C)$ = 11.0 Hz, *m*-CH(Ph)), 134.1 (d, $^{4}J(^{31}P,^{13}C)$ = 3.3 Hz, *p*-CH(Ph)), 134.6 $^{2}J(^{31}P,^{13}C)$ = 43.4 Hz, *i*-CNP), 149.1 (d, $^{3}J(^{31}P,^{13}C)$ = 11.0 Hz, *o*-$(CH_3)_3$CC), 154.8 (d, $^{5}J(^{31}P,^{13}C)$ = 7.6 Hz, *p*-$(CH_3)_3$CC); $\delta(^{19}F\{^{1}H\})$ -78.1 ("s", $^{1}J(^{19}F,^{13}C)$ = 318 Hz); $\delta(^{31}P\{^{1}H\})$ 41 ("s", SPC, $^{1}J(^{31}P,^{13}C)$ = 86 Hz), 79 (s, NPS).

Table 8.1: Summary of crystal data, data collection, and refinement conditions for [Mes*NP•Py]OTf.

	[Mes*NP•Py]OTf[d] (2.7)
Empirical formula	$C_{24}H_{34}F_3N_2O_3PS$
Formula weight (g mol^{-1})	518.57
Crystal system	triclinic
Space group	*P*-1(No. 2)
a (Å)	10.298(3)
b (Å)	16.842(4)
c (Å)	8.835(2)
α (deg)	95.69(2)
β (deg)	112.24(2)
γ(deg)	80.66(2)
V (Å^3)	1398.4(6)
Z	2
D_x (Mg m^{-3})	1.231
Radiation, λ (Å)	Cu-Kα, 1.54178
μ (mm^{-1}), *F*(000)	1.972, 548.00
Crystal size (mm^3)	0.08 × 0.10 × 0.12
Crystal colour, habit	light-yellow, block
Diffractometer	Rigaku AFC5R
Scan type	ω-2θ
Temperature (K)	293(2)
Absorption correction method	Ψ-scans
Reflections collected	3143
Independent reflections	2932
Observed reflections ($I > 3\sigma(I)$)	1354
R_{int}, 2θ (deg)	0.046, 119.6
Index ranges *h*, *k*, *l*	0 → 10, -18 → 16, 8 → -8
Parameters, restraints	228, 0
R,[a] *wR*[b] (observed data)	0.057, 0.060
Decay (%)	0
Goodness-of-fit *S*[c]	1.95
Final max. and min. for ρ (e Å^{-3})	0.25, -0.22
Comments	Some non-hydrogen atoms refined isotropically.

([a]) $R = (\Sigma (||F_o| - |F_c||) / \Sigma |F_o|)$.

([b]) $wR = (\Sigma w(|F_o| - |F_c|)^2 / \Sigma w(F_o)^2)^{1/2}$.

([c]) $S = ((\Sigma w(|F_o| - |F_c|)^2) / (n - p))^{1/2}$, where *n* and *p* denote the number of reflections used in refinement and the number of parameters, respectively. Unit weighting scheme (*w*) employed.

([d]) Values obtained from reference 215.

Table 8.2: Summary of crystal data, data collection, and refinement conditions for [Mes*NP•Qncd]OTf, [Mes*NP•Dipy]OTf•CH_2Cl_2, and [Mes*NP•Im]OTf.

	[Mes*NP•Qncd]OTf[d] (2.8)	[Mes*NP•Dipy]OTf•CH_2Cl_2[d] (2.9)	[Mes*NP•Im]OTf[e] (3.14)
Empirical formula	$C_{26}H_{42}F_3N_2O_3PS$	$C_{30}H_{39}Cl_2F_3N_3O_3PS$	$C_{30}H_{49}F_3N_3O_3PS$
Formula weight (g mol^{-1})	550.65	680.57	619.75
Crystal system	orthorhombic	monoclinic	orthorhombic
Space group	$P2_12_12_1$ (No. 19)	$P2_1/a$ (No. 14)	*P*bca (No. 61)
a (Å)	29.469(2)	18.4174(9)	10.6688(2)
b (Å)	10.0650(6)	10.9488(6)	15.2337(3)
c (Å)	9.7745(6)	19.2129(10)	42.5078(6)
α (deg)	90	90	90
β (deg)	90	116.924(1)	90
γ (deg)	90	90	90
V ($Å^3$)	2899.2(3)	3454.3(3)	6908.6(2)
Z	4	4	8
D_x (Mg m^{-3})	1.262	1.309	1.192
Radiation, λ (Å)	Mo-Kα, 0.71069	Mo-Kα, 0.71069	Mo-Kα, 0.71069
μ (mm^{-1}), *F*(000)	0.215, 1176	0.345, 1424	0.189, 2656
Crystal size (mm^3)	0.3 × 0.3 × 0.3	0.4 × 0.2 × 0.2	0.35 × 0.30 × 0.10
Crystal colour, habit	red, block	red, block	purple, plate
Diffractometer	Bruker 1KCCD	Bruker 1KCCD	Siemens/Bruker CCD
Scan type	Φ and ω	Φ and ω	Φ and ω
Temperature (K)	193(2)	193(2)	213(2)
Absorption correction method	empirical	empirical	empirical
Reflections collected	18488	20945, 8095[a]	23185
Independent reflections	6851	8094	5361
Observed reflections ($I > 2\sigma(I)$)	5710	4722	3752
R_{int}, range for θ (deg)	0.0323, 1.38 to 28.30	0.0369, 2.21 to 28.35	0.0857, 1.92 to 24.00
Index ranges *h*, *k*, *l*	-38 → 39 -13 → 12 -11 → 13	0 → 24, -14 → 14, -25 → 22	-11 → 12, -15 → 17, -45 → 48
Parameters, restraints	326, 0	404, 29	370, 0
R_1,[b] wR_2[c] (observed data)	0.0530, 0.1294	0.1000, 0.2381	0.0892, 0.1502
R_1,[b] wR_2[c] (all data)	0.0668, 0.1395	0.1457, 0.2621	0.1360, 0.1699
Extinction coefficient	-	0.0008(7)	
Goodness-of-fit *S*[d]	1.038	1.173	1.215
Final max. and min. for ρ (e $Å^{-3}$)	0.589, -0.309	0.926, -0.722	0.399, -0.318
Comments	Absolute structure could not be determined. Flack parameter = 0.48(9).	Disordered CF_3 group in triflate. Solvate (CH_2Cl_2) disordered.	

([a]) Number of reflections after averaging. ([b]) $R_1 = (\Sigma |F_o| - |F_c|) / (\Sigma |F_o|)$.
([c]) $wR_2 = ((\Sigma w(F_o^2 - F_c^2)^2) / (\Sigma w(F_o^2)^2))^{1/2}$. ([d]) $S = ((\Sigma w(F_o^2 - F_c^2)) / (n - p))^{1/2}$, where *n* and *p* denote the number of reflections used in refinement and the number of parameters, respectively.
Weight schemes: $w = ((\sigma^2 \times F_o^2) + (A \times P)^2 + (B \times P))^{-1}$, where $P = 1/3(F_o^2 + 2F_c^2)$ and *A*, *B* = 0.0702, 1.0800 [Mes*NP•Qncd]OTf; 0.0800, 4.0000 [Mes*NP•Dipy]OTf; 0.134, 23.7562 [Mes*NP•Im]OTf.
Extinction $F_c^* = kF_c (1 + 0.001(F_c^2 \times \lambda^3) / \mathrm{Sin}(2\theta)))^{-1/4}$, where *k* is the overall scaling factor, 0.35889 for [Mes*NP•Dipy]OTf. ([d]) Values obtained from reference 216. ([e]) Values obtained from reference 215.

Table 8.3: Summary of crystal data, data collection, and refinement conditions for Mes*NP(Cl)•Im, Mes*NPSi(OTf)DAB, and [Mes*NP•OPPh$_3$]OTf.

	Mes*NP(Cl)•Im[d] (3.15)	Mes*NPSi(OTf)DAB (4.7 X = OTf)	[Mes*NP•OPPh$_3$]OTf (5.4 Ch = O)
Empirical formula	$C_{29}H_{49}ClN_3P$	$C_{29}H_{49}F_3N_3O_3PSSi$	$C_{37}H_{44}F_3NO_4P_2S$
Formula weight (g mol^{-1})	506.13	635.83	717.73
Crystal system	monoclinic	monoclinic	monoclinic
Space group	$P2_1/c$ (No. 14)	$P2_1/c$ (No. 14)	$P2_1/c$ (No. 14)
a (Å)	21.8062(3)	10.3568(1)	8.5855(8)
b (Å)	8.5184(1)	10.2140(2)	11.1407(11)
c (Å)	17.8511(2)	33.0100(2)	38.545(3)
α (deg)	90	90	90
β (deg)	110.892(1)	94.448(1)	91.059(2)
γ (deg)	90	90	90
V (Å^3)	3097.90(7)	3481.42(8)	3686.1(6)
Z	4	4	4
D_x (Mg m^{-3})	1.085	1.213	1.293
Radiation, λ (Å)	Mo-Kα, 0.71069	Mo-Kα, 0.71069	Mo-Kα, 0.71069
μ (mm^{-1}), F(000)	0.195, 1104	0.221, 1360	0.229, 1512
Crystal size (mm^3)	0.40 × 0.30 × 0.30	0.40 × 0.40 × 0.30	0.10 × 0.21 × 0.30
Crystal colour, habit	orange, block	dark blue, plate	light orange, plate
Diffractometer	Siemens/Bruker CCD	Siemens/Bruker CCD	Bruker P4/RA (CCD)
Scan type	Φ and ω	Φ and ω	Φ and ω
Temperature (K)	213(2)	173(2)	193(2)
Absorption correction method	empirical	empirical	empirical
Reflections collected	9422	14207	17982
Independent reflections	4217	6130	7550
Observed reflections ($I > 2\sigma(I)$)	3497	5314	3015
R_{int}, range for θ (deg)	0.0402, 2.00 to 23.00	0.0263, 1.24 to 26.00	0.0940, 1.06 to 26.40
Index ranges h, k, l	-14 → 23 - 9 → 8 -19 → 19	-12 → 12, -11 → 11, -37 → 40	-10 → 8, -13 → 13, -48 → 31
Parameters, restraints	307, 0	385, 0	443, 41
R_1,[a] wR_2[b] (observed data)	0.0850, 0.2371	0.0633, 0.1419	0.0925, 0.2417
R_1,[a] wR_2[b] (all data)	0.1075, 0.2753	0.0752, 0.1516	0.2072, 0.2996
Extinction coefficient	-	-	0.0016(9)
Goodness-of-fit S	1.082	1.144	0.930
Final max. and min. for ρ (e Å^{-3})	0.644, -0.692	0.950, -0.723	0.876, -0.893
Comments			Disordered SO_3 and CF_3 groups in triflate. P(1) also disordered over two positions.

([a]) $R_1 = (\Sigma |F_o| - |F_c|) / (\Sigma |F_o|)$. ([b]) $wR_2 = ((\Sigma w(F_o^2 - F_c^2)^2) / (\Sigma w(F_o^2)^2))^{1/2}$.
([c]) $S = ((\Sigma w(F_o^2-F_c^2)) / (n - p))^{1/2}$, where n and p denote the number of reflections used in refinement and the number of parameters respectively. Weight schemes: $w = ((\sigma^2 \times F_o^2) + (A \times P)^2 + (B \times P))^{-1}$, where $P = 1/3(F_o^2 + 2F_c^2)$ and A, B = 0.1374, 12.8850 Mes*NP(Cl)•Im; 0.0414, 7.5874 Mes*NPSi(OTf)DAB; 0.1612, 0 [Mes*NP•OPPh$_3$]OTf. Extinction $F_c^* = kF_c (1 + 0.001(F_c^2 \times \lambda^3) / \mathrm{Sin}(2\theta)))^{-1/4}$, where k is the overall scaling factor, 0.07135 for [Mes*NP•OPPh$_3$]OTf. ([d]) Values obtained from reference 215.

Table 8.4: Summary of crystal data, data collection, and refinement conditions for [Mes*NP•OIm]OTf•$(C_6H_5CH_3)_{0.5}$, [Mes*NP•SIm]OTf, and Mes*NP•SeIm]OTf.

	[Mes*NP•OIm]OTf•$(C_6H_5CH_3)_{0.5}$ (5.3 Ch = O)	[Mes*NP•SIm]OTf (5.3 Ch = S)	[Mes*NP•SeIm]OTf (5.3 Ch = Se)
Empirical formula	$C_{33.50}H_{53}F_3N_3O_4PS$	$C_{30}H_{49}F_3N_3O_3PS_2$	$C_{30}H_{49}F_3N_3O_3PSSe$
Formula weight (g mol^{-1})	681.82	651.81	698.71
Crystal system	monoclinic	monoclinic	monoclinic
Space group	$P2_1/n$ (No. 14)	$P2_1/c$ (No. 14)	$P2_1/c$ (No. 14)
a (Å)	9.5517(12)	19.8669(14)	19.8797(13)
b (Å)	30.214(4)	10.4930(7)	10.5398(7)
c (Å)	13.1803(15)	18.2872(14)	18.0832(11)
α (deg)	90	90	90
β (deg)	95.816(3)	114.911(2)	113.840(1)
γ (deg)	90	90	90
V (Å^3)	3784.1(8)	3457.5(4)	3465.7(4)
Z	4	4	4
D_{calc} (Mg m^{-3})	1.197	1.252	1.339
Radiation, λ (Å)	Mo-Kα, 0.71069	Mo-Kα, 0.71069	Mo-Kα, 0.71069
μ (mm^{-1}), F(000)	0.180, 1460	0.250, 1392	1.239, 1464
Crystal size (mm^3)	0.10 × 0.18 × 0.50	0.30 × 0.20 × 0.10	0.10 × 0.30 × 0.40
Crystal colour, habit	orange-yellow, prism	orange, prism	orange, prism
Diffractometer	Bruker P4/RA (CCD)	Bruker P4/RA (CCD)	Bruker P4/RA (CCD)
Scan type	Φ and ω	Φ and ω	Φ and ω
Temperature (K)	193(2)	193(2)	193(2)
Absorption correction method	empirical	empirical	empirical
Reflections collected	18727	17783	16793
Independent reflections	7719	7076	7096
Observed reflections ($I > 2\sigma(I)$)	2868	4199	4267
R_{int}, range for θ (deg)	0.1022, 1.35 to 26.45	0.0524, 1.13 to 26.40	0.0550, 1.12 to 26.39
Index ranges h, k, l	-11 → 11 -37 → 35 -16 → 6	-24 → 24, -13 → 10, -22 → 22	-23 → 24, -13 → 12, -22 → 9
Parameters, restraints	426, 74	379, 0	434, 84
R_1,[a] wR_2[b] (observed data)	0.0749, 0.1656	0.0503, 0.1229	0.0409, 0.0827
R_1,[a] wR_2[b] (all data)	0.2061, 0.2111	0.0929, 0.1386	0.0835, 0.0924
Extinction coefficient	0.0010(5)	-	0.0006(1)
Goodness-of-fit S[c]	0.882	0.929	0.881
Final max. and min. for ρ (e Å^{-3})	0.500, -0.509	0.365, -0.360	0.398, -0.415
Comments	Disordered *p-tert*-butyl group on Mes*. Disordered solvate (toluene) and CF_3 group on triflate.		Disordered *p-tert*-butyl group on Mes*. Disordered CF_3 group on triflate.

([a]) $R_1 = (\Sigma |F_o| - |F_c|) / (\Sigma |F_o|)$. ([b]) $wR_2 = ((\Sigma w(F_o^2 - F_c^2)^2) / (\Sigma w(F_o^2)^2))^{1/2}$.
([c]) $S = ((\Sigma w(F_o^2 - F_c^2)) / (n - p))^{1/2}$, where n and p denote the number of reflections used in refinement and the number of parameters respectively. Weight schemes: $w = ((\sigma^2 \times F_o^2) + (A \times P)^2)^{-1}$, where $P = 1/3(F_o^2 + 2F_c^2)$ and A = 0.927 [Mes*NP•OIm]OTf•$(C_6H_5CH_3)_{0.5}$; 0.718 [Mes*NP•SIm]OTf; 0.3095 [Mes*NP•SeIm]OTf. Extinction: $F_c^* = kF_c (1 + 0.001(F_c^2 \times \lambda^3) / \mathrm{Sin}(2\theta))^{-1/4}$, where k is the overall scaling factor, 0.07699 for [Mes*NP•OIm]OTf•$(C_6H_5CH_3)_{0.5}$ and 0.08282 for [Mes*NP•SeIm]OTf.

Table 8.5: Summary of crystal data, data collection, and refinement conditions for 1,3-diisopropyl-4,5-dimethyl-imidazol-2-ylidene Im (**3.1**), and 1,3-diisopropyl-4,5-dimethylimidazlidin-2(*3H*)-thione SIm, (**5.2** Ch = S).

	Im (**3.1**)	SIm (**5.2** Ch = S)
Empirical formula	$C_{11}H_{20}N_2$	$C_{5.50}H_{10}N_1S_{0.50}$
Formula weight (g mol^{-1})	180.29	106.18
Crystal system	orthorhombic	monoclinic
Space group	*Pccn* (No. 56)	*C2/c* (No. 15)
a (Å)	9.1543(6)	10.024(7)
b (Å)	9.3381(6)	11.298(7)
c (Å)	13.4586(8)	11.358(7)
α (deg)	90	90
β (deg)	90	102.63(5)
γ (deg)	90	90
V (Å^3)	1150.49(13)	1255(1)
Z	4	4
D_x (Mg m^{-3})	1.041	1.124
Radiation, λ (Å)	Mo-Kα, 0.71069	Mo-Kα, 0.71069
μ (mm^{-1}), F(000)	0.062, 400	0.226, 464
Crystal size (mm^3)	0.42 × 0.35 × 0.34	0.90 × 0.20 × 0.15
Crystal colour, habit	colourless, prism	colourless, prism
Diffractometer	Bruker P4/RA (CCD)	Rigaku AFC5R
Scan type	Φ and ω	ω-2θ
Temperature (K)	193(2)	293(2)
Absorption correction method	empirical	Ψ-scan
Reflections collected	6717	1535
Independent reflections	1188	1435
Observed reflections ($I > 2\sigma(I)$)	1063	1370
R_{int}, range for θ (deg)	0.0290, 3.12 to 26.39	0.10108, 2.76 to 30.07
Index ranges h, k, l	-11 → 11 -11 → 11 -16 → 15	0 → 11, 0 → 15, -15 → 15
Parameters, restraints	61, 0	84, 33
R_1,[a] wR_2[b] (observed data)	0.0400, 0.1096	0.0433, 0.1168
R_1,[a] wR_2[b] (all data)	0.0438, 0.1128	0.2557, 0.1833
Extinction coefficient	-	0.002(2)
Goodness-of-fit S[c]	1.092	0.936
Final max. and min. for ρ (e Å^{-3})	0.239, -0.152	0.177, -0.147
Comments		Disordered *iso*-propyl and methyl groups.

([a]) $R_1 = (\Sigma |F_o| - |F_c|) / (\Sigma |F_o|)$. ([b]) $wR_2 = ((\Sigma w(F_o^2 - F_c^2)^2) / (\Sigma w(F_o^2)^2))^{1/2}$.
([c]) $S = ((\Sigma w(F_o^2 - F_c^2)) / (n - p))^{1/2}$, where n and p denote the number of reflections used in refinement and the number of parameters, respectively.
Weight schemes: $w = ((\sigma^2 \times F_o^2) + (A \times P)^2 + (B \times P))^{-1}$, where $P = 1/3(F_o^2 + 2F_c^2)$ and A, B = 0.0600, 0.2199 Im; 0, 0.0738 SIm.
Extinction: $F_c^* = kF_c (1 + 0.001(F_c^2 \times \lambda^3) / \mathrm{Sin}(2\theta)))^{-1/4}$, where k is the overall scaling factor.

References

1. Norman, N. C. *Periodicity and the p-Block Elements*; Oxford University Press: New York, 1994; Vol. 16, pp 52-54.

2. Norman, N. C. *Polyhedron* **1993**, *12*, 2431-2446.

3. Schoeller, W. W. In *Multiple Bonds and Low Coordination in Phosphorus Chemistry*; Regitz, M., Scherer, O. J., Eds.; Thieme Medical Publishers: New York, 1990; pp 5-32.

4. Kutzelnigg, W. *Angew. Chem., Int. Ed. Engl.* **1984**, *23*, 272-295.

5. Pauling, L. *The Nature of the Chemical Bond*; 3rd ed.; Cornell University Press: Ithaca, NY, 1960, pp 79-83.

6. Allen, L. C. *J. Am. Chem. Soc.* **1989**, *111*, 9003-9014.

7. Dasent, W. E. *Nonexistent Compounds. Compounds of Low Stability*; Marcel Dekker: New York, 1965, pp 163-164.

8. Cowley, A. H.; Norman, N. C. In *Prog. Inorg. Chem.*; Lippard, S. J., Ed.; John Wiley and Sons: New York, 1986; Vol. 34, pp 1-63.

9. Mingos, D. M. P. *Essential Trends in Inorganic Chemistry*; Oxford University Press: New York, 1998, pp 113-115.

10. Yoshifuji, M. *J. Organomet. Chem.* **2000**, *611*, 210-216.

11. Burford, N.; Clyburne, J. A. C.; Chan, M. S. W. *Inorg. Chem.* **1997**, *36*, 3204-3206.

12. Burford, N.; Clyburne, J. A. C.; Mason, S.; Richardson, J. F. *Inorg. Chem.* **1993**, *32*, 4988-4989.

13. Scherer, O. J.; Kuhn, N. *J. Organomet. Chem.* **1974**, *82*, C3-C6.

14. Markovskii, L. N.; Romanenko, V. D.; Drapailo, A. B.; Ruban, A. V.; Chernega, A. N.; Antipin, M. Y.; Struchkov, Y. T. *Zh. Obshch. Khim.* **1986**, *56*, 2231-2242.

15. Markovskii, L. N.; Romanenko, V. D.; Klebanskii, E. O.; Povolotskii, M. I.; Chernega, A. N.; Antipin, M. Y.; Struchkov, Y. T. *Zh. Obshch. Khim.* **1986**, *56*, 1721-1737.

16. Blättner, M.; Nieger, M.; Ruban, A.; Schoeller, W. W.; Niecke, E. *Angew. Chem., Int. Ed. Engl.* **2000**, *39*, 2768-2771.

17. Meisel, M.; Lönnecke, P.; Grimmer, A.-R.; Wulff-Molder, D. *Angew. Chem., Int. Ed. Engl.* **1997**, *36*, 1869-1870.

18. Suresh, C. H.; Koga, N. *Inorg. Chem.* **2000**, *39*, 3718-3721.

19. Driess, M.; Grützmacher, H. *Angew. Chem., Int. Ed. Engl.* **1996**, *35*, 826-856.

20. Abrams, M. B.; Scott, B. L.; Baker, R. T. *Organometallics* **2000**, *19*, 4944-4956.

21. Burford, N.; Royan , B. W.; Linden, A.; Cameron, T. S. *J. Chem. Soc., Chem. Commun.* **1988**, 842-844.

22. Burford, N.; Royan , B. W.; Linden, A.; Cameron, T. S. *Inorg. Chem.* **1989**, *28*, 144-150.

23. Burford, N.; Losier, P.; Bakshi, P. K.; Cameron, T. S. *J. Chem. Soc., Dalton Trans.* **1993**, 201-202.

24. Burford, N.; Losier, P.; Macdonald, C.; Kyrimis, V.; Bakshi, P. K.; Cameron, T. S. *Inorg. Chem.* **1994**, *33*, 1434-1439.

25. Burford, N.; Cameron, T. S.; Clyburne, J. A. C.; Eichele, K.; Robertson, K. N.; Sereda, S.; Wasylishen, R. E.; Whitla, W. A. *Inorg. Chem.* **1996**, *35*, 5460-5467.

26. Carmalt, C. J.; Lomeli, V.; McBurnett, B. G.; Cowley, A. H. *J. Chem. Soc., Chem. Commun.* **1997**, 2095-2096.

27. Cowley, A. H.; Cushner, M. C.; Szobota, J. S. *J. Am. Chem. Soc.* **1978**, *100*, 7784-7786.

28. Cowley, A. H.; Cushner, M. C.; Lattman, M.; McKee, M. L.; Szobota, J. S.; Wilburn, J. C. *Pure Appl. Chem.* **1980**, *52*, 789-797.

29. Cowley, A. H.; Lattman, M.; Wilburn, J. C. *Inorg. Chem.* **1981**, *20*, 2916-2919.

30. Cowley, A. H.; Kemp, R. A. *Chem. Rev.* **1985**, *85*, 367-382.

31. Denk, M. K.; Gupta, S.; Ramachandran, R. *Tetrahedron Lett.* **1996**, *37*, 9025-9028.

32. Denk, M. K.; Gupta, S.; Lough, A. J. *Eur. J. Inorg. Chem.* **1999**, 41-49.

33. Drapailo, A. B.; Chernega, A. N.; Romanenko, V. D.; Madhouni, R.; Sotiropoulos, J. M.; Lamandé, L.; Sanchez, M. *J. Chem. Soc., Dalton Trans.* **1994**, 2925-2931.

34. Gudat, D.; Haghverdi, A.; Hupfer, H.; Nieger, M. *Chem. Eur. J.* **2000**, *6*, 3414-3425.

35. Gudat, D.; Nieger, M.; Niecke, E. *J. Chem. Soc., Dalton Trans.* **1989**, 693-700.

36. Jones, V. A.; Thornton-Pett, M.; Kee, T. P. *J. Chem. Soc., Chem. Commun.* **1997**, 1317-1318.

37. Jones, V. A.; Sriprang, S.; Thornton-Pett, M.; Kee, T. P. *J. Organomet. Chem.* **1998**, *567*, 199-218.

38. Niecke, E.; David, G.; Detsch, R.; Kramer, B.; Nieger, M.; Wenderoth, P. *Phosphorus, Sulfur Silicon Relat. Elem.* **1993**, *76*, 25-28.

39. Nieger, M.; Niecke, E.; Detsch, R. *Z. Kristallogr.* **1995**, *210*, 971-972.

40. Payrastre, c.; Madaule, Y.; Wolf, J. G.; Kim, T. C.; Mazières, M. R.; Wolf, R.; Sanchez, M. *Heteroat. Chem.* **1992**, *3*, 157-162.

41. Sanchez, M.; Mazières, M. R.; Lamandé, L.; Wolf, R. In *Multiple Bonds and Low Coordination in Phosphorus Chemistry*; Regitz, M., Scherer, O. J., Eds.; Thieme Medical Publishers: New York, 1990; pp 129-148.

42. Reed, R. W.; Xie, Z.; Reed, C. A. *Organometallics* **1995**, *14*, 5002-5004.

43. Schultz, C. W.; Parry, R. W. *Inorg. Chem.* **1976**, *15*, 3046-3050.

44. Thomas, M. G.; Schultz, C. W.; Parry, R. W. *Inorg. Chem.* **1977**, *16*, 994-1001.

45. Veith, M.; Kruhs, W.; Huch, V. *Phosphorus, Sulfur Silicon Relat. Elem.* **1995**, *105*, 217-220.

46. Carré, F.; Chuit, C.; Corriu, R. J. P.; Mehdi, A.; Reyé, C. *J. Organomet. Chem.* **1997**, *529*, 59-68.

47. Carré, F.; Chuit, C.; Corriu, R. J. P.; Monforte, P.; Nayyar, N. K.; Reyé, C. *J. Organomet. Chem.* **1995**, *499*, 147-154.

48. Kuhn, N.; Fahl, J.; Blaser, D.; Boese, R. *Z. Anorg. Allg. Chem.* **1999**, *625*, 729-734.

49. Rosenthal, M. R. *J. Chem. Educ.* **1973**, *50*, 331-335.

50. Bochmann, M. *Angew. Chem., Int. Ed. Engl.* **1992**, *31*, 1181-1182.

51. Strauss, S. H. *Chem. Rev.* **1993**, *93*, 927-942.

52. Steudel, R.; Nachod, F. C.; Zukerman, J. J. *Chemistry of the Non-metals*; Walter de Gruyter and Company: Berlin, 1977, pp 69-71.

53. Enjalbert, R.; Savariault, J.-M.; Legros, J.-P. *C. R. Acad. Sc. Paris* **1980**, *C290*, 239-241.

54. Kibardin, A. M.; Litvinov, I. A.; Naumov, V. A.; Struchkov, Y. T.; Gryaznova, T. V.; Mikhalov, Y. B.; Pudovik, A. N. *Dokl. Akad. Nauk SSSR* **1988**, *298*, 369-373.

55. Emsley, J. *The Elements*; 3rd ed.; Clarendon Press: Oxford, 1998.

56. Dean, J. A. *Lange's Handbook of Chemistry*; 15th ed.; McGraw-Hill: New York, 1999, pp 4.30-4.34.

57. Ladd, M. F. C. *Structure and Bonding in Solid State Chemistry*; Ellis Horwood: New York, 1979, p 253.

58. Lambert, J. B.; Zhang, S.; Stern, C. L.; Huffman, J. C. *Science* **1993**, *260*, 1917-1918.

59. Schleyer, P. v. R.; Buzek, P.; Müller, T.; Apeloig, Y.; Siehl, H.-U. *Angew. Chem., Int. Ed. Engl.* **1993**, *32*, 1471.

60. Pauling, L. *Science* **1994**, *263*, 983-983.

61. Quin, L. D. *A Guide to Organophosphorus Chemistry*; John Wiley and Sons: New York, 2000, pp 8-10.

62. Wolf, R. *Pure Appl. Chem.* **1980**, *152*, 1141-1150.

63. Nelson, P. G. *J. Chem. Educ.* **1997**, *74*, 465-470.

64. Maier, L. In *Prog. Inorg. Chem.*; Cotton, F. A., Ed.; Interscience: New York, 1963; Vol. 5, pp 27-210.

65. Levason, W. In *The chemistry of organophosphorus compounds; primary, secondary, and tertiary phosphines, polyphosphines and heterocyclic organophosphorus(III) compounds*; Hartley, F. R., Ed.; John Wiley and Sons: New York, 1990; Vol. 1, pp 567-642.

66. McAuliffe, C. A. In *Comprehensive Coordination Chemistry*; Wilkinson, G., Gillard, R. D., McCleverty, J. A., Eds.; Pergamon Press: New York, 1987; Vol. 2, pp 989-1066.

67. Regitz, M. In *Multiple Bonds and Low Coordination in Phosphorus Chemistry*; Regitz, M., Scherer, O. J., Eds.; Thieme Medical Publishers: New York, 1990; pp 58-111.

68. Regitz, M. In *Heteroatom Chemistry*; Block, E., Ed.; VCH Publishers: Weinheim, 1990; pp 295-322.

69. Nixon, J. F. *Chem. Rev.* **1988**, *88*, 1327-1362.

70. Appel, R. In *Multiple Bonds and Low Coordination in Phosphorus Chemistry*; Regitz, M., Scherer, O. J., Eds.; Thieme Medical Publishers: New York, 1990; pp 157-219.

71. Märkl, G. In *Multiple Bonds and Low Coordination in Phosphorus Chemistry*; Regitz, M., Scherer, O. J., Eds.; Thieme Medical Publishers: New York, 1990; pp 220-257.

72. Schmidpeter, A.; Karaghiosoff, K. In *Multiple Bonds and Low Coordination in Phosphorus Chemistry*; Regitz, M., Scherer, O. J., Eds.; Thieme Medical Publishers: New York, 1990; pp 258-292.

73. Dillon, K. B.; Mathey, F.; Nixon, J. F. *Phosphorus: The Carbon Copy*; John Wiley and Sons: New York, 1998, pp 1-13.

74. Niecke, E.; Böske, J.; Gudat, D.; Güth, W.; Lysek, M.; Symalla, E. *Nova Acta Leopold* **1985**, *59*, 83-91.

75. Niecke, E.; Gudat, D.; Leuer, M.; Lysek, M.; Symalla, E. *Phosphorus, Sulfur Silicon Relat. Elem.* **1987**, *30*, 467-470.

76. Gudat, D. *Eur. J. Inorg. Chem.* **1998**, 1087-1094.

77. Gudat, D. *Coord. Chem. Rev.* **1997**, *163*, 71-106.

78. Yoshifuji, M. In *Multiple Bonds and Low Coordination in Phosphorus Chemistry*; Regitz, M., Scherer, O. J., Eds.; Thieme Medical Publishers: New York, 1990; pp 321-337.

79. Niecke, E.; Rüger, R. *Angew. Chem., Int. Ed. Engl.* **1983**, *22*, 155-156.

80. Gevrey, S.; Taphanel, M.-H.; Morizur, J.-P. *J. Mass. Spec.* **1998**, *33*, 399-402.

81. Cowley, A. H.; Kemp, R. A.; Lasch, J. G.; Norman, N. C.; Stewart, C. A.; Whittlesey, B. R.; Wright, T. C. *Inorg. Chem.* **1986**, *25*, 740-749.

82. SooHoo, C. K.; Baxter, S. G. *J. Am. Chem. Soc.* **1983**, *105*, 7443-7444.

83. Niecke, E.; Lysek, M. *Tetrahedron Lett.* **1988**, *29*, 605-606.

84. Romanenko, V. D.; Drapailo, A. B.; Ruban, A. V.; Markovskii, L. N. *Zh. Obshch. Khim.* **1987**, *57*, 1402-1403.

85. Gonbeau, D.; Pfister-Guillouzo, G.; Barrans, J. *Can. J. Chem.* **1983**, *61*, 1371-1378.

86. Schoeller, W. W.; Niecke, E. *J. Chem. Soc., Chem. Commun.* **1982**, 569-570.

87. Niecke, E.; Gudat, D.; Schoeller, W. W.; Rademacher, P. *J. Chem. Soc., Chem. Commun.* **1985**, 1050-1051.

88. David, G.; Von der Gönna, V.; Niecke, E.; Busch, T.; Schoeller, W. W.; Rademacher, P. *J. Chem. Soc., Faraday Trans.* **1994**, *90*, 2611-2616.

89. Scherer, O. J. *Angew. Chem., Int. Ed. Engl.* **1985**, *24*, 924-943.

90. Niecke, E. In *Multiple Bonds and Low Coordination in Phosphorus Chemistry*; Regitz, M., Scherer, O. J., Eds.; Thieme Medical Publishers: New York, 1990; pp 293-320.

91. Burford, N.; Losier, P.; Bakshi, P. K.; Cameron, T. S. *J. Chem. Soc., Chem. Commun.* **1996**, 307-308.

92. David, G.; Niecke, E.; Nieger, M.; Radseck, J.; Schoeller, W. W. *J. Am. Chem. Soc.* **1994**, *116*, 2191-2192.

93. Burford, N.; Clyburne, J. A. C.; Bakshi, P. K.; Cameron, T. S. *Organometallics* **1995**, *14*, 1578-1585.

94. Burford, N.; Clyburne, J. A. C.; Bakshi, P. K.; Cameron, T. S. *J. Am. Chem. Soc.* **1993**, *115*, 8829-8830.

95. Romanenko, V. D.; Rudzevich, V. L.; Rusanov, E. B.; Chernega, A. N.; Senio, A.; Sotiropoulos, J. M.; Pfister-Guillouzo, G.; Sanchez, M. *J. Chem. Soc., Chem. Commun.* **1995**, 1383-1385.

96. Bouhadir, G.; Reed, R. W.; Réau, R.; Bertrand, G. *Heteroat. Chem.* **1995**, *6*, 371-375.

97. Reed, R.; Réau, R.; Dahan, F.; Bertrand, G. *Angew. Chem., Int. Ed. Engl.* **1993**, *32*, 399-401.

98. Sanchez, M.; Cosledan, F.; Sotiropoulos, J. M.; Lamandé, L.; Drapailo, A. B.; Gudima, A. O.; Romanenko, V. D. *Tetrahedron Lett.* **1995**, *36*, 2085-2088.

99. Wiberg, N.; Schurz, K.; Müller, G.; Riede, J. *Angew. Chem., Int. Ed. Engl.* **1988**, *27*, 935-936.

100. Patsanovskii, I. I.; Stepanova, Y. Z.; Ishmaeva, É. A.; Romanenko, V. D.; Markovskii, L. N. *Zh. Obshch. Khim.* **1993**, *63*, 561-564.

101. Patsanovskii, I. I.; Stepanova, Y. Z.; Ishmaeva, É. A.; Romanenko, V. D.; Markovskii, L. N. *Zh. Obshch. Khim.* **1990**, *60*, 502-504.

102. Niecke, E.; Gudat, D. *Angew. Chem., Int. Ed. Engl.* **1991**, *30*, 217-237.

103. Markovskii, L. N.; Romanenko, V. D.; Ruban, A. V. *Zh. Obshch. Khim.* **1987**, *57*, 1433-1464.

104. Fluck, E. In *Topics in Phosphorus Chemistry*; Grayson, M., Griffith, E. J., Eds.; John Wiley and Sons: New York, 1980; Vol. 10, pp 291-481.

105. Neilson, R. H. In *Encyclopedia of Inorganic Chemistry*; King, R. B., Ed.; John Wiley and Sons: New York, 1994; Vol. 6, pp 3180-3199.

106. Niecke, E.; Lysek, M.; Symalla, E. *Chimia* **1986**, *40*, 202-205.

107. Ahlemann, J.-T.; Roesky, H. W.; Murugavel, R.; Parisini, E.; Noltemeyer, M.; Schmidt, H.-G.; Müller, O.; Herbst-Irmer, R.; Markovskii, L. N.; Shermolovich, Y. G. *Chem. Ber.* **1997**, *130*, 1113-1121.

108. Chernega, A. N.; Antipin, M. Y.; Struchkov, Y. T.; Ruban, A. V.; Romanenko, V. D. *Zh. Strukt. Khim.* **1987**, *28*, 105-110.

109. Zurmühlen, F.; Regitz, M. *New J. Chem.* **1989**, *13*, 335-340.

110. Schick, G.; Loew, A.; Nieger, M.; Niecke, E. *Heteroat. Chem.* **1996**, *7*, 427-435.

111. Niecke, E.; Detsch, R.; Nieger, M. *Chem. Ber.* **1990**, *123*, 797-799.

112. Detsch, R.; Niecke, E.; Nieger, M.; Reichert, F. *Chem. Ber.* **1992**, *125*, 321-330.

113. Schoeller, W. W.; Busch, T.; Niecke, E. *Chem. Ber.* **1990**, *123*, 1653-1654.

114. Schoeller, W. W.; Busch, T.; Haug, W. *Phosphorus, Sulfur Silicon Relat. Elem.* **1990**, *49/50*, 285-288.

115. Glaser, R.; Horan, C. J.; Choy, G. S.-C.; Harris, B. L. *J. Phys. Chem.* **1992**, *96*, 3689-3697.

116. Glaser, R.; Horan, C. J.; Choy, G. S.-C.; Harris, B. L. *Phosphorus, Sulfur Silicon Relat. Elem.* **1993**, *77*, 73-76.

117. Gudat, D.; Niecke, E. *Fresenius. J. Anal. Chem.* **1997**, *357*, 482-484.

118. Rozhenko, A. B.; Povolotskii, M. I.; Polovinko, V. V. *Magn. Reson. Chem.* **1996**, *34*, 269-275.

119. Gudat, D.; Hoffbauer, W.; Rozhenko, A. B.; Schoeller, W. W.; Povolotskii, M. I. *Magn. Reson. Chem.* **2000**, *38*, 861-866.

120. Bulloch, G.; Keat, R.; Thompson, D. G. *J. Chem. Soc., Dalton Trans.* **1977**, 99-104.

121. Zeiss, W.; Weis, J. *Z. Naturforsch., B: Chem. Sci.* **1977**, *32*, 485-487.

122. Kagan, H. B.; Sasaki, M. In *The chemistry of organophosphorus compounds; primary, secondary, and tertiary phosphines, polyphosphines and heterocyclic organophosphorus(III) compounds*; Hartley, F. R., Ed.; John Wiley and Sons: New York, 1990; Vol. 1, pp 51-102.

123. Niecke, E.; Nieger, M.; Reichert, F. *Angew. Chem., Int. Ed. Engl.* **1988**, *27*, 1715-1716.

124. Chernega, A. N.; Korkin, A. A.; Aksinenko, N. E.; Ruban, A. V.; Romanenko, V. D. *Zh. Obshch. Khim.* **1990**, *60*, 2462-2469.

125. Enjalbert, R.; Galy, J. *Acta Crystallogr., Sect. B* **1979**, *35*, 546-550.

126. Lance, E. T.; Haschke, J. M.; Peacor, D. R. *Inorg. Chem.* **1976**, *15*, 780-781.

127. Chernega, A. N.; Korkin, A. A.; Romanenko, V. D.; Koidan, G. N.; Marchenko, A. P. *Struct. Chem.* **1997**, *8*, 343-352.

128. Romanenko, V. D.; Kachkovskaya, L. S.; Povolotskii, M. I.; Chernega, A. N.; Antipin, M. Y.; Struchkov, Y. T.; Markovskii, L. N. *Zh. Obshch. Khim.* **1988**, *58*, 849-858.

129. Chernega, A. I.; Antipin, M. Y.; Struchkov, Y. T.; Ruban, A. V.; Romanenko, V. D. *Zh. Strukt. Khim.* **1990**, *31*, 134-140.

130. Niecke, E.; Detsch, R.; Nieger, M.; Reichert, F.; Schoeller, W. W. *Bull. Soc. Chim. Fr.* **1993**, *130*, 25-31.

131. Allen, F. H.; Kennard, O.; Watson, D. G.; Brammer, L.; Orpen, G. A.; Taylor, R. *J. Chem. Soc., Perkin Trans. 2* **1987**, S1-S19.

132. Olah, G. A.; Prakash, G. K. S.; Sommer, J. *Superacids*; John Wiley and Sons: New York, 1985, pp 36-37.

133. Lawrance, G. A. *Chem. Rev.* **1986**, *86*, 17-33.

134. Dixon, N. E.; Lawrance, G. A.; Lay, P. A.; Sargeson, A. M.; Taube, H. In *Inorganic Syntheses; Reagents for Transition Metal Complex and Organometallic Synthesis*; Angelici, R. J., Ed.; John Wiley and Sons: New York, 1990; Vol. 28, pp 70-76.

135. Gudat, D.; Schiffner, H. M.; Nieger, M.; Stalke, D.; Blake, A. J.; Grondey, H.; Niecke, E. *J. Am. Chem. Soc.* **1992**, *114*, 8857-8862.

136. Barion, D.; Gartner-Winkhaus, C.; Link, M.; Nieger, M.; Niecke, E. *Chem. Ber.* **1993**, *126*, 2187-2195.

137. Niecke, E.; Gudat, D. In *Phosphorus-31 NMR Spectral Properties in Compound Characterization and Structural Analysis*; Quin, L. D., Verkade, J. G., Eds.; VCH Publishers: Weinheim, 1994; pp 159-174.

138. Niecke, E.; Nieger, M.; Reichert, F.; Schoeller, W. W. *Angew. Chem., Int. Ed. Engl.* **1988**, *27*, 1713-1714.

139. Pötschke, N.; Barion, D.; Nieger, M.; Niecke, E. *Tetrahedron* **1995**, *51*, 8993-8996.

140. Niecke, E.; Hein, J.; Nieger, M. *Organometallics* **1989**, *8*, 2290-2291.

141. Pötschke, N.; Nieger, M.; Niecke, E. *Acta Chem. Scand.* **1997**, *51*, 337-339.

142. Romanenko, V. D.; Reitel, G. V.; Kachkovskaya, L. S.; Mikolaichik, M.; Omelyanchuk, Y.; Pérlikovska, V. *Zh. Obshch. Khim.* **1993**, *63*, 1182-1184.

143. Romanenko, V. D.; Ruban, A. V.; Reitel, G. V.; Povolotskii, M. I.; Markovskii, L. N. *Zh. Obshch. Khim.* **1989**, *59*, 2129-2131.

144. Niecke, E.; Nieger, M.; Gärtner-Winkhaus, C.; Kramer, B. *Chem. Ber.* **1990**, *123*, 477-479..

145. David, G.; Niecke, E.; Nieger, M.; von der Gönna, V.; Schoeller, W. W. *Chem. Ber.* **1993**, *126*, 1513-1517.

146. Barion, D.; David, G.; Link, M.; Nieger, M.; Niecke, E. *Chem. Ber.* **1993**, *126*, 649-655.

147. Hein, J.; Gärtner-Winkhaus, C.; Nieger, M.; Niecke, E. *Heteroat. Chem.* **1991**, *2*, 409-415.

148. Romanenko, V. D.; Ruban, A. V.; Reitel, G. C.; Chernega, A. N.; Markovskii, L. N. *Dokl. Akad. Nauk SSSR* **1990**, *313*, 869-872.

149. Markovskii, L. N.; Romanenko, V. D.; Ruban, A. V.; Sarina, T. V.; Povolotskii, M. I.; Luré, L. F. *Zh. Obshch. Khim.* **1991**, *61*, 401-406.

150. Burford, N.; Clyburne, J. A. C.; Bakshi, P. K.; Cameron, T. S. *Phosphorus, Sulfur Silicon Relat. Elem.* **1994**, *93*, 379-380.

151. Burford, N.; Clyburne, J. A. C.; Gates, D. P.; Schriver, M. J.; Richardson, J. F. *J. Chem. Soc., Dalton Trans.* **1994**, 997-1001.

152. Burford, N.; Clyburne, J. A. C.; Losier, P.; Parks, T. M. In *Synthetic Methods of Organometallic and Inorganic Chemistry*; Karsch, H. H., Ed.; Georg Thieme Verlag: Stuttgart, 1996; Vol. 3, pp 21-28.

153. Markovskii, L. N.; Ruban, A. V.; Chernega, A. N.; Povolotskii, M. I.; Reitel, G. V.; Romanenko, V. D. *Dokl. Akad. Nauk SSSR* **1989**, *306*, 1137-1140.

154. Niecke, E.; Altmeyer, O.; Barion, D.; Detsch, R.; Gärtner, C.; Hein, J.; Nieger, M.; Reichert, F. *Phosphorus, Sulfur Silicon Relat. Elem.* **1990**, *49/50*, 321-324.

155. Niecke, E.; Kröher, R. *Angew. Chem., Int. Ed. Engl.* **1976**, *15*, 692-693.

156. Oberdörfer, R.; Nieger, M.; Niecke, E. *Chem. Ber.* **1994**, *127*, 2397-2401.

157. Cowley, A. H.; Kemp, R. A. *J. Chem. Soc., Chem. Commun.* **1982**, 319-320.

158. Cowley, A. H.; Kemp, R. A. *Inorg. Chem.* **1983**, *22*, 547-550.

159. Curtis, J. M.; Burford, N.; Parks, T. M. *Org. Mass Spectrom.* **1994**, *29*, 414-418.

160. Zollinger, H. *Angew. Chem., Int. Ed. Engl.* **1978**, *17*, 141-150.

161. Schoeller, W. W.; Tubbesing, U. *J. Mol. Struct. (Theochem)* **1995**, *343*, 49-55.

162. David, G.; Niecke, E.; Nieger, M. *Tetrahedron Lett.* **1992**, *33*, 2335-2338.

163. Laplaza, C. E.; Davis, W. M.; Cummins, C. C. *Angew. Chem., Int. Ed. Engl.* **1995**, *34*, 2042-2044.

164. Niecke, E.; Nixon, J. F.; Wenderoth, P.; Passos, B. F. T.; Nieger, M. *J. Chem. Soc., Chem. Commun.* **1993**, 846-848.

165. Brown, I. D.; Skowom, A. *J. Am. Chem. Soc.* **1990**, *112*, 3401-3403.

166. Gutmann, V. *Angew. Chem., Int. Ed. Engl.* **1970**, *9*, 843-860.

167. Schmutzler, R. In *Halogen Chemistry*; Gutmann, V., Ed.; Academic Press: New York, 1967; Vol. 2, pp 31-113.

168. Dean, P. A. W.; Gillespie, R. J.; Hulme, R.; Humphreys, D. A. *J. Chem. Soc. A* **1971**, 341-346.

169. Sheldrick, W. S.; Kiefer, J. *Z. Naturforsch., B: Chem. Sci.* **1989**, *44*, 609-611.

170. Sheldrick, W. S.; Schmidpeter, A.; Zwaschka, F.; Dillon, K. B.; Platt, A. W. G.; Waddington, T. C. *J. Chem. Soc., Dalton Trans.* **1981**, 413-418.

171. Chernega, A. N.; Korkin, A. A.; Antipin, M. Y.; Struchkov, Y. T.; Ruban, A. V.; Romanenko, V. D. *Zh. Obshch. Khim.* **1989**, *59*, 2243-2253.

172. Eichele, K.; Wasylishen, R. E.; Schurko, R. W.; Burford, N.; Whitla, W. A. *Can. J. Chem.* **1996**, *74*, 2372-2377.

173. Penner, G. H.; Wasylishen, R. E. *Can. J. Chem.* **1989**, *67*, 1909-1913.

174. Dixon, K. R. In *Multinuclear NMR*; Mason, J., Ed.; Plenum Press: New York, 1987; pp 369-402.

175. Berger, S.; Braun, S.; Kalinowski, H.-O. *NMR Spectroscopy of the Non-Metallic Elements*; John Wiley and Sons: New York, 1997, pp 756-758.

176. Wong, C. Y.; Kennepohl, D. K.; Cavell, R. G. *Chem. Rev.* **1996**, *96*, 1917-1951.

177. Webster, M. *Chem. Rev.* **1966**, *66*, 87-118.

178. Beattie, I. R.; Webster, M. *J. Chem. Soc., Dalton Trans.* **1961**, 1730-1733.

179. Muetterties, E. L.; Bither, T. A.; Farlow, M. W.; Coffman, D. D. *J. Inorg Nucl. Chem.* **1960**, *16*, 52-59.

180. Cameron, T. S.; Chan, C.; Chute, W. J. *Acta Crystallogr.*, **1980**, *B36*, 2391-2393.

181. Deng, R. M. K.; Dillon, K. B. *J. Chem. Soc., Dalton Trans.* **1984**, 1917-1920.

182. Schmidpeter, A.; von Criegern, T.; Blanck, K. *Z. Naturforsch., B: Chem. Sci.* **1976**, *31*, 1058-1063.

183. Dillon, K. B.; Reeve, R. N.; Waddington, T. C. *J. Chem. Soc., Dalton Trans.* **1978**, 1318-1323.

184. Deng, R. M. K.; Dillon, K. B. *J. Chem. Soc., Dalton Trans.* **1984**, 1911-1916.

185. Sheldrick, W. S. *J. Chem. Soc., Dalton Trans.* **1974**, 1402-1405.

186. Averbuch-Pouchot, M. T.; Meisel, M. *Acta Crystallogr., Sect. C* **1989**, *45*, 1937-1939.

187. Beattie, I. R.; Gilson, T. R.; Ozin, G. A. *J. Chem. Soc. A* **1968**, 2772-2778.

188. Meyer, B. N.; Ishley, J. N.; Fratini, A. V.; Knachel, H. C. *Inorg. Chem.* **1980**, *19*, 2324-2327.

189. Ishley, J. N.; Knachel, H. C. *Inorg. Chem.* **1975**, *14*, 2558-2560.

190. Well, M.; Jones, P. G.; Schmutzler, R. *J. Fluorine Chem.* **1991**, *53*, 261-275.

191. Von Criegern, T.; Schmidpeter, A. *Z. Naturforsch., B: Chem. Sci.* **1979**, *34*, 762-763.

192. John, K.-P.; Schmutzler, R.; Sheldrick, W. S. *J. Chem. Soc., Dalton Trans.* **1974**, 1841-1846.

193. Lamandé, L.; Munoz, A. *Tetrahedron Lett.* **1991**, *32*, 75-78.

194. Kerbs, B.; Schmutzler, R.; Schomburg, D. *Polyhedron* **1989**, *8*, 731-738.

195. Kaukorat, T.; Jones, P. G.; Schmutzler, R. *Z. Naturforsch., B: Chem. Sci.* **1992**, *47*, 755-759.

196. Kaukorat, T.; Jones, P. G.; Schmutzler, R. *Heteroat. Chem.* **1991**, *2*, 81-86.

197. Becker, W.; Jones, P. G.; Schomburg, D.; Schmutzler, R. *Chem. Ber.* **1990**, *123*, 1759-1766.

198. Yoshifuji, M.; Sangu, S.; Kamijo, K.; Toyota, K. *Chem. Ber.* **1996**, *129*, 1049-1055.

199. Kamijo, K.; Otoguro, A.; Toyota, K.; Yoshifuji, M. *Bull. Chem. Soc. Jpn.* **1999**, *72*, 1335-1342.

200. Wong, C. Y.; McDonald, R.; Cavell, R. G. *Inorg. Chem.* **1996**, *35*, 325-334.

201. Dillon, K. B.; Reeve, R. N.; Waddington, T. C. *J. Chem. Soc., Dalton Trans.* **1978**, 1465-1471.

202. Sheldrick, W. S.; Schmidpeter, A.; von Criegern, T. *Z. Naturforsch., B: Chem. Sci.* **1978**, *33*, 583-587.

203. Ziegler, M. L.; Weiss, J. *Angew. Chem., Int. Ed. Engl.* **1968**, *8*, 455-456.

204. Timosheva, N. V.; A., C.; Day, R. O.; Holmes, R. R. *Inorg. Chem.* **1998**, *37*, 4945-4952.

205. Holmes, R. R. *J. Am. Chem. Soc.* **1960**, *82*, 1295-1299.

206. Chuit, C.; Corriu, R. J. P.; Monforte, P.; Reyé, C.; Declercq, J.-P.; Dubourg, A. *J. Organomet. Chem.* **1996**, *511*, 171-175.

207. Chauhan, M.; Chuit, C.; Corriu, R. J. P.; Reyé, C.; Declercq, J.-P.; Dubourg, A. *J. Organomet. Chem.* **1996**, *510*, 173-179.

208. Chuit, C.; Corriu, R. J. P.; Monforte, P.; Reyé, C.; Declercq, J.-P.; Dubourg, A. *Angew. Chem., Int. Ed. Engl.* **1993**, *32*, 1430-1432.

209. Chuit, C.; Reyé, C. *Eur. J. Inorg. Chem.* **1998**, 1847-1857.

210. Roper, W. R.; Wilkins, C. J. *Inorg. Chem.* **1964**, *3*, 500-502.

211. Weiss, R.; Engel, S. *Angew. Chem., Int. Ed. Engl.* **1992**, *31*, 216-217.

212. Bezombes, J.-P.; Carré, F.; Chuit, C.; Corriu, R. J. P.; Mehdi, A.; Reyé, C. *J. Organomet. Chem.* **1997**, *535*, 81-90.

213. Losier, P. Dissertation, Dalhousie University: Halifax, NS, 1995.

214. Blättner, M.; Ruban, A. V.; Gudat, D.; Nieger, M.; Niecke, E. *Phosphorus, Sulfur Silicon Relat. Elem.* **1999**, *147*, 31.

215. Burford, N.; Cameron, T. S.; LeBlanc, D. J.; Phillips, A. D.; Concolino, T. E.; Lam, K.-C.; Rheingold, A. L. *J. Am. Chem. Soc.* **2000**, *122*, 5413-5414.

216. Burford, N.; Cameron, T. S.; Robertson, K. N.; Phillips, A. D.; Jenkins, H. A. *J. Chem. Soc., Chem. Commun.* **2000**, 2087-2088.

217. Trinquier, G. *J. Am. Chem. Soc.* **1986**, *108*, 568-577.

218. Benoit, R. L.; Lefebvre, D.; Fréchette, M. *Can. J. Chem.* **1987**, *65*, 996-1001.

219. Benoit, R. L.; Mackinnon, M. J.; Bergeron, L. *Can. J. Chem.* **1981**, *59*, 1501-1504.

220. Howard, P. H.; Meylan, W. M., Eds. *Handbook of Physical Properties of Organic Chemicals*; CRC Press: Bocta Raton, Fl, 1997, p 318.

221. Perrin, D. D. *Dissociation Constants of Organic Bases in Aqueous Solution*; Butterworths: London, 1965, p 1032.

222. Lide, D. R. *CRC Handbook of Chemistry and Physics*; 81st ed.; CRC Press: Boca Raton, Fl., 2000, pp 8-44.

223. Schoeller, W. W.; Schneider, R.; Tubbesing, U. *Phosphorus, Sulfur Silicon Relat. Elem.* **1999**, *144-146*, 781-784.

224. Mootz, D.; Wussow, H.-G. *J. Chem. Phys.* **1981**, *75*, 1517-1522.

225. Ülkü, D.; Huddle, B.; Morrow, J. C. *Acta Crystallogr., Sect. B* **1971**, *27*, 432-436.

226. Töpel, v. K.; Hensen, K.; Bats, J. W. *Acta Crystallogr., Sect. C* **1984**, *40*, 828-830.

227. Banks, R. E.; Besheesh, M. K.; Pritchard, R. G.; Sharif, I. *Acta Crystallogr., Sect. C* **1993**, *49*, 1804-1806.

228. Blackstock, S. C.; Lorand, J. P.; Kochi, J. K. *J. Org. Chem.* **1987**, *52*, 1451-1460.

229. Fourme, R. *Journal de Physique* **1979**, *40*, 557-561.

230. Merritt, L. L.; Schroeder, E. D. *Acta Crystallogr.*, **1956**, *9*, 801-804.

231. Dedert, P. L.; Sorrell, T.; Marks, T. J.; Ibers, J. A. *Inorg. Chem.* **1982**, *21*, 3506-3517.

232. Gudat, D.; Niecke, E.; Grossmann, G.; Krüger, K. *Magn. Reson. Chem.* **1999**, *37*, 43-47.

233. Constable, E. C. *Metals and Ligand Reactivity: an introduction to the organic chemistry of metal complexes. New, rev. and expanded ed.*; VCH Publishers: Weinheim, 1996, pp 26-27.

234. Castellano, S.; Günther, H.; Ebersole, S. *J. Phys. Chem.* **1965**, *69*, 4166-4176.

235. Batterham, T. J. *NMR Spectra of Simple Heterocycles*; John Wiley and Sons: New York, 1973, p 26.

236. Bellavance, P.; Corey, E. R.; Corey, J. Y.; W., H. G. *Inorg. Chem.* **1977**, *16*, 462-467.

237. Griffith, W. P. In *Developments in Inorganic Nitrogen Chemistry*; Colburn, C. B., Ed.; Elsevier Science Publishing: Amsterdam, 1966; Vol. 1, pp 242-306.

238. Reedijk, J. In *Comprehensive Coordination Chemistry*; Wilkinson, G., Gillard, R. D., McCleverty, J. A., Eds.; Pergamon Press: New York, 1987; Vol. 2, pp 73-98.

239. Kettle, S. F. A. *Physical Inorganic Chemistry. A Coordination Chemistry Approach*; Spektrum Academic: Oxford, 1996, pp 84-89.

240. Hitchcock, P. B.; Lappert, M. F.; Rai, A. K.; Williams, H. D. *J. Chem. Soc., Chem. Commun.* **1986**, 1633-1634.

241. Chernega, A. N.; Korkin, A. A.; Romanenko, V. D. *Zh. Obshch. Khim.* **1995**, *65*, 1823-1833.

242. Chernega, A. N.; Antipin, M. Y.; Struchkov, Y. T.; Drapailo, A. B.; Romanenko, V. D. *Zh. Strukt. Khim.* **1990**, *31*, 124-133.

243. Pohl, S. *Chem. Ber.* **1979**, *112*, 3159-3165.

244. Chernega, A. N.; Korkin, A. A.; Antipin, M. Y.; Struchkov, Y. T. *Zh. Obshch. Khim.* **1988**, *58*, 2045-2056.

245. Niecke, E.; Altmeyer, O.; Nieger, M. *Angew. Chem., Int. Ed. Engl.* **1991**, *30*, 1136-1138.

246. Storzer, W.; Schomburg, D.; Röschenthaler, G.-V.; Schmutzler, R. *Chem. Ber.* **1983**, *116*, 367-374.

247. Kennepohl, D. K.; Pinkerton, A. A.; Lee, F. Y.; Cavell, R. G. *Inorg. Chem.* **1990**, *29*, 5088-5096.

248. Becker, W.; Schomburg, D.; Schmutzler, R. *Phosphorus, Sulfur Silicon Relat. Elem.* **1989**, *42*, 21-35.

249. Liu, X.-D.; Verkade, J. G. *Inorg. Chem.* **1998**, *37*, 5189-5197.

250. Kaukorat, T.; Ernst, L.; Schmutzler, R.; Schomburg, D. *Polyhedron* **1990**, *9*, 1463-1467.

251. John, K.-P.; Schmutzler, R.; Sheldrick, W. S. *J. Chem. Soc., Dalton Trans.* **1974**, 2466-2468.

252. Kaukorat, T.; Jones, P. G.; Schmutzler, R. *Phosphorus, Sulfur Silicon Relat. Elem.* **1992**, *68*, 9-13.

253. Kaukorat, T.; Jones, P. G.; Schmutzler, R. *Chem. Ber.* **1991**, *124*, 1335-1346.

254. Tang, J.; Mohan, T.; Verkade, J. G. *J. Org. Chem.* **1994**, *59*, 4931-4938.

255. Gudat, D.; Hoffbauer, W.; Niecke, E.; Schoeller, W. W.; Fleischer, U.; Kutzelnigg, W. *J. Am. Chem. Soc.* **1994**, *116*, 7325-7331.

256. Markovskii, L. N.; Romanenko, V. D.; Ruban, A. V.; Drapailo, A. B.; Reitel, G. V.; Chernega, A. N.; Povolotskii, M. I. *Zh. Obshch. Khim.* **1990**, *60*, 2453-2462.

257. Cowley, A. H.; Kemp, R. A.; Wilburn, J. C. *Inorg. Chem.* **1981**, *20*, 4289-4293.

258. Arduengo, A. J. III; Harlow, R. L.; Kline, M. *J. Am. Chem. Soc.* **1991**, *113*, 361-363.

259. Arduengo, A. J. III *Acc. Chem. Res.* **1999**, *32*, 913-921.

260. Alder, R. W.; Allen, P. R.; Murray, M.; Orpen, G. A. *J. Chem. Soc., Chem. Commun.* **1996**, 1121-1123.

261. Alder, R. W.; Butts, C. P.; Orpen, G. A. *J. Am. Chem. Soc.* **1998**, *120*, 11526-11527.

262. Bourissou, D.; Bertrand, G. *Adv. Organomet. Chem.* **1999**, *44*, 175-219.

263. Igau, A.; Grutzmacher, H.; Baceiredo, A.; Bertrand, G. *J. Am. Chem. Soc.* **1988**, *110*, 6463-6466.

264. Arduengo, A. J. III; Goerlich, J. R.; Marshall, W. J. *J. Am. Chem. Soc.* **1995**, *117*, 11027-11028.

265. Denk, M. K.; Thadani, A.; Hatano, K.; Lough, A. J. *Angew. Chem., Int. Ed. Engl.* **1997**, *36*, 2607-2608.

266. Kuhn, N.; Kratz, T. *Synthesis* **1993**, 561-562.

267. Arduengo, A. J. III; Dias, H. V. R.; Harlow, R. L.; Kline, M. *J. Am. Chem. Soc.* **1992**, *114*, 5530-5534.

268. Boesveld, W. M.; Gehrhus, B.; Hitchcock, P. B.; Lappert, M. F.; Schleyer, P. v. R. *J. Chem. Soc., Chem. Commun.* **1999**, 755-756.

269. Arduengo, A. J. III; Goerlich, J. R.; Marshall, W. J. *Liebigs Ann. Chem.* **1997**, 365-374.

270. Alder, R. W.; Allen, P. R.; Williams, S. J. *J. Chem. Soc., Chem. Commun.* **1995**, 1267-1268.

271. Bourissou, D.; Guerret, O.; Gabbaï, F. P.; Bertrand, G. *Chem. Rev.* **2000**, *100*, 39-91.

272. Regitz, M. *Angew. Chem., Int. Ed. Engl.* **1996**, *35*, 725-728.

273. Carmalt, C. J.; Cowley, A. H. In *Advances in Inorganic Chemistry*; Sykes, A. G., Cowley, A. H., Eds.; Academic Press: New York, 2000; Vol. 50, pp 1-32.

274. Arduengo, A. J. III; Krafczyk, R.; Marshall, W. J.; Schmutzler, R. *J. Am. Chem. Soc.* **1997**, *119*, 3381-3382.

275. Kuhn, N.; Gohner, M.; Henkel, G. *Z. Anorg. Allg. Chem.* **1999**, *625*, 1415-1416.

276. Arduengo, A. J. III; Dias, H. V. R.; Calabrese, J. C. *Chem. Lett.* **1997**, 143-144.

277. Arduengo, A. J. III; Calabrese, J. C.; Cowley, A. H.; Dias, H. V. R.; Goerlich, J. R.; Marshall, W. J.; Reigel, B. *Inorg. Chem.* **1997**, *36*, 2151-2158.

278. Arduengo, A. J. III; Carmalt, C. J.; Clyburne, J. A. C.; Cowley, A. H.; Pyati, R. *J. Chem. Soc., Chem. Commun.* **1997**, 981-982.

279. Schmidpeter, A. In *Multiple Bonds and Low Coordination in Phosphorus Chemistry*; Regitz, M., Scherer, O. J., Eds.; Thieme Medical Publishers: New York, 1990; pp 149-154.

280. Dimroth, K. In *Top. Curr. Chem.*, 1973; Vol. 38, pp 7-19.

281. Schinkels, B.; Ruban, A.; Nieger, M.; Niecke, E. *J. Chem. Soc., Chem. Commun.* **1997**, 293-294.

282. Poetschke, N.; Nieger, M.; Khan, M. A.; Niecke, E.; Ashby, M. T. *Inorg. Chem.* **1997**, *36*, 4087-4093.

283. Ruban, A.; Nieger, M.; Niecke, E. *Eur. J. Inorg. Chem.* **1998**, 83-85.

284. Ashby, M. T.; Li, Z. *Inorg. Chem.* **1992**, *31*, 1321-1322.

285. Izod, K. In *Advances in Inorganic Chemistry*; Sykes, A. G., Cowley, A. H., Eds.; Academic Press: New York, 2000; Vol. 50, pp 33-107.

286. Dunne, B. J.; Orpen, A. G. *Acta Crystallogr., Sect. C* **1991**, *47*, 345-347.

287. Appel, R.; Knoll, F. In *Advances in Inorganic Chemistry*; Sykes, A. G., Ed.; Academic Press: New York, 1989; Vol. 33, pp 259-361.

288. Grützmacher, H.; Pritzkow, H. *Angew. Chem., Int. Ed. Engl.* **1992**, *31*, 99-101.

289. Kuhn, N.; Bohnen, H.; Fahl, J.; Bläser, D.; Boese, R. *Chem. Ber.* **1996**, *129*, 1579-1586.

290. Romanenko, V. D.; Sanchez, M. *Coord. Chem. Rev.* **1997**, *158*, 275-324.

291. Akitt, J. W. *Prog. NMR Spec.* **1989**, *21*, 1-149.

292. Power, P. P. *Angew. Chem., Int. Ed. Engl.* **1990**, *29*, 449-460.

293. Markovskii, L. N.; Romanenko, V. D.; Pidvarko, T. I. *Zh. Obshch. Khim.* **1982**, *52*, 1925-1926.

294. Grützmacher, H.; Pritzkow, H. *Angew. Chem., Int. Ed. Engl.* **1991**, *30*, 709-710.

295. Heim, U.; Pritzkow, H.; Schönberg, H.; Grützmacher, H. *J. Chem. Soc., Chem. Commun.* **1993**, 673-674.

296. Igau, A.; Baceiredo, A.; Grützmacher, H.; Pritzkow, H.; Bertrand, G. *J. Am. Chem. Soc.* **1989**, *111*, 6853-6854.

297. Loss, S.; Widauer, C.; Grützmacher, H. *Angew. Chem., Int. Ed. Engl.* **1999**, *38*, 3329-3331.

298. Trinquier, G.; Ashby, M. T. *Inorg. Chem.* **1994**, *33*, 1306-1313.

299. Morris, E. D. J.; Nordman, C. E. *Inorg. Chem.* **1969**, *8*, 1673-1676.

300. Romanenko, V. D.; Ruban, A. V.; Markovski, L. N. *J. Chem. Soc., Chem. Commun.* **1983**, 187-189.

301. Roberts, B. P.; Singh, K. *J. Chem. Soc., Perkin Trans. 2* **1981**, 866-869.

302. Hein, J.; Niecke, E.; Nieger, M.; Wenderoth, P.; Nixon, J. F.; Passos, B. F. T.; Meidine, M. F. *Phosphorus, Sulfur Silicon Relat. Elem.* **1993**, *77*, 242.

303. Markovsky, L. N.; Romanenko, V. D.; Ruban, A. V.; Drapailo, A. B.; Reitel, G. C.; Sarina, T. V. *Phosphorus, Sulfur Silicon Relat. Elem.* **1990**, *49/50*, 329-332.

304. Chernega, A. N.; Antipin, M. Y.; Struchkov, Y. T.; Ruban, A.; Romanenko, V. D. *Zh. Strukt. Khim.* **1988**, *29*, 133-142.

305. Schmidpeter, A.; Gebler, W.; Zwaschka, F.; Sheldrick, W. S. *Angew. Chem., Int. Ed. Engl.* **1980**, *19*, 722-723.

306. Chernega, A. N.; Ruban, A. V.; Romanenko, V. D.; Markovski, L. N.; Korkin, A. A.; Antipin, M. Y.; Struchkov, Y. T. *Heteroat. Chem.* **1991**, *2*, 229-241.

307. Chernega, A. N.; Antipin, M. Y.; Struchkov, Y. T.; Boldeskul, I. E.; Sarina, T. V.; Romanenko, V. D. *Dokl. Akad. Nauk SSSR* **1984**, *278*, 1146-1150.

308. Day, R. O.; Willhalm, A.; Holmes, J. M.; Holmes, R. R.; Schmidpeter, A. *Angew. Chem., Int. Ed. Engl.* **1985**, *24*, 764-765.

309. Weber, L.; Uthmann, S.; Bögge, H.; Müller, A.; Stammler, H.-G.; B., N. *Organometallics* **1998**, *17*, 3593-3598.

310. Curtis, R. D.; Schriver, M. J.; Wasylishen, R. E. *J. Am. Chem. Soc.* **1991**, *113*, 1493-1498.

311. Povolotskii, M. I.; Negrebetskii, V. A.; Ruban, A. V.; Romanenko, V. D.; Chernega, A. N.; Muzyka, P. V.; Markovskii, L. N. *Zh. Obshch. Khim.* **1991**, *61*, 79-86.

312. Issleib, K.; Leißring, E.; Riemer, M.; Oehme, H. *Z. Chem.* **1983**, *23*, 99-100.

313. Oehme, H.; Leißring, E.; Meyer, H. *Z. Chem.* **1981**, *21*, 407-408.

314. Weber, L.; Kaminski, O. *Synthesis* **1995**, 158.

315. Schmidpeter, A.; Lochschmidt, S.; Willhalm, A. *Angew. Chem. Suppl.* **1983**, 710-717.

316. West, R.; Denk, M. *Pure Appl. Chem.* **1996**, *68*, 785-788.

317. Denk, M.; Lennon, R.; Hayashi, R.; West, R.; Belyakov, A. V.; Verne, H. P.; Haaland, A.; Wagner, M.; Metzler, N. *J. Am. Chem. Soc.* **1994**, *116*, 2691-2692.

318. Haaf, M.; Schmiedl, A.; Schmedake, T. A.; Powell, D. R.; Millevolte, A. J.; Denk, M.; West, R. *J. Am. Chem. Soc.* **1998**, *120*, 12714-12719.

319. Haaf, M.; Schmedake, T. A.; West, R. *Acc. Chem. Res.* **2000**, *33*, 704-714.

320. Gehrhus, B.; Lappert, M. F.; Heinicke, J.; Boese, R.; Bläser, D. *J. Chem. Soc., Chem. Commun.* **1995**, 1931-1932.

321. Arduengo, A. J. III; Bock, H.; Chen, H.; Denk, M.; Dixon, D. A.; Green, J. C.; Herrmann, W. A.; Jones, N. L.; Wagner, M.; West, R. *J. Am. Chem. Soc.* **1994**, *116*, 6641-6649.

322. Denk, M.; Green, J. C.; Metzler, N.; Wagner, M. *J. Chem. Soc., Dalton Trans.* **1994**, 2405-2410.

323. Heinemann, C.; Herrmann, W. A.; Thiel, W. *J. Organomet. Chem.* **1994**, *475*, 73-84.

324. Kira, M.; Ishida, S.; Iwamoto, T.; Kabuto, C. *J. Am. Chem. Soc.* **1999**, *121*, 9722-9723.

325. Weidenbruch, M. *Coord. Chem. Rev.* **1994**, *130*, 275-300.

326. Metzler, N.; Denk, M. *J. Chem. Soc., Chem. Commun.* **1996**, 2657-2658.

327. Timms, P. L. *Inorg. Chem.* **1968**, *7*, 387-389.

328. Schäfer, A.; Weidenbruch, M.; Saak, W.; Pohl, S. *Angew. Chem., Int. Ed. Engl.* **1987**, *26*, 776-777.

329. Weidenbruch, M.; Olthoff, S.; Peters, K.; von Schnering, H. G. *Chem. Commun.* **1997**, 1433-1434.

330. Clendenning, S. B.; Gehrhus, B.; Hitchcock, P. B.; Nixon, J. F. *J. Chem. Soc., Chem. Commun.* **1999**, 2451-2452.

331. Driess, M.; Rell, S.; Pritzkow, H. *J. Chem. Soc., Chem. Commun.* **1995**, 253-254.

332. Sheldrick, W. S. In *The Chemistry of Organic Silicon Compounds Part 1*; Patai, S., Rappoport, Z., Eds.; John Wiley and Sons: New York, 1989; pp 227-303.

333. Belzner, J.; Schär, D.; Kneisel, B. O.; Herbst-Irmer, R. *Organometallics* **1995**, *14*, 1840-1843.

334. Brook, M. A. *Silicon in Organic, Organometallic, and Polymer Chemistry*; John Wiley and Sons: New York, 2000, pp 31-34.

335. Chernega, A. N.; Antipin, M. Y.; Struchkov, Y. T.; Ruban, A. V.; Romanenko, V. D.; Markovskii, L. N. *Dokl. Akad. Nauk SSSR* **1989**, *307*, 610-612.

336. Marsmann, H. In *NMR, Basic Prinicples and Progress; Oxygen-17 and Silicon-29*; Diehl, P., Fluck, E., Kosfeld, R., Eds.; Springer-Verlag: New York, 1981; Vol. 17, pp 65-235.

337. Brook, M. A. *Silicon in Organic, Organometallic, and Polymer Chemistry*; John Wiley and Sons: New York, 2000, pp 40-51.

338. Denk, M. K.; Hatano, K.; Lough, A. J. *Eur. J. Inorg. Chem.* **1998**, 1067-1070.

339. Lambert, J. B.; Zhang, S.; Ciro, S. M. *Organometallics* **1994**, *13*, 2430-2443.

340. Denk, M.; Hayashi, R.; West, R. *J. Am. Chem. Soc.* **1994**, *116*, 10813-10814.

341. Straus, D. A.; Zhang, C.; Quimbita, G. E.; Grumbine, S. D.; Heyn, R. H.; Tilley, T. D.; Rheingold, A. L.; Geib, S. J. *J. Am. Chem. Soc.* **1990**, *112*, 2673-2681.

342. Wanandi, P. W.; Tilley, T. D. *Organometallics* **1997**, *16*, 4299-4313.

343. Boese, R.; Klingebiel, U. *J. Organomet. Chem.* **1986**, *315*, C17-C21.

344. Stalke, D.; Pieper, U.; Vollbrecht, S.; Klingebiel, U. *Z. Naturforsch., B: Chem. Sci.* **1990**, *45*, 1513-1516.

345. Mix, A.; Berlekamp, U. H.; Stammler, H.-G.; Neumann, B.; Jutzi, P. *J. Organomet. Chem.* **1996**, *521*, 177-183.

346. Schmedake, T. A.; Haaf, M.; Paradise, B. J.; Powell, D.; West, R. *Organometallics* **2000**, *19*, 3263-3265.

347. Denk, M.; Hayashi, R.; West, R. *J. Chem. Soc., Chem. Commun.* **1994**, 33-34.

348. Perti, S. H. A.; Eikenberg, D.; Neumann, B.; Stammler, H.-G.; Jutzi, P. *Organometallics* **1999**, *18*, 2615-2618.

349. Altmeyer, O.; Niecke, E.; Nieger, M.; Busch, T.; Schoeller, W. W.; Stalke, D. *Heteroat. Chem.* **1990**, *1*, 191-194.

350. Romanenko, V. D.; Ruban, A. V.; Drapailo, A. B.; Markovskii, L. N. *Zh. Obshch. Khim.* **1985**, *55*, 2793-2795.

351. Smit, C. N.; Bickelhaupt, F. *Organometallics* **1987**, *6*, 1156-1163.

352. Bender, H. R. G.; Niecke, E.; Nieger, M. *J. Am. Chem. Soc.* **1993**, *115*, 3314-3315.

353. tom Dieck, H.; Zettlitzer, M. *Chem. Ber.* **1987**, *120*, 795-801.

354. Gregor, I. K. *Aust. J. Chem.* **1965**, *18*, 2035-2038.

355. Gregor, I. K. *Aust. J. Chem.* **1966**, *19*, 1977-1982.

356. Von Binder, H.; Fluck, E. *Z. Anorg. Allg. Chem.* **1969**, *365*, 166-169.

357. Von Binder, H.; Fluck, E. *Z. Anorg. Allg. Chem.* **1969**, *365*, 170-175.

358. Searles, S. J.; Tamres, M. In *The Chemistry of the Ether Linkage*; Patai, S., Ed.; John Wiley and Sons: New York, 1967; pp 243-308.

359. Pinkus, A. G.; Ma, S. Y.; Custard, H. C. J. *J. Am. Chem. Soc.* **1961**, *83*, 3917-3918.

360. Well, M.; Fischer, A.; Jones, P. G.; Schmutzler, R. *Chem. Ber.* **1993**, *126*, 1765-1768.

361. Holmes, R. R. *Chem. Rev.* **1996**, *96*, 927-950.

362. Prakasha, T. K.; Day, R. O.; Holmes, R. R. *Inorg. Chem.* **1992**, *31*, 3391-3397.

363. Chandrasekaran, A.; Sood, P.; Day, R. O.; Holmes, R. R. *Inorg. Chem.* **1999**, *38*, 3369-3376.

364. Sood, P.; Chandrasekaran, A.; Day, R. O.; Holmes, R. R. *Inorg. Chem.* **1998**, *37*, 3747-3752.

365. Chandrasekaran, A.; Day, R. O.; Holmes, R. R. *J. Am. Chem. Soc.* **1997**, *119*, 11434-11441.

366. Sood, P.; Chandrasekaran, A.; Day, R. O.; Holmes, R. R. *Inorg. Chem.* **1998**, *37*, 6329-6336.

367. Holmes, R. R.; Prakasha, T. K.; Day, R. O. *Inorg. Chem.* **1993**, *32*, 4360-4367.

368. Sherlock, D. J.; Chandrasekaran, A.; Day, R. O.; Holmes, R. R. *Inorg. Chem.* **1997**, *36*, 5082-5089.

369. Prakasha, T. K.; Day, R. O.; Holmes, R. R. *J. Am. Chem. Soc.* **1993**, *115*, 2690-2695.

370. Sherlock, D. J.; Chandrasekaran, A.; Day, R. O.; Holmes, R. R. *J. Am. Chem. Soc.* **1997**, *119*, 1317-1322.

371. Cavell, R. G.; The, K. I.; Griend, L. V. *Inorg. Chem.* **1981**, *20*, 3813-3818.

372. Cavell, R. G.; Griend, L. V. *Inorg. Chem.* **1986**, *25*, 4699-4704.

373. Burford, N.; Kennepohl, D.; Cowie, M.; Ball, R. G.; Cavell, R. G. *Inorg. Chem.* **1987**, *26*, 650-657.

374. Timosheva, N. V.; Chandrasekaran, A.; Day, R. O.; Holmes, R. R. *Inorg. Chem.* **1998**, *37*, 3862-3867.

375. Rasley, B. T.; Rapta, M.; Kulawiec, R. J. *Acta Crystallogr., Sect. C* **1995**, *51*, 523-525.

376. Livant, P.; Sun, Y. J.; Webb, T. R. *Acta Crystallogr., Sect. C* **1991**, *47*, 1003-1005.

377. Chaloner, P. A.; Harrison, R. M.; Hitchcock, P. B. *Acta Crystallogr., Sect. C* **1993**, *49*, 1072-1075.

378. Light, R. W.; Hutchins, L. D.; Paine, R. T.; Campana, C. F. *Inorg. Chem.* **1980**, *19*, 3597-3604.

379. Ramírez-Arizmendi, L. E.; Yu, Y. Q.; Kenttämaa, H. I. *Am. Soc. Mass. Spec.* **1999**, *10*, 379-385.

380. Kuhn, N.; Henkel, G.; Kratz, T. *Z. Naturforsch., B: Chem. Sci.* **1993**, *48*, 973-977.

381. Kuhn, N.; Henkel, G.; Kratz, T. *Chem. Ber.* **1993**, *126*, 2047-2049.

382. Baker, M. J.; Harrison, K. N.; Orpen, G. A.; Pringle, P. G.; Shaw, G. *J. Chem. Soc., Dalton Trans.* **1992**, 2607-2614.

383. Burford, N.; Royan, B. W.; White, P. S. *Acta Crystallogr., Sect. C* **1990**, *46*, 274-276.

384. Cetinkaya, B.; Hitchcock, P. B.; Lappert, M. F.; Thorne, A. J.; Goldwhite, H. *J. Chem. Soc., Chem. Commun.* **1982**, 691-693.

385. Ruck, M. *Z. Anorg. Allg. Chem.* **1994**, *620*, 1832-1836.

386. Keder, N. L.; Shibao, R. K.; Eckert, H. *Acta Crystallogr., Sect. C* **1992**, *48*, 1670-1671.

387. Nieger, M. Dissertation, University of Bonn: Bonn, 1989; pp 54-56.

388. Burford, N.; Spence, E. v. H.; Rogers, R. D. *J. Chem. Soc., Dalton Trans.* **1990**, 3611-3619.

389. Burford, N.; Spence, R. E. v. H.; Linden, A.; Cameron, T. S. *Acta Crystallogr., Sect. C* **1990**, *46*, 92-95.

390. Burford, N. *Coord. Chem. Rev.* **1992**, *112*, 1-18.

391. Ansell, G. B.; Forkey, D. M.; Moore, D. W. *J. Chem. Soc., Chem. Commun.* **1970**, 56-57.

392. Frampton, C. S.; Parkes, K. E. B. *Acta Crystallogr., Sect. C* **1996**, *52*, 3246-3248.

393. Ueda, H.; Onishi, H.; Nagai, T. *Acta Crystallogr., Sect. C* **1986**, *42*, 462-464.

394. Kapon, M.; Reisner, G. M. *Acta Crystallogr., Sect. C* **1989**, *45*, 780-782.

395. Kuhn, N.; Fawzi, R.; Kratz, T.; Steimann, M.; Henkel, G. *Phosphorus, Sulfur Silicon Relat. Elem.* **1996**, *108*, 107-119.

396. Kuhn, N.; Bohnen, H.; Kreutzberg, J.; Bläser, D.; Boese, R. *J. Chem. Soc., Chem. Commun.* **1993**, 1136-1137.

397. Williams, D. J.; Fawcett-Brown, M. R.; Raye, R. R.; Van Derveer, D.; Pang, Y. T.; Jones, R. L.; Bergbauer, K. L. *Heteroat. Chem.* **1993**, *4*, 409-414.

398. Romanenko, V. D.; Ruban, A. V.; Chernega, A. N.; Markovskii, L. N. *Zh. Obshch. Khim.* **1988**, *58*, 2802-2803.

399. Albright, T. A.; Freeman, W. J.; Schweizer, E. E. *J. Org. Chem.* **1975**, *40*, 3437-3441.

400. Schmidpeter, A.; Brecht, H. *Z. Naturforsch., B: Chem. Sci.* **1969**, *24*, 179-192.

401. Burford, N.; Royan , B. W.; Spence, E. v. H.; Cameron, T. S.; Linden, A.; Rogers, R. D. *J. Chem. Soc., Dalton Trans.* **1990**, 1521-1528.

402. Kuhn, N.; Kratz, T.; Henkel, G. *Chem. Ber.* **1994**, *127*, 849-851.

403. Milicev, S.; Hadzi, D. *Inorg. Chim. Acta* **1977**, *21*, 201-207.

404. Goggin, P. L. In *Comprehensive Coordination Chemistry*; Wilkinson, G., Gillard, R. D., McCleverty, J. A., Eds.; Pergamon Press: New York, 1987; Vol. 2, pp 487-514.

405. Socrates, G. *Infrared Characteristic Group Frequencies*; 2nd ed.; John Wiley and Sons: New York, 1994, p 183.

406. Nyquist, R. A.; Putzig, C. L.; Clark, T. D. *Vib. Spectrosc.* **1996**, *12*, 81-91.

407. Lin-Vien, D.; Colthup, N. B.; Fateley, W. G.; Grasselli, J. G. *The Handbook of Infrared and Raman Characteristic Frequencies of Organic Molecules*; Academic Press: New York, 1991, p 146.

408. Person, R. G. *Inorg. Chem.* **1988**, *27*, 734-740.

409. Perrin, D. D. *Dissociation Constants of Organic Bases in Aqueous Solution*; Butterworths: London, 1965, p 432.

410. Arnett, E. M.; Wu, C. Y. *J. Am. Chem. Soc.* **1960**, *82*, 4999-5000.

411. Wiberg, N.; Schurz, K.; Reber, G.; Müller, G. *J. Chem. Soc., Chem. Commun.* **1986**, 591-592.

412. Silverstein, R. M.; Bassler, G. C.; Morrill, T. C. *Spectrometric Identification of Organic Compounds*; 5th ed.; John Wiley and Sons: New York, 1991, pp 113-123.

413. Burford, N.; Phillips, A. D.; Schurko, R. W.; Wasylishen, R. E.; Richardson, J. F. *J. Chem. Soc., Chem. Commun.* **1997**, 2363-2364.

414. Lappert, M. F.; Martin, T. R. *J. Chem. Soc., Chem. Commun.* **1980**, 635-637.

415. Gysling, H. J. *Coord. Chem. Rev.* **1982**, *42*, 133-244.

416. Chernega, A. N.; Ruban, A. V.; Romanenko, V. D. *Zh. Strukt. Khim.* **1991**, *32*, 158-160.

417. Markovskii, L. N.; Romanenko, V. D.; Ruban, A. V.; Drapailo, A. B.; Chernega, A. N.; Antipin, M. Y.; Struchkov, Y. T. *Zh. Obshch. Khim.* **1988**, *58*, 291-295.

418. Nieger, M.; Hupfer, H.; Niecke, E.; Reichert, F. *Cambridge Database* **1998**.

419. Sheldrick, W. S.; Hewson, M. J. C. *Z. Naturforsch., B: Chem. Sci.* **1978**, *33*, 834-837.

420. Podlaha, J.; Podlahová, J.; Trísková, R.; Novotny, J. *Phosphorus, Sulfur Silicon Relat. Elem.* **1992**, *66*, 289-295.

421. Wood, J. S.; Wikholm, R. J.; McEwen, W. E. *Phosphorus Sulfur Relat. Elem.* **1977**, *3*, 163-169.

422. Sood, P.; Chandrasekaran, A.; Prakasha, T. K.; Day, R. O.; Holmes, R. R. *Inorg. Chem.* **1997**, *36*, 5730-5734.

423. Golic, L.; Milicev, S. *Acta Crystallogr., Sect. B* **1978**, *34*, 3379-3381.

424. Kepert, D. L.; Taylor, D.; White, A. H. *J. Chem. Soc., Dalton Trans.* **1973**, 1658-1662.

425. Thomas, J. A.; Hamor, T. A. *Acta Crystallogr., Sect. C* **1993**, *49*, 355-357.

426. Nardelli, M.; Pelizzi, C.; Pelizzi, G. *J. Organomet. Chem.* **1976**, *112*, 263-272.

427. Bittner, A.; Männig, D.; Nöth, H. *Z. Naturforsch., B: Chem. Sci.* **1986**, *41*, 587-591.

428. Romanenko, V. D.; Ruban, A. V.; Drapailo, A. B.; Povolotskii, M. I.; Markovskii, L. N. *Zh. Obshch. Khim.* **1987**, *57*, 235-236.

429. Burford, N.; Clyburne, J. A. C.; Silvert, D.; Warner, S.; Whitla, W. A.; Darvesh, K. V. *Inorg. Chem.* **1997**, *36*, 482-484.

430. Mitzel, N. W.; Smart, B. A.; Dreihäupl, K.-H.; Rankin, D. W. H.; Schmidbaur, H. *J. Am. Chem. Soc.* **1996**, *118*, 12673-12682.

431. Scherer, O. J. In *Multiple Bonds and Low Coordination in Phosphorus Chemistry*; Regitz, M., Scherer, O. J., Eds.; Thieme Medical Publishers: New York, 1990; pp 112-128.

432. Obase, H.; Tsuji, M.; Nishimura, Y. *Chem. Phys.* **1983**, *74*, 89-95.

433. Allen, F. H.; Harris, S. E. *Acta Crystallogr., Sect. B* **1995**, *51*, 378-381.

434. Lundgren, J.-O. *Acta Crystallogr.*, **1978**, *B34*, 2428-2431.

435. Bürger, H.; Burczyk, K.; Blaschette, A. *Monatsh. Chem.* **1970**, *101*, 102-119.

436. Karaghiosoff, K. In *Encyclopedia of Nuclear Magentic Resonance*; Grant, D. M., Harris, R. K., Eds.; John Wiley and Sons: New York, 1996; Vol. 6, pp 3612-3619.

437. Karaghiosoff, K. In *Multiple Bonds and Low Coordination in Phosphorus Chemistry*; Regitz, M., Scherer, O. J., Eds.; Thieme Medical Publishers: New York, 1990; pp 463-471.

438. Gudat, D.; Hoffbauer, W.; Niecke, E. *Phosphorus, Sulfur Silicon Relat. Elem.* **1993**, *77*, 237.

439. Schmidt, H. M.; Stoll, H.; Preuss, H.; Becker, G.; Mundt, O. *J. Mol. Struct. (Theochem)* **1992**, *262*, 171-185.

440. Arif, A. M.; Barron, A. R.; Cowley, A. H.; Hall, S. W. *Chem. Commun.* **1988**, 171-172.

441. Hemme, I.; Klingebiel, U. In *Adv. Organomet. Chem.*; Stone, F. G. A., West, R., Eds.; Academic Press: New York, 1996; Vol. 39, pp 159-192.

442. Walter, S.; Klingebiel, U. *Coord. Chem. Rev.* **1994**, *130*, 481-508.

443. Niesmann, J.; Klingebiel, U.; Schäfer, M.; Boese, R. *Organometallics* **1998**, *17*, 947-953.

444. Cameron, T. S. *Unpublished results.*

445. Blake, A. J.; Radek, C.; Schröder, M. *Acta Crystallogr., Sect. C* **1993**, *49*, 1652-1654.

446. Xue, W.-M.; Wang, Y.; Chan, M. C.-W.; Su, Z.-M.; Cheung, K.-K.; Che, C.-M. *Organometallics* **1998**, *17*, 1946-1955.

447. Bakir, M.; Sullivan, B. P. *J. Chem. Soc., Dalton Trans.* **1995**, 1733-1738.

448. Haiduc, I.; Silaghi-Dumitrescu, I. *Coord. Chem. Rev.* **1986**, *74*, 127-270.

449. Izatt, R. M.; Lamb, J. D.; Swain, C. S.; Christensen, J. J.; Haymore, B. L. *J. Am. Chem. Soc.* **1980**, *102*, 3032-3034.

450. Zollinger, H. *Diazo Chemistry I; Aromatic and Heteroaromatic Compounds*; VCH Publishers: Weinheim, 1994, pp 289-303.

451. Beck, W.; Sünkel, K. *Chem. Rev.* **1988**, *88*, 1405-1421.

452. Wilke, G.; Eckerle, A. In *Applied Homogeneous Catalysis with Organometallic Compounds, A Comprehensive Handbook: Applications and Developments*; Cornils, B., Herrmann, W. A., Eds.; VCH-Wiley: Weinheim, 2000; pp 358-373.

453. Romanenko, V. D.; Rudzevich, V. L.; Rusanov, E. B.; Chernega, A. N.; Senio, A.; Sotiropoulos, J. M.; PfisterGuillouzo, G.; Sanchez, M. *Phosphorus, Sulfur Silicon Relat. Elem.* **1996**, *111*, 832-832.

454. Komiya, S. In *Synthesis of Organometallic Compounds*; Komiya, S., Ed.; John Wiley and Sons: New York, 1997; pp 35-55.

455. Salzer, A. In *Syntheic Methods of Organometallic and Inorganic Chemistry. Volume 1. Literature, Laboratory Techniques, and Common Starting Materials*; Herrmann, W. A., Salzer, A., Eds.; Georg Thieme Verlag: Stuttgart, 1996; Vol. 1, pp 8-28.

456. Shriver, D. F.; Drezdzon, M. A. *The Manipulation of Air-Sensitive Compounds*; 2nd ed.; John Wiley and Sons: New York, 1986.

457. Burford, N.; Muller, J.; Parks, T. M. *J. Chem. Educ.* **1994**, *71*, 807-809.

458. Perrin, D.; Armarego, W. L. F. *Purification of Laboratory Chemicals*; 3rd ed.; Pergamon Press: New York, 1988.

459. Gerhardt, V. W. *J. Prakt. Chem.* **1968**, *4*, 77-87.

460. Corbridge, D. E. C. *Studies in Inorganic Chemistry: Phosphorus; An Outline of its chemistry, biochemistry and technology*; 4th ed.; Elsevier Science Publishing: Amsterdam, 1990; Vol. 10, pp 1063-1065.

461. Luxon, S. G. *Hazards in the Chemical Laboratory*; 5th ed.; Royal Society of Chemistry: Cambridge, U.K., 1992.

462. Budzelaar, P. H. M., gNMR, 1998; Cherwell Scientific Publishing, Palo Alto, CA.

463. Mason, J. *Solid State Nucl. Magn. Res.* **1993**, *2*, 285-288.

464. Eichele, K.; Wasylishen, R. E., WSolids, 1997; University of Alberta, Edmonton, AB.

465. Stout, G. H.; Jensen, L. H. *X-Ray Structure Determination: A Practical Guide*; 2nd ed.; John Wiley and Sons: New York, 1989, p 77.

This page has been intentionally left blank.